


DOTTORATO DI RICERCA IN INGEGNERIA CIVILE PER L'AMBIENTE ED IL TERRITORIO
X Ciclo - Nuova Serie (2008-2011)
Dipartimento di Ingegneria Civile, Università degli Studi di Salerno

IL CONTRIBUTO DELLA IDRO-GEOMORFOLOGIA NELLA VALUTAZIONE DELLE PIENE IN CAMPANIA

THE CONTRIBUTE OF THE HYDRO-GEOMORPHOLOGY IN THE EVALUATION OF THE FLOOD DISCHARGE IN CAMPANIA REGION

ing. Albina Cuomo

Relatore:
prof. geol. Domenico Guida

Coordinatore
prof. ing. Leonardo Cascini

Correlatore:
prof. ing. Fabio Rossi

THE CONTRIBUTE OF THE HYDRO-GEOMORPHOLOGY IN THE EVALUATION OF THE PEAK DISCHARGE IN CAMPANIA REGION

Finito di stampare il 17/03/2012

CONTENTS

LIST OF FIGURES

LIST OF TABLES

SOMMARIO

Uno dei rischi naturali cui è esposto sin dal passato il territorio nazionale, ed anche la regione Campania, è quello legato alle piene alluvionali. Uno dei problemi centrali nella valutazione di tale rischio è la definizione delle portate massime di piena con assegnato periodo di ritorno. Attualmente in Campania, per la valutazione di tale parametro, si fa riferimento alla metodologia VAPI-Campania (1995). Il VAPI- Campania si basa su un modello geomorfo-climatico, valido a scala regionale, che, ai fini della valutazione delle piogge critiche, ha individuato sette aree omogenee dal punto di vista pluviometrico utile per il calcolo dell'intensità di pioggia con durata pari al tempo di ritardo del bacino, mentre, ai fini della trasformazione afflussi-deflussi, ha previsto la suddivisione del territorio regionale in tre classi di permeabilità. In occasione del XXX° Convegno Nazionale di Idraulica e Costruzioni Idrauliche (IDRA2006), il gruppo di lavoro dell'Università di Salerno, coordinato dai Proff. F. Rossi e P. Villani, presentò una relazione di studio che illustrava le premesse per una rivisitazione di carattere metodologico e procedurale del VAPI. In particolare, la relazione focalizzò l'attenzione su due problematiche fondamentali: i) la presenza ed il ruolo delle barriere orografiche ai fini di valutare l'intensità, la durata e la persistenza delle precipitazioni estreme e ii) l'individuazione degli idro-geomorfotipi, ai fini della più adeguata trasformazione afflussi-deflussi alla scala di bacino e sottobacino. L'obiettivo generale della ricerca illustrata nella presente tesi riguarda, quindi, l'approfondimento del contributo che l'idro-geomorfologia può offrire per la risoluzione delle due tematiche specifiche sopra citate. La prima tematica di ricerca affrontata riguarda la messa a punto di una procedura per la automatica individuazione ed oggettiva delimitazione delle barriere orografiche. In particolare, a partire da una preesistente delimitazione delle barriere orografiche della Campania, basata su giudizio esperto geomorfologico, implementata nel modello semplificato di amplificazione orografica di Rossi et al. (2005), la ricerca perviene ad una procedura fondata sui concetti base della orometria gerarchica (hierarchical mountain geomorphometry): prominenza e parent relationship, per individuare le montagne in modo orografico nella scal spazio-temporale. Inoltre, la procedura consente di individuare

geomorfologicamente le montagne e le sue componenti principali quali fondovalle, versante e crinale utilizzando attributi quali pendenza, rilievo relativo ed esposizione rispetto alla direzione principale delle perturbazioni. La procedure, inoltre, individua i rilievi orografici secondo una procedura gerarchico-multiscalare al fine di utilizzarle alle diverse scale spazio-temporali di analisi idrologica o metereologica. La seconda tematica riguarda la definizione degli idro-geomorfotipi significativi alle diverse scale di analisi idrologiche. La procedura adottata sviluppa la proposta di Guida et al. (2007), che identifica in ambiente GIS grid-based gli idro-geomorfotipi solo sull'areale piroclastico campano e la integra per identificare i diversi meccanismi di deflusso, ed uno schema decisionale di utile all'individuazione dei meccanismi dominanti di formazione del ruscellamento. Detta procedura prototipale, è stata oggettivata ed automatizzata con l'individuazione su DEM, in ambiente GIS object based, delle nove forme elementari del paesaggio di Troch et al.(2002) alle quali associa la risposta idrologica in termini di deflusso superficiale, sub-superficiale ed immagazzinamento di acqua nel sottosuolo. Tale procedura ha consentito di produrre la carta degli idro-geomorfotipi su cui vengono identificate e delimitate le aree del territorio con meccanismi dominanti di trasformazione afflusso-deflusso: eccesso di infiltrazione o hortoniano, eccesso di saturazione e sub-superficiale e di contributo ritardato da deflusso profondo. Ai fini dalla calibrazione e validazione della procedura, sono state effettuate analisi idro-geomorfologiche su alcuni bacini campione opportunamente strumentati, anche utilizzando i dati idro-pluviometrici forniti, dietro richiesta ufficiale, dal Centro Funzionale Regionale del Settore di Protezione Civile della Regione Campania. Le analisi effettuate hanno consentito di proporre, in linea con recenti indicazioni bibliografiche un nuovo indice idrologico, denominato Runoff Index (RI), che potrebbe consentire una migliore valutazione del coefficiente di deflusso nei bacini non strumentati. Inoltre, i risultati delle elaborazioni effettuate su altri bacini strumentati, con analoghe caratteristiche di quelli campione, ha consentito l' estensione della procedura alla regione Campania. Infine, viene discussa l'implementazione, in software di larga diffusione tecnico-scientifica, delle procedure sopra sinteticamente illustrate nella modellazione idrologica distribuita.

ABSTRACT

Italy and, in particular, the Campania region, has been exposed to Hydraulic Risk since long ago. In hydraulic risk analysis the definition of maximum flood discharge with a specific return time (T) is crucial and, to this aim, the VAPI- Campania procedure (1995) was adopted in the Campania region. The VAPI method is based on a geo-morphoclimatic model, identifying 7 climatic homogenous areas with respect to the rainfall probability density function and 3 classes of permeability for the rainfall-runoff transformation model. At the XXX National Congress on the Hydraulic and Hydraulic Engineering (IDRA 2006), the hydrological working group of Salerno University (Rossi and Villani (2006)), pointed out guidelines for up-dating the VAPI-Campania and, in particular the role of: orographic barriers in the evaluation of intensity and persistence of the extreme rainfalls; and the individuation of hydro-geomorphotypes for the rainfall-runoff modeling at the catchments and sub-catchments scales. In this framework, the present thesis gives a contribution to a hydro-geomorphological approach to achieve the two guidelines mentioned above. This research focuses first on the automatic individuation and objective delimitation of the orographic barriers in order to upgrade the heuristic delimitation (expert judgment) used in the simplified model of orographically induced rainfall of Rossi et al. (2005). The proposed procedure is based on the basic concepts of the hierarchic orometry (hierarchical mountain geomorphometry), prominence and parent relationships, to delineate the 'orographic mountain' in various spatial scale (hierarchical- multiscale approach). Also, the procedure defines the 'morphologic mountains' and its components (ridge, plain and hillslope) using slope, altitude, relief ratio and exposition with respect to the dominant perturbation fronts and its moving direction. The second topic of research deals with the individuation of the hydro-geomorphotypes. To this aim, the prototypal work of Guida et al. (2007), was taken into account as a guideline in the identification of the hydro-geomorphotypes and the decisional scheme of Scherrer and Naef (2003), here modify, allowed the identification of the three dominant runoff mechanisms on the Campania region. In particular, the prototypal

procedure of Guida has been here objectified and automatized, defining the 9 elementary landscape forms (Troch et al., 2002), characterized in terms of sub-surface flow and soil moisture storage, under an object-based GIS environment. The procedure here presented allowed identification on the hydro-geomorphological map, and of the runoff mechanisms: Hortonian overland flow for excess of saturation, sub-surface flow, and deep percolation.
In order to test the procedure some hydro-geomorphological analysis have been carried out based on data from two instrumented experimental catchments and on rainfall data from the Regional Functional Center of the Campania Civil Protection Sector. The results allowed to calculate the hydrologic index named Runoff Index, which improves the evaluation of the runoff coefficient (Cf) for un-gauged basins. Other analyses were performed on further 4 catchments with similar hydrologic and geologic behavior in order to extended the procedure to the whole Campania region. Also, conceptual discussions on the implementation of the Runoff Index in the rainfall-runoff transformation operated with a largely used hydrologic software, HEC-HMS, was made, in order to evaluate the feasibility of the procedure proposed in the present research and improve the RI in hydraulic risk evaluation at a regional scale.

ACKNOWLEDGMENTS

I would here like to express my deeply-felt thanks to the kind people who have been very helpful to me during the time it took me to write this thesis. This thesis would not have been possible without the help, support and patience of my principal supervisor, Prof. Guida Domenico, not to mention his advice and unsurpassed knowledge of Geomorphologies and geomorphologic catography. The good advice and support of my second supervisor, Prof. Rossi Fabio, has been invaluable on both an academic and a personal level, for which I am extremely grateful. I would like to acknowledge the academic and technical support of the University of Salerno and the CUGRI. I am most grateful to the doctors V. Siervo, V. Palmieri and A. Cestari for providing me GIS software knowledge and the answers to every questions I've ever asked them regarding GIS tools and the geomorphological mapping. For this research, data were essential. I collected a lot of data thanks to Pasquale Lovisi. It was particularly kind of him to allow me to collected the discharge data on the Bussento river. There were many people who gave interesting feedback e valuable suggestions, for which I would like to thank them.
Above all, I would like to thank my husband Antonio for his personal support and great patience at all times. My parents and sisters have given me their unequivocal support throughout, as always, for which my mere expression of thanks likewise does not suffice.

ABOUT THE AUTHOR

Albina Cuomo, Degree in Civil Engineering for the environment and the territory at the University of Salerno. She was a Philosophy Doctor Student at the University of Salerno, Department of Civil Engineering, 2008-2011 period, on the research activity regarding the role of Hydro-geomorphology in the evaluation of fluvial flood in Campania Region.
She attended courses (Short course "Gis terrain analysis for hydro-geomorphological applications") and workshops (IDRA 2010, EGU 2010) where in oral session presented the procedure for the identification of the orographic barrier. She is author of the paper entitled "Digital orographic map of peninsular and insular Italy" published on "journal of maps'. On Dicember 2011 a book chapter entitled " Water Resources Assessment for Karst Aquifer Conditioned River Basins: Conceptual Balance Model Results and Comparison with Experimental Environmental Tracers Evidences" was published as a co-author on a book "Earth and Environmental Sciences".

1 INTRODUCTION

1.1 RELEVANCE OF THE PROBLEM

Earthquakes, floods, drought, and other natural hazards continue to cause tens of thousands of deaths, hundreds of thousands of injuries, and billions of dollars in economic losses each year around the world (Dilley, et al., 2005).
During the last years, all the natural hazards have had an exponential increase, especially from 1960 to 2000. It could be associated to several factors, such as the increased of population in areas subject to disasters (Berz, 1997), the climate change, that for many researches it is the principal cause of the dramatically increases of disasters (Augusti, et al., 2001, Frich, et al., 2002) and the human causes, which make possible to the hazard to became a disaster (Cannon, 1994).

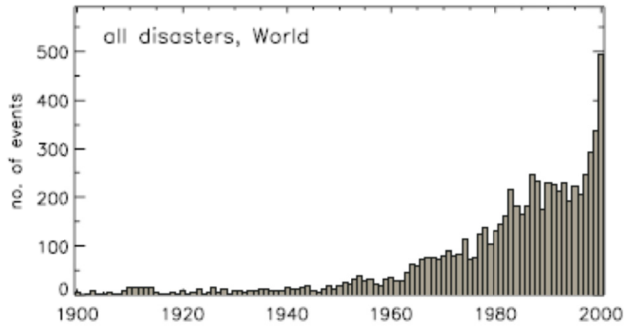

Figure 1.1: Annual global frequency of recorded climate-related disasters for all disaster types (Brooks, et al., 2003)

All the disasters to which each continent is exposed, can cause damage, as well as loss of human life, even to the environmental and urban heritage. If we consider the flood risk, as shown in the figure 1.2, the major mortality occurs in the poorest countries of the world, while the major economic losses occur for the countries with advanced economy.

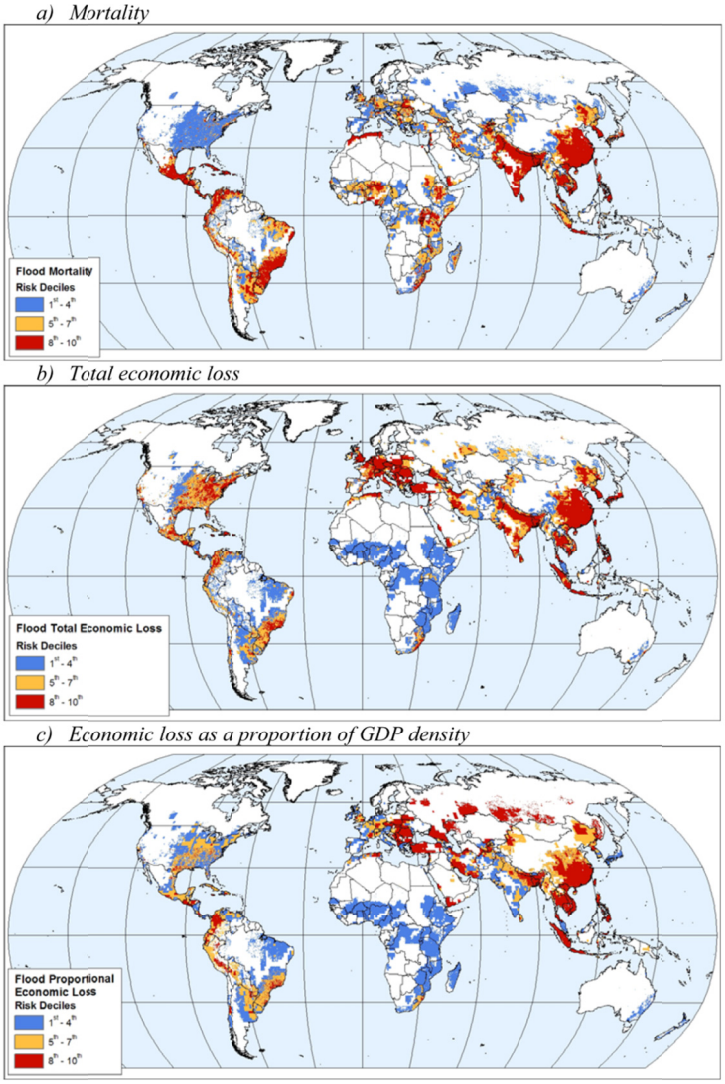

Figure 1.2: Global distribution of flooding risk (modified from Vos, et al., 2010)

In Europe, as we can see in the figure 1.3, the major risk is associated to the climatological factors, instead Asia and Oceania are exposed principally to the geophysical risks. For the Americas, the percent of occurrence of the climatological, hydrological and meteorological risk are comparable, instead in Africa the major risk to which the population is exposed is the hydrological ones.

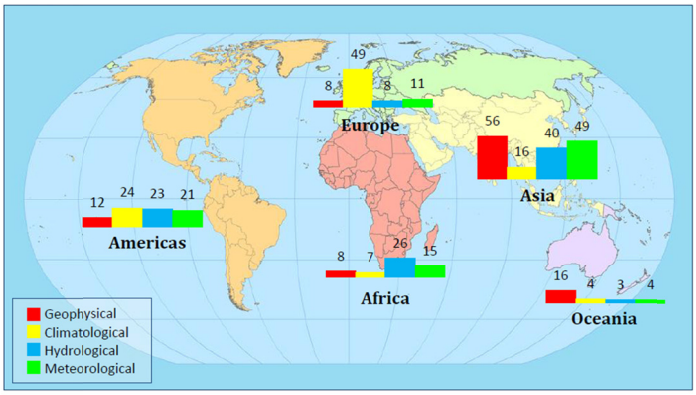

Figure 1.3: Percent share of reported occurrence by disaster sub-group and continent in 2009 (Vos, et al., 2010)

At a national scale, all studies on the overall natural risks to which the Italy is subjected estimated that almost half of the municipalities, are subjected to the risk of flooding. In particular, the Campania Region is the third region after Lombardia and Piemonte regions, with a bigger number of municipality exposed to hydrogeological risks.

Figure 1.4: Number and axtension of municipality areas exposed to the hydro-geological risk (source: Ministry for the Environment).

In the research of the Lastoria et al. (2006), a collection of the major foods occurred in 2003 (figure 1.5) is made. Fifty-five flood events have been collected in the historical archive and Piemonte, Liguria, Sicilia, Toscana, Lombardia, Calabria and Campania result to be the Italian regions more often struck by major floods.

Region	Hydrographic basin	Flood time period	Total duration (h)	Max precipitation (mm/24 h)	Rain gauge name
Molise	Biferno – Fortore – Trigno	23–26 Jan 2003	84	187.8	Casacalenda
Abruzzo	Pescara – Sangro – Trigno	23–26 Jan 2003	72	354.0	–
Puglia	Candelaro – Carapellotto – Celone Cervaro – Fortore – Sannoro – Triolo	24-26 Jan. 2003	–	–	–
Campania	Calore – Miscano – Ufita – Volturno	24–26 Jan 2003	108	77.6	Rotondi
Friuli	Fella (Tagliamento)	29–30 Aug 2003	21	396.2	Pontebba
Puglia	Lato – Tara	8 Sep 2003	9	244.2	Castellaneta
Campania	Irno – Sarno	9 Sep 2003	4	87.0	Capodimonte
Sicilia	Anapo	17–18 Sep 2003	120	234.0 398,4	Melilli-Siracusa Siracusa
Toscana	Carrione	23–24 Sep 2003	20	332.6	Orto di Donna
Sicilia	Salso	15–18 Oct 2003	–	109.0	Aidone
Calabria	Ancinale – Mesima – Petrace	11–13 Dec 2003	36	320.2	Gambarie

Figure 1.5: Italian major floods in 2003 with indication of struck hydrological basins (Lastoria, et al., 2006)

In figure 1.6, Lastoria et al. (2006) reported the results of the study on the total damage, compared to the Gross Domestic Product (GDP), for the major events of Italy, in order to permit the comparison between the economic losses caused by flood events occurred in different historical periods and in different economic conditions. The data source of the research was the AVI (Aree Vulnerate Italiane) database, edited by APAT (Agenzia per la Protezione dell'Ambiente e del Territorio) in the chapter "*Natural Hazards*" of "*Italian Environmental Data Year–book*". In the above research, Lastoria et al. (2006) considered as relevant only the flood events having either generated a casualty at least or economic damages higher than 0.001% of GDP.

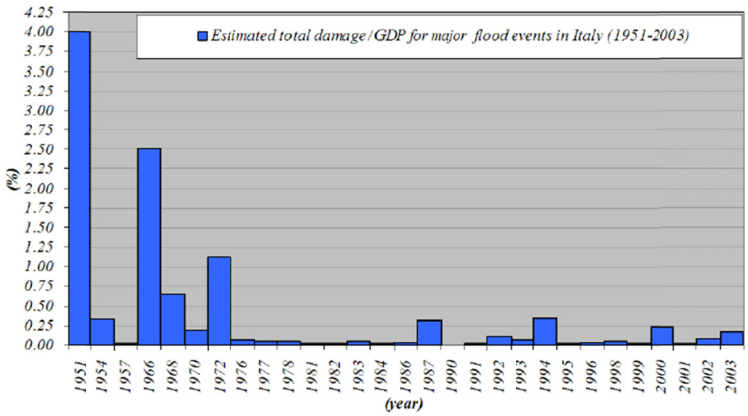

Figure 1.6: Estimated total damage updated in relation with the GDP, for the major flood events in Italy (1951-2003) (Lastoria, et al., 2006)

Another study on the distribution of the Italian municipalities struck by flood event was carried out by Salvati et al. (2010) collecting the data for 1419 years from 590 to 2008. They found that on 81072 municipalities, 1378 of this experienced fatal event and other 1428 with casualties.

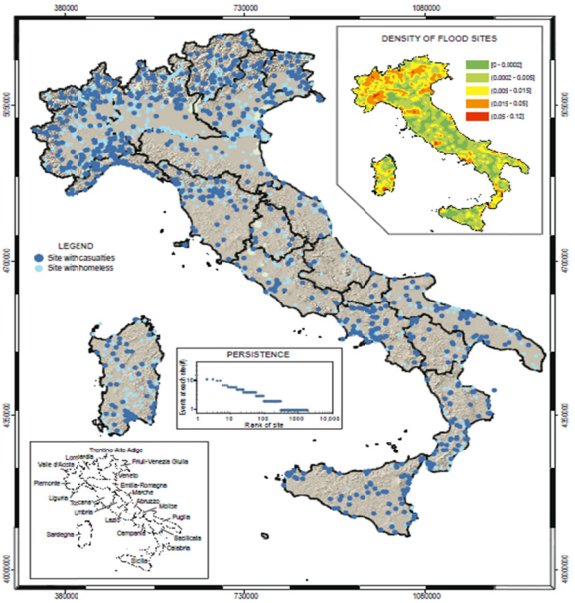

Figure 1.7: Map showing the location of 1836 sites affected by flood events with direct consequences to the population on Italy, in the 1419 – year period 590-2008 (Salvati, et al., 2010)

It is evident that Italy has a long history on natural catastrophes as inundation or flooding, which occurs every year causing significant economic damage and social distress. Several are the causes of the natural disasters and, in particular, for the hydrological ones high intensity rainfall, steep slopes, easily eroded rocks and inappropriate land management. Since past, researchers have performed hydrological and hydraulic studies to assess flooding hazard, mitigate flood risks and support the land management. Thus, in the following paragraphs, will be revised the hydrologic catchment modeling ranging from the Rational method to the recent distributed models.

1.2 BACKGROUND AND APPROACHES

The central problem in the definition of the flood risk assessment is the evaluation of the peak flood discharge following trainfall extreme events. The estimation of this parameter is crucial to both small and large-scale, respectively, and is performed by combining watershed hydrological and channel hydraulic models in the delimitation of the flooding areas and definition of the design parameters useful for the mitigation of hydraulic risk. Then, watershed models and, more precisely, the rainfall-runoff transformation procedures are fundamental to assess the water resources and manage the hydrogeological risks (Singh, et al., 2002).
The scientific literature concerning the hydrological modeling it is very wide and results hard to synthetize a systematic review of the several models existing. Only some hydrologists have attempted this review, among others: Clarke (1973) discussed on the several hydrological model identification and parameter estimation. Todini (1988, 2007) reviewed the historical development of mathematical method used in the rainfall-runoff modeling; El- Kady (1989) reviewed the hydrologic models pointing on the surface-groundwater linkage. Goodrich and Woolhiser (1991) reviewed advances in catchment hydrology in the United States, Horneberger and Boyer (1995) emphasized the importance of the spatial and temporal variability of the hydrological responses and the need to explicitly consider the linkage among the hydrology and the other disciplines, comparing modeling concepts and challenges. More recently, Singh and Woolhiser (2002) reviewed the 72 catchment hydrological models more widely used.

Considering the large number of existing watershed models in the literatures, only the fundamental ones will be cited in the present chapter.

The basic classification of the existing hydrological models distinguishes them in lumped or distributed models. Beven (2000) defined the first one as a model describing the catchment hydrological response referred to a single structural and functional component. This last can be represented by means an unique hydrologic variable representing the average descriptor values over the catchment area. Differently, in the distributed modeling the catchment is discretized into a grid squares and to everyone is associated the specific state variables representing the local average. With respect to the most general formulation of the hydrologic models involving partial differential equations in 3D space and time, if the spatial variation of the hydrologic parameter is ignored, the model is namely "lumped", otherwise if the outputs are function of the space and the time, it is said to be "distributed" (Singh & Woolhiser, 2002).

The origin of the mathematical hydrological modeling date back to the Rational formula, a method proposed by Mulvani (1850) that relate the concept of time of concentration to the maximum runoff value. In 1921, Ross (1921) introduced a distributed hydrological model and his idea was to split the catchment in areas on the basis of the travel time to the catchment outlet. The problem of Ross time-area concept was deciding which area of the catchment would contribute to the different zones (Beven, 2000). This problem was avoided by Shermann (1932) with the introduction of concept of Unit Hydrograph (UH) of a watershed, defined as the direct runoff hydrograph resulting from a unit volume of excess rainfall of constant intensity and uniformly distributed over the drainage area (Ramírez, 2000). The UH introduced by Sherman was successively interpreted as the Instantaneous Unit Hydrograph, or IUH, defined as the hydrograph of direct surface runoff caused by one inch of precipitation excess being released instantaneously and uniformly over a catchment basin (Phillippee, et al., 1969).

In the more recent time Chow et al. (1998) categorized the Syntetic Unit Hydrograph in three procedures:

1) the first one is done by Nash (1957) and Dooge (1959) based on the models of watershed storage;

2) the second one was based on a dimensionless unit hydrograph, e. g. Soil Conservation Service, (1972);

3) the third one was relating to the hydrograph characteristics, as the time to peak, or to the watershed characteristics, as the GIUH, introduced by Rodríguez-Iturbe and Valdés (1979).
The practical limitation in the all above watershed hydrologic models is the scarcity of data and parameters which do not permit a fully distributed characterization of the watershed.
In the 1980s a great deal of attention was done to the new data collection as the remote sensing, satellites and radar which provides data regarding spatial distribution of meteorological inputs, soil and land-use parameter, inventories of water bodies, etc. (Singh, et al., 2002). Another advances, concerning the physical characteristics of a watershed, such as soil, land use and topography which vary spatially, consisted in essential materials and new tools such as the digital terrain (DTM or DEM) or GIS. The first one represents the 3D nature of the landscape and it automatically extracts topographic variables, such as basin geometry, stream networks, slope, aspect, relief, etc. (Singh, et al., 2002).
Singh and Fiorentino (1996) expressed the effectiveness of the GIS Database for processing large quantities of data. Leavesley and Stannard (1990) used the environmental Gis employed automated methods to derive parameter for delineating the Hydrological Response Units (HRUs). Hydrologic models with the spatial structure are being increasingly based on detailed DEM or DTM (Moore, et al., 1988 a,b) and many existing models used data structures in grid or cell networks as their basic structure , such as SHE (Abbott, et al., 1986a, b) , TOPMODEL (Beven and Kirkby, 1979), ANSWERS (Beasley, et al., 1980) and AGNPS (Young, et al., 1989). There are well known general watershed models used elsewhere, from the HEC-HMS , NWS and MMS models in the United States to the RORB and WBN models in Australia, or TOPMODELS and SHE models in Europe.
More recently, Rigon et al. (2011) developped a theoretical framework to investigate peakflow dipendence on geomorphic properties of the river basin, demostrating its no dependence on channel velocity but on geomorphic properties.
Nowadays data structures are being increasingly based on the Object-Oriented (OO). It is a way to organize the system as a collection of discrete objects (Simonovic, et al., 1997) which could be concrete (such as a river reach) or conceptual, such as a policy decision (Elshorbagy, et al., 2006). There are a few applications of OOD in hydrological simulation in the past decade (Wang, et al., 2005a; Band, et al., 2000).

These applications have made valuable attempts using OO Programming (OOP) in hydrological modeling, but there is no detailed discussion of OO Design (OOD) principles and how to systematically implement them in watershed model design (Wang, et al., 2005b).

1.2.1 Background and Approaches: Italy and Campania region

The hydrological model briefly illustrated in the previous paragraph, although rigorous and physically-based, have afew limitations in regional food hazard planning and practical applications.
In Italy, the shared approach used in Italy for evaluating the peak discharge for regional flood hazard assessment is based on the VAPI method (VAlutazione delle PIene) (Rossi and Villani, 1994).
Since 1994 in Italy, the National Group of Defense from Hydrogeological Disasters (GNDCI) of Italian National Research Council (CNR), started a National Research Program in order to define the peak discharge in basin at regional scale with respect to the hydro-geomorpho-climate controls. The result of a decadal effort carried out by GNDCI were the several research group contributions at regional level (Versace et al. 1989, Cao et al. 1991, Copertino and Fiorentino 1992, Cannarozzo et al. 1993, Rossi and Villani 1994, Villi and Bacchi 2001).
In the figure 1.8 are shown the book covers of the evaluation of the peak discharge in some regions of Italy.

Figure 1.8: VAPI Report covers of the flood evaluation of a few regions of Italy.

In the Campania region, the research program was directed by professors F. Rossi and P. Villani (VAPI, 1994)- Department of Civil Engineering, University of Salerno, 1.9 Operative Unit of GNDCI (Ferrari et al., 1990; Rossi e Villani, 1994). Part of the same research group performed the VaPi Piedmont on behalf the CUGRI Salerno

(Contract 21 giugno 1999, n. 1776), as a hydrological model developed to organizing the ongoing knowledge relating to formation processes of the flood discharges following short and intense rainfall events previously gained within the VAPI project (National Project for Assessment of Floods in Italy).
The two-component extreme value distribution TCEV (Rossi et al., 1984) was adopted in the VAPI procedure to studying the extreme precipitation pattern. The TCEV represents the distribution of the maximum value, in a given time interval, of a random variable distributed according to the mixture of two exponentials:
- the low component (low intensity and high frequency);
- the high component (high intensity and low frequency).

If X is the random variable and X_T is the value of the variable X at a specific return period flow T:

$$X_T = K_T\, m(X) \qquad \textbf{Equation 1.1}$$

Where: m(X) = mean value of the random variable X; K_T = probability factor of growth, increasing with the return period.
Adopting the TCEV distribution, the following relation was done between the K_T and T:

$$T = \frac{1}{1-\exp(-\Lambda_1 e^{-k\eta} - \Lambda_1 \Lambda_* e^{-k\eta/\theta_*})} \qquad \textbf{Equation 1.2}$$

Where: Λ_1 is a scale parameter; $\theta_* = \theta_2/\theta_1$ e $\Lambda_* = \Lambda_2/\Lambda_1 1/\theta_*$ are the shape parameters of the distribution; η depend on Λ_1, Λ_* e θ_* (Rossi e Villani, 1994).
In the practical application it possible to adopting the following simple formulation:

$$K_T = \left(\frac{\theta_* \Lambda_\upsilon \Lambda_*}{\eta} + \frac{\Lambda_\upsilon \Lambda_1}{\eta}\right)\frac{\theta_*}{\eta}\Lambda_\upsilon T \qquad \textbf{Equation 1.3}$$

For the parameters of the TCEV distribution estimated for the Campania region, the equation 1.3, becomes:

$$K_T=-0.0373+0.517\ Ln(T) \qquad \textbf{Equation 1.4}$$

In the table 1.1 area reported the K_T values calculated for some return period T.

Table 1.1: Value of the K_T coefficient estimated for the Campania region for some return period T

T (year)	2	5	10	20	25	40	50	100	200
K_T	0.87	1.16	1.38	1.64	1.72	1.92	2.03	2.36	2.71

For the evaluation of the annul mean of the peak discharge m(X) it is possible to use four method: two of that compared the m(X) to the area of the watershed, on the contrary in the rational and the geomopho-climatic approaches the m(X) is calculated considering the precipitation and the geomorphologic features of the basins.
In the following will describe the geomorpho-climatic approach, only, to calculate the mean annual peak discharge m(X):

$$m(x) = \frac{C_f \times q \times K_A(t_r) \times m[I(t_r)] \times A}{3.6} \qquad \textbf{Equation 1.5}$$

Where A is the area of the basin (km^2), m $[I(t_r)]$ is annual average of the maximum rainfall intensity on a fixed term (mm), C_f is the runoff coefficient, Ka is the areal reduction factor and t_r is the delay time of the basin (h), q is the attenuation coefficient of peak discharge.
The annual average of the maximum rainfall intensity on a fixed term d, is calculated with the following formulation for the Campania:

$$m[I(d)] = \frac{m(I_0)}{(1+\frac{d}{d_c})^{\beta}} \qquad \textbf{Equation 1.6}$$

where d e d_c are in hour, $m[I_O]$ e m[I(d)] are in mm/hour and

$$\beta = C - D * Z$$ **Equation 1.7**

The parameters of equations 1.6 and 1.7 are constants for each pluviometric homogenous areas. For the Campania region six pluviometric homogenous areas were identified (table 1.2).

Table 1.2: Statistical parameters for each climatologically homogenous areas of the Campania region.

Homogenous areas	m(h_O) (mm/hour)	d_C (hour)	C	D * 10^5
1	77.1	0.3661	0.7995	8.6077
2	83.8	0.3312	0.7031	7.7381
3	116.7	0.0976	0.7360	8.7300
4	78.6	0.3846	0.8100	24.874
5	231.8	0.0508	0.8351	10.800
6	87.9	0.2205	0.7265	8.8476

The areal reduction factor K_A, can be calculated in the following way:

$$K_A(d) = 1 - [\ (1 - \exp(-c_1 A))\exp(-c_2 d^{c_3})\ ]$$ **Equation 1.8**

where: A is the area of the basin, in km^2; c_1 = 0.0021;c_2 = 0.53; c_3 = 0.25.
In the VAPI Campania, is proposed to splitting the basins in three classes of permeability to evaluating the the runoff coefficient and the delay time:

- Permeable areas without forest (A_1)
- Impermeable areas (A_2)
- Permeable areas with forest (A_3)

The coefficient at the basis of the runoff coefficient is to assign the coefficient to each homogenous areas in terms of permeability and then provided to the balanced average of that:

$$C_f = C_{f1}\frac{A_1}{A} + C_{f2}\frac{A_2}{A} + C_{f3}\frac{A_3}{A}$$ **Equation 1.9**

dove:
C_{f1} = runoff coefficient for the permeable area without forest = 0.42;
C_{f2} = runoff coefficient for the impermeable area = 0.56;
C_{f3} = runoff coefficient for the permeable with forest= 0.00.

The delay time is calculated with the following formula:

$$tr = \frac{C_{f1} A_1}{C_f A} \frac{1{,}25\sqrt{A_1}}{3{,}6 c_1} + \frac{C_{f2} A_{2_1}}{C_f A} \frac{1{,}25\sqrt{A_2}}{3{,}6 c_2}$$

Where: c_1 is the mean flood wave celerity of channel network for the permeable areas without forest = 0.23 m/s; c_2 is the mean flood wave celerity of channel network for the impermeable areas = 1.87 m/s.

The attenuation coefficient of the peak discharge is calculated considering the law of pluviometric probability and the response time of the river. This formulation has taken into account the mistake made adopting a duration time of the precipitation equal to the delay time of the basin.

$$q = \begin{cases} 0.60 \quad se \quad 0.25 \le n' = 1 + k_1 \cdot A - \dfrac{\beta \cdot t_r / d_c}{1 + t_r / d_c} \le 0.45 \\ 0.65 \quad se \quad 0.45 \le n' = 1 + k_1 \cdot A - \dfrac{\beta \cdot t_r / d_c}{1 + t_r / d_c} \le 0.65 \end{cases}$$

Where:

- β = (C - D·z) e d_c are the parameters of the law of the pluviometric probabilities;
- k_1 is a numeric coefficient equal to $1.44 \cdot 10^{-4}$ if the area A is expressed in km^2 and the delay time t_r in hour.

1.3 OBJECTIVES OF THE THESIS

After ten years from the publication of the VAPI method, Rossi and Villani (2006) have presented at the National Conference of Hydraulics and Hydraulics engineering in Rome (IDRA 2006) the research guidelines for the VAPI procedure up-dating.
More precisely, the aim of the research group is to updated the methodology in the evaluation of the maximum annual precipitation and the runoff coefficient (C_f), at basins scale. In particular they have pointed the attention on three themes:

1. the estimation of the precipitation pattern with a new probability distribution function;
2. the effects of the orographic barrier on the precipitation pattern on the windward and leeward side of the mountains;
3. the identification of the hydro-geomophotypes to performed the hydrologic analysis at catchment and sub-catchment scales, taking into account in more detail the hydrologic response of the basin and the geo-morphological factors for a re-calibration of the runoff coefficient (C_f).

About the second theme, in the 2005, the same research group of Salerno University presented at the European Geosciences Union (EGU) a simplified model to estimate the rainfall amplification and attenuation factors, respectively on windward and leeward side of the mountains, by analyzing the historical dataset on the annual maximum intensity. This study was carried out considering the orographic barrier map performed on heuristic basis (Rossi et al. 2005).
About the third theme, in the XXX Conference on Hydraulics and Hydraulic Constructions (IDRA2006), Rossi and Villani (2006) highlight the need to introduce the hydro-geomophotype concept in the hydrologic updating of the VAPI procedure and provided a preliminary method to identify them in the pyroclastic-cover on carbonate bedrock landscapes in the Campania Region.
Starting from these premises, the aims of the present research were to provide the requested hydro-geomorphological contributions to the second and third themes of the up-to-dating VAPI procedure.

Therefore, the present research is based on two main topics: the orographic barrier, in order to improve extreme precipitations orographically-induced and the hydro-geomorphotypes, to support rainfall-runoff transformation models.
Regarding to the orographic barrier topic, the research proposal is oriented to their objective individuation and delimitation, hierarchical characterization and multi-scale mapping. The individuation and delimitation of the orographic barriers will carried-out by an automated GIS-based procedure. The objective identification of the orography will be used by the researchers for the analysis in the anomaly of the precipitation pattern at a regional and local scales..
The second topic is the definition of the basic hydro-geomorphological units which are relevant for the analysis at a different scales of the hydrologic analysis. The objective of the studies is the identification of units with a specific hydrological and morphological characteristics which go beyond the basin subdivision in the three classical VAPI permeability classes (see par. 2.1.1). The implementation of the terrain morphologies could be relevant to evaluate the sub-surface response of basins, i.e., to highlight the fast and delayed response of a basins to the rainfall inputs.
The procedures proposed and exposed in the following paragraphs will be validated on a dataset on discharge and precipitation data collected at the a basin outlet which are the historical ones for the study of the VAPI procedure. The discharge data were collected by a monitoring system of the hydro-geomorphological working group of the Salerno University and the rainfall dataset were provided by the courtesy of the Campania Region Civil Protection.

1.4 STRUCTURE OF THE THESIS

The structure of the thesis has been organized to facilitate the understanding of the background approaches, procedures, materials, analysis and results on the topics.
In the chapter 2, methods and procedure adopted will be described. In particular in the first part will be explained the interdisciplinary nature of the research which is the current tendency of the international scientific researches. Then, will be described the multiscalar procedure and the

hierarchical approach used to identify, with the GIS tools, the spatial extent of the Hydro-geomorphotypes and the orographic barriers, both often hierarchically organized. The description of the study area will be made in the chapter 3 and in the chapter 4, materials utilized will show. In the following chapters 5 and 6 will described the procedures adopted for the identification, respectively, of orographic barriers and hydro-geomorphotypes, as well as the thematic maps derived from them.
Finally, in the chapter 7, the discussion to the case study will be performed. In this chapter will be show, with a rainfall-runoff model applied in HEC-HMS software, the linkage between the orographic barriers, inducing the variation of the rainfall intensity, and hydro-geomorphotypes, utilized to evaluate the sub-surface response of basins.

2 METHODS

2.1 INTERDISCIPLINARITY

The research here presented uses an interdisciplinary science, the hydro-geomorphology, that focuses on the interaction and linkage of hydrologic processes with landforms and the interrelation of geomorphic processes with surface and subsurface water, in various temporal and spatial dimensions.
The interdisciplinarity is an useful working method of two or more academic fields in order to pursuing common research tasks. So, its development has led to the training of experts of two or more disciplines at the same time, with a greater understanding of complex phenomena whose study does not requires the simply sum of its disciplinary parts (Klein and Newell, 1998). The current tendency of the scientific community is oriented to a such approaches, as the hydro-ecology, hydro-meteorology, hydro-geomorphology and so on.
The research here presented is oriented to the above introduced hydro-geomorphology based on the concepts of other scientific areas, the geology, geomorphology, land cover, slope, lithology, hydrology and climatology, (e.g. Sidle and Onda 2004; Bisson and Lehr 2004; Babar 2005).
The morphology of terrestrial surface is a major structural determinant of many surface hydrological processes, as well as of many coupled quantitative processes and interfaces with the groundwater, the cryosphere and the atmosphere dynamics. Conversely, hydrology is a major driving force of geomorphological dynamics, under climatic forcing and in relation to both tectonics and geography, the topography is modified in a long times. This refers to various issues, from palaeo-hydrology to landslide hazard assessment, and even to hydrological interpretations of planetary morphologies.
Several focal areas it is possible to study with hydrogemorphology science as runoff processes influenced by lithology and geomorphology, surface and mass erosion processes and linkage to stream, modeling hydrological factors affecting landslides initiation and environment,

impact of distributed land-use practices on soil and water resources, effects of global climate change, land-use planning and so on (Sidle and Onda 2004).
Some interesting works stressed the importance of the relationships between geomorphology and groundwater approaches with other emerging scientific domains, such as hydro-ecology or hydro-geoecology (Loague et al., 2006; Hancock et al. 2009), hydropedology (Espinha Marques et al., 2006, 2007), urban hydrogeology (Alonso et al. 2006).
In figure 2.1 is shown, as example, the procedural scheme adopted by Teixeira et al. (2008) for evaluating the groundwater resources, with an integrated approach hydro-geomorphology and GIS mapping.

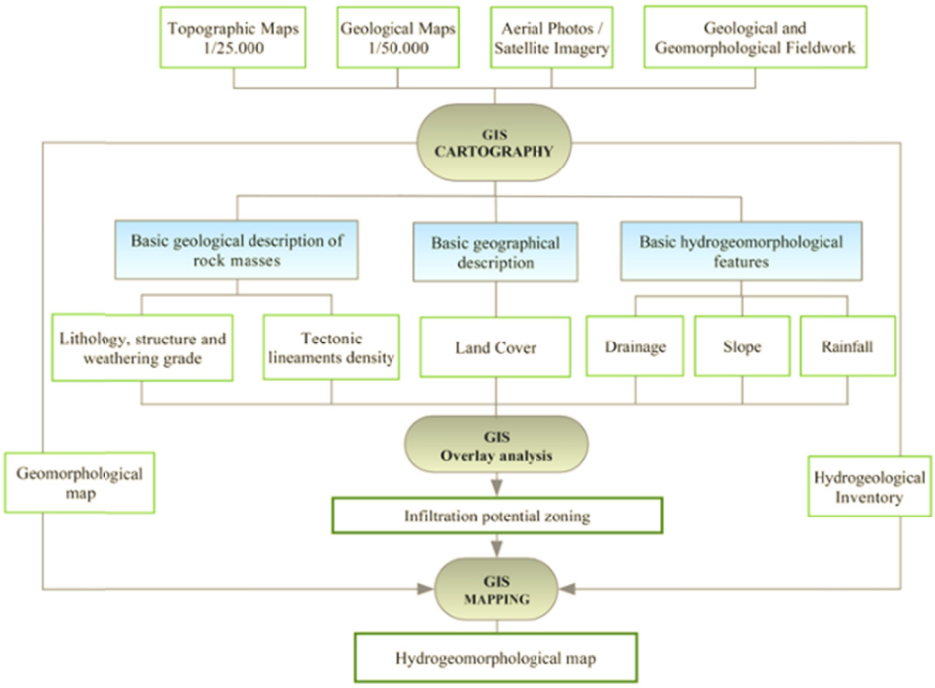

Figure 2.1: Interdisciplinary procedural scheme adopted for a GIS-based evaluation of the groundwater resources, modified from Teixeira et al. (2008)

Since the 60ths of the past century, the professor Tsukamoto (1961) developped the variable source-area concept in streamflow generation model. Sccessively, the professor Kazuo Okunishi in 1989 articulated many of the processes-based concepts in hydro-geomorphology approaches (Okunishi, 1991, 1994).
In Europe, a large contribute to the hydro-geomorphology has been done by Kirkby and Chorley (1967) and Anderson and Burth (1978) and in North America by Hack and Goodlett (1960), Hewlett and Hibbert, (1967) and Dunne and Black (1970). In 1972, Scheidegger (1972) defined, in a review paper, the hydro-geomorphology as the study of landforms as caused by the action of water, discussing examples of the mechanical interaction of surface water, groundwater and seas with landscapes and ocean bottom.
The definitive scientific definition of "hydro-geomorphology" was provided by Sidle R. C. and Onda Y. (2004), in a special issue of Hydrological Processes Journal, representing a collection of contributions on "*Interaction between geomorphic changes and hydrological circulation*", as proceedings of the Fifth International Conference on Geomorphology (ICG-5), held in Tokyo, Japan, from 23 to 28 August 2004.

2.2 HIERARCHICY AND MULTISCALARITY

As above cited, the present research deals with two topics: the identification and delimitation of the orographic barriers and hydro-geomorphotypes. To this goal the hierarchical multiscale approach was adopted. Following the recent research study of Dramis et al.(2011), the problem of the multiscale geomorphological mapping may be approached adopting the *principles of allometry* (Bull, 1975) that is the space-time relationships of landforms and the *Hierarchical theory*, that allows the definition of nested object of size orders and taxonomical complexity (Dikau, 1990).
In particular, the hierarchical procedure is based on the general Hierarchy Theory widely applied in ecology (O'Neill, 1988) (O'Neill *et al.* 1986; Klijn 1988) as well as in the Land System evaluations (Speight, 1988). In the geomorphological mapping this approach is used for the

spatial definition and characterization of the landforms (Linton 1951, Wright 1972). Dramis et al. (2011) approached to the hierarchical procedure for the geomorphological mapping, in order to define the taxonomy, adopting the symmetrical, horizontal and asymmetrical upwards/downwards relationships (Koestler, 1967; Webster, 1977; O'Neil et al., 1986; Haigh, 1987; Seelbach et al., 1997; Wu, 1999; Krönert et al., 2001; Pereira, 2002) (figure 2.2).

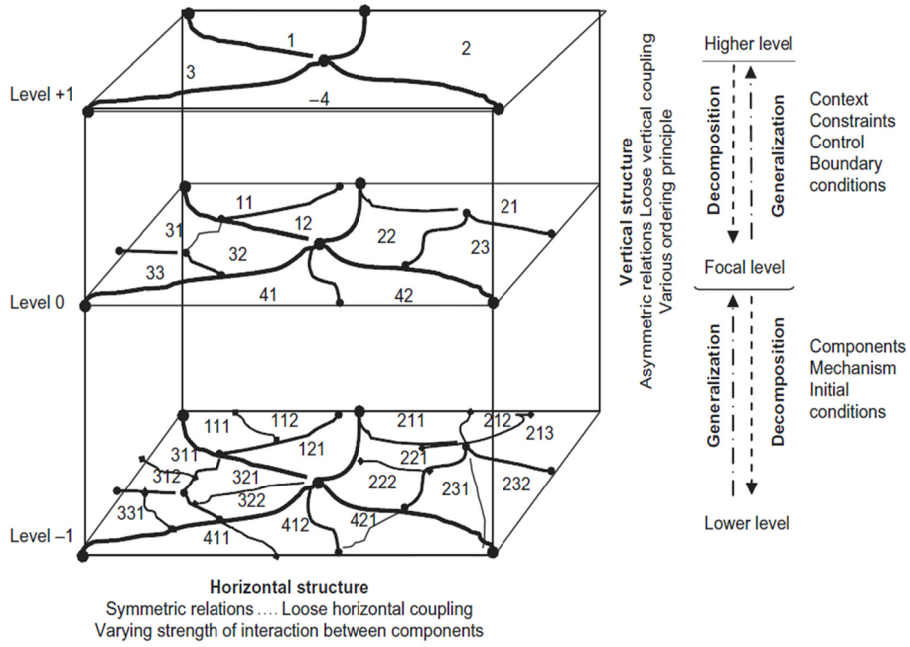

Figure 2.2: Illustration of hierarchical ordering/coding and horizontal/vertical relationship between the focal (initial) level and the higher/lower levels. In the focal to higher level transition, a set of generalization algorithms allows the adaptation of time-spatial context, number and typology of control factors and boundary conditions. In the focal versus L-level transition, a set of decomposition algorithms are involved to extract basic components and mechanisms, modifying the previous initial conditions. (modified from Dramis et al., 2011)

Adopting this procedure, the land surface can be viewed splitted in geomorphometric object that can be decomposed into smaller ones increasing observation detail and generalized in the bigger ones decreasing the observation detail. The taxonomical complexity comprises the simple facets, form elements and complex relief forms and relief form association (Dikau, 1990). In the figure 2.3 is reported the figure of the hierarchical taxonomic suggested in geomorphological mapping by Dramis et al. (2011).

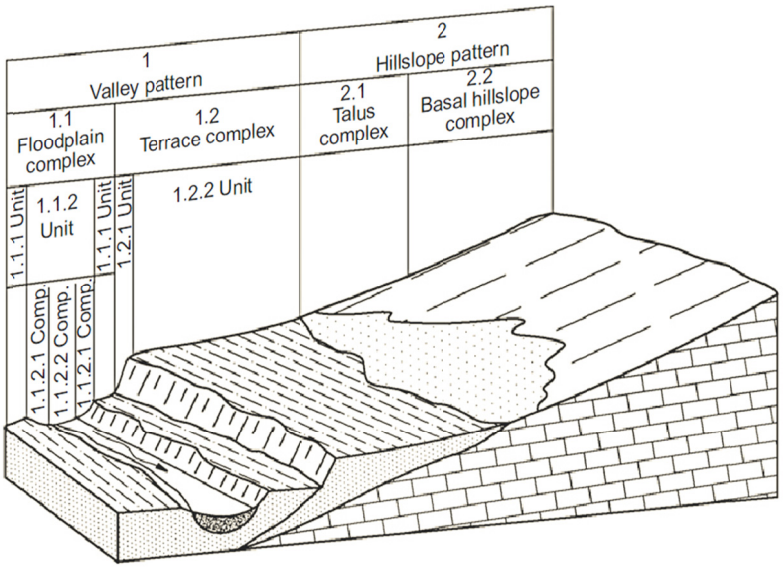

Figure 2.3: Nested hierarchic sequence of landforms (Dramis et al. 2011)

So, the nested hierarchical multiscale approach allowed in the identification of geomorphological units at a different scale, as proposed by Dramis et al. (2011):

Table 2.1: Hierarchical Multiscale Taxonomy (from Dramis et al., 2011)

Level	Scale Range	Land Features Taxonomy	Corresponding Land Units in Other Classification Schemes	Persistence Time
1	<1:1,000,000	Physiographic domain	Physiographic domain (MacMillan et al., 2000a) Land region *p.p.* (Crofts, 1991) Land system *p.p.* (Linton, 1951)	10^8–10^9 years
2	1:1,000,000 1:500,000	Physiographic region	Physiographic region (MacMillan et al., 2000a) Land region *p.p.* (Crofts, 1991) Land system *p.p.* (Linton, 1951) Geotectonic region (Blasi et al., 2007)	10^8 years
3	1:500,000 1:250,000	Physiographic province	Physiographic province (MacMillan et al., 2000a) Land region (Crofts, 1991) Land system *p.p.* (Linton, 1951) Morphotectonic province (Guida et al., 1996; Blasi et al., 2007)	10^7–10^8 years
4	1:250,000 1:100,000	Landform system	Physiographic system *p.p.* (MacMillan et al., 2000a) Land region (Linton, 1951) Morphological system *p.p.* (Guida et al., 1996; Blasi et al., 2007)	10^7 years
5	1:100,000 1:50,000	Landform sub-system	Land system *p.p.* (Linton, 1951) Land system (Crofts, 1991) Morphological system *p.p.* (Guida et al., 1996; Blasi et al., 2007)	10^6 years
6	1:50,000 1:25,000	Landform pattern	Landform type *p.p.* (MacMillan et al., 2000a) Land facet (Crofts, 1991) Facet (Linton, 1951) Morphological unit (Guida et al., 1996; Blasi et al., 2007)	10^5–10^6 years
7	1:25,000 1:10,000	Landform complex	Landform type *p.p.* (MacMillan et al., 2000a) Land facet *p.p.* (Crofts, 1991) Facet *p.p.* (Linton, 1951)	10^4–10^5 years
		unit	(MacMillan et al., 2000a)	years
	1:5000		Land site *p.p.* (Crofts, 1991) Site *p.p.* (Linton, 1951)	
9	>1:5000	Landform element	Landform element *p.p.* (MacMillan et al., 2000a) Land site *p.p.* (Crofts, 1991) Site *p.p.* (Linton, 1951)	10^2 years or less

The scale issue is very important in hydrology, too (Dooge, 1982, 1986; Klemes, 1983; Wood et al., 1990; Beven, 1991; Mackay and Riley, 1991;

Rodriguez-Iturbe and Gupta, 1983; Gupta et al., 1986). The hydrological processes occur in a wide range of scales, from the unsaturated flow in a 1 m of soil profile to flood in a river systems of a million square of kilometers; from flash floods of several minute durations to flow in aquifers over one hundred years (Blösch and Silvapan, 1995).
The figure 2.4, based on both data and heuristic considerations, attempts a classification of hydrological processes and precipitation according to the length and time scales. Blosch and Silvapan (1955) believe that all the hydrological processes occur in response to a precipitation at a similar length scales, with a delay in the time response.

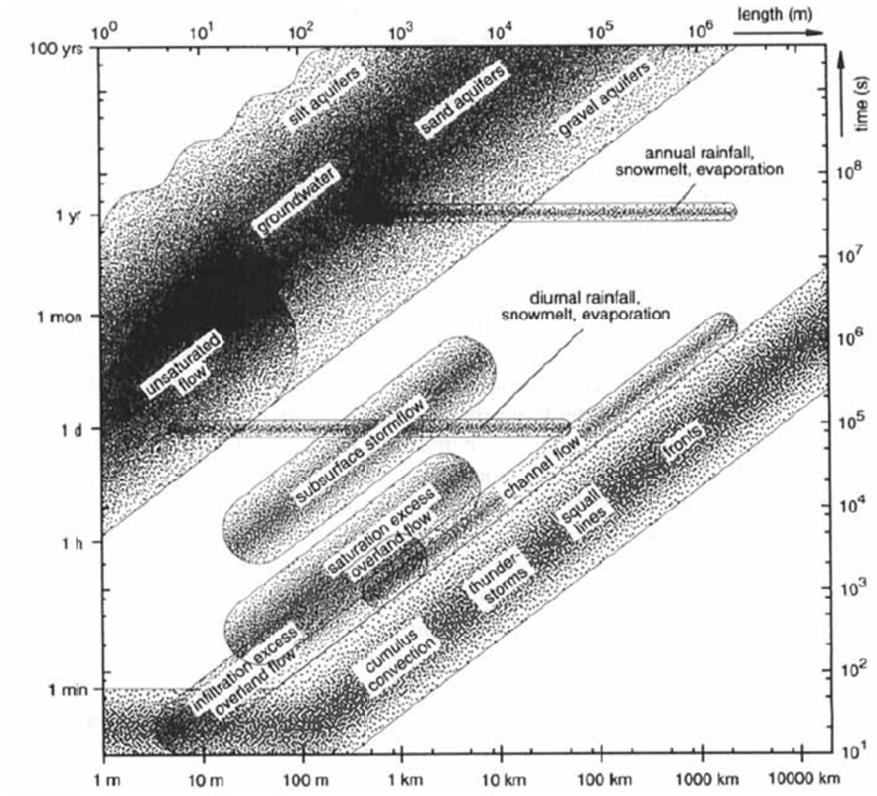

Figure 2.4: Hydrological processes at a range of characteristic space time scales (from Blosch and Silvapan, 1995).

The meteorological phenomena, too, can see at different spatial –time scale, i.e. it will occur the isolated cells at a scale of 1 km and several minutes, or the frontal system at a scale of 1000 km and the duration is more of 1 day (Austin and Houze, 1972; Orlanski, 1975).

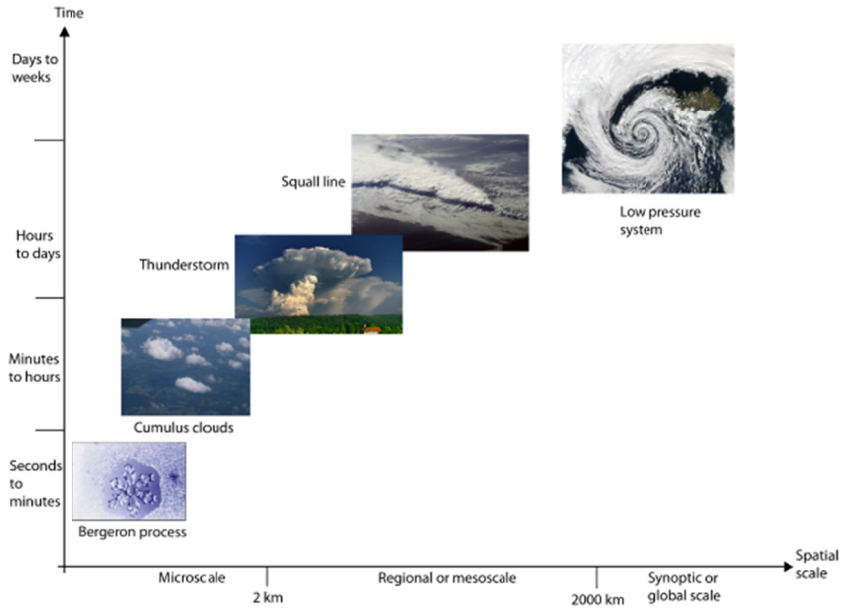

Figure 2.5: Scale definition modified from Orlansky (1975)

It is evident that to studying an event involving the interdisciplinary approach, as the hydro-geomorphology, depending by scale, it is crucial individuate, at any time or spatial scale, the correspondence between the hydrological and geomorphic units or processes. To this aim, Cuomo and Guida (2010) proposed, on the heuristics basis, a comparative table between the orography unit and the atmospheric phenomena.

2.3 TRAINING-TARGET APPROACH

Another aspect of the research is applied the proposed procedures firstly on tested areas to evaluate its reliability and then extended to the region of interest. This method used an articulate approach widely employed in other inter-disciplinary researches (Carrara et al., 1983, 1991, 1992, 1995), and is based on the following three steps (fig. 2.6):

- Analysis on the "Methodological Training areas", which are areas of particular significance to the phenomena of interest;
- Extension of the obtained results to the "target areas", depending on the population of the events that will occur with the same characteristics of that verified in the training areas;
- Operative applications of the results on the "experimental training areas".

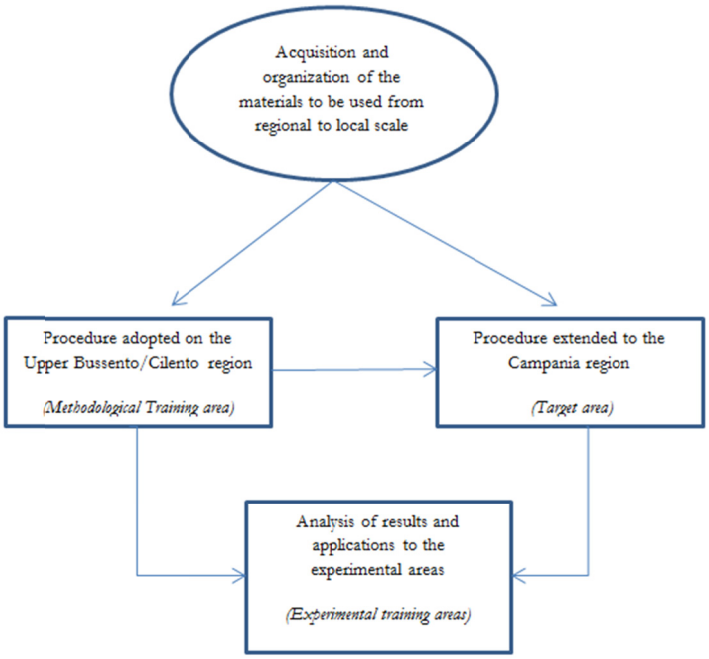

Figure 2.6: Scheme of the methodological approach used in the research

3 TARGET AND TRAINING STUDY AREAS

3.1 INTRODUCTION

Following the above illustrated hierarchical, multiscale and training-target approaches, the above study areas of the research were chosen:

- Campania region as target area of the research, at a regional scale, limited to the drainage basins flowing toward the Tyrrhenian Sea, from the Volturno to Bussento river basins. The data source for this level was the GNDCI-VAPI Campania Report (Rossi and Villani, 1994);

- The Bussento basin river as a methodological training area, at basin scale, located in the National Park of the Cilento and Vallo Diano;
- The Upper Bussento sub-basin river, as experimental training area, at catchment scale, chosen for the availability of hydro-geomorphological and hydrological dataset.

These last were choice because the drainage basins are hydro-geomorphologically complexes, but representative for many drainage basin of the Campania region, comprising the karst features.

3.2 REGIONAL TARGET AREA: CAMPANIA REGION

3.2.1 Physiography and Climate

The physiography of the Campania region landscape is very complex, depending on geology, morpho-structural setting and morpho-genesis.

In general, it is possible to define three sectors: coastal plains (about 25% in area), filled by fluvial and marine clastic successions, marly-clayey, anti-apennine hilly landscape (31%) and carbonate and terrigenous mountain landscape (44%) (fig. 3.1).

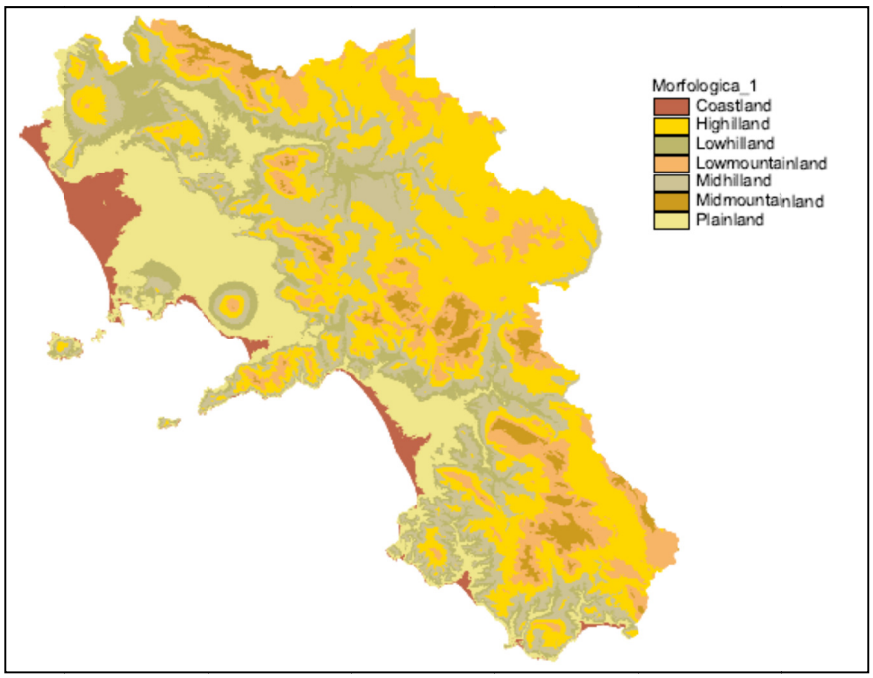

Figure 3.1: Physiography of the Campania region.

Climatically, Blasi et al. (2000) recognize three climatic regions in the Campaia region: mediterranean, temperate and transition (Fig. 3.2).

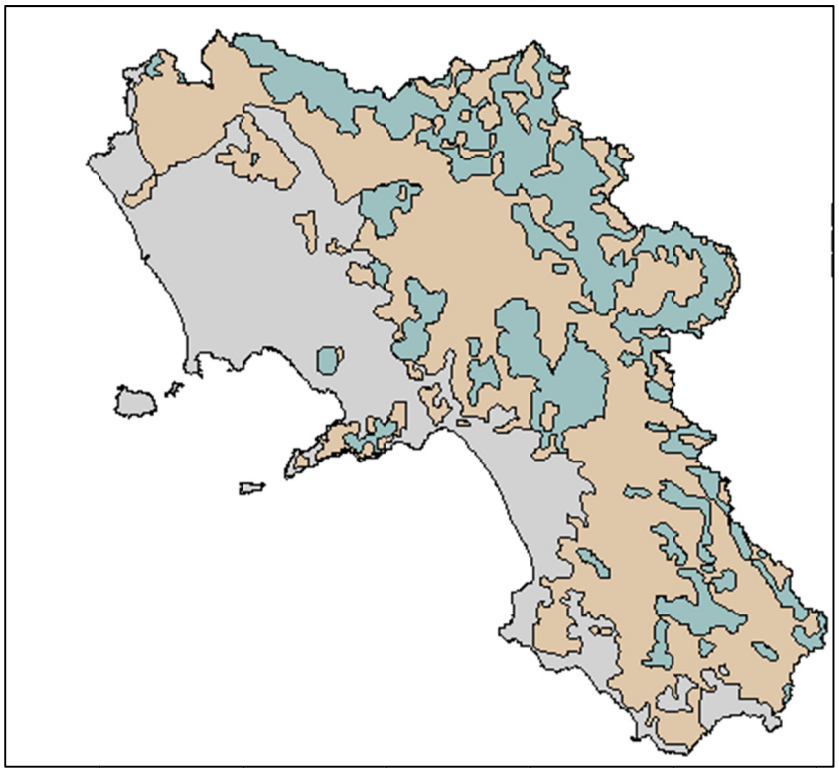

Figure 3.2: Climate regions of the Campania region
Legend: light grey: Mediterranean, beige: transition, grey: temperate

3.2.2 Regional geology and geomorphology

The Campania region corresponds geo-tectonically to the peri-Tyrrhenian sector of the Campano-lucanian orogenetic Arc within the Southern Apennine Chain (Patacca et al., 1992). This one represents a segment of a larger fold-and-thrust belt built up in Central Tethys between late Cretaceous and Pleistocene, as consequences of interaction between the European and African plates, spreading of the Tyrrhenian oceanic basin and anti-clockwise rotation of the orogenic front. Due to long-time and complex litho-genetic history, tectono-sedimentary events and orogenetic displacements, several litho-stratigraphic units, stacked in form of normal overthrusts and/or irregular sequence, can be distinguished (fig. 3.3).

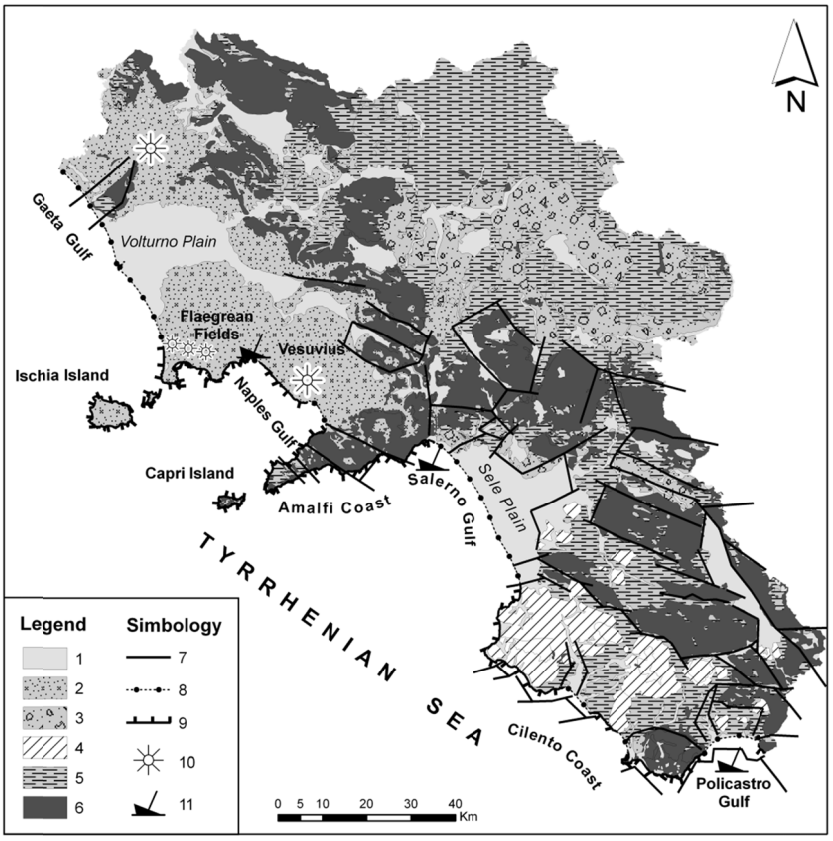

Figure 3.3: Geo-structural setting of the Campania region.

Legend: 1. Quaternary and Post-orogenic clastic Units; 2. Volcanic and volcano-clastic deposits; 3. Neogenic Sinorogenic Units, including continental, transition and marine clastic sediments; 4. Internal Units, with deep basin marly, varicoloured clay at the base, passing above in calcarenites, calcilutites, often cherty, argillites, sandstones and rare conglomerate; 5. The External Units, slope, reef and back-reef of carbonate platform sediments ; 6. Lagonegro Units, with cherty limestones at the base and marly clay at the top, deposited in a deep, marine basin; 7. Apulia Units , reef and back-reef carbonate of Apulia Foreland.

The Internal Units, Mesozoic to Tertiary aged, (Bonardi et al., 1988; Cammarosano et al., 2000) are made up at the base prevalently by marly, varicoloured clay, in oceanic plain sedimentary facies, passing above to calcarenites, calcilutites, often cherty, argillites, sandstones and rare conglomerate deposited in a distal turbidite basin. At present, the main outcrops are located in the hilly area exclusively in Cilento. The External Units are constituted mainly by neritic, carbonate sediments of Mesozoic and Tertiary age which show sedimentary environments going from the shallow water carbonates with back-reef facies to slope and deep water

carbonates (D'Argenio et al., 1975; Mostardini and Merlini, 1986). These units form the main mountainous massifs of Campania region located both inland and coastal areas; they constitute the bedrock of major karst massifs in the Matese M.nts, Camposauro-Taburno M.nts, Avella-Partenio M.nts, Sorrento Peninsula, Picentini M.nts, as well as in the Cilento. The Lagonegro Units are made up of cherty limestones at the base and marly clayey at the top, likely deposited in a deep marine basin (D'Argenio et al., 1975; Mostardini and Merlini, 1986), outcropping exclusively along the axis of Apennine Chain. The Apulia Units represent the remnants of Apulia Foreland, in progressive lowering under the Foretrough and Chain by deep normal and listric faults. In disconformity, there are the Neogenic Sinorogenic Units, represented by several terrigenous formations and units referred to Miocene-Pliocene age, lying on previous units and in the Bradanic Forethrough. They are mostly in turbidite facies, from wild-flysch to submarine fan sedimentary characters (Patacca et al., 1992). For instance, Cilento Group (Amore et al., 1988; Cammarosano et al., 2000) is one of these units, which is the most widespread unit in the homonymous area and along the corresponding coast; a minor unit outcrops in Sorrento Peninsula. Surrounding the Somma-Vesuvius volcanic complex and Phlaegrean Phields, near Naples city and Ischia and Procida volcanic islands, large surfaces are covered by volcanic formations and volcano-clastic deposits, Pleistocene in age (De Vivo et al., 2001). They are known as the peri-Tyrrhenian volcanism due to the deepest crossing normal faults of the Campania Plain Graben (Florio et al., 1999). The Quaternary Post-orogenic Units include all the continental, transition and marine clastic sediments, deposited after the final emersion of Apennine Chain, from Late Pliocene to Early Pleistocene and Holocene. They are represented by aeolian, fluvial, piedmont, lacustrine and travertine deposits along the river valleys and coastal plains. Such units can show intercalation of the products of Vesuvian and Phlaegrean volcanic activity, previously considered. The present day structural setting results in a duplex, NE-vergent , multiple thrusting deep structure (Patacca et al., 1992) of the above mentioned units built-up from Middle Miocene to Middle Pleistocene age. Since then, only trans-tensive and relative, vertical uplift occurs, resulting in graben-horst structures, along faults in Apennine (NW-SE) and anti-Apennine (NE-SW) directions (D'Argenio et al., 1973). The above geological and tectonic setting, induces a prevalent morpho-structural control of the Campania landscape, with steep

hillslopes resulting from retreat and replacement evolution model of the previous fault scarps and fault-line scarps, alternating to hillscape and terraced plains and shorelines. Based on tectonical and lithological characters several Lithological Systems can be recognized (fig. 3.4).

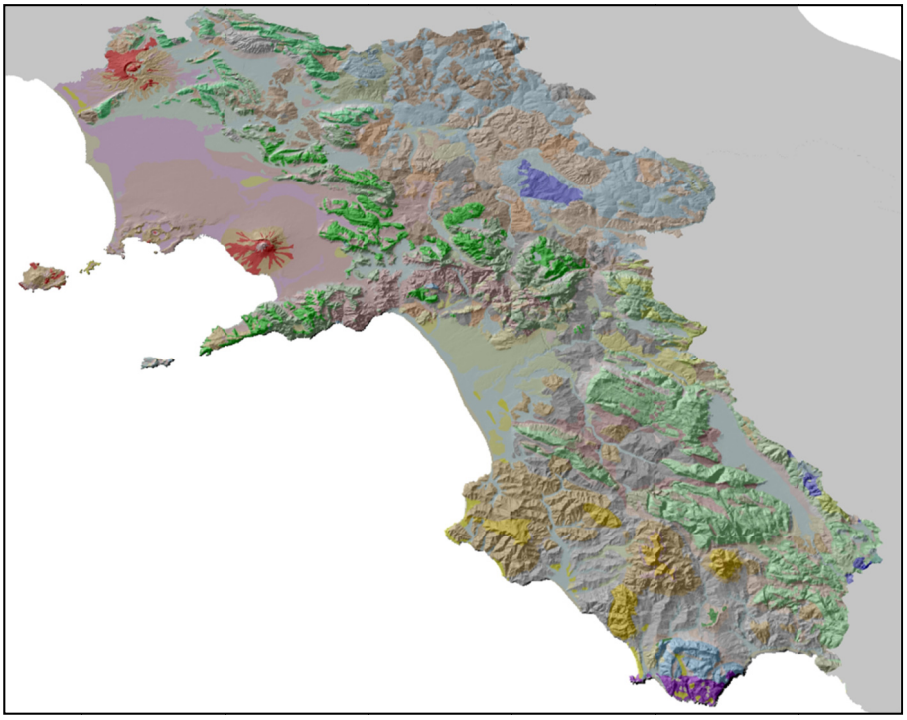

Figure 3.4: Lithological Systems of the Campania region.

Legend: Green: Limestone System; Brown: Terrigenous System; Blue: Dolomite-marly System; Pink: Marly-clayey System; Red: Volcanic System; Gray: Clastic System.

Geomorphology of the Campania region is heavily conditioned by the above illustrated morpho-structural arrangement and lithological nature of the bedrock. Combining basic landforms and elevation, the Morphological Systems can be defined and mapped (tab.3.1 and fig.3.5).

Table 3.1: Matrix of the Morphological System of the Campania region.

LANDFORM / ELEVATION	Canyon incised stream 1	Midslope drainage valley 2	Upland drainage headwater 3	U-shaped valley (Piedmont) 4	Plain (Terrace) 5	Open slope Piedmont 6	Upper slope Mesas 7	Local ridge Hillvalley 8	Midslope ridge Hillvalley 9	Montaintop Highridge 10
Coastland 1	Coastal Canyon 1	Coastal Valley 2	Coastal Valley 2	Coastal Valley (?) 2	Coastal beach 3	Coastal cliff 4	Coastal Terrace 5	Headland 6	Headland 6	Headland 6
Plainland 2	Plain Canyon 7	Plain Valley 8	Plain Valley 8	Plain Valley 8	Coastal Plain 9	Plain Scarp 10	Plain Terrace 11	Hill Plain 12	Hill Plain 12	Plain Ridge 13
Lowhillland 3	Hill Canyon 14	Hill Valley 15	Hill Valley 15	Hill Valley 15	Flood Plain 16	Hill Slope 17	Hill Terrace 18	Hill Ridge 19	Hill Ridge 19	Hill Ridge 19
Midhilland 4	Hill Canyon 14	Hill Valley 15	Hill Valley 15	Hill Valley 15	Flood Plain 16	Hill Slope 17	Hill Terrace 18	Hill Ridge 19	Hill Ridge 19	Hill Ridge 19
Highilland 5	Hill Canyon 14	Hill Valley 15	Hill Valley 15	Hill Valley 15	Flood Plain 16	Hill Slope 17	Hill Terrace 18	Hill Ridge 19	Hill Ridge 19	Hill Ridge 19
Lowmountainland 6	Mountain Canyon 20	Mountain Valley 21	Mountain Valley 21	Mountain Valley 21	Mountain Plain 22	Mountain Slope 23	Mountain Terrace 24	Mountain Ridge 25	Mountain Ridge 25	Mountain Ridge 25
Midmountainland 7	Mountain Canyon 20	Mountain Valley 21	Mountain Valley 21	Mountain Valley 21	Mountain Plain 22	Mountain Slope 23	Mountain Terrace 24	Mountain Ridge 25	Mountain Ridge 25	Mountain Ridge 25
Highmountainland 8	Mountain Canyon 20	Mountain Valley 21	Mountain Valley 21	Mountain Valley 21	Mountain Plain 22	Mountain Slope 23	Mountain Terrace 24	Mountain Ridge 25	Mountain Ridge 25	Mountain Ridge 25

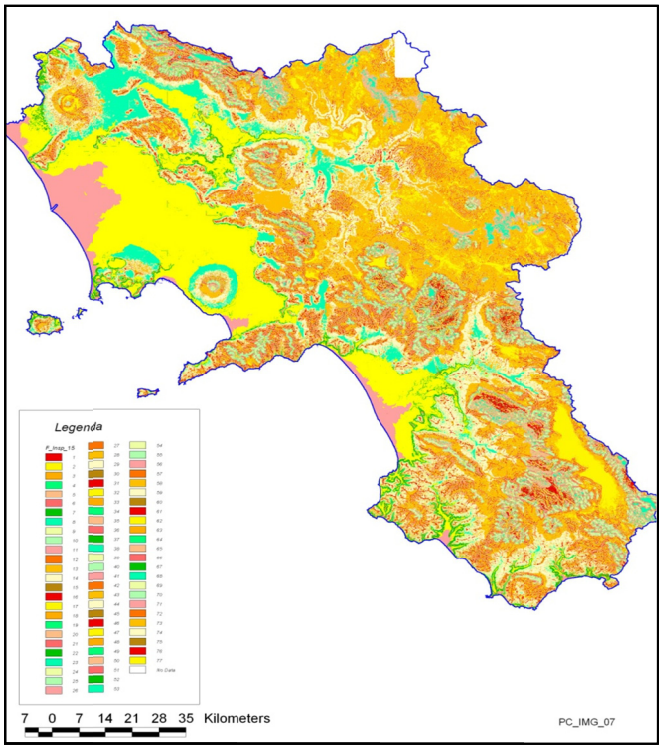

Figure 3.5: Morphological System of the Campania. For legend, see tab. 3.1.

3.2.3 Hydrography, Hydrology and Hydrogeology

The hydrography of the Campania region is influenced, at regional scale, by the morpho-structural setting (grabens, fault and overthrust systems) and by relief and lithology at basin scale. In the karst carbonate landscape (Matese, Taburno, Avella and Alburno–Cervati) the drainage is coarse and poor developed due to highly permeability of the bedrock and blind valleys. The drainage, located in marly-clayey landscapes, have dendritic pattern with prevalent surficial runoff (figure 3.6).

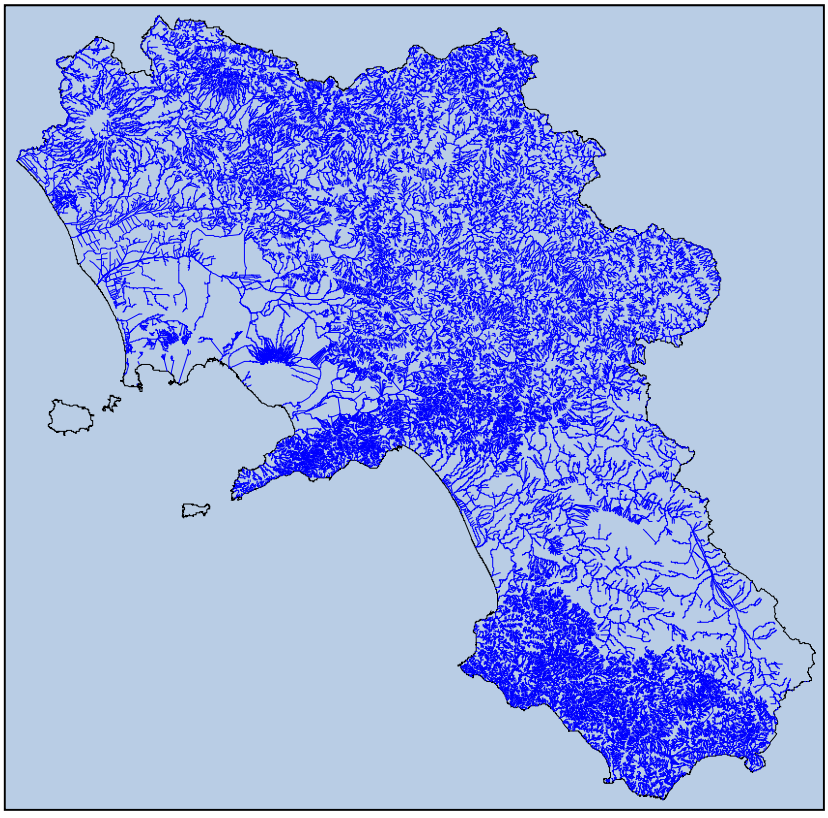

Figure 3.6: Hydrography Map of the Campania region

The main river and drainage network is the Volturno river basin, about 170 km long, occupying the 40% of the regional area, with two sub-basin: the Upper Volturno and the Calore Irpino. The second drainage system of Campania is the Sele river, 65 Km long and another ones are: Sarno, Tusciano, Alento, Bussento, Mingardo, Picentino, Lambro and Regi Lagni channel.
Hydrologically, the Campania region is drained by 37 drainage basins and sectors (figure 3.7 and table 3.2).

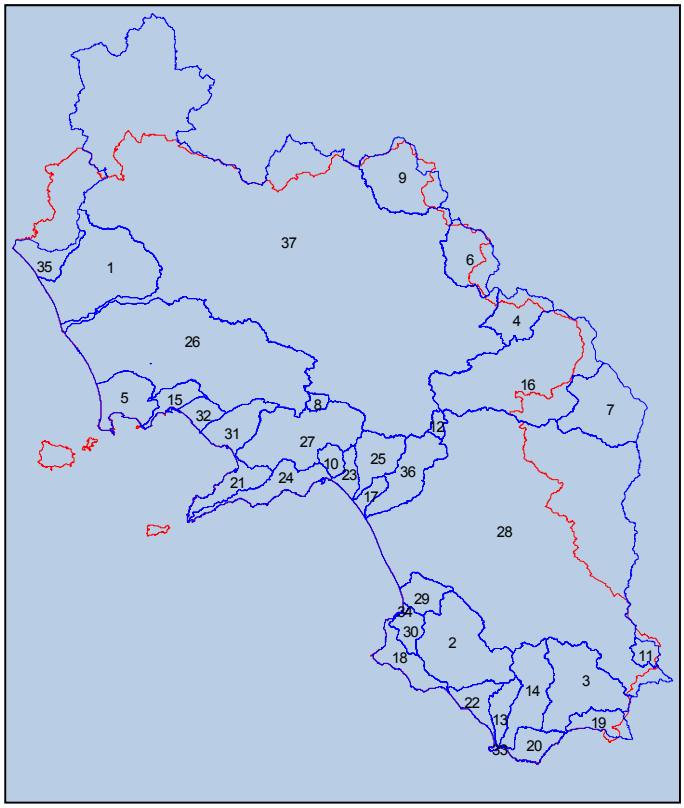

Figure 3.7: Drainage basins and sector in the Campania region.

Table 3.2: List of the drainage basins and sectors in the Campania region.

Code	Basin or Sector Name	Area (Km^2)	Perimeter (m)
1	Agnena-Savone	506	138
2	Alento	408	141
3	Bussento	342	143
4	Calaggio	152	95
5	Campi Flegrei	170	78
6	Cervaro	196	91
7	Fiumara d'Atella	313	104
8	Forino	22	28
9	Fortore	288	100
10	Irno	44	39
11	Spigno - Magorno - Cessuta Lakes	42	38
12	Laceno Lake	23	30
13	Lambro	76	64
14	Mingardo	223	117
15	Naples and Sebeto	72	72
16	Ofanto	790	208
17	Picentino to Tusciano Basins	39	42
18	Agropoli to Alento Basins	123	99
19	Bussento to Mezzanotte Basins	85	69
20	Mingardo to Bussento Basins	88	65
21	Sarno to Punta Campanella Basins	110	98
22	Alento to Lambro Basins	92	85
23	Irno to Picentino Basins	52	49
24	Punta Campanella to Irno Basins	153	139
25	Picentino	145	79
26	Regi Lagni	1231	256
27	Sarno	395	146
28	Sele	3357	452
29	Solofrone	93	58
30	Testene and minor creek from Solofrone to Agropoli	66	54
31	Vesuvian creek from T. del Greco to Sarno	140	74
32	Vesuvian creek from Sebeto to Torre del Greco	61	39
33	Lambro to Mingardo Basins	0,154	2
34	Solofrone to Testene Basins	3,1	10
35	Minor creek from Garigliano to Torre S.Limato	97,3	70
36	Tusciano	200	107
37	Volturno	5582	810

The hydrogeological setting of the Campania, at regional level, is shown in the figure 3.8.

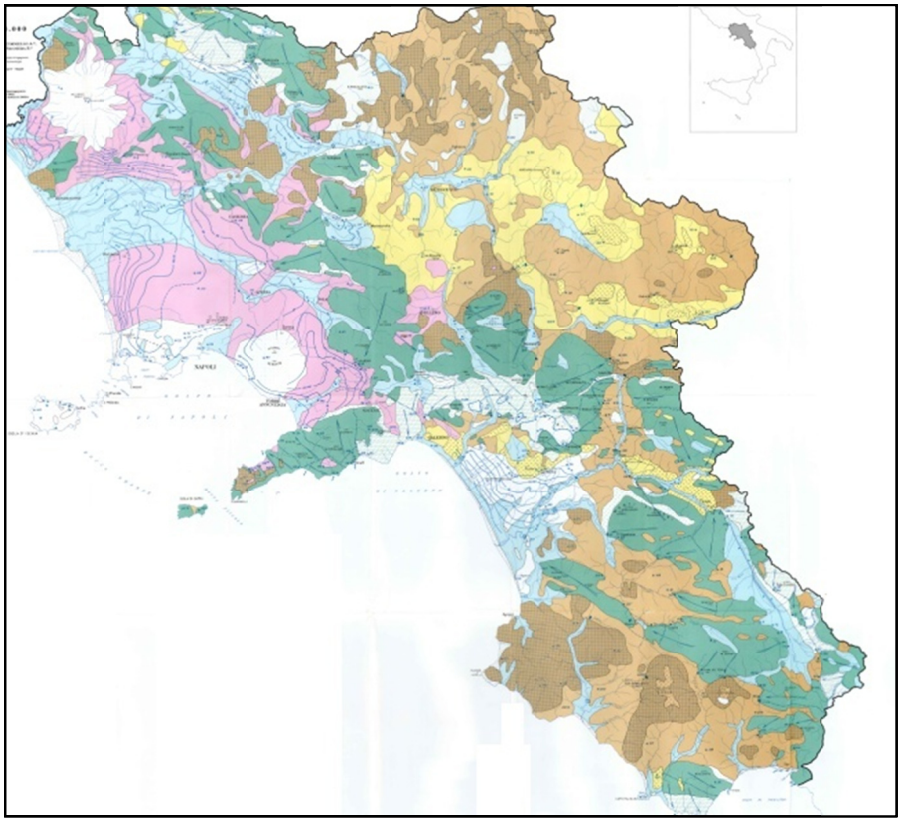

Figure 3.8: Hydrological map of the Campania region.

Legend: green: carbonate karst aquifer; brown: terrigemous aquifers; yellow: clastic aquifer; light blue: alluvial aquifer; pink: volcanic aquifer; lines: iso-piezometric

The above drainage basins and aquifers are included in the National, Interregional and Regional Basin Authorities (figure 3.9).

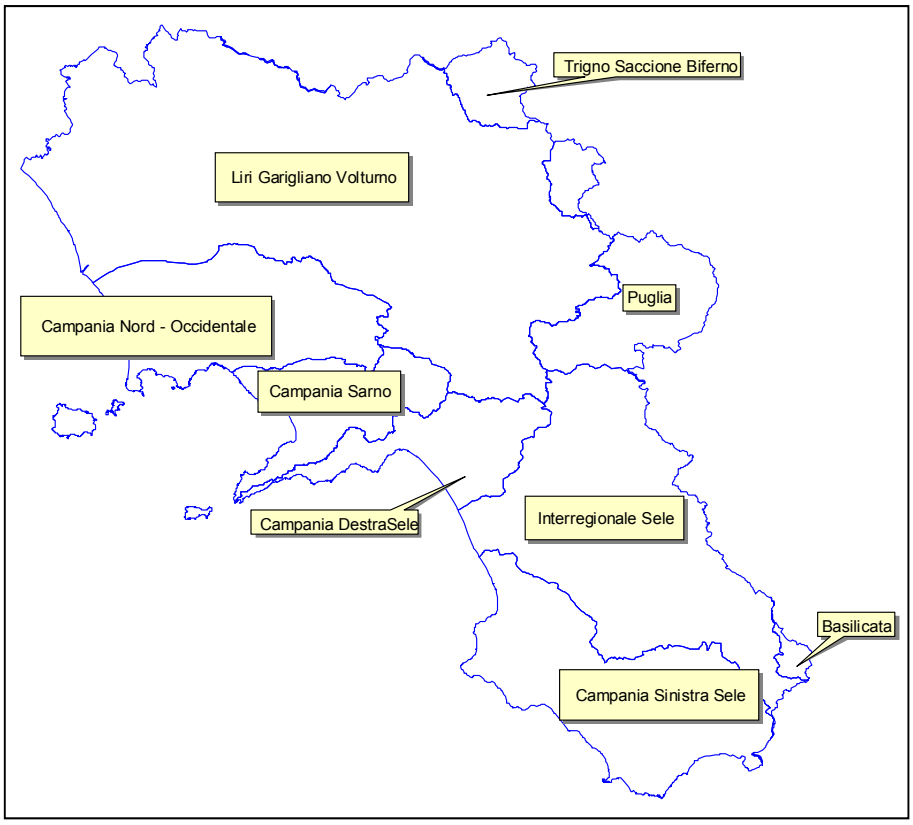

Figure 3.9: Basin Authorities in the Campania region.

3.3 METHODOLOGICAL TRAINING AREA AT BASIN LEVEL: BUSSENTO RIVER BASIN

3.3.1 Location

The Bussento river drainage basin is one of the major and complex drainage river system of the SE of the Campania region (Southern Italy), located in the Cilento and Vallo di Diano National Park, recently designed in the European and Global Geopark Network (figure 3.10).

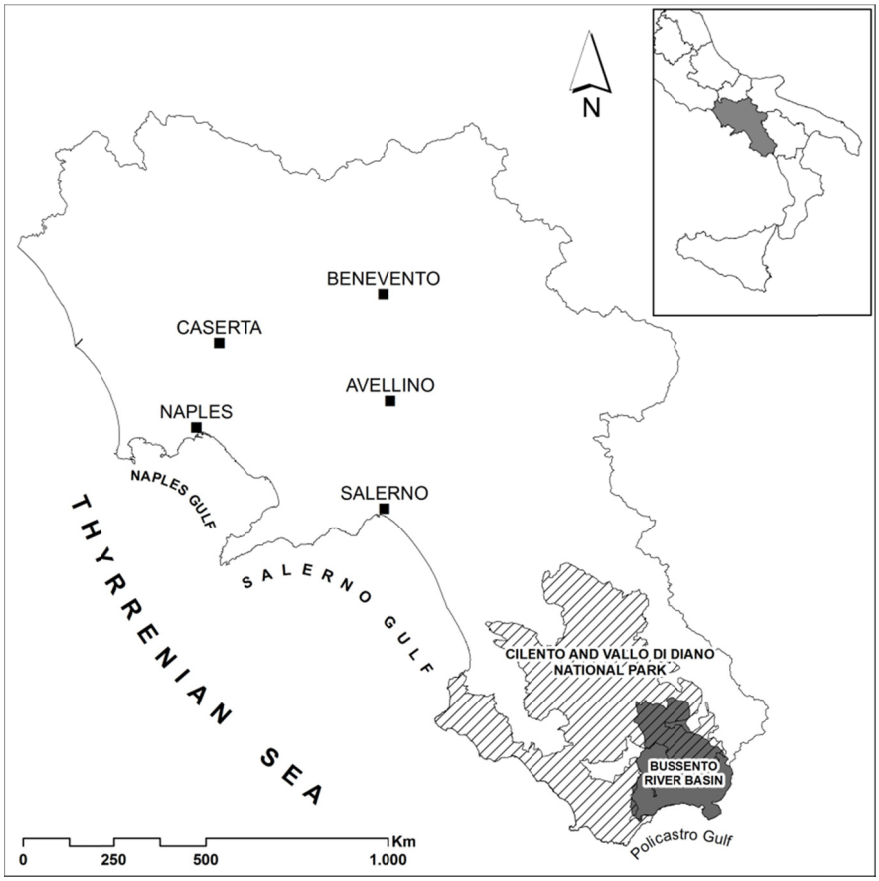

Figure 3.10: Location of the Bussento river basin.

3.3.2 Basin Hydrogeomorphological setting

The objective "complex" is due to the highly hydro-geomorphological conditioning induced by the karst landforms and processes. In fact, it is well known to geomorphologists and hydrogeologists for its widely and deeply karst features, like summit karst highlands with dolines and poljes, lowlands with blind valleys, streams disappearing into sinkholes, cave systems, and karst-induced groundwater aquifers and gravitational karst-induced depressions (figure 3.11).

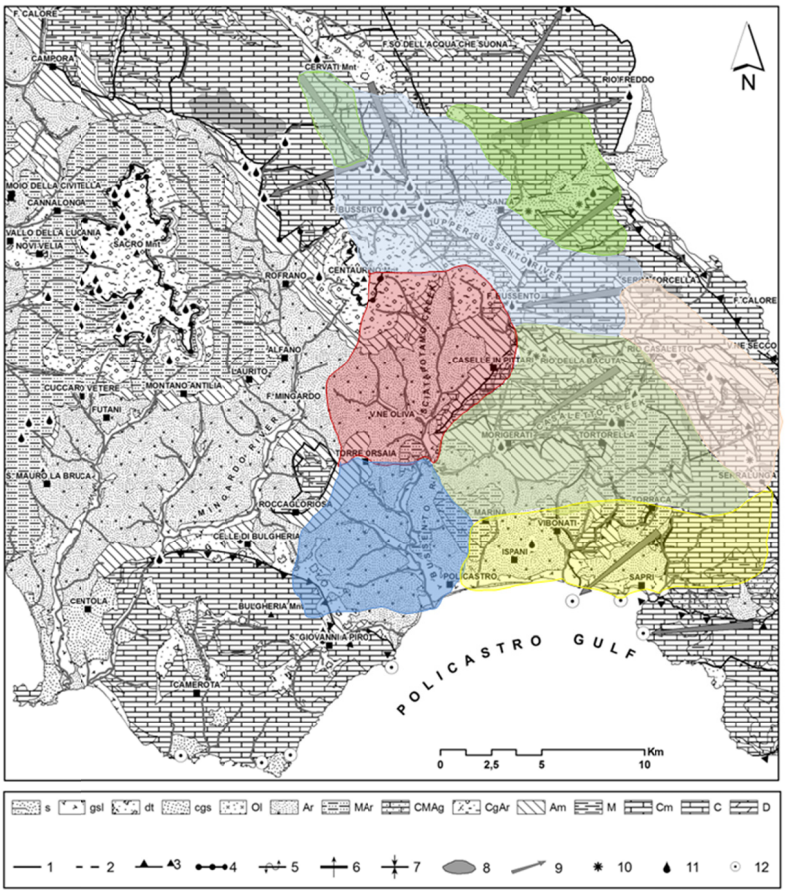

Figure 3.11: Hydro-geomorphological map of Bussento river and surrounding areas.

Legend: Hydrogeological Complex: s)Sand and gravelly sand; gsl) Fluvial sandy gravel; dt) Slope debris; cgs) Sandy conglomerate; Ol) clayey Olistostrome; Ar) Sandstone and marls; MAr) Marl and Sandstone; CMAg) Marl and Conglomerate; CGAr) Conglomerate and Sandstone; Am) marly shale;M) Silty marl "fogliarina"; Cm) Marly limestone; C) Limestone; D) Dolostone. Symbology:1) Fault; 2) Hypotisized fault; 3) Overthrust; 4) Permeability limit; 5) Groundwater exchange; 6) Losing river; 7) Gaining river); 8)Karst summit; 9) Probable groundflow direction;10) Sinkhole; 11) Main spring; 12) Coastal and submarine spring. Sub-basins: light blue: Upper Bussento; green on light blue: Endorheic Upper Bussento basins; pink, Eastern Bussento; green: Middle Bussento River-Kars System; light brown: Western Bussento; blue, Lower Bussento.

Therefore, the Bussento river basin can be considered a "prototypal" hydro-geomorphological system, which cannot be fully understood without considering break down, significant components of the hydrological and hydrogeological basin, variously interacting in the same

areas. In this sense, the whole basin can be sub-divided in the following sub-basins (colored areas in the figure 3.11):

- **Upper Bussento Sub-basin**, in light blue in the figure 3.11, with two inter-connected endorheic basins (Vallivona and Sanza) and Karst Highlands, in light green transparent on light blue in the fig. 3.11,
- **Eastern Bussento Sub-basin**, with terminal outlet to Capello Spring Oasis, near Casaletto Spartano village and small endorheic basins (Affunnaturo) and large Karst Highlands;
- **Middle Bussento Sub-basin**, heavily conditioned by the **Middle Bussento Karst System**, illustrated in the following paragraph;
- **Western Bussento Sub-basin**, in light brown on figure 3.11, greatly corresponding to the Sciarapotamo creek basin, conditioned by summit conglomerate aquifers and marly-clayey succession in lower sector;
- **Lower Bussento Sub-basin**, the blue area, on figure 3.11, includes the catchments from the Bulgheria and Roccagloriosa carbonate secondary aquifer and alluvial and coastal clastic valley fillings;
- **Bussento-Policastro gulf system**, a complex and still unknow groundwater system with interconnections aquifer and huge Submarine Groundwater Discharges.

3.3.3 Climate and Geomorphic setting

The study area is characterized by a typical Mediterranean climatic regime, tending to the temperate one from the coast to the mountain reliefs. The 50-years (1921-1977) mean annual rainfall and mean annual temperature for historical meteorological stations of Morigerati, Caselle in Pittari, Casaletto Spartano and Sanza, located within the Bussento River watershed, are shown in table 3.3.

Table 3.3: Climate outline of the Bussento river basin, mod. from Guida et al. (1980).

Station	Elevation (m a.s.l.)	Mean annual Precipitation (mm)	Mean annual Temperature (°C)	Mean annual Potential Evapotranspiration (mm)	Effective Precipitation (mm)
Morigerati	300	1439	15.9	820	619
Caselle in Pittari	315	1657	15.3	788	869
Casaletto Spartano	310	1811	15.3	789	1022
Sanza	569	1596	12.2	668	928

Bussento river basin is one of 36 VAPI Training Basins, considered in three outlet sections: Bussento at Caselle in Pittari, Bussento at Sicilì and Bussento at the mouth.
The geomorphic characteristics of the Bussento river are shown in the tables 3.4, 3.5 and 3.6 and figure 3.12 from VAPI Report (Rossi and Villani, 1994).

Table 3.4: Morphometric characteristics of the basins (from Rossi and Villani, 1994)

Bacino	Area km^2	D_d km/km^2	N_f 1/km
Bussento a Caselle in Pittari	113	1.501	2.94
Bussento a Sicilì	228	2.624	5.68
Bussento alla foce	352	2.858	5.95

Table 3.5: Altimetric features of the basins (from Rossi and Villani, 1994)

Bacino	zero idr. m s.l.m.m.	H_{max} m s.l.m.m.	H_m m s.l.m.m.	dist. foce km
Bussento a Caselle in Pittari	350.00	1899	850	21
Bussento a Sicilì	60.00	1899	750	13
Bussento alla foce	-	1899	604	-

Table 3.6: Morphometric features of the basins (from Rossi and Villani, 1994)

Bacino	Ordine w	Rami N(w)	$L_{tot}(w)$ km	$L_{med}(w)$ km	$R_l(w)$ (-)	$R_b(w)$ (-)
	1	985	327,72	0,37		
Bussento a Sicilì	2	243	134,54	0,55	1,466	4,053
	3	50	61,64	1,23	2,226	4,860
	4	13	28,24	2,17	1,762	3,846
	5	3	44,89	14,96	6,889	4,333
	6	1	1,25	1,25	0,083	3,000
					R_L=1,599	**R_B=4,054**
	1	257	91,87	0,35		
Bussento a Caselle in Pittari	2	60	36,02	0,60	1,681	4,283
	3	12	29,94	2,49	4,158	5,000
	4	2	4,07	2,03	0,816	6,000
	5	1	7,74	7,74	3,803	2,000
					R_L=2,090	**R_B=4,263**
	1	1578	560,62	0,35		
Bussento alla foce	2	398	220,63	0,55	1,561	3,965
	3	89	108,91	1,22	2,209	4,472
	4	23	46,33	2,01	1,645	3,870
	5	5	51,28	10,25	5,092	4,600
	6	2	7,63	3,81	0,372	2,500
					R_L=1,783	**R_B=3,560**

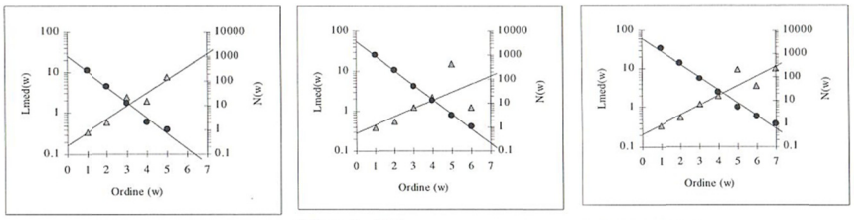

1 - Bussento a Caselle in Pittari

2 -Bussento a Sicilì

3 - Bussento alla foce

Figure 3.12: The quantitative geomorphic analysis (from Rossi and Villani, 1994)

3.3.4 Hydrography and Karst-conditioning Hydrology

The main stream of the Bussento river originates from the upland springs of M.nt Cervati (1.888 m asl), one of the highest mountain ridge in the Southern Apennines, flowing downstream, partly in wide alluvial valleys (i.e., Sanza valley) and, partly, in steep gorges and canyons, where a number of springs delivering fresh water from karst aquifers into the streambed and banks, increasing progressively the river discharge. The upper right area is characterized by marly-arenaceous rocks outcrops (Marchese Hills), while the left upper area is characterized by limestone sequences (M.nt Rotondo and Serra Forcella highlands). More downstream, near Caselle in Pittari village, the Bussento river and adjacent neighbours minor creeks flow, respectivelys into "La Rupe " (Bussento Upper Cave), Orsivacca and Bacuta-Caravo sinkholes, channelling the entire fluvial surface streamflow drained from the upper Bussento basin into the a hypo-karst cave system and re-emerging about four kilometers downstream, in the neighbourhood of the Morigerati town, from the resurgence, called "Bussento Lower Cave". Downstream the resurgence, the Bussento river joints with Bussentino creek, originating from the eastern sectors of the drainage basin and, flows along deep canyons and deep gorges, carved into the meso-cainozoic litho-stratigraphic limestone sequences, prevalently constitute of limestone and marly limestone, referred to Alburno-Cervati Unit (D'Argenio et al., 1973). In the western and southern sectors of the basin (Sciarapotamo creek sub-basin), marly-clayey successions of the Liguride and "affinità Sicilide" Units (Cammarosano et al., 2000) dominate the hilly landscape, whereas they underlie the arenaceous-conglomerate sequences at the Mount Centaurino M.nt (Bonardi et al.,1988). Downstream the confluence with Sciarapotamo creek, the Bussento river flows, as a meander stream, in a terraced floodplain and, finally in the Policastro coastal plain.

Surface and groundwater circulation in the basin results very complex. Groundwater inflows from outside of the hydrological watershed and groundwater outflows towards surrounding drainage systems, frequently, occur. This complexity is due to the occurrence of soils and rocks with highly different hydraulic permeabilities and to the highly hydrogeological conditioning induced by the karst features. Bussento river regime is also affected by a very complex hydropower and drinking water system, which retains and diverts the river discharge within dams,

an artificial lake and weirs. This drainage sector refers to the Middle Bussento river Karst System (MBKS) (figure 3.13).

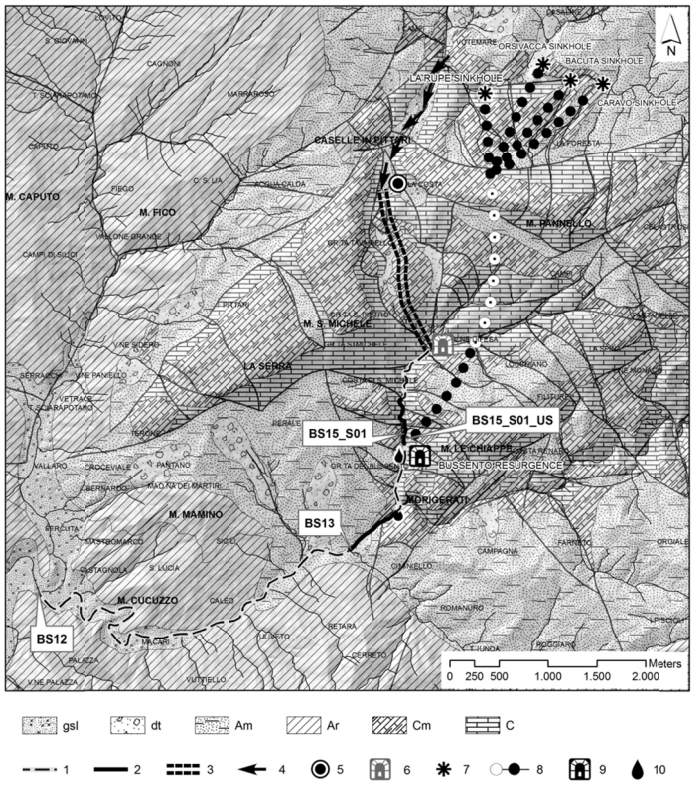

Figure 3.13: Detailed hydro-geomorphological map of the MBKS.

Legend: Hydrogeological complexes: gsl) Fluvial sandy gravel; dt) Slope debris; Am) marly shale; Ar) Sandstone and marls; Cm) Marly limestone; c) Limestone. Symbology: 1) Location of fluvial segment of interest; 2) Location of the fluvial reaches of interest; 3) Abandoned subterranean flowpath of the Palaeo-Bussento River ; 4) Abandonned surface flowpath of the Palaeo-Bussento river; 5) Abandoned sinkhole of the Palaeo-Bussento river; 6) Abandoned resurgence of the Palaeo-Bussento river ; 7) Upper Bussento active sinkhole; 8) Explored (grey circle) and no-explored (withe circle) subterranean flowpath of present-day Bussento river; 9) Active resurgence of the Bussento river; 10) Main karst spring.

This karst system develops within the carbonate ridge of the S. Michele-M.te Pannello-Zepparra M.ts, between the four sinkholes east Caselle in Pittari (SA) and the final fluvial reach of the gorge SE Sicilì village (Sicilì bridge), up to the Bussento hydropower central, just downstream the

confluence with Sciarapotamo creek. The Figure 3.13 reports the Hydro-geomorphological map of the area, with the hydrogeological complexes and main springs, the hypothesized palaeo- and present-day sink-cave-resurgence system, and the river segments and reference reaches of interest. The Middle Bussento segment and Oasis WWF reach are located in the Morigerati gorge, a typical epigenetic valley (Lambiase and Ruggiero 1980, D'Elia et al., 1987), along which groundwater influxes from both epikarts spring, conduit spring (Old Mill Spring) and cave spring (Bussento Resurgence) supply a perennial streamflow in a step-and-pool river type (Montgomery and Buffington, 1998).

The Middle-lower segment and the Sicilì bridge reach are located downstream the previous from the end of the Morigerati gorge to Sciarapotamo creek confluence, along which three reach can be recognized from downvalley: the downstream, in correspondence of the Bussento Hydropower Central, results a typical riffle-pool river (Montgomery and Buffington, 1998), as a entrenched meander in fluvial and strath terraces, the second upstream reach, Bottelli House reach, results a riffle-pool river along low order alluvial terraces and finally the third, the above cited Sicilì Bridge reach, a plane bed river slightly entrenched in alluvial terrace.

The hydro-geomorphological setting, above briefly illustrated, induces a very complex surface- groundwater interaction and exchanges. Therefore, groundwater inflows from outside of the hydrological watershed and groundwater outflows towards surrounding drainage systems, frequently occur, influencing the basin water budget and streamflow regime. The Bussento river regime is also affected by a very complex hydropower plant system, which retains and diverts the river discharge in the Sabetta reservoir and the Casaletto weirs, respectively, from the upper Bussento river and the Bussentino creek reaches segment to the Lower Bussento fluvial segment.

In order to provide a physical scheme of the complex recharge, storage and routing system of the Middle Bussento karst area, a preliminary, conceptual model has been built-up, accounting for an interconnected sequence of geologic substrates, structural discontinuities, type and rate in permeability distribution, recharge areas and discharge points, that collectively provide a physical scheme of the recharge system, the storage system and the routing system. With reference Guida et al. (2005), the conceptual hydro-geomorphological model of the MBKS contains

three nested hydrological domains i) a hydrogeologic domain; ii) a hydro-geomorphological domain and iii) an aquifer-river domain (figure 3.14). The hydrogeological domain represents the 3-D structure of aquifer, aquitard and aquiclude, conditioning the groundwater circulation and storage, vertically differentiated in the classic subdivision of karst hydro-structures (Bakalowicz, 1995): epikarst, vadose, percolation and saturated or phreatic zones (Ford and Williams, 1989). The last one is hydro-dynamically subdivided in cave, conduit and fracture routing system (White, 1969).

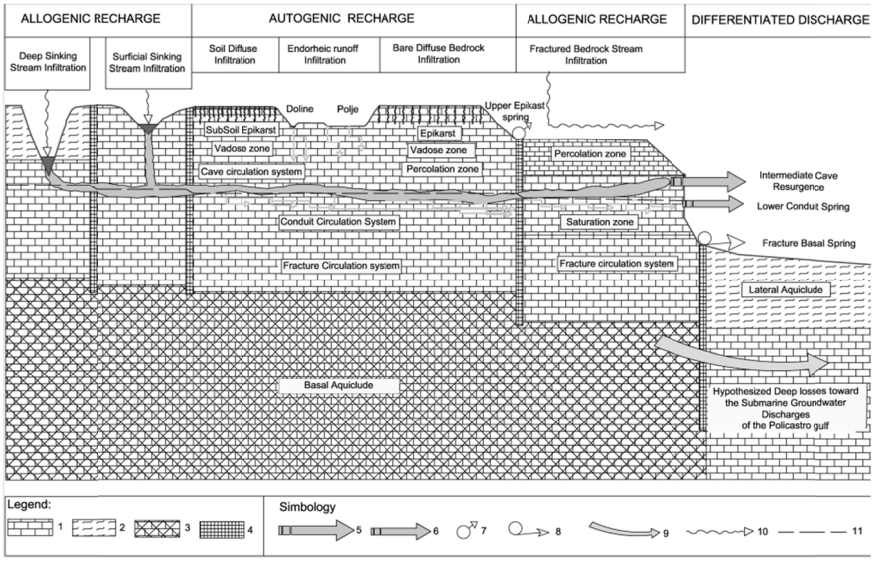

Figure 3.14: Conceptual hydro-geomorphological model of the Middle Bussento river Karst System (MBKS).

Legend: 1) Limestone aquifer; 2) Marly shale aquiclude; 3) Basal highly fractured limestone aquitard; Lateral fractured fault-induced aquitard; 5) Intermediate cave resurgence; 6) lower conduit spring; 7) Upper epikarst spring; 8) Basal fracture spring; 9) Probable groundwater losses toward marine spring; 10) Infiltration of streamwater along the river bed; 11) Water table.

The hydro-geomorphological domain comprises fluvio-karst landforms and processes, conditioning groundwater recharge ("*karst input control*", sensu Ford and Williams, 1989), by means of the infiltration and runoff processes, including: a) allogenic recharge from surrounding impervious drainage basins into deep and shallow sinking stream infiltration points, and fractured bedrock stream infiltration; b) autogenic recharge, including sub-soil and bare diffuse epikarst infiltration, endorheic runoff infiltration in dolines and poljes; c) groundwater discharge ("*karst ouput*

control", sensu Ford andWilliams, 1989), differentiated in the groundwater-river interactions within the aquifer-river domain. This last comprises the complex interactions between the streambed-springs system, which generally results in a downstream river discharge increasing, occurring generally in typical bedrock streams, flowing in gorge and canyons carved in enlarged fractured limestone sequences. Following the routing karst system, the springs inflowing into streamlow can be characterized in: i) upper epikarst springs, ii) intermediate cave resurgence springs, iii) lower conduit springs and iv) basal fracture springs. Figure 3.14 highlights, also, the hypothesized deep losses toward the Submarine Groundwater Discharges (SGD), emerging in the Policastro gulf. Each of the mentioned components corresponds, in the modelling conceptualization of the scheme, to a linear storage, releasing streamflow as a function of water storage and characteristic delay time. The characteristic time indicates that there is a delay between the recharge to the system and the output from the system itself, and this delay is greater for deeper aquifers. The number of storages, each representing, thus, a different process, contributes to the total streamflow through a recharge coefficient, that is a measure of the magnitude of the single storage. The application of a conceptual model, such as the one briefly described, requires the calibration of the model parameters, and in particular of the characteristic delay time and of the recharge coefficient of each single storage. In the complex catchments, such as the Bussento River System, characterized by a large impact of karstic phenomena, raw streamflow data are not sufficient to the quantification of the contribute and magnitude of the single storage, runoff production and flood routing, therefore, are not sufficient to calibrate the model.

To overcoming this issue, field activities and interdisciplinary researches were started by the Salerno University Hydro-workgroup to (see chapter 4): i) Integrate Hydro-geomorphological Minitoring System; ii) improve the Semi-distributed hydrological model and iii) implement natural radioactive tracer techniques.

Such researches were carried out both at basin and sub-basin scale, as will illustrated in the following chapter.

3.4 SPERIMENTAL TRAINING AREA AT CATCHMENT LEVEL: UPPER BUSSENTO RIVER SUB-BASIN

3.4.1 Location

The Upper Bussento Sub-basin and included catchments are located upstream the La Rupe Sinkhole and Sabetta Reservoir (figure 3.14).

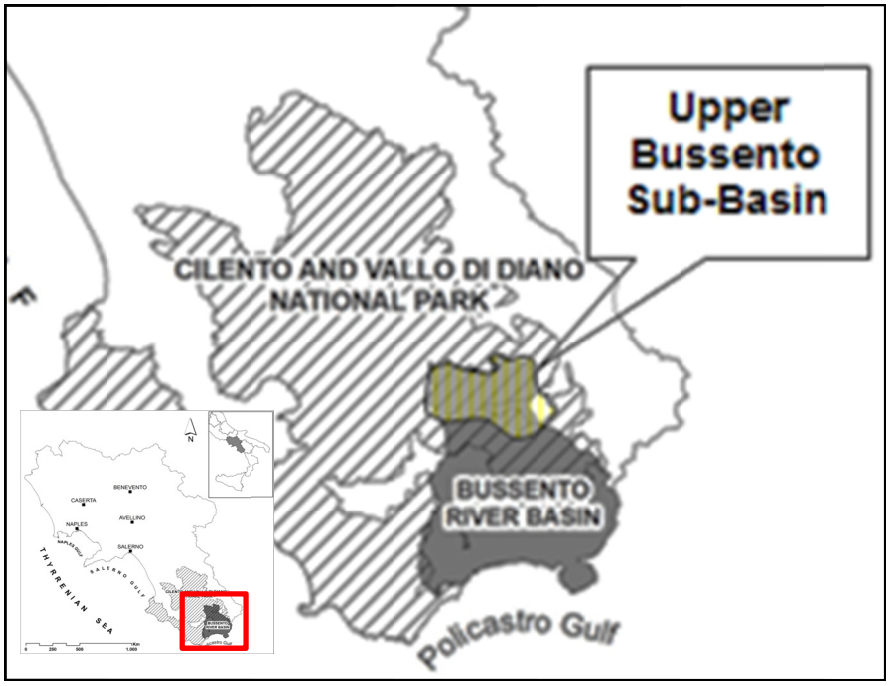

Figure 3.15: Location of Upper Bussento Sub-basin in the Bussento river basin.

3.4.2 Hydro-geomorphological setting

The mainstream originates from south-western upland valley of the Mount Cervati (Vallivona and Mezzana valleys), where many, low discharge springs from shallow aquifer in debris cover on marly-clayey bedrock originate ephemeral creek flowing into the Vallivona Affunnaturo sinkhole. From the Varco la Peta spring-resurgence, the Inferno creek flows southward, carving steep gorges in form of a typical bedrock stream, with cascade and rapids, where further springs (Montemezzano spring), along the streambed, increasing progressively the river discharge, as well as along the piedmont (Sanza Fistole spring groups). The true Bussento river begins downstream the junction of the above cited Inferno creek and the Persico creek. This last flows at the bottom of an asymmetric valley, characterized at the left side by the above cited steep, carbonate southern mountain front of M.nt Cervati and at the right by the gentle northern terrigenous mountain slope of the M.nt Centaurino (1551 m asl). The middle right side of the basin is characterize by marly-arenaceous rocks outcrop (M.nt Marchese hilly ridge), while the left middle side is characterized by limestone sequences (M.nt Rotondo and Serra Forcella), figure 3.16.

The geological constraints and the permeability variability in type and rate induce a very complex hydrogeological behaviour to coupled aquifer-river system (figure 3.17).

In the northern sector of the basin, is located one of the main karst aquifer of the Southern Apennine: Cervati Aquifer (AQ_CRV). The hydrogeological boundaries of this aquifer are: at the northern side, a set of compressive tectonic lines (reverse faults, overthrusts), at the S and SW, is confined by the impermeable "bends" of the marly-clayey aquicludes, connected to carbonate aquifer by normal faults or stratigraphical limits. Inside aquifer, shear zones due to compressive and extensional tectonics originate intermediate aquitard, controlling a "segmentation" of multilayered aquifers, with karst spring at various elevations (see hydrogeological section below the figure 3.17 and table 3.7).

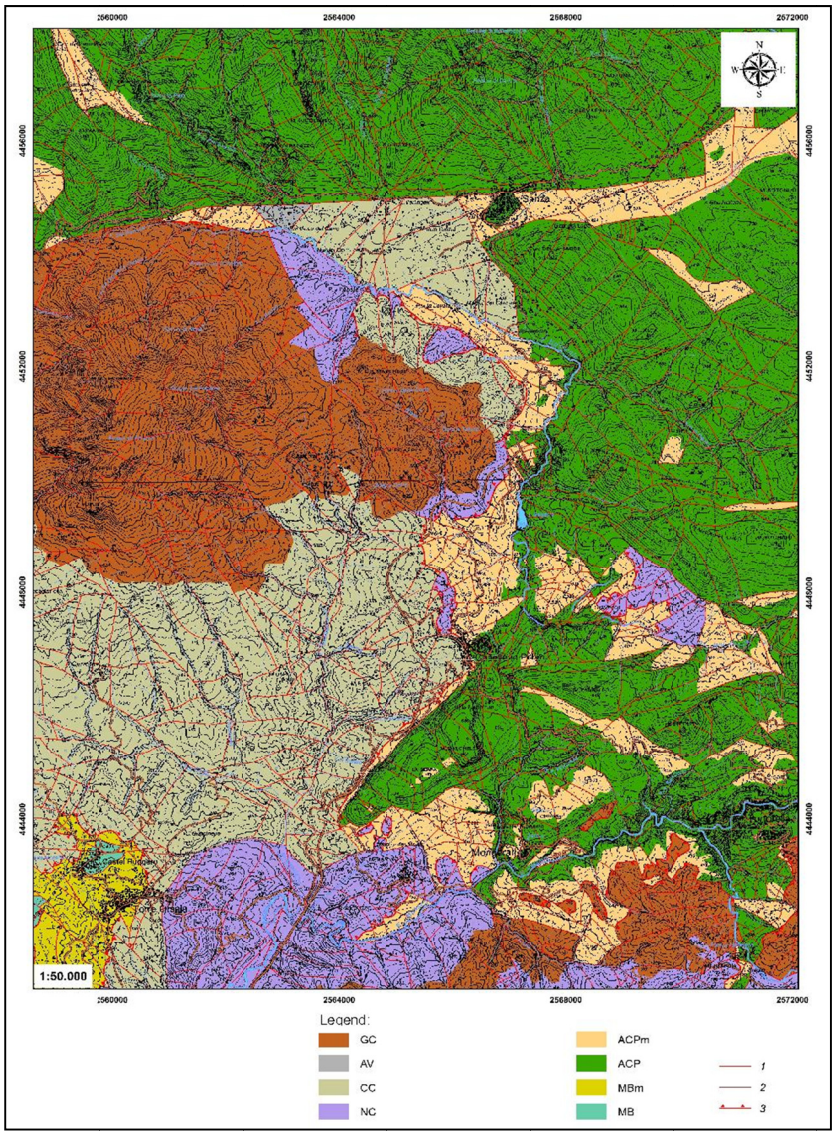

Figure 3.16:Geological map of the Upper Bussento river (1:50.000 scale).

Legend: GC. Cilento group; AV. Sicilide Unit; CC. Castelnuovo unit; NC. Nord Calabrian Unit; ACPm. Alburni – Cervati -Pollino unit - Piaggine formation; ACP. Alburni – Cervati -Pollino unit; MBm. Bulgheri- Roccagloriosa Unit - Marls; MB. Bulgheri- Roccagloriosa Unit- Limestone; 1. Fault; 2. Stratigraphical unit, 3. Overthrust.

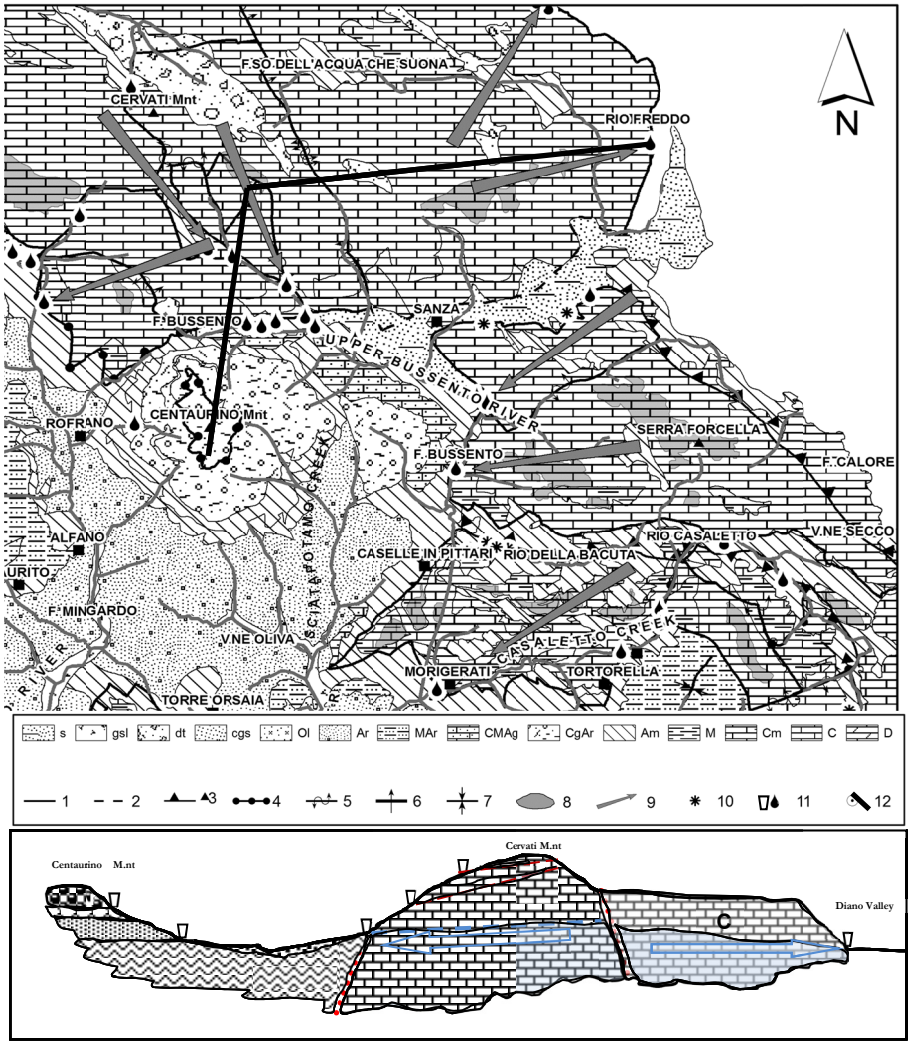

Figure 3.17: Hydro-geomorphological map of the Upper Bussento river and related hydro-geomorphological features.

Legend: s. Sandy conglomerate complex; gsl. Gravelly sandy silty complex; dt. Debris complex; Ol. Blocky clayey olistostrome complex; Ar. Sandstone complex; MAr. Marly sandstone complex; CMAg. Marly conglomerate sandstone complex; Am. Silty Sandstone complex; M. Marly complex; Cm. Marly limestone complex; C. Limestone complex; D. Dolomite complex. 1. Permeability limit; 2. Buried permeability limit; 3. Overtrusth hydro-geological limit; 4. Syncline hydro-geological limit; 5. Overturned strata; 6. Horizontal strata; 7. Sincline; 8. Karst summit; 9. Hypnotized groundwater flow direction; 10. Sinkhole; 11. Main spring; 12. Section line.

Table 3.7: Main karst springs from Cervati Aquifer.

Spring name	Sub-aquifer name	Elevation (m a.s.l.)	Mean Annual Discharge (l/s)	Ground Water Direction
Rio Freddo	M.nt Arsano	470	750	E
Fontanelle Soprane	M.nt Arsano	470	800	N-E
Fontanelle Sottane	M.nt Arsano	460	400	N-E
Varco la Peta	Vallivona	1200	450	S
Montemezzano	Inferno creek	900	100	S
Sanza Fistole Group	Basal Southern Cervati	470		S
Faraone Fistole Group	Pedale Raia	450	400	W
Calore Group	Neviera	1150	100	N
Sant'Elena Group	Rotondo	420	400	N-W
Laurino Group	Scanno Tesoro	330-400	600	N-W
Capodifiume Group	Chianiello-Vesole	30-35	2900	N-W
Paestum-Cafasso Group	Chianiello-Vesole	1-10	750	N-W
Acqua Solfurea Group	Chianiello-Vesole	5	250	N-W

3.4.3 Hydrography and Hydrology

A Drainage Network Analysis was carried out on the Upper Bussento river basin, starting from the Horton-Schumm ordering (figure 3.18).

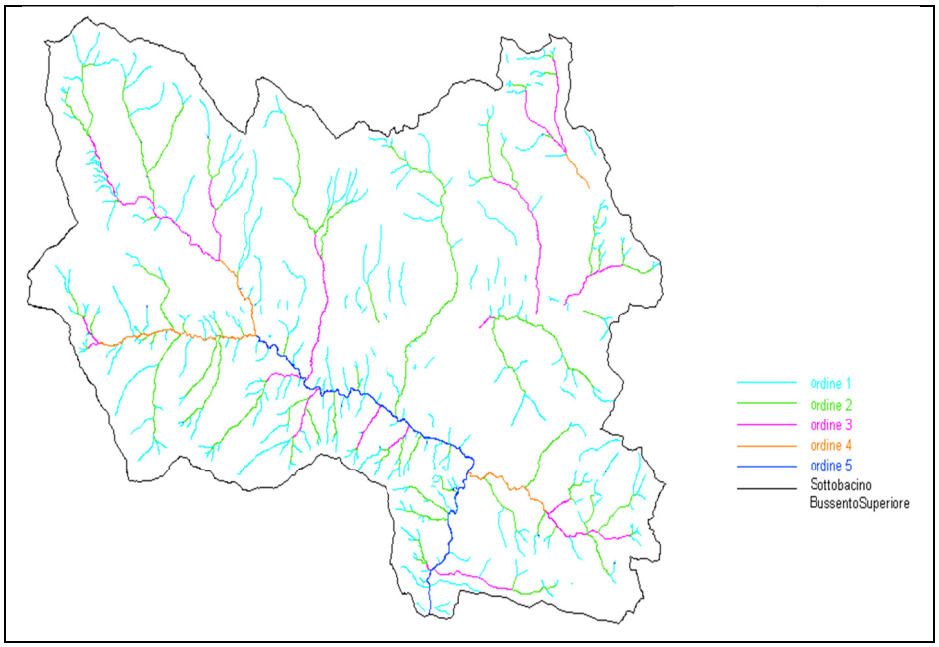

Figure 3.18: Drainage network and Horton stream ordering.

Based on the above hydro-geomorphological and hydrographical settings, the Main Monitoring Point (MMP) River Reach were identificated and located (figure 3.19 and table 3.8).

Table 3.8:Main River Reaches along the Upper Bussento Segment

N°	Reach Name	Reach Code	Dowstream MMP	Upstream MMP	Lenght (m)	Slope (%)
1	Tredici Fistole	BS17_BS18	BS17	BS18	1670,62	1,31
2	Farnetani Spring	BS18_BS19	BS18	BS19	2478,56	1,25
3	Farnetani Bridge	BS19_BS20	BS19	BS20	3277	1,46
4	Ponte L'Abate	BS20_BS22	BS20	BS22	2118,88	1,98
5	Varco Carro Bridge	BS22_BS22_07	BS22	BS22_07	4745	8,09
6	Inferno Bridge	BS21JBS22_ BS21_04	BS21JBS22	BS21_04	5004	13,73

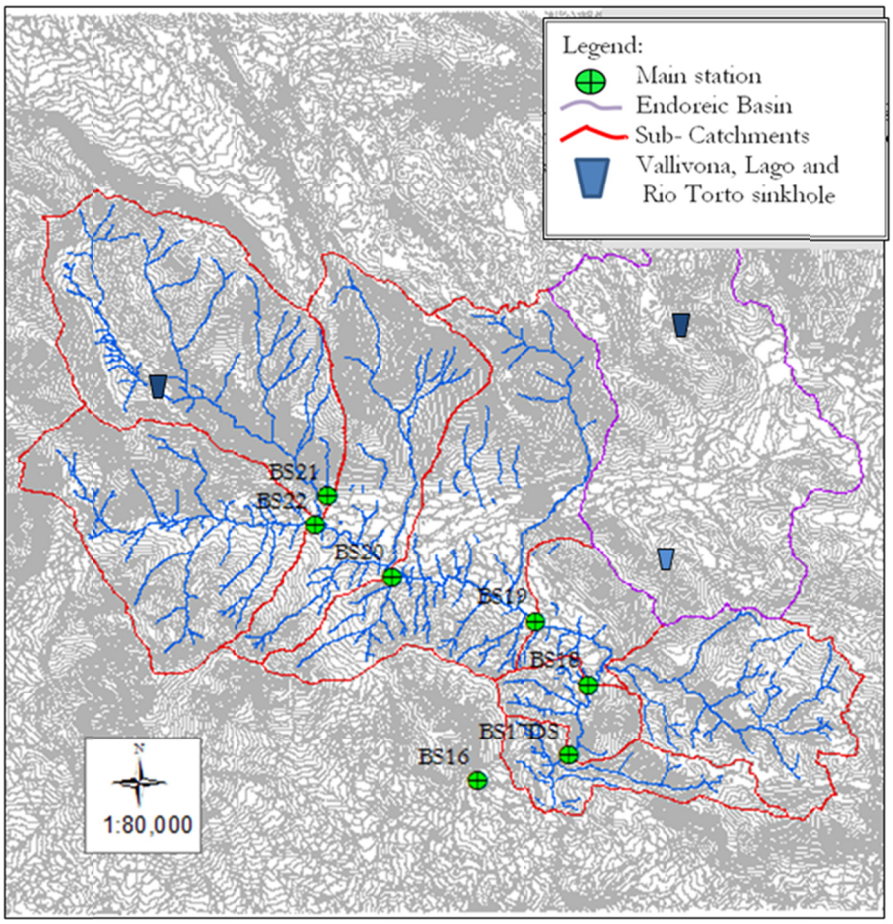

Figure 3.19:Relevant Hydrological Points and Main Monitoring Points (MMP) location along the Upper Bussento Segment.

Along the Main River Segment were drawn the longitudinal profiles from the outlet section of the Sub-basin toward the headwaters of the BS21 and BS22 (figures 3.20-3.22).

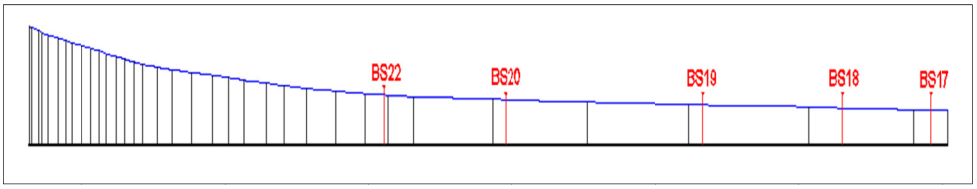

Figure 3.20 : Longitudinal profile along the BS22.

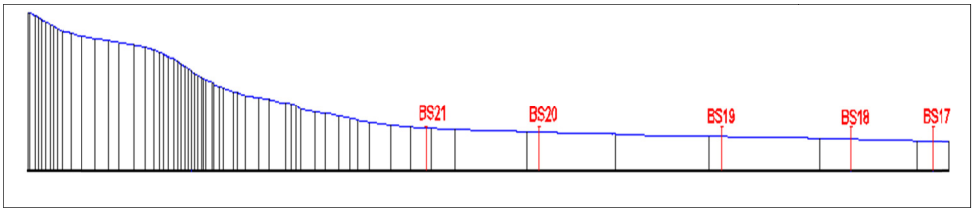

Figure 3.21 : Longitudinal profile along the BS21, whitout the Vallivona endorheic basin.

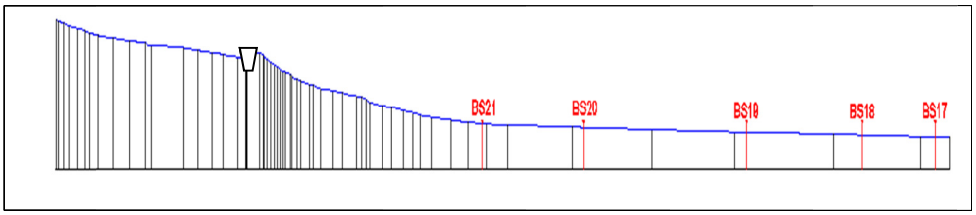

Figure 3.22 : Longitudinal profile along the BS21, comprising the Vallivona endoreic basin and sinkhole (see the symbol)

Further longitudinal profile was drawn along the BS21 to extend analysis to Vallivona endorheic basin, recently affected by sub-terranean hydraulic works (figures 3.21 and 3.22).

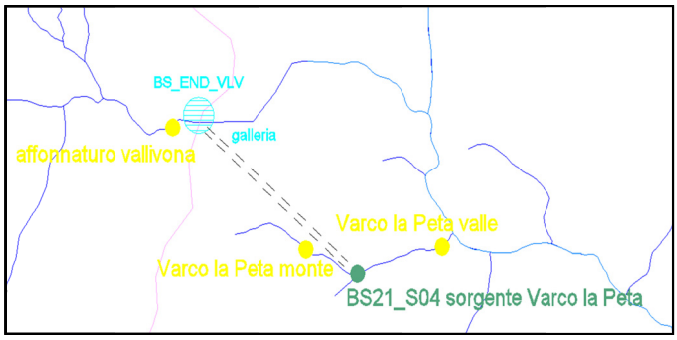

Figure 3.23 : ***Vallivona sinkhole- Varco La Peta system.***

The successive phase of analysis was the Main Catchment identification and characterization (figure 3.24 and table 3.9).

Table 3.9: Geometric parameters of the Main Catchments of the Upper Bussento

	Outlet Code	Area (m^2)	Perimeter (m)	Lenght (m)	Width (m)
Catchments	BS22	14727513,67	16547,1611	5537,2846	4517,86
	BS21	19325148,96	19552,4478	7256,01	3955,81
Basin Sector	BS20	47201996,21	57671,3862	9013,71	8928,97
	BS19	66842393,94	84538,7562	11757,74	9409,46
	BS18	107719093,6	122411,746	13250,69	13480,57
	BS17	110396713,5	130259,286	14609,1	13480,57
	BS17	114827287	144131,404	15675,07	13480,57

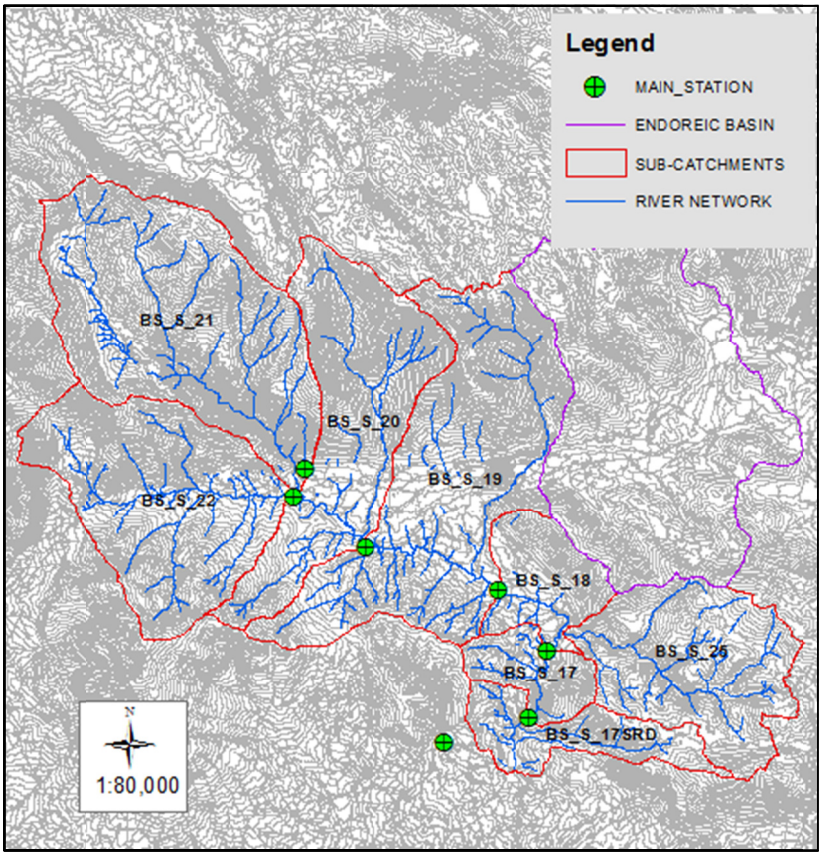

Figure 3.24: Main Catchments of the Upper Bussento

A Form Analysis of Main and Secondary Catchment and Basin Sector was carried out, as show in the figure 3.25.

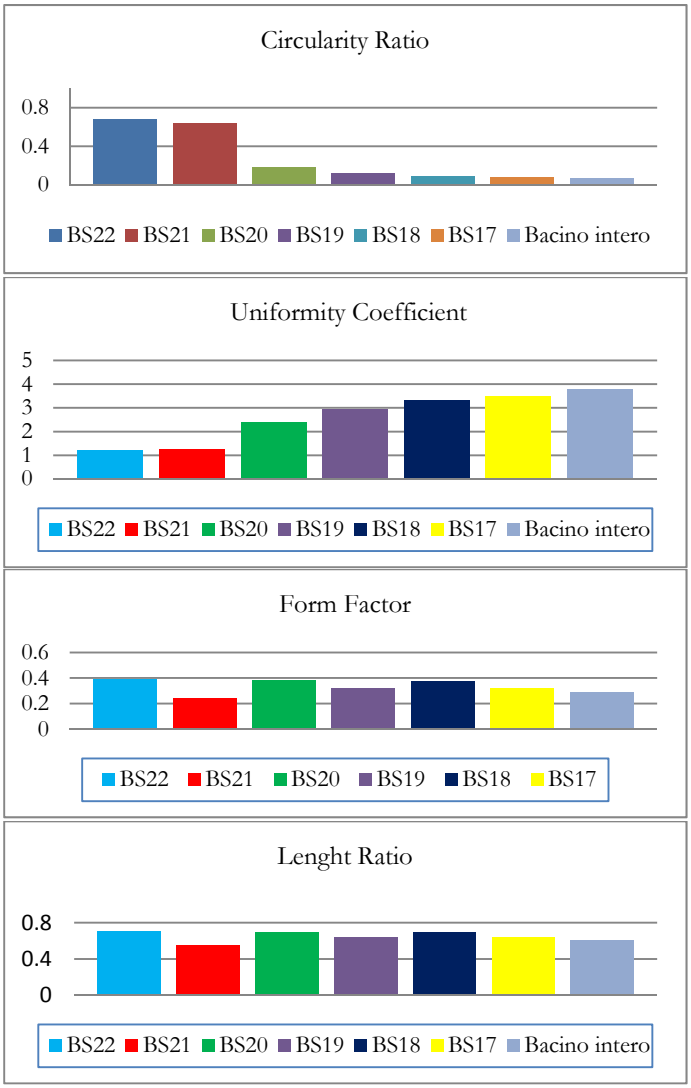

Figure 3.25: Main Catchment Form Analysis

The figure 3.26 and table 3.10 show the Secondary Catchment Map and their geometric parameters and geomorphic ratios respectively (figure 3.27).

Table 3.10:Geometric parameters of the Upper Bussento Secondary Catchments

Code	*Name*	*Area m²*	*Perimeter m*	*Lenght m*	*Width m*
BS35	Vallone Surice	575111,69	3578,71	1457,92	626,88
BS25	Vallone di Paolo	10914022,06	15706,837	4789,63	3550,26
BS34	Vallone Nocella 2	906420,07	4030,32	1403,66	1024,72
BS27	Vallone Diavoli	11111785,02	17371,83	6402,23	3503,77
BS33	Vallone Nocella 1	493025,04	3331,97	1417,92	922,38
BS32	Vallone Giardino	470596,29	3029,73	1337,61	512,8
BS30	Vallone Giumenta	2809199,98	7325,63	2978,6813	1673,97
BS28	Vallone Secco	7728992,91	15023,76	6343,31	2876,31
BS31	Vallone Rosso	2544087,6	7842,398	3315,38	1193,2587
BS24	Vallone Panniere2	1075927,44	5699,8158	2544,76	1218,63
BS23	Vallone Panniere1	391742,88	4082,02	1982,674	394,72
BS26	Vallone Pezza	3251503,69	7769,203	3139,41	2312,08

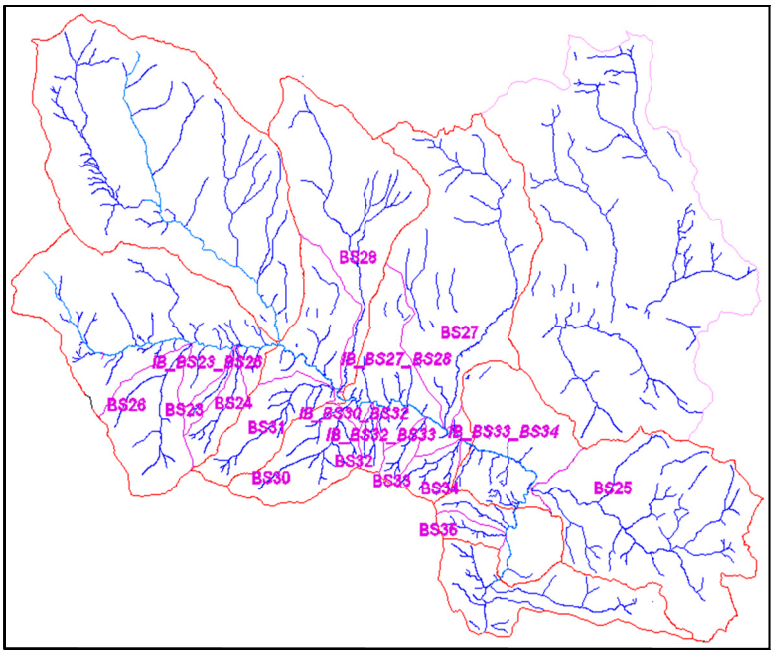

Figure 3.26: Secondary Catchments of the Upper Bussento

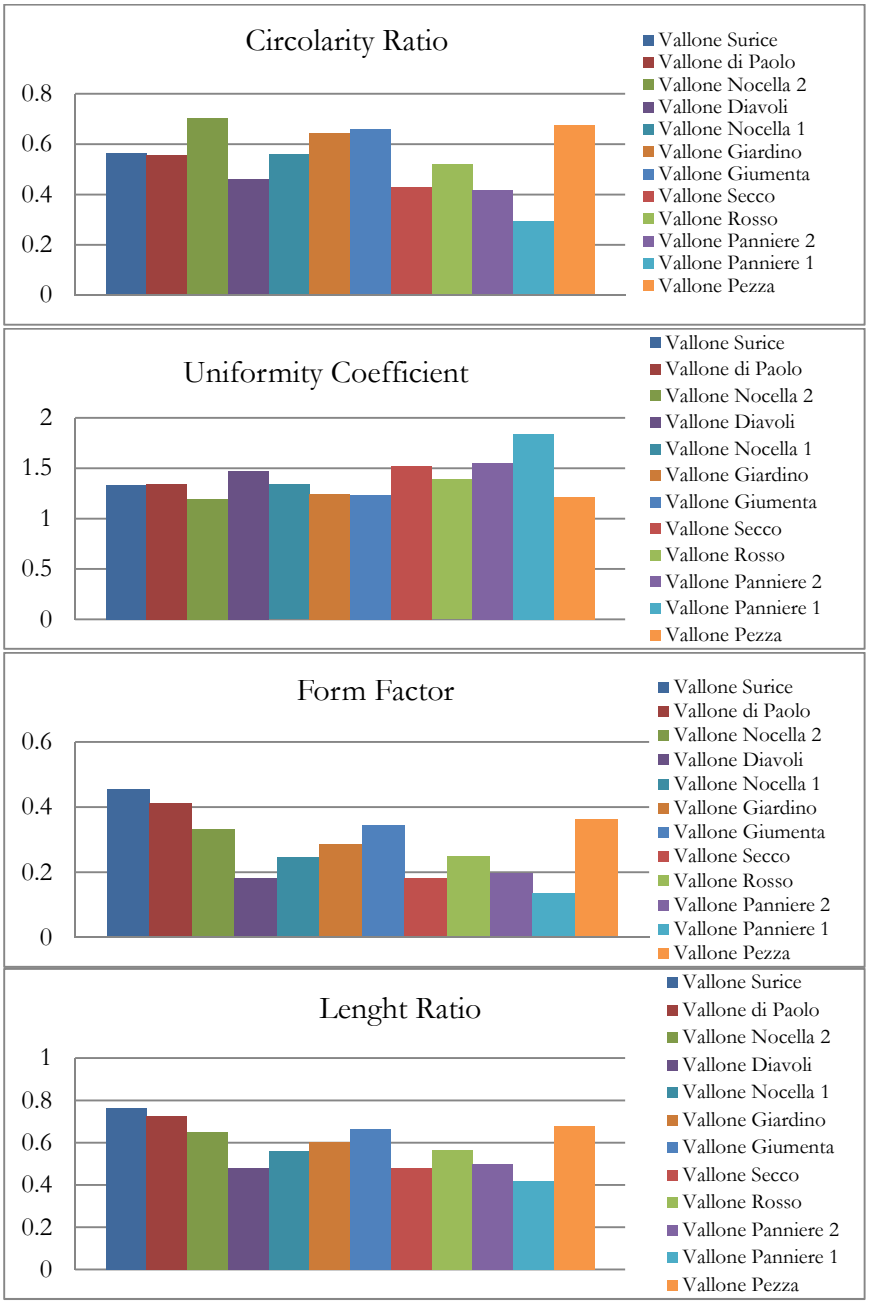

Figure 3.27: Secondary Catchment Analysis

Considering the karst-conditioning of the basin, the Endorheic basins (figure 3.28 and table 3.11) were mapped and measured because their direct contributions to streamflow from endokarst circulation.

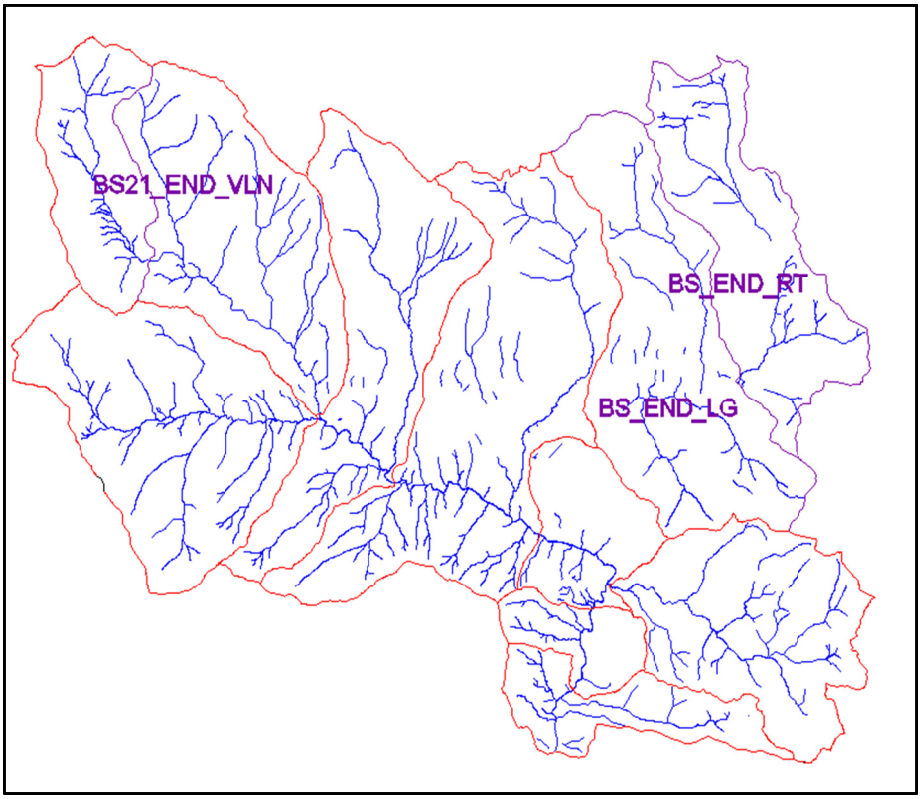

Figure 3.28: Endorheic basins and relate sinkholes.

Table 3.11: Geometric features of the Endorheic basins.

Code	Name	Area (Km^2)	Perimeter (Km)
BS21_END_VLN	Vallivona	6,2	12
BS_END_RT	Rio Torto	10,5	18,6
BS_END_LG	Lago	15,6	13,1

Further karst-conditioning features on hydrology of the Upper Bussento river basin, relevant for water budget definition are the Karst Uplands (figure 3.29 and table. 3.12). These features result in "no contribution areas" for direct runoff production, but play a role in groundwater contribution to streamflow.

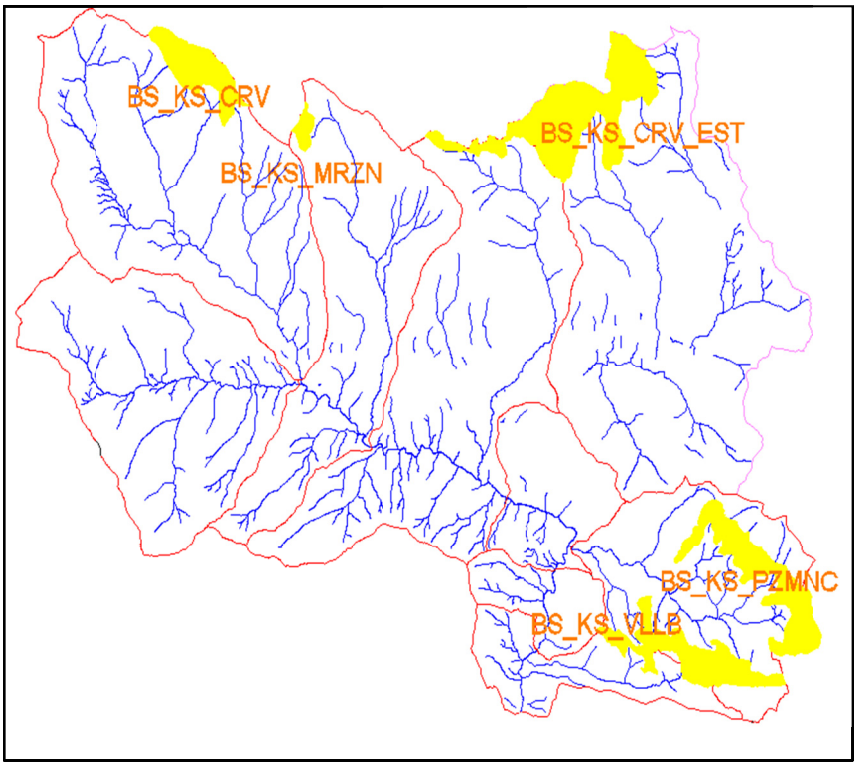

Figure 3.29: Karst Upland Map.

Table 3.12: Karst Uplands and thier characteristics.

Code	Name	Area (Km^2)	Perimeter (Km)	Groundwater Discharge
BS_KS_VLLB	Valle d'Alba	1,4	12	Inside Basin
BS_KS_PZMNC	Pozzi Monaci	17,8	11,5	Inside Basin
BS_KS_CRV_EST	Cervati Est	2,9	15	Outside Basin
BS_KS_MRZN	Monte Arzano	16	20	Outside Basin
BS_KS_CRV	Cervati Summit	0,99	5,7	Outside Basin

4 THE INTEGRATE MONITORING SYSTEM

4.1 HISTORICAL HYDROLOGICAL MONITORING SYSTEM

The VAPI procedure is based on statistical analysis on the pluviometric and hydrometric datasets collected at national, regional and basins scales. So, the first, structured and systematic hydro-meteorological database of the Campania region and Bussento river basin was performed within the development of the VAPI procedure.
The source datasets were the hydrological data recorded by the rain gauges and streamflow stations managed by the SIMI (Servizio Idrografico e Mareografico Italiano), compartment of Naples. In particular, at the third level of regionalization of the VAPI (Rossi and Villani, 1995) concerning the analysis on the annual mean of the daily and hourly rainfalls, were utilized 231 rain gauges stations with more than 10 years of observations; at the second level, 129 rain gauges with more than 30 years of observations and, finally, at the first, 112 rain gauges with more than 40 years of observations. Figure 4.1 shows the location of the Historical Hydro-meteorological Monitoring System in Campania region and surroundings.

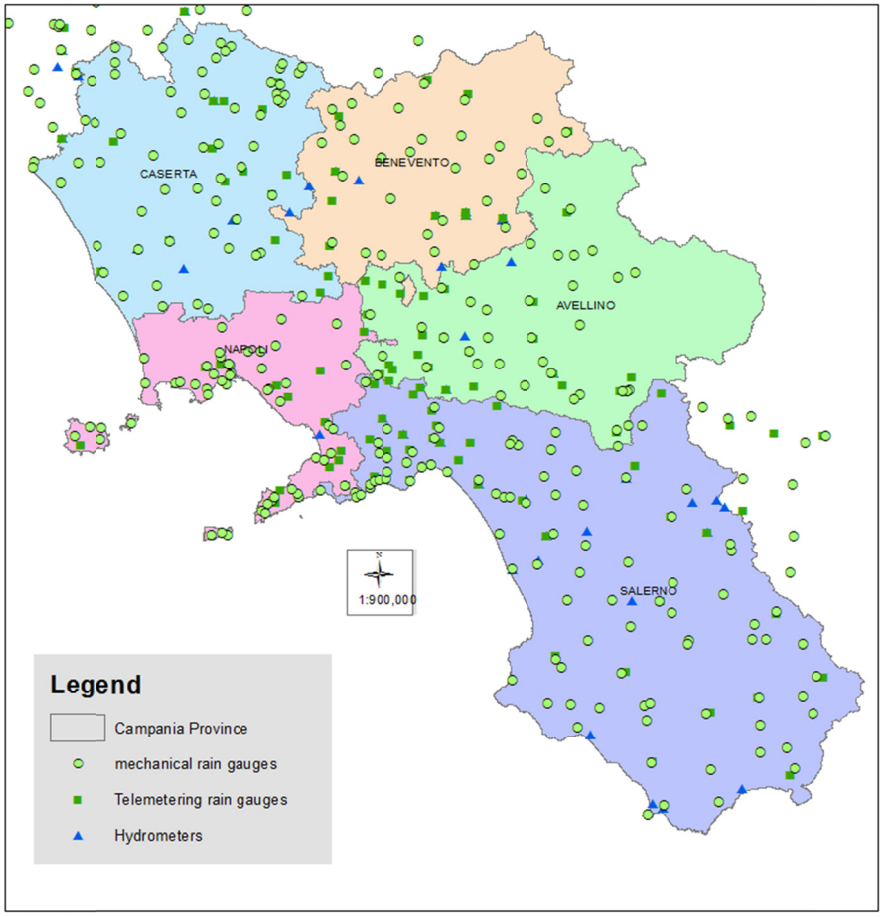

Figure 4.1: Rain gauge station location of the Hystorical Monitoring System in the Campania region and surroundings.

Statistical analysis of this dataset was used to individuate the six "Homogeneous Pluviometric Areas" (HPA) of the Campania region and surroundings (figure 4.2), as Areas with similar pluviometric behavior in extreme rainfall events.

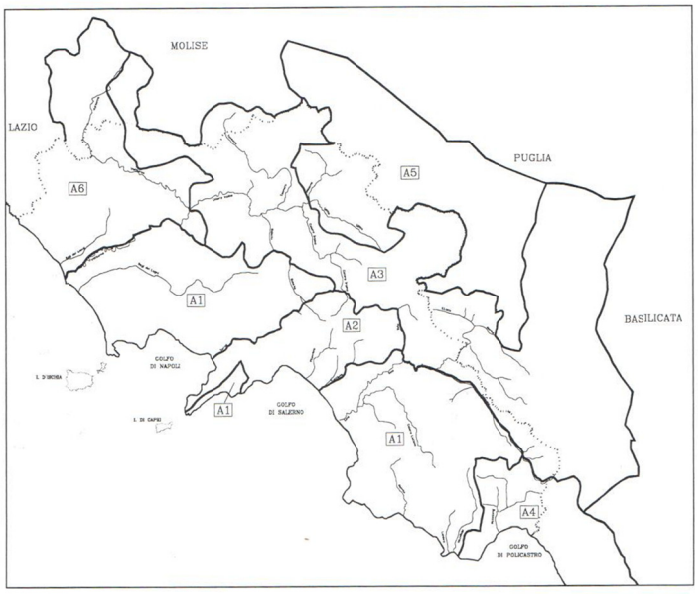

Figure 4.2: Schematic chorography of the six "Homogeneous Rainfall Areas" individuated and delimitated in the Campania region and surroundings.

The Bussento river basin resulted included in the A_4 Homogeneous Pluviometric Area, to which were attributed the statistical parameters derived from the regression law analysis between the annual hourly rainfall vs. elevation, as shown in the table 4.1.

Table 4.1: Statistical parameters of the linear regression law between the means of annual hourly rainfall ([hg(0)]) and elevation (Z) for the six HPA. In red, are listed the values for the Bussento river basin (VAPI, 2005).

HPA	N. of Station	A	$B \cdot 10^4$	$\mu[h_g(0)]$(mm)	$\mu[h_{g(1000)}]$(mm)	ρ^2
1	70	1.769	1.552	58.8	84.0	0.59
2	30	1.935	1.292	86.1	116.0	0.47
3	55	1.674	1.614	47.2	68.4	0.68
4	28	1.800	2.700	63.1	118.0	0.64
5	22	1.499	2.331	31.6	54.0	0.70
6	28	1.870	1.332	74.1	101.0	0.57

In the extreme flood analysis concerning the annual maximum discharge data were used: at the first level of regionalization, 28 hydrometric stations, with more than 5 years of observations; at the second level, 36 hydrometric stations, (21 of these falling between the Volturno and the Bussento river basins); at the third level, 22 measurement stations with more than 5 years of observations. Table 4.2 reports the fundamental land use (% in forest), morphologic (Mean elevation and Slope), and hydrologic (%Imp.= percent of area with impervious soils and bedrock; $m[I_A(g)]$: Maximum Hourly Rainfall expected and m[Q]= Peak Hourly Discharge) features at "Bussento at Caselle in Pittari" hydrometrograph, now re-named BS17 "Tredici Fistole" station.

Table 4.2: Fundamental land use, morphologic, and hydrologic features of the Bussento at Caselle in Pittari hydro-metrograph station.

Station	N. years	Area (Km^2)	Mean elevation (m.asl)	Mean slope (%)	% Imp.	% forest	$m[I_A(g)]$ (mm/hour)	m[Q] (m^3/s)
Bussento	17	113	850	15.96	30	55	4.32	56

Figures 4.3-4.19 shown daily hydrographs from Caselle in Pittari Hydrometrograph Station Monitoring DataSet from 1952 to the 1968, plotted in the hydrological year (t=0 is for first of October). Table 4.3 ~~is~~ reports annual maximum discharge, maximum daily discharge and mean value at the Bussento Caselle in Pittari river station.

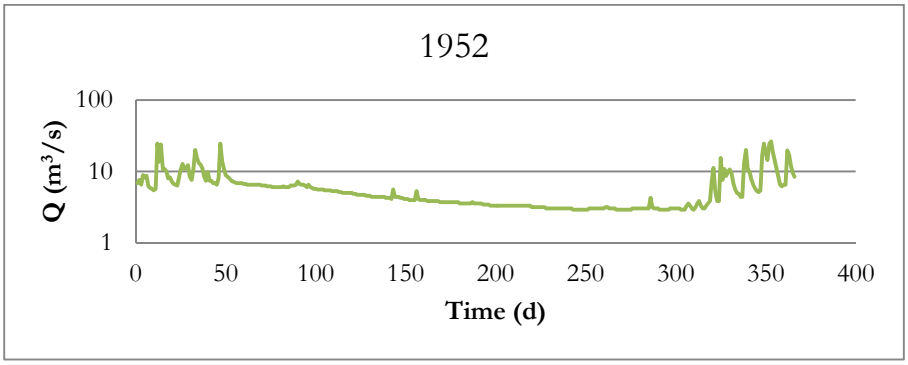

Figure 4.3: Annual hydrograph plotting discharge measurements, detected in the 1952 to the historical Caselle in Pittari Hydrometrograph

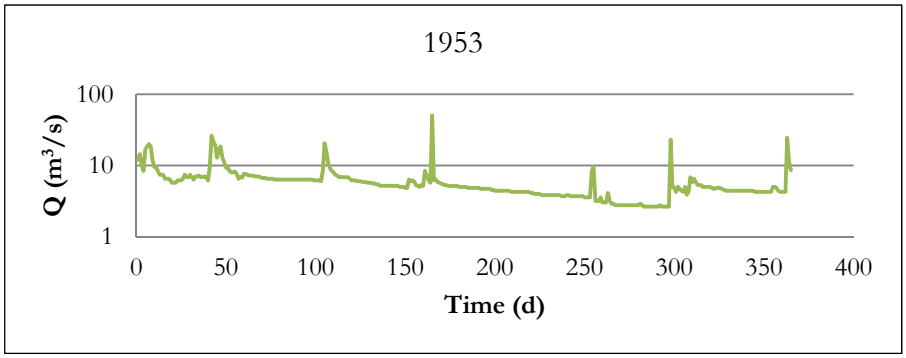

Figure 4.4: Annual hydrograph plotting discharge measurements, detected in the 1953 to the historical Caselle in Pittari Hydrometrograph

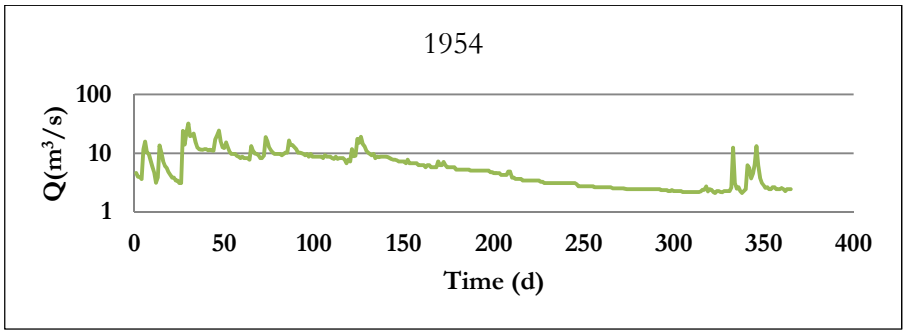

Figure 4.5: Annual hydrograph plotting discharge measurements, detected in the 1954 to the historical Caselle in Pittari Hydrometrograph

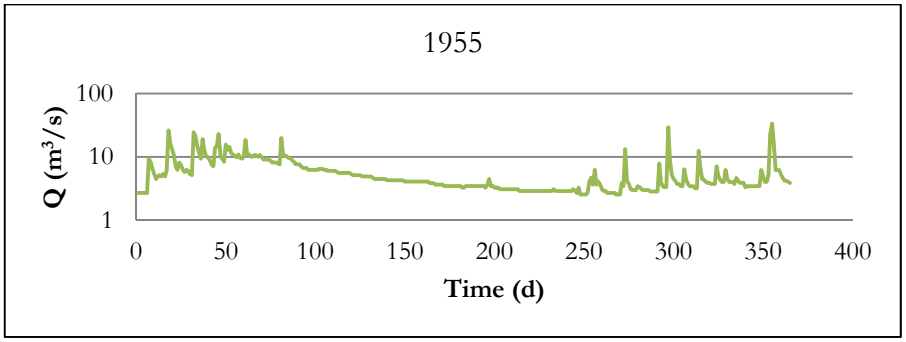

Figure 4.6: Annual hydrograph plotting discharge measurements, detected in the 1955 to the historical Caselle in Pittari Hydrometrograph

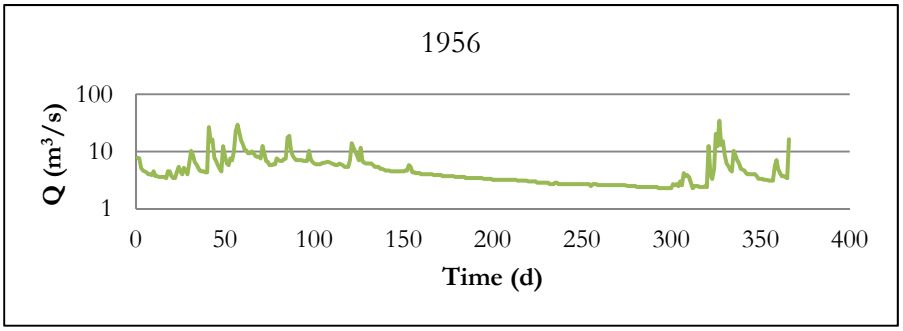

Figure 4.7: Annual hydrograph plotting discharge measurements, detected in the 1956 to the historical Caselle in Pittari Hydrometrograph

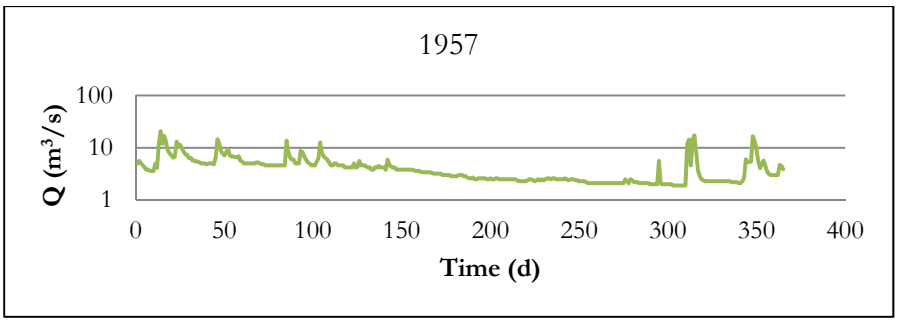

Figure 4.8: Annual hydrograph plotting discharge measurements, detected in the 1957 to the historical Caselle in Pittari Hydrometrograph

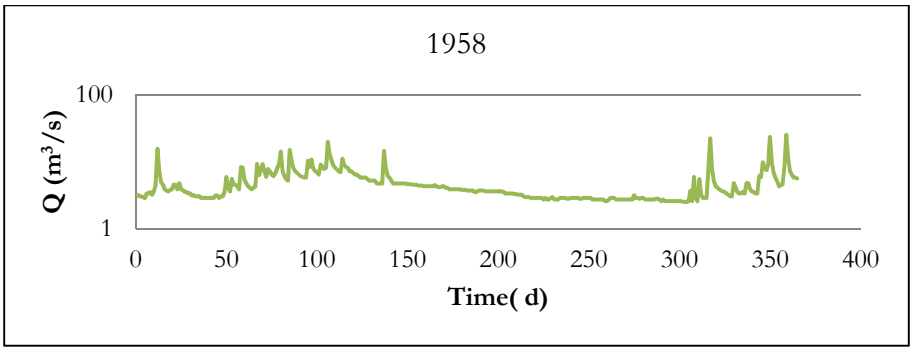

Figure 4.9: Annual hydrograph plotting discharge measurements, detected in the 1958 to the historical Caselle in Pittari Hydrometrograph

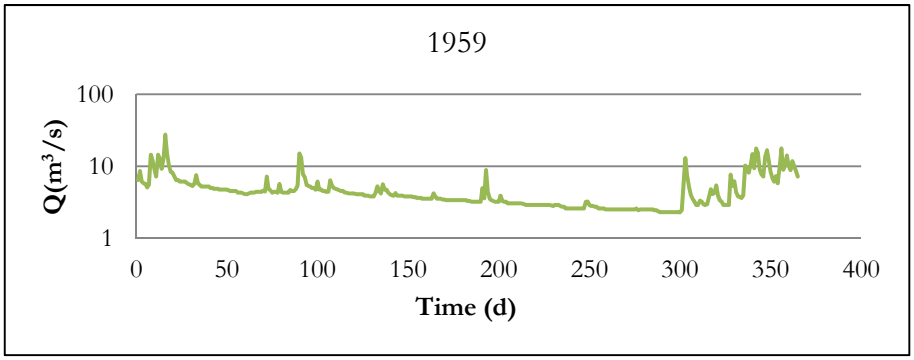

Figure 4.10: Annual hydrograph plotting discharge measurements, detected in the 1959 to the historical Caselle in Pittari Hydrometrograph

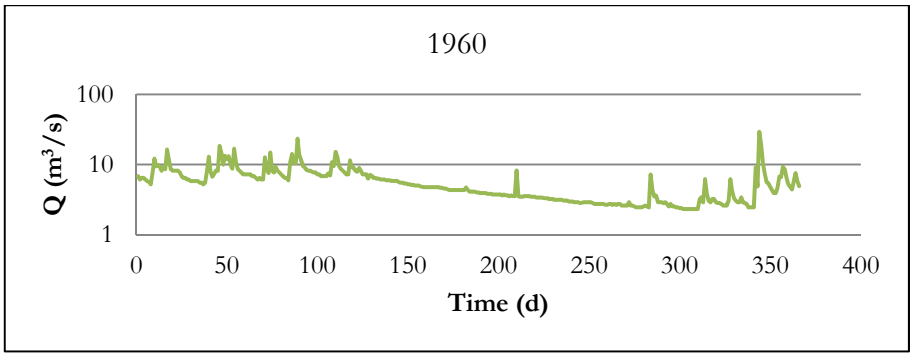

Figure 4.11: Annual hydrograph plotting discharge measurements, detected in the 1960 to the historical Caselle in Pittari Hydrometrograph

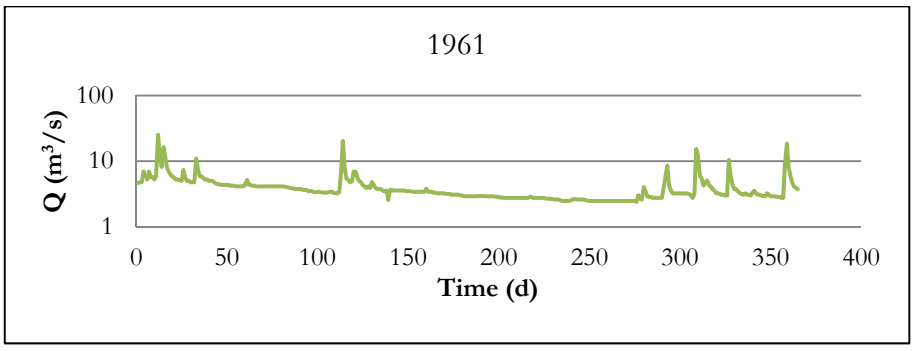

Figure 4.12: Annual hydrograph plotting discharge measurements, detected in the 1961 to the historical Caselle in Pittari Hydrometrograph

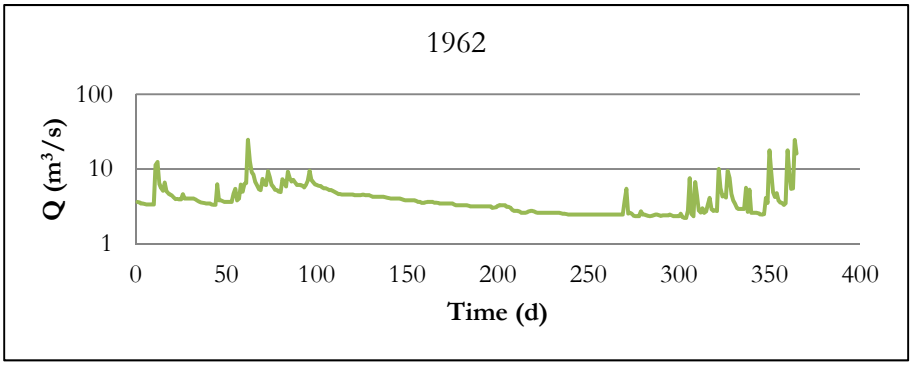

Figure 4.13: Annual hydrograph plotting discharge measurements, detected in the 1962 to the historical Caselle in Pittari Hydrometrograph

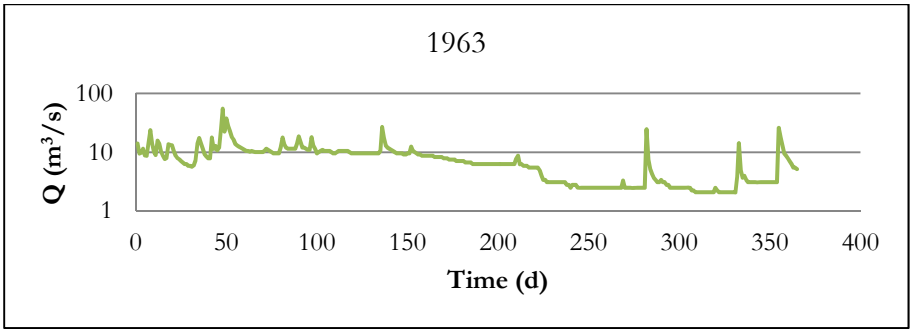

Figure 4.14: Annual hydrograph plotting discharge measurements, detected in the 1963 to the historical Caselle in Pittari Hydrometrograph

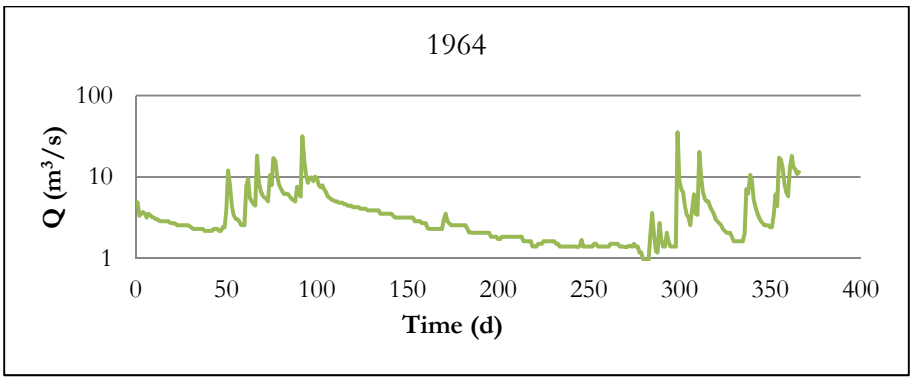

Figure 4.15: Annual hydrograph plotting discharge measurements, detected in the 1964 to the historical Caselle in Pittari Hydrometrograph

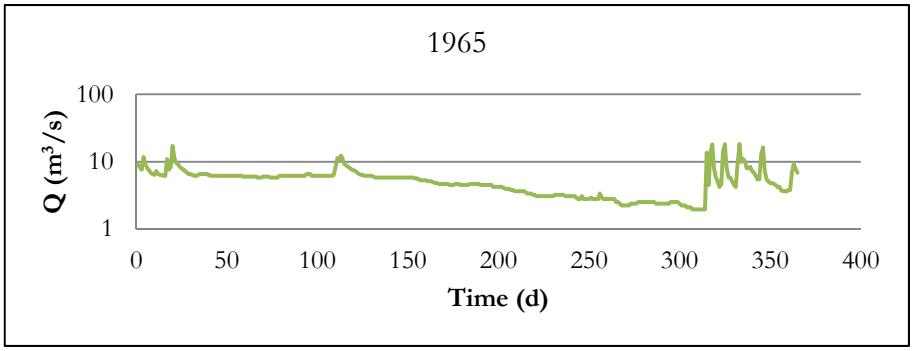

Figure 4.16: Annual hydrograph plotting discharge measurements, detected in the 1965 to the historical Caselle in Pittari Hydrometrograph

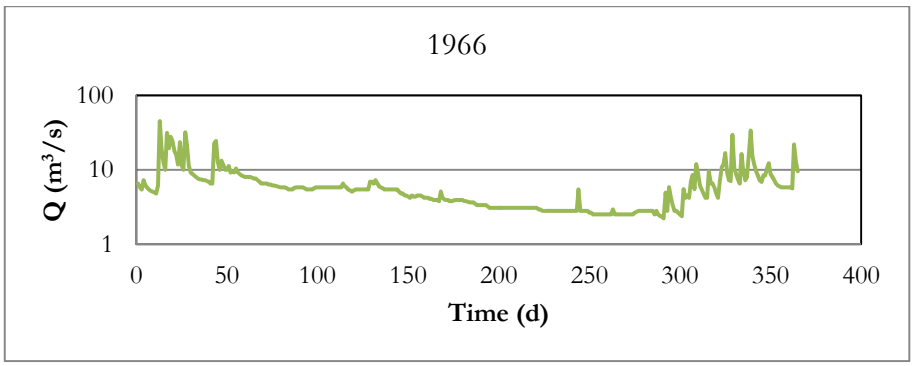

Figure 4.17: Annual hydrograph plotting discharge measuremets, detected in the 1966 to the historical Caselle in Pittari Hydrometrograph

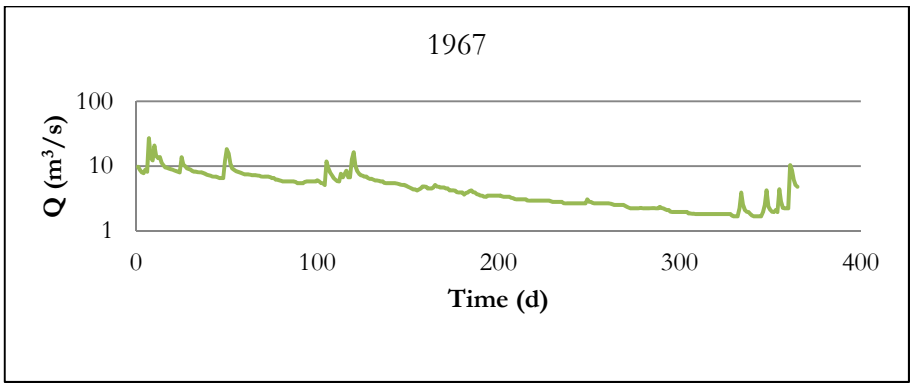

Figure 4.18: Annual hydrograph plotting discharge measurements, detected in the 1967 to the historical Caselle in Pittari Hydrometrograph

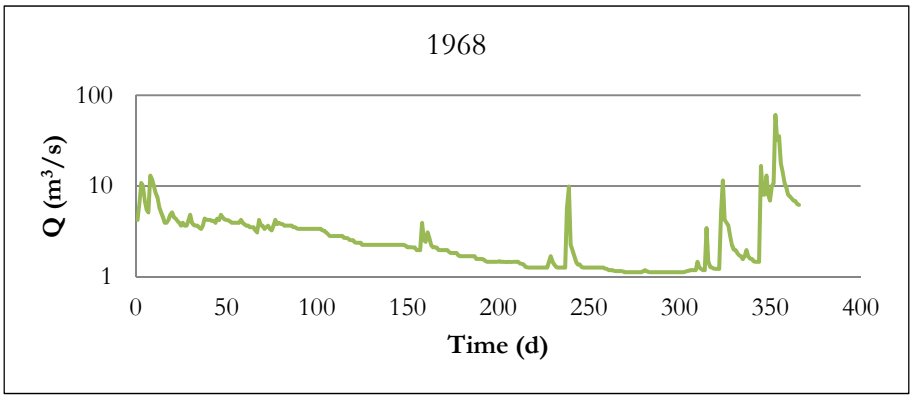

Figure 4.19: Annual hydrograph plotting discharge measurements, detected in the 1968 to the historical Caselle in Pittari Hydrometrograph

Table 4.3: Full, maximum daily and mean value discharge at the Bussento Caselle in Pittari river station.

N.	Years	$Q_{full}(m^3/s)$	$Q_{daily}(m^3/s)$	$Q_{mean,f}(m^3/s)$	$Q_{mean,d}(m^3/s)$
1	1952	61.7	26.2	55.7	32.1
2	1953	36.5	26.2		
3	1954	36.8	32.1		
4	1955	41	33.6		
5	1956	65.4	34.5		
6	1957	33.5	20.7		
7	1958	38.6	25.1		
8	1959	33.6	27.4		
9	1960	41.4	29.2		
10	1961	47	25.3		
11	1962	39	24.5		
12	1963	82.6	55		
13	1964	82	35.4		
14	1965	90.3	18.3		
15	1966	71.8	45.1		
16	1967	58	27		
17	1968	88.5	60.7		

4.2 INTER-INSTITUTIONAL BUSSENTO BASIN MONITORING SYSTEM

To improve the knowledge of the hydrologic and hydrogeologic features of the Bussento and other river basins and provide major informations on the interaction between groundwater and surface waters, the hystorical dataset of the VAPI project was integrated by an Interistitutionale Basin Monitoring System managed by the CUGRI (Centro Universitario per la Gestione del Rischio Idrogeologico) and Left Sele River Basin Authority. Therefore, in order to complete the knowledge of the study areas, were collected the data from the CUGRI Hydro-geomorphological DataBase. In the following, are shown example of maps and data used.

1) Upper Bussento Sub-basin Hydrogeological Map (figure 4.20);

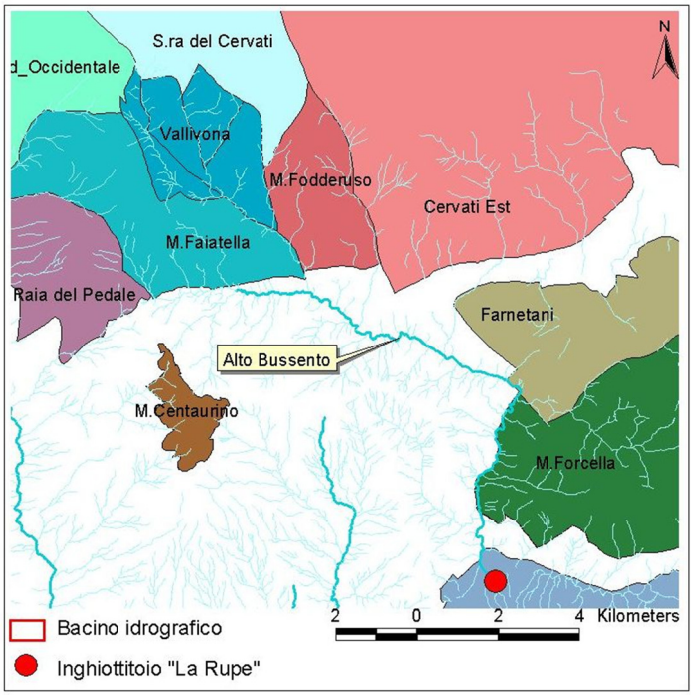

Figure 4.20: Aquifer of the Upper Bussento river Basin.

2) Montemezzano Spring map and monthly flow rate (figures 4.21 and 4.22):

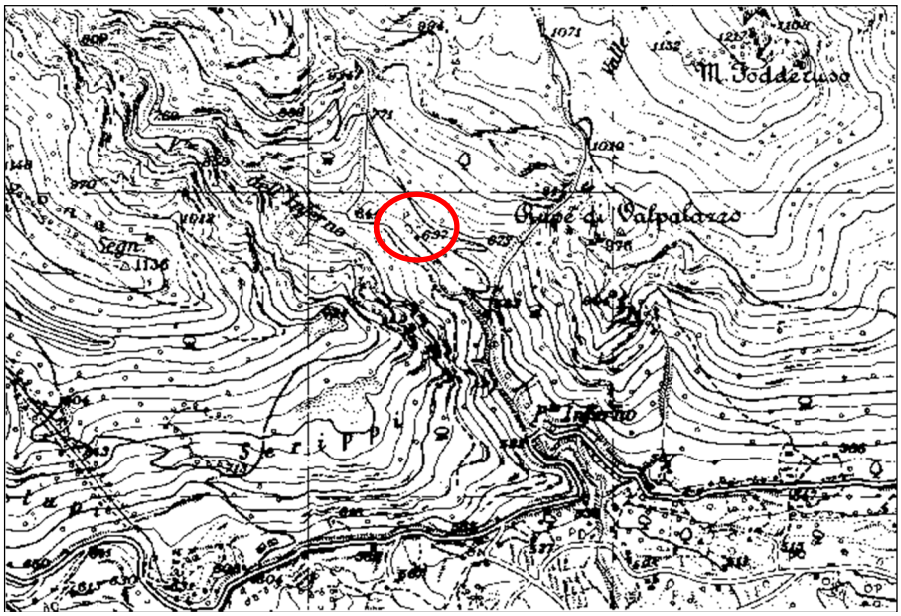

Figure 4.21: Montemezzano Spring location; Sanza Municipality, Upper Bussento Sub-basin; Gauss-Boaga Coordinates: X = 2562341; Y = 4455861; Elevation: 637 m asl).

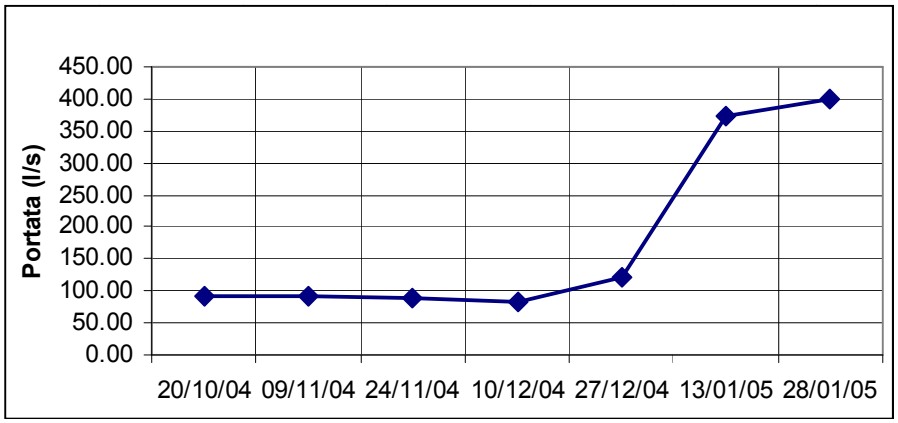

Figure 4.22: Montemezzano Spring flow rate.

3) Fistole di Sanza Spring location and flow rate(figg. 4.23-4.24);

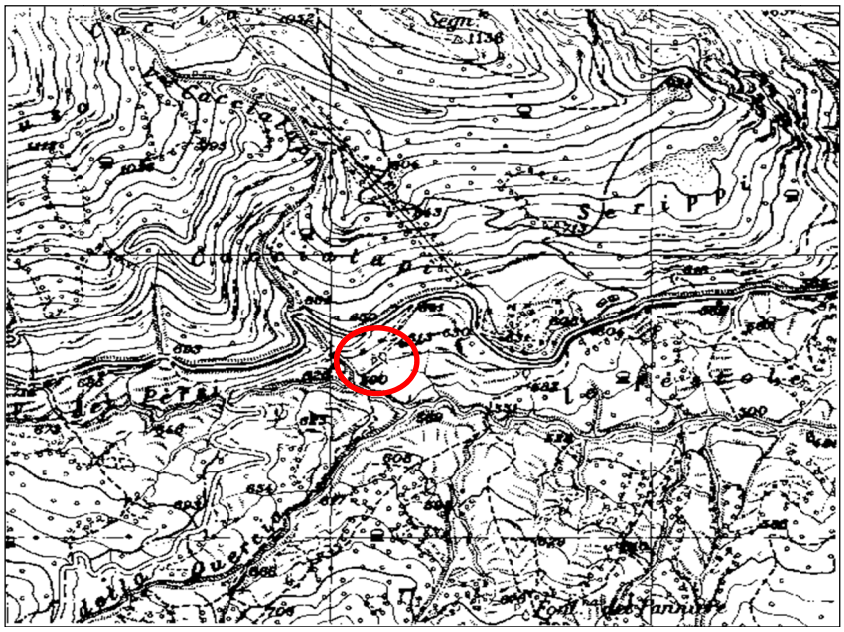

Figure 4.23: Upper Fistole di Sanza spring location. Sanza Municipality, Sub-basin Upper Bussento; Gauss-Boaga Coordinate: X = 256116, Y = 4454641; Elevation: 610 m s.l.m.

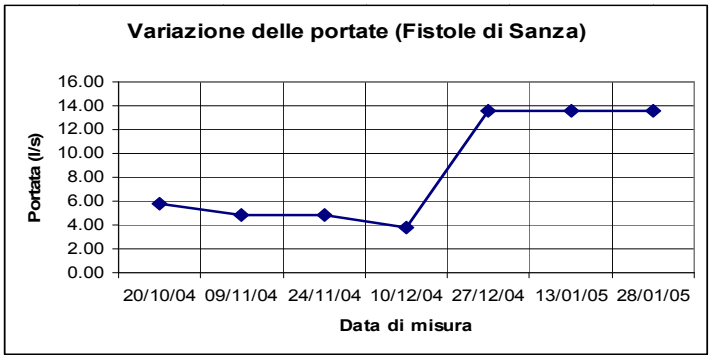

Figure 4.24: Upper Fistole di Sanza Spring flow rate.

4) The stream and spring flow monitoring system was integrated by Radon stations and measures(figures 4.25 and 4.26, tables 4.4, 4.5), in order to use natural isotopic signature in separating surface, sub-surface and groundwater and their interations.

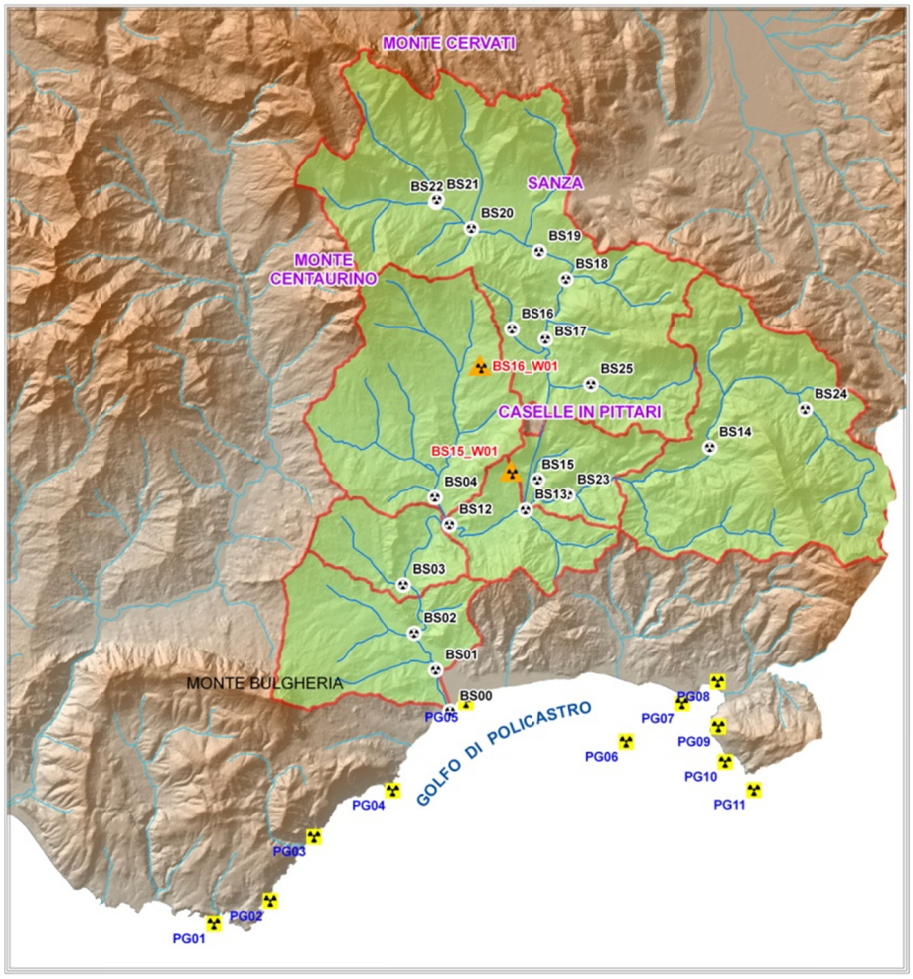

Figure 4.25: Radon Monitoring River-Sea Stations in river (Guida et al., 2008)

Monitoring stations on land were integrated with the coastal and off-share station in the Policastro gulf to detect radon concentration surrounding sub- marine springs (i. e. vuddu submarine springs).
The table 4.4 lists a short dataset of radon measurements from stream on spring stations.

Table 4.4: 2007-2008 instream Radon-222 Measurement campains and results (Guida et al. 2008)

STATION NAME	*CODE*	*09/07*	*12/07*	*01/08*	*02/08*	*03/08*	*04/08*	*05/08*
Bussento Mouth	BS00	1,95	2,75	1,9	1,5	0,4	1,6	1,3
Bussento SS18 Bridge	BS01	1,8	1,1	2,1	1,4	0,8	0,98	2,3
Railway Bridge	BS02	1,6	2,1	0,34	1,95	1,3	1,7	2,8
Sciarapotamo Bridge	BS04	1,28	1,2	1,5	1,8	0,7	1,6	1,5
Hydropower	BS12	0,975	0,9	0,7	1,1	0,6	0,8	0,7
Sicili Bridge	BS13	2,1	2,4	2,2	1,7	1,1	7,5	8,7
Rio Casaletto Capello	BS14	3,03	3,47	6,1	2,05	0,8	10,6	14,9
Oasi WWf Bridge	BS15	4,56	5,8	6,1	0,9	0,6	1,55	1,7
T. Ciciniello	BS16	0,61	0,565	0,58	0,435	0,32	0,45	0,48
Sabetta Reservoir	BS17	8,3	7,5	6	2,3	1,2	4,2	3,9
Acquevive Bridge	BS18	8,4	2,2	0,95	1,7	1,3	4,6	7,7
Farnetani Bridge	BS19	1,2	0,4	0,15	0,43	0,2	0,95	0,3
L'Abate Bridge	BS20	0,25	0,38	0,8	0,21	0,37	0,42	0,34
V.ne Inferno Bridge	BS21	1,9	2,5	0,7	0,68	0,46	0,38	0,15
Varco del Carro Bridge	BS22	1,02	1,3	0,9	0,5	0,39	0,85	0,7
Bussentino Bridge	BS23	0,77	0,83	4,2	0,35	0,33	0,65	0,92
Bacuta Sinkhole	BS25	0,37	0,4	0,32	0,18	0,22	0,3	0,35

In order to detect the surface-groundwater interactions, a more detailed monitoring system was build-up in the upper Bussento river basin (fig.4.26).

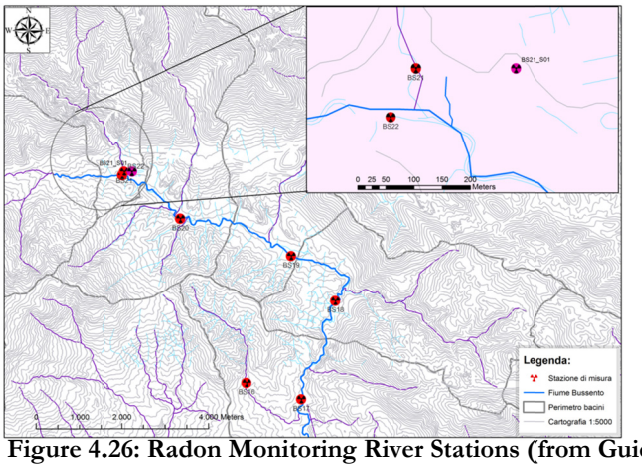

Figure 4.26: Radon Monitoring River Stations (from Guida et al., 2008)

The table 4.5 lists Rn-measurement valuea from September 2007 to December 2008 at the upper Bussento stations.

Table 4.5: 2007-2008 Instream Radon222 Concentration (Guida et al. 2008)

STATION Name and Code	Sabetta Reservoir BS17	Acquevive Bridge BS18	Farnetani Bridge BS19	L'Abate Bridge BS20	Inferno Creek BS21	Persico Bridge BS22
Campaign	[222-Rn] (Bq/l)	[222-Rn] (Bq/l)	[222-Rn] (Bq/l)	[222-Rn] (Bq/l)	[222-Rn] (Bq/l)	[222-Rn] (Bq/l)
Sept.07	6 ± 4	4,2 ± 0,6	0,5 ± 0,3	-	-	-
Dec.07	8 ± 7	4,8 ± 0,8	0,4 ± 0,3	-	2,5 ± 0,8	-
Ian.08	6,0 ± 1,8	3,3 ± 0,9	0,2 ± 0,1	0,8 ± 0,4	0,7 ± 0,5	0,9 ± 0,3
Feb.08	2,2 ± 1,3	4,1 ± 0,8	-	-	-	-
Mar.08	-	.	-	-	-	-
Apr.08	4,2 ± 0,8	4,6 ± 0,8	0,9 ± 0,2	0,4 ± 0,2	0,4 ± 0,1	0,9 ± 0,4
May.08	-	7,7 ± 1,0	0,3 ± 0,2	-	0,2 ± 0,1	0,7 ± 0,4
Jun.08	-	7,9 ± 0,9	0,5 ± 0,3	0,3 ± 0,1	0,4 ± 0,3	0,3 ± 0,2
Oct.08	-	-	-	0,4 ± 0,3	0,7 ± 0,6	0,5 ± 0,3
Nov.08	-	4,3 ± 0,9	0,5 ± 0,4	0,4 ± 0,3	0,2 ± 0,2	0,5 ± 0,2
Dec.08	-	5,0 ± 0,4	0,3 ± 0,2	0,4 ± 0,1	0,3 ± 0,3	0,5 ± 0,3

5) Monthly discharge measurements (2006-2007);

At the same radon-222 river stations, during the hydrological year 2006-2007 were carried out, simultaneously, the discharge measurement campaigns (tables 4.6, 4.7).

Table 4.6: 2006 discharge measurements in m3/s

Previous Code	New Code	Station Name	ott-06	nov-06	dic-06
B_AS01	BS21	Inferno Lower Bridge	47.20	119.19	145.35
B_AS06	BS21_S01	Lower Fistole Sanza	99.64	104.92	115.41
	BS22	Varco Carro Bridge	37.70	68.14	97.93
B06	BS19	Farnetani Bridge	293.08	342.7742	331.76
B06	BS19	Farnetani Bridge	293.08	342.7742	331.76
B_AS04	BS18	Acquevive Bridge	373.75	414.60	451.32
	BS18_S0N	Farnetani Spring Group	80.66	71.83	119.55
B03*	BS13_US	Upper Stream Sicili Bridge	838.77	975.51	1018.34
B03	BS13	Sicili Bridge	969.99	1106.32	1150.55
	BS13_S0N	**Cillito Spring Group**	131.22	130.82	132.21
B03	BS13	Sicili Bridge	969.99	1106.32	1150.55
B02	BS12	HydroPower	1093.43	1215.79	1377.81
		Mid-Lower Bussento Cathments	123.45	109.46	227.26
B02	BS12	HydroPower	1093.43	1215.79	1377.81
B01	BS01	SS18 Bridge	1534.13	1630.92	1703.68
		W-L Catchments	440.70	415.14	325.88
B_AS02	BS14US	Capello Upstream	291.57	366.24	337.47
B_AS03	BS14DS	Capello Downstream	379.71	457.92	466.61
	BS14_S01	**Capello Spring**	88.14	91.68	129.14

Table 4.7: 2007 spring and river discharge measurement data

Previous Code	gen-07	feb-07	mar-07	apr-07	mag-07	lug-07	set-07	nov-07	dic-07
B_AS01	305.28	193.89	565.15	580.14	256.69	88.16	23.82	97.72	295.93
B_AS06	68.99	114.16	176.35	156.31	76.81	101.64	67.64	102.83	86.61
B06	588.30	434.68	1121.81	1116.61	610.65	172.50	102.71	325.91	604.21
B06	588.30	434.68	1121.81	1116.61	610.65	172.50	102.71	325.91	604.2123
B_AS04	696.88	604.61	2180.19	2219.57	887.65	327.89	318.55	418.82	712.86
B_AS04	696.88	604.61	2180.19	2219.57	887.65	327.89	318.55	418.82	712.86
B03	1295.84	1268.16	1679.45	1759.21	1241.72	1088.48	978.84	1127.33	1450.89
B03*	986.87	938.24	1351.87	1403.25	978.11	889.87	847.12	916.40	1136.69
B03	1295.84	1268.16	1679.45	1759.21	1241.72	1088.48	978.84	1127.33	1450.89
B03	1295.84	1268.16	1679.45	1759.21	1241.72	1088.48	978.84	1127.33	1450.89
B02	1451.45	1389.31	1780.12	1835.42	1375.76	1076.71	1006.11	1381.11	1855.25
B02	1451.45	1389.31	1780.12	1835.42	1375.76	1076.71	1006.11	1381.11	1855.25
B01	1855.56	1782.29	2614.75	2739.56	2405.74	1450.84	1226.29	1675.01	2342.46
B_AS02	357.67	293.24	610.02	770.10	351.36	282.26	282.04	381.38	365.92
B_AS03	478.72	384.39	930.81	1050.67	426.84	367.90	344.15	487.84	451.87

6) Scheme of the Bussento Hydro-system.

On the base of previous data and hydro-geomorphological surveys, a conceptual model of Bussento Hydrogeological System (BHS) was draw-up, as represented in Figure 4.27.

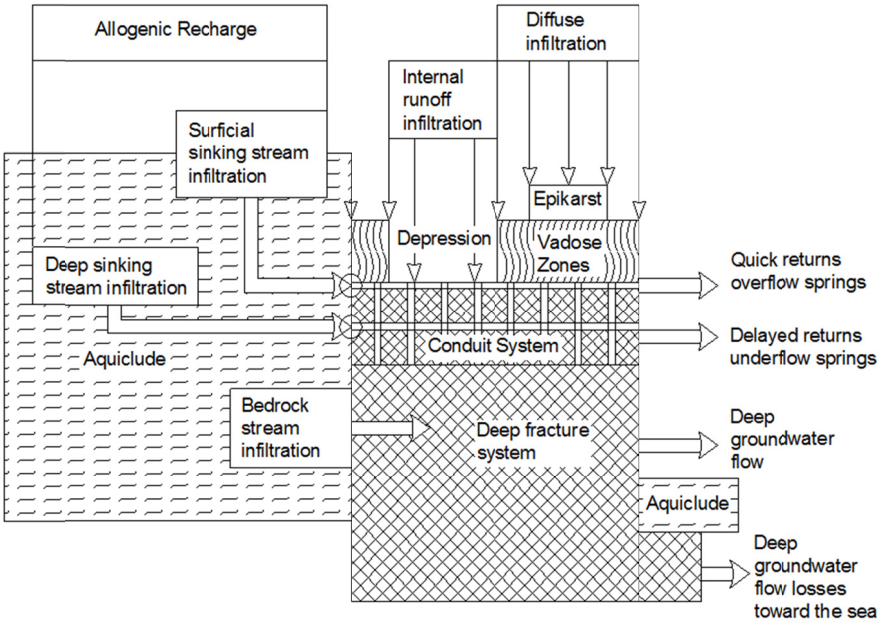

Figure 4.27: Conceptual model of Bussento Hydrogeological System (BHS) (modified from Guida at al., 2003)

Four sources of recharge for karst aquifers can be recognized: i) allogenic recharge; ii) internal runoff recharge; iii) diffuse infiltration recharge and iv) recharge from fractured bedrock streams.

A distinguishing feature of Bussento Hydrogeological System (BHS) is that most of the groundwater is discharged through a small number of large springs. Figure 4.28 illustrates a simplified scheme of the Bussento river surface network indicating the complex interactions between the streambed springs system, which generally results in an increase in river discharge, and the anthropic impact, i.e. the hydroelectric system, which generally results in a decrease in river discharge, retained and diverted within dams, artificial lake and weirs for human water uses.

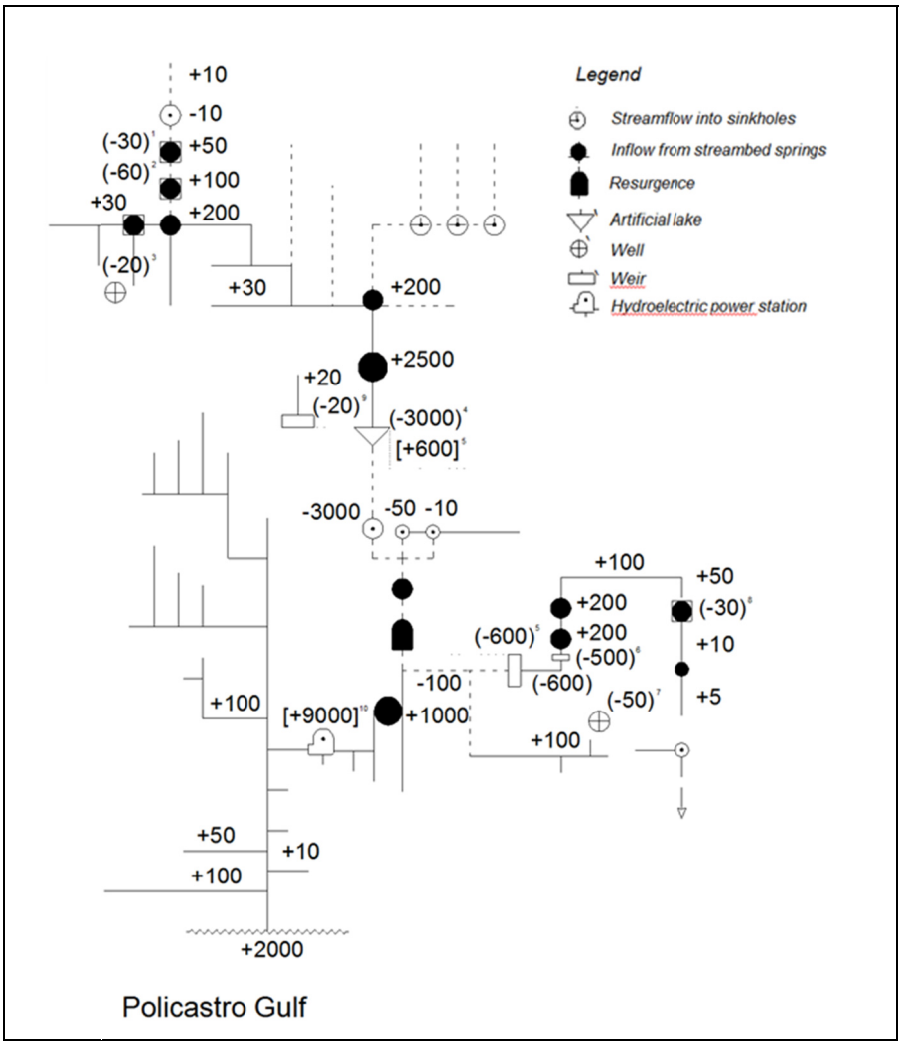

Figure 4.28: Water resources and human uses in the Bussento river basin.

Based on the above hydro-geomorphological considerations and water uses, the definitive Hydro-geomorfological Monitoring System was established, as in figure 4.29 and listed in the table 4.8.

Figure 4.29: Integrate Monitoring System of the Bussento River basin.

Table 4.8: Bussento Monitoring stations

Code	Station Name	Latitude	Longitude	Distance (m)
BS00	Mouth	543605,3366	4435295,3874	0
BS01*	SS18 Bridge	543365,5730	4435974,7175	740
BS02	FS Bridge	542247,8301	4438272,0435	3680
BS03	Vallonaro Creek	541834,8402	4440099,9059	6200
BS12	Hydro-power	543583,6737	4442368,8007	10246
BS04	SS517 Bridge	543412,8693	4442664,5218	10930
BS13*	Sicilì Bridge	546446,5601	4442939,8484	14100
BS15	Capello Oasis	546915,6349	4444081,9437	15580
BS23	Ponte Morigerati	548065,3782	4443510,8961	15995
BS14	WWF Oasis	553475,0352	4445318,3639	22717
BS24	Melette Bridge	557102,7175	4446756,1804	28734
BS25	Bacuta Sinkhole	548948,4602	4447695,8382	20500
BS17**	Sabetta Reservoir	547207,9202	4449424,2903	20900
BS18	Acquevive Bridge	548000,0954	4451699,0969	23534
BS19	Ponte Farnetani	546973,6582	4452744,0284	25550
BS20	Ponte l'Abate	544406,0243	4453604,0162	28460
BS22	Varco Carro Bridge	543049,7711	4454630,4533	30095
BS21	V.ne Inferno Bridge	543083,6774	4454695,1836	30300
BS16	Ciciniello Bridge	545934,8916	4449803,4248	22300

**** Same location of the station having managed by the Campania Regional Civil Defence Sector***
***** Same location of the Bussento at Caselle managed by National Hydrographic Service and Reference station for VAPI Bussento at Caselle.***

4.3 SUB-BASIN MONITORING SYSTEM

On the base of above hydro-geomorphological setting and human use features, the CUGRI and the Environmental Hydro-geomorphological Workgroup of the Salerno University have build-up the Upper Bussento Hydro-geomorphological Monitoring System (UBS_HGMS), according to the National Park of the Cilento and Vallo Diano – Geopark and Left Sele River Regional Basin Authority (figure 4.30).

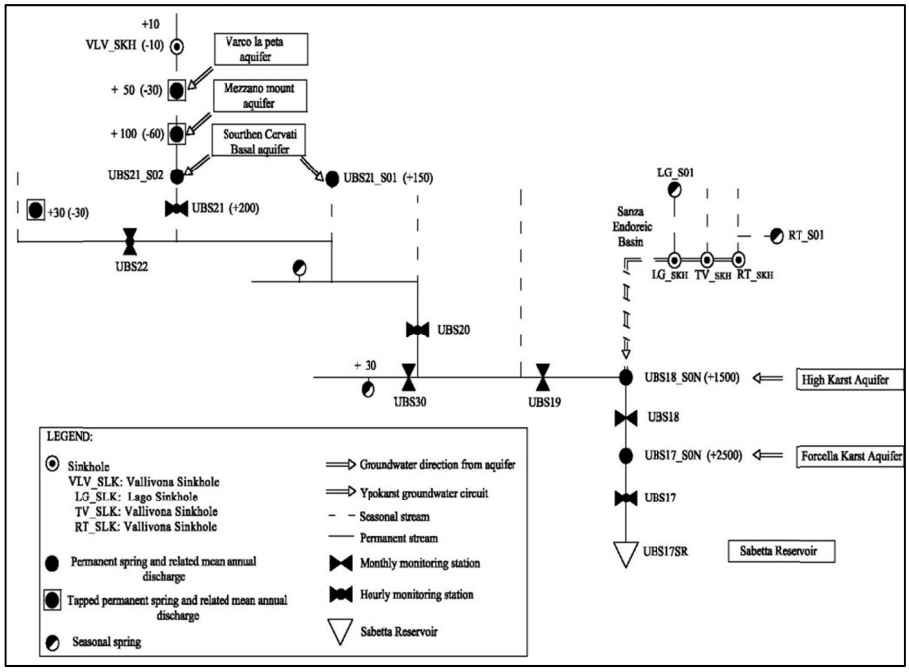

Figure 4.30: Upper Bussento network, hydro-geological features, water resources plant and monitoring stations. (Longobardi et al., 2011)

The UBS_HGMS, designed and managed by the Hydro-Geomorphological Research Group (responsible prof. Domenico Guida and the undersigned ing. Albina Cuomo), has different type of station: main, secondary and temporary. Figure 4.31 and the table 4.9 shown location and listed code, name, geographical coordinates, elevation, distance from outlet station, mean slope of upstream reach (BS17), measurement type and interval of the main station, respectively.

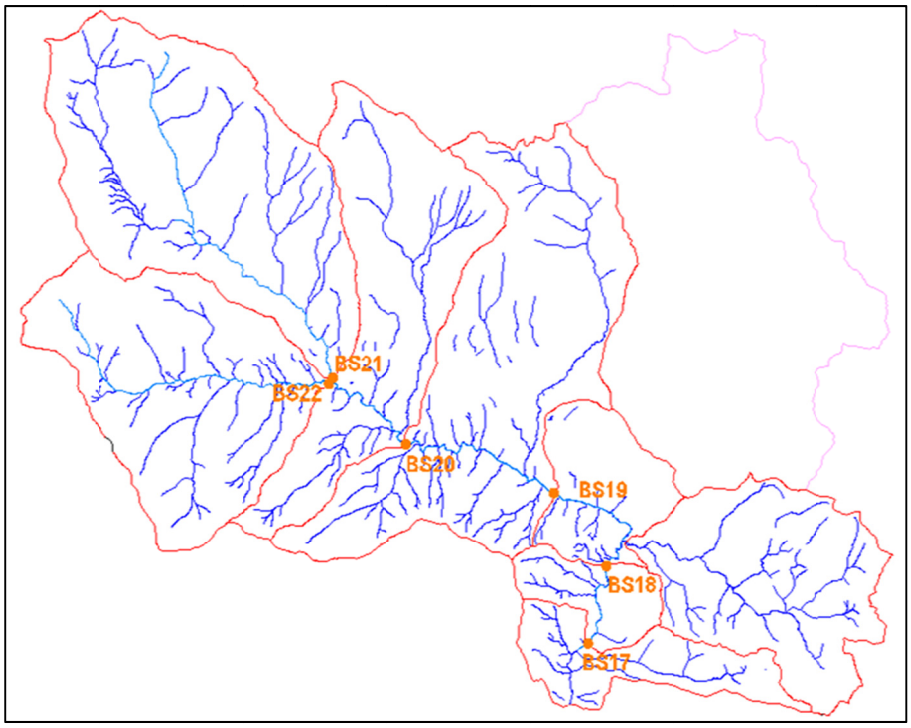

Figure 4.31: Location of the Main Stations of the UBS_HGMS

Table 4.9: Main stations of the UBS_HGMS

Station Code	Station Name	X	Y	Height (m asl)	Distance from BS17	Slope BS17	Measure Type	Measure Time
BS17	Tredici Fistole	2567521,9	4450092	320	0	0	Stage Current-meter	Hourly Weekly
BS18	Acquevive Bridge	2567840,2	4451369	342,69	1526,087	1,486	Current-meter	1.Weekly
BS19	Farnetani Bridge	2566935,5	4452581	373,15	3959,83	1,342	Current-meter	2.Weekly
BS20	L'Abate Bridge	2564359,9	4453401	421,83	7383,24	1,379	Current-meter	1.Weekly
BS21	Lower Inferno Bridge	2563047,4	4454497	463	9516,99	1,502	Stage Current-meter	Hourly Weekly
BS22	Varco Carro Bridge	2563006,5	4454424	464,97	9497,832	1,526	Stage Current-meter	Hourly Weekly

Figure 4.32 and table 4.10 shown and listed code, name, geographical coordinates, elevation of the secondary stations, respectively. The measurement type is carried with current-meter and the measurements are monthly collected.

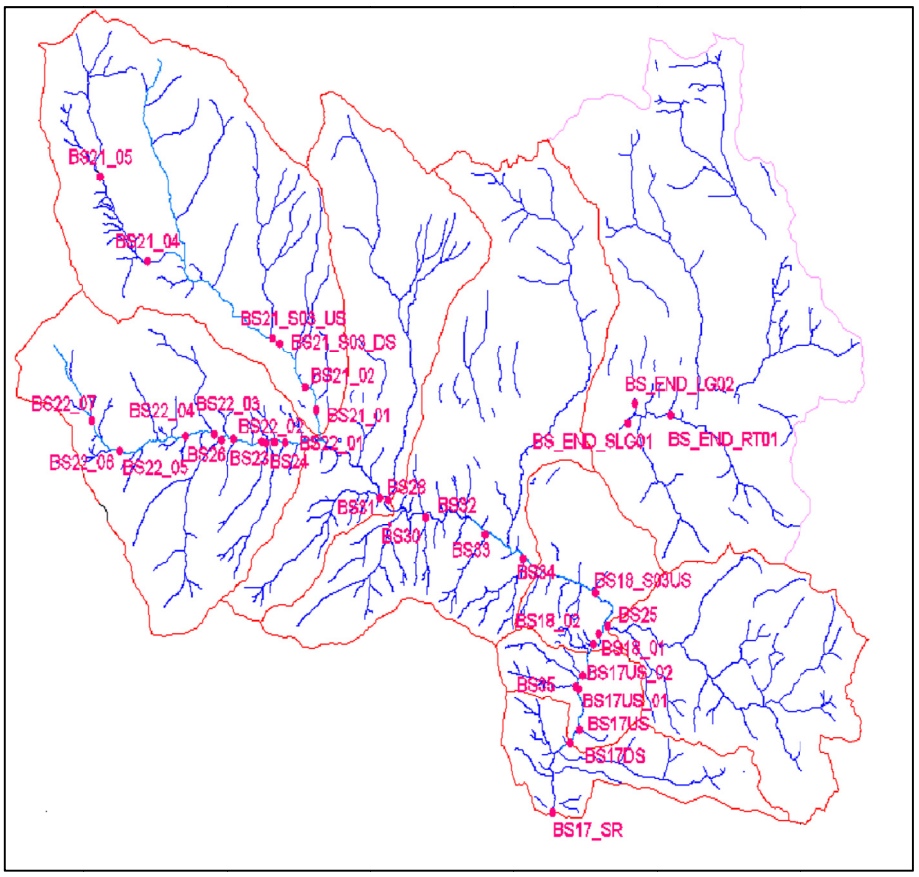

Figure 4.32: Location of the Secondary Stations of the UBS_HGMS

Table 4.10: Secontary stations of the UBS_HGMS

Station Code	Station Name	X	Y	Elevation (masl)
BS17_SR	Sabetta Reservoir	2567354	4449994,5	300
BS17DS	Tredici Fistole DS	2567515,3	4450081,4	318,9
BS17US	Tredici Fistole US	2567672,4	4450262,7	321,6
BS17US_01	Tredici Fistole US_01	2567645,3	4450866,2	332,65
BS35	Vallone Surice	2567605,2	4450878,1	337,57
BS17US_02	Tredici Fistole US_02	2567724,5	4451048,7	336,03
BS18_01	Acquevive Bridge US_01	2567917,4	4451496,4	346,6
BS18_02	Acquevive Bridge US_02	2568012,2	4451637,9	352,53
BS25	Vallone Paolo	2568191,6	4451773	364,09
BS18_S03US	Farnetani Springs US	2567945,8	4452231,8	360,72
BS19DS_S01	Salice Spring DS	2567845,8	4452221,8	373,9
BS34	Vallone Nocella 2	2566724	4452701	377,43
BS33	Vallone Nocella 1	2566014,2	4453072,9	392,62
BS32	Vallone Giardino	2564914,6	4453315,8	414,05
BS30	Vallone Giumenta	2564318,8	4453225	429,11
BS28	Vallone Secco	2564251,7	4453565,6	425,99
BS31	Vallone Rosso	2564125,8	4453607,8	428,755
BS21_01	Upper Fistole Bridge	2562959,6	4454838,7	481,05
BS21_02	Upper Inferno Bridge	2562769	4455172,6	518,24
BS21_S03_DS	Montemezzano Spring DS	2562315,4	4455807,4	614,62
BS21_S03_US	Montemezzano Spring US	2562191,2	4455884,6	632,41
BS21_S04DS	Varco La Peta Spring DS	2560651,4	4456717,6	952,41
BS21_S04US	Varco La PetaSpring US	2560310,6	4456709,7	1172,49
BS21_04	Vallivona Sinkhole	2559962,4	4456967,1	1126,69
BS21_05	Ruscio Bridge	2559153,9	4458179,8	1264,09
BS22_01	Panniere DS	2562425,6	4454383,4	486,98
BS24	Vallone Panniere 2	2562190,9	4454397,5	507,14
BS23	Vallone Panniere 1	2562088,3	4454353,6	517,38
BS22_02	Caccialupi	2562007,9	4454381,8	509,83
BS22_03	Crepabuoi	2561494,9	4454435,7	546,7

BS26	Vallone Pezza	2561241,3	4454419,5	572,92
BS22_04	Vallone Pezza US	2561141,6	4454496,7	579,62
BS22_05	Persico Bridge	2560633	4454480,4	624,71
BS22_06	Cornitiello	2559476,1	4454256,9	736,97
BS22_07	Mezzana Bridge	2558971,5	4454703,6	847,54
BS_END_LG01	Lago Sinkhole US	2568530,7	4454671,4	497,61
BS-END_LG02	Taverne Lago DS	2568661,8	4454940,9	500,51
BS_END_RT01	Rio Torto Sinkhole US	2569313,5	4454784,9	503,42

Figure 4.33 and table 4.11 shown and listed code, name, geographical coordinates, elevation of the spring stations, respectively. The measurement type are indirect, specifically the discharge is calculated as Upstream-Downstream difference discharge measurements.

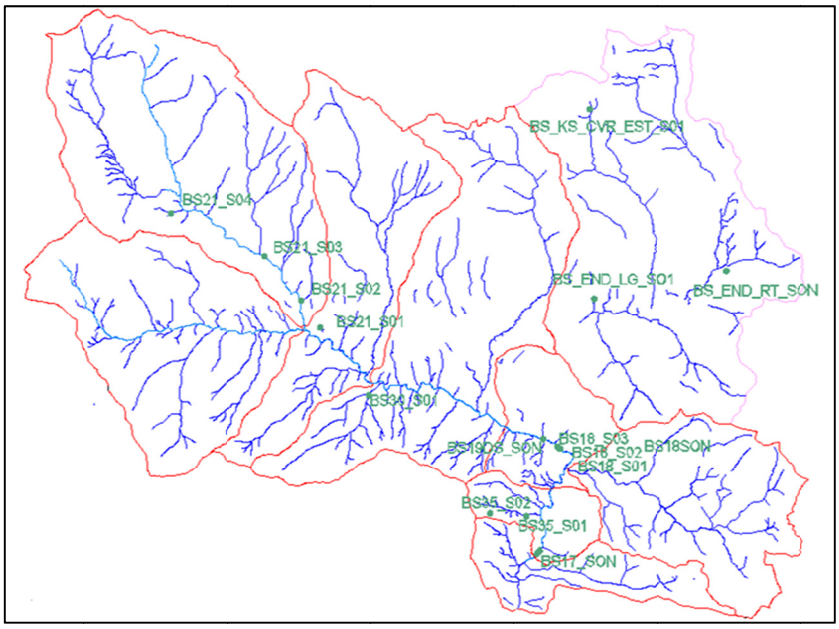

Figure 4.33: Location of the Spring Stations of the UBS_HGMS

Table 4.11: Spring stations of the UBS_HGMS

Code	Spring Name	X (m)	Y (m)	Z (m)
BS17SON	Tredici Fistole Spring Group	2567578	4450192	320,2
BS18SON	Farnetani Spring Group	2567998	4452169	358,9
BS19DS_SON	Bonomo Mil Spring Group	2567680	4452349	364,2
BS30_S01	Giumenta Spring	2564271	4453127	437
BS21_S01	Lower Sanza Fistole Spring Group	2563307	4454458	475
BS21_S02	Upper Fistole Sanza Spring Group	2562974	4455003	493,9
BS21_S03	Montemezzano Spring	2562288	4455877	650
BS21_S04	Varco La Peta Spring	2560440	4456657	1108
BS_END_LG_S01	Lago Spring	2568657	4455005	502,7
BS_END_RT_SON	Rio Torto Spring	2571200	4455540	550
BS_KS_CVR_EST_S01	Est Cervati Spring	2568570	4458656	1025

Figure 4.34 and table 4.12 shown and listed code, name, geographical coordinates, elevation of the creek-Bussento confluence stations, respectively, where visual observations are temporary make.

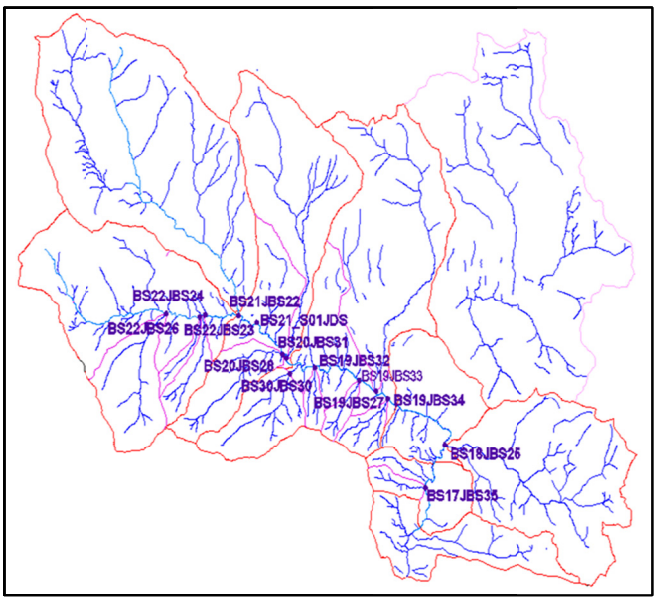

Figure 4.34: Confluence stations of influent Creek-Bussento of the UBS_HGMS

Table 4.12: The Creek-Bussento confluence stations of the UBS_HGMS

Code	Name	X (m)	Y (m)	Elevation (m)
BS17JBS35	Vallone Surice	2567645,38	4450886,1	332,78
BS18JBS25	Vallone di Paolo	2568108,11	4451768,75	352,74
BS19JBS34	vallone Nocella 2	2566730,38	4452716,22	375,73
BS19JBS27	Vallone Diavoli	2566433,79	4452858,58	381,55
BS19JBS33	Vallone Nocella 1	2566026,98	4453090,07	388,21
BS19JBS32	Vallone Giardino	2564934,26	4453356,72	408,48
BS19JBS30	Vallone Giumenta	2564586,28	4453400,73	416,53
BS20JBS28	Vallone Secco	2564225,58	4453560,29	425,39
BS20JBS31	Vallone Rosso	2564155,35	4453611,59	428,38
BS21_S01IDS	Fistole Sanza Basse	2563503,26	4454252,3	446,97
BS21JBS22	Persico Inferno	2563063,91	4454417,08	461,79
BS22JBS24	Confluenza Vallone Panniere 2	2562222,8	4454420,79	499,18
BS22JBS23	Confluenza Vallone Panniere 1	2562076,84	4454380,06	508,52
BS22JBS26	Confluenza Vallone Pezza	2561270,08	4454452,18	565,91

Figure 4.35 and the table 4.12 shown and listed code, name, geographical coordinates, elevation of the sinkhole stations, respectively, were visual observations and temporally measurements are make.

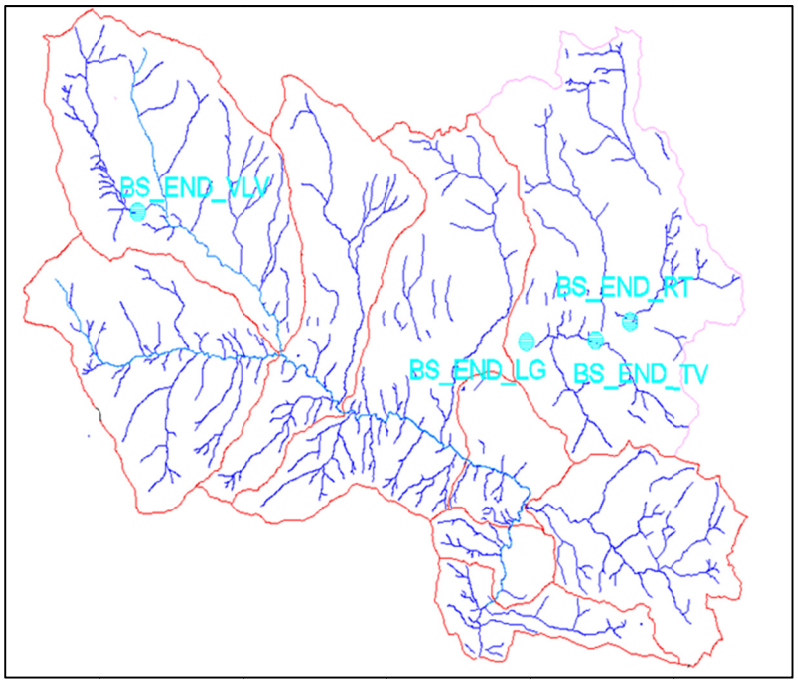

Figure 4.35: Location of the sinkhole station of the UBS_HGMS

Table 4.13: The sinkhole station of the UBS_HGMS

Code	Name	X [m]	Y [m]
BS_END_LG	Lago	2568273,2	4454550,1
BS_END_RT	Rio Torto	2570506,1	4454935
BS_END_TV	Taverne		
BS_END_VLV	Vallivona	2560027,7	4456981,5

4.4 WEEKLY DELAYED AND BASE FLOW DIRECT MEASUREMENTS

The direct discharge measurements were carried out using the Swoffer 3000 current meters (figure 4.36).

Figure 4.36: Current meter Swoffer 3000

The protocol used was DISCH (figure 4.37) and the collected data of water depth, velocity and discharge were processing with a form (figure 4.38) and implemented in a specific data base.

Figure 4.37: Direct discharge measurements with Swoffer 3000.

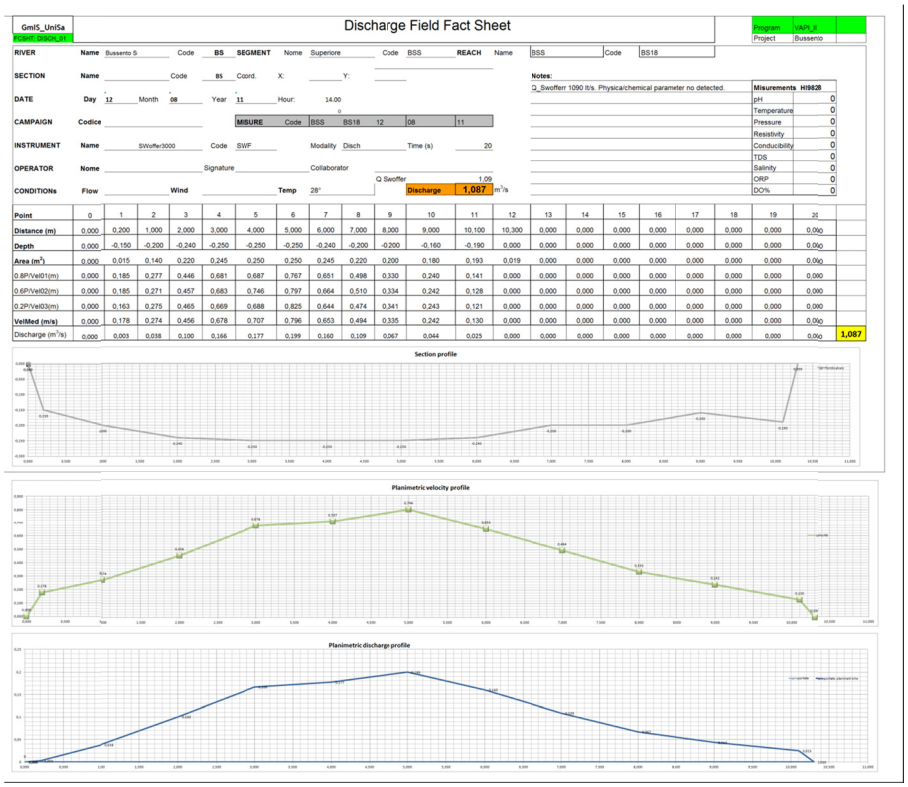

Figure 4.38: Fact sheet for discharge field measurements.

Following the systematic procedure above described, since November 2009 streamflow discharge data were collected. The figure 4.39 shown as example, the annual 2009-2010 streamflow hydrographs collected weekly at the BS21 and BS22 river stations.

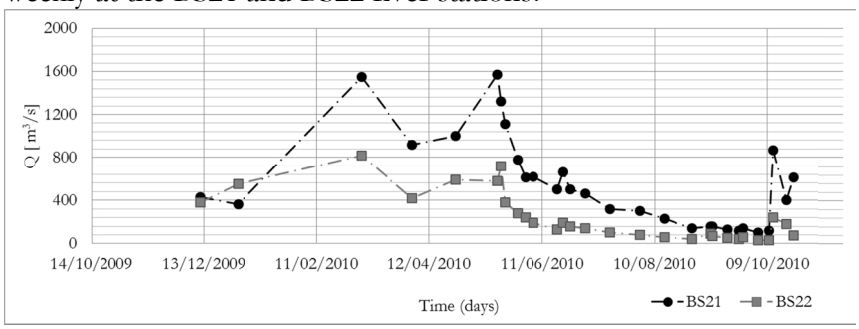

Figure 4.39: The annual hydrographs of the streamflow collected weekly at the BS21 and BS22 river stations in the 2009-2010 years.

4.5 AUTHOMATIC, INTEGRATE HOURLY MONITORING REGISTRATIONS

The three stations BS17, BS21 and Bs22 were equipped by authomatic measurement and registration of water level, using DL/N70 Data Logger (STS spa). At the BS21 station, a Data Logger with hourly Temperature and Electrical Conductivity was placed. An example of integrate measurements at BS21 is shown in the figure 4.40.

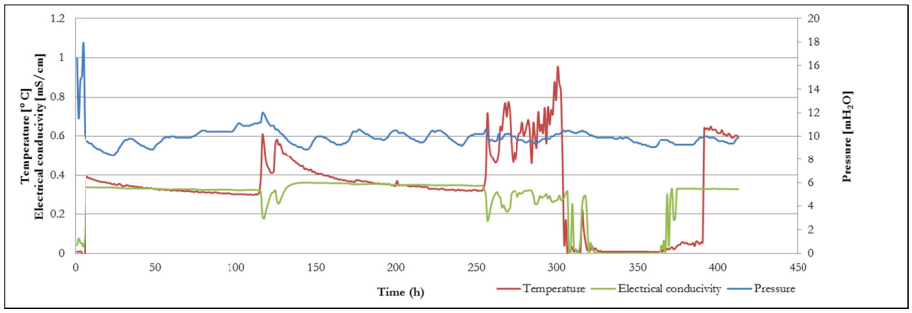

Figure 4.40: Integrate measurement plots (Water Level, Temperature and Electrical Conductivity) at BS21 (Inferno Bridge) station during the November 2010 Flood Event. Note the no-registration due to instrument damage (fig. 4.41).

Figure 4.41:The instrument damage at BS21 station during the 10-11 November 2010 flood event.

The weekly discharge dataset are used to calculate the relationship existing between the water-surface stage and the simultaneous streamflow. Stage-discharge relation was made for the BS21 and BS22 sections (figures 4.42 and 4.43).

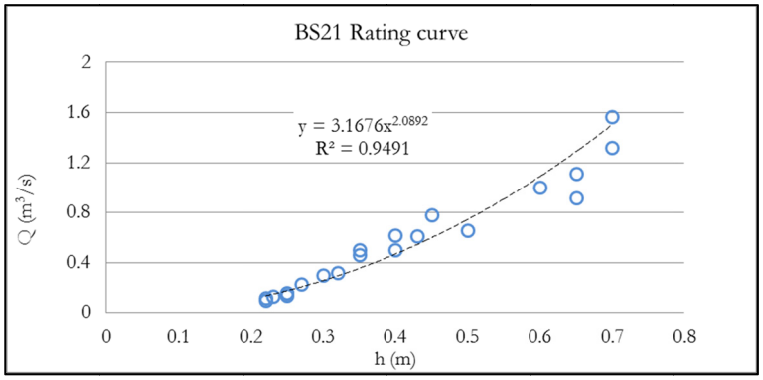

Figure 4.42: Rating curve of the BS21 river section

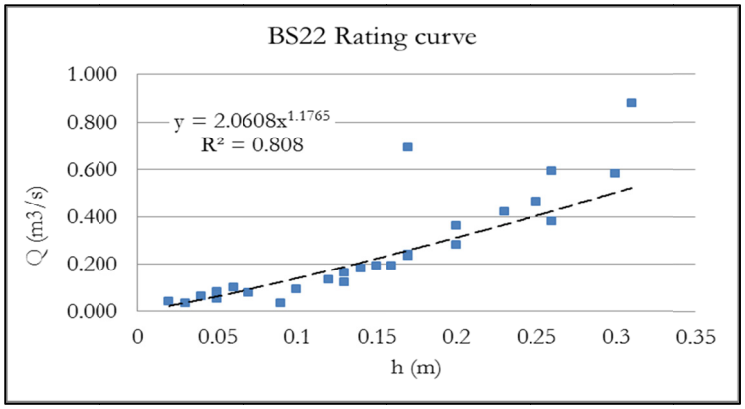

Figure 4.43: Rating curve of the BS22 river section

Figures 4.44 and 4.45 shown exsamples of hydrographs detected at the BS21 and BS22 stations, used in the following chapter to testing the procedure for the the implementation of the hydro-geomorphotypes in runoff-rainfall transformation models at catchment scale.

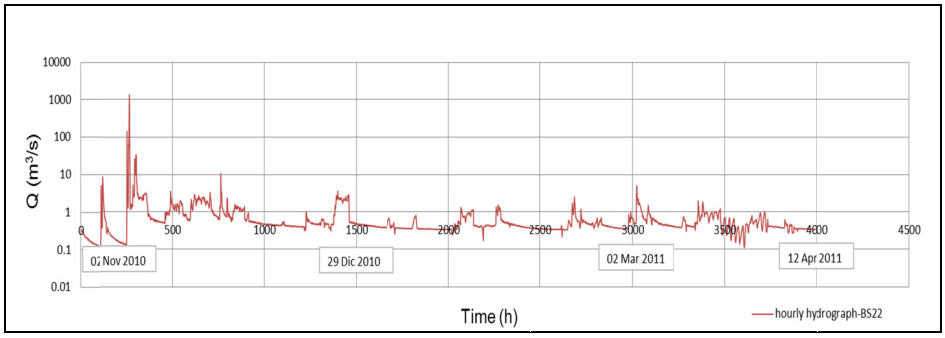

Figure 4.44: Hydrograph performed with hourly stream flow data colleted at the BS22 river station.

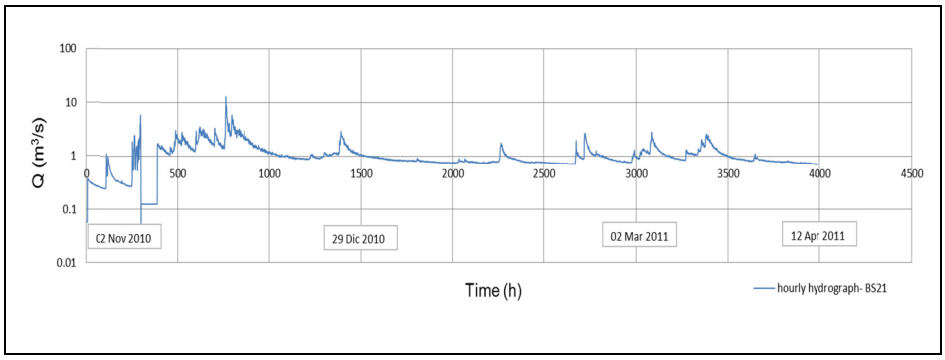

Figure 4.45: Hydrograph performed with hourly stream flow data collected at the BS21 river station. In the circle, the no-data detection

4.5.1 Radon-222 measurements

As previously cited, in addition to the streamflow and physical measurements, were carried out measurements of Radon (222-Rn) activity concentration using RAD7 detector at the river and spring stations.
Radon data will be used as isotope aid in hydrograph separation techniques (Longobardi et al., 2011). Figures 4.46-4.48 shown the time variability of Radon concentration in stream and spring of some river stations of the Bussento.

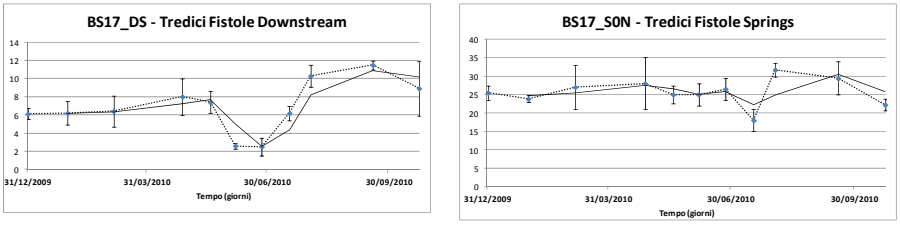

Figure 4.46: Temporal Radon concentrations pattern at the BS17 and BS17_S0N spring stations

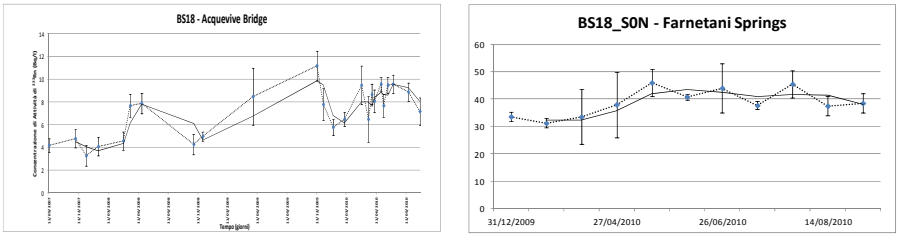

Figure 4.47: Temporal Radon concentrations pattern at the BS18 and BS18_S0N spring stations

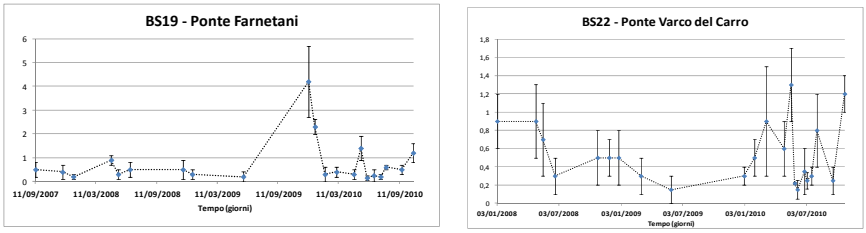

Figure 4.48: Temporal Radon concentrations pattern at the BS19 and BS22 stations

5 THE OROGRAPHIC BARRIERS

5.1 INTRODUCTORY REMARKS

This chapter illustrates the first main topic of the research: the procedure adopted for the objective identification and delimitation of mountains, as orographical features influencing meteorological and hydrological analysis.
This topic is useful for the hydrologists for two main raisons: i) the orography or the mountains are the most important sources of freshwater ("*water towers*") for the adjacent lowlands and plains (Viviroli et al. 2004, 2007, 2011); ii) the presence of a mountainous orography acts as a barrier for a normal movement of the wet air masses influencing the distribution, intensity and persistence of the precipitations (Roe et al., 2005). The above raisons gives a double, relevant importance to the orographical issues in hydro-geomorphology, both on the rainfall and the runoff production. The present chapter deals with the above last topic and it is organized as follows. The paragraph 5.2 introduces the need of an interdisciplinary approach between geomorphology and atmospheric sciences in orographic precipitations (Garlewsky et al. 2008) and points-out on the scientific background about importance of the orographic barrier in global, continental and local scales of atmospheric circulation (Roe, 2005). The paragraph 5.3 discusses a short systematic review on the methods and modeling of the orographic precipitation at international, national, academic and institutional level. The paragraph 5.4 introduces and synthesizes the researches carried out by the hydrological research group of the University of Salerno, directed by the profs. Fabio Rossi and Paolo Villani about the role of the orographic barriers on extreme rainfall events and the importance of their objective identification and delimitation at multi-scale levels.

The paragraphs 5.5 to 5.8 illustrate the results of the original researches carried out by the writer, from GIS-based procedures and methods (5.5), to multiscale mapping and applications.

5.2 INTERDISCIPLINARY APPROACHES AND SCIENTIFIC BACKGROUND

In the recent years a growing attention arises about the link between geomorphology, atmospheric sciences and other disciplines, as hydrology and ecology (Galewsky et al. 2008).
The workshop held in Boulder (Col. USA) in the October 2007, has focused the need of interaction especially between the orographic precipitations and regional and global dynamics. During the workshop, geomorphologists, atmosphere scientists and hydrologists give a great interest in the integrated studies concerning hydrological cycle, particularly in land/atmosphere interactions as wind dynamics, precipitation distributions and evaporation (Pielke, 2001).
Of all the meteorological phenomena, the most relevant in humid regions are precipitations delivered by atmosphere to the landscape as intense rainfalls and storms. The physical basis of the storms events is sufficiently well understood, whilst the understanding of extreme events and ability to accurately and quantitatively predict precipitation location and magnitude is still limited (Sun et al., 2007).
Within the general statements of the geomorphology, hydrology and atmospheric science, the most important issues are the real-time monitoring technology and high-resolution atmospheric modeling in understanding main factors controlling both topographically-driven climate and geomorphic processes.
The state-of-the-art in atmospheric researches, developed on body of theory based on the general principles of geophysical fluid-dynamics, provides good explanation for the basic pattern of the large-scale atmospheric circulation and allows to perform useful weather predictions. At the present, most of the climate models work less well at regional and basin scale and, especially in forecasting location, intensity and frequency of extreme events.
Process models do not have a predictive capability, but have produced valuable insights into the processes mostly relevant to geomorphology,

i.e. precipitations in mountainous regions (Rotunno and Ferretti 2001, Miglietta and Rotunno, 2005), the development of mid-latitude and tropical cyclones (Thorncroft et al., 1993) and organized moist convection (Robe and Emanuel, 2001).
One of main scientific goals of the above cited workshop was, letterally (Galewsky et al., 2008) : " *we need a global survey of geomorphic processes and morphology (landscape metrics, or geomorphometry) the examines its dependency on the probability distribution of climate*" and weather.
Another interdisciplinary research field suggested during the workshop was a new perspective on orographic precipitations such as the development of linear models, isotopic signatures of drying ratios.
One of the exciting challenges that geomorphology researches offer to atmospheric sciences is the need to understand occurring weather systems across a wide range of spatial-time interacting scales, from seconds-parcel scale to hundreds of years-continental scale, and beyond (Holley, B. P. 1969).
Meentemeyer (1989) pointed-out that in geographical related disciplines, as atmospheric science, geomorphology and hydrology, scale has always been a major issue, debating about the appropriate and shared scale of analysis for various processes (Nir, 1987).
The above authors proposed a correspondence among time scales, scales of the atmospherical variables and more frequently used topographical variables (Basist, 1989) in orographic precipitation studies (Table 5.1).

Table 5.1: Correspondences between the time scale, atmospheric parameter and topographic variables (modified from Meentemeyer, 1989)

Time	Atmospheric variable	Topographic variable
Minute	Local convenction, dew point depression	Slope %
Hour	Feedere cloud, potential instability, wind speed	Orientation, Elevation
Day	Synoptic events, Vorticity, Short-wave pattern	Esposure
Year	Precipitable H_2O, Upper level divergence, Baroclinic zones, SST and ENSO	Elevation, Slope Orientation

5.3 OROGRAPHIC PRECIPITATIONS: MECHANISMS AND MODELLING

The presence of relief on the land surfaces assumes a central role for studying the dynamics of the earth science events. Significant interactions between climate and topography play a primary role in external geodynamics and landscape evolution (Bush et al., 2004).
Mountain range creation affects deeply the mesoscale weather and climate of a landscape. Landscape topography and its changes depend to a large extent on the complex interactions between hillslope and channel processes, controlled by regularly exceeding thresholds for runoff erosion during large and heavy storms (Horton,1945; Montgomery and Dietrich, 1989).
Consequently, rainfall is one of the most important factors in hillslope evolution, coupling with fluvial network characteristics and dynamics, as erosion/flooding processes, primarily in active mountain belts (Bonnet and Crave, 2003; Coppus and Imeson, 2002; Tucker and Bras, 1998).
Over long span of time, the influence of the orogenic belt creation on climatic change at continental scale is recognized. Many studies over the last 30 years focused on investigating the large-scale variability of the Asian monsoon climate with respect to the role of the Tibetan Plateau (e.g. Hahn and Manabe 1975, Murakami 1987, 1983; Webster, 1987).
The terrain variations (e.g. orography, surface characteristics) possessing mesoscale spatial dimensions can provide a direct forcing of the atmosphere and its processes, as external mesoscale forcing. The topographic relief is the best first-order meso-scale rainfall predictor and the relief changing along an orocline can alter rainfall distribution (Bookhagen and Strecker 2008). Rainfall enhancement in intensity, frequency and distribution on windward mountain flanks is highly variable and results from complex atmospheric-orographic interactions (Barros and Lettenmaier, 1994, Roe 2005).
Over short-term, orographic barriers influence the annual, monthly and daily distribution, intensity and frequency of precipitations (Roe 2005). In fact, on a smaller scale, on a mountain basins with prevailing wind, precipitation is enhanced on the windward side of mountains and much reduced on the lee side (Jiang 2003).
Besides, precipitations, associated with orographic forcing, results an order of magnitude bigger than the other events, such as frontal precipitation (Smith and Bastard, 2004). Following Orlanvski (1975),

macro-, meso- and micro-scale hierarchy in climate analysis can be recognized. To each of above climate scenarios, specific atmospheric events, selected control factors and space-time range can be related (Table 5.2).

Table 5.2: Atmospheric scale definitions (modified from Lin, 2007)

Horizontal Scale	Lifetime	Stull (1988)	Pielke (2002)	Orlanski (1975)	Thunis and Bornstein (1996)	Atmospheric Phenomena
10 000 km	1 month	Macro	Synoptic Regional	Macro-α	Macro-α	General circulation, long waves
2000 km	1 week			Macro-β	Macro-β	Synoptic cyclones
200 km	1 day		Meso	Meso-α	Macro-γ	Fronts, hurricanes, tropical storms, short cyclone waves, mesoscale convective complexes
20 km	1 h	Meso		Meso-β	Meso-β	Mesocyclones, mesohighs, supercells, squall lines, inertia-gravity waves, cloud clusters, low-level jets thunderstorm groups, mountain waves, sea breezes
2 km				Meso-γ	Meso-γ	Thunderstorms, cumulonimbi, clear-air turbulence, heat island, macrobursts
200 m	30 min	Micro	Micro	Micro-α	Meso-δ	Cumulus, tornadoes, microbursts, hydraulic jumps
20 m	1 min			Micro-β	Micro-β	Plumes, wakes, waterspouts, dust devils
2 m	1 s	Micro δ		Micro-γ	Micro-γ	Turbulence, sound waves
					Micro-δ	

The orography-induced precipitations are related to meso-scale β scenarios with a 20 Km space dimensions and the day as temporal span. The orography inducing effects on atmospheric flow can produce or modify precipitating clouds through orographic lifting, triggering of convection, indirect effects of flow splitting or blocking, and induced waves (Figure 5.1). The common mechanism of orographic precipitation is the "stable upslope ascent" (figure 5.1 a). This mechanism occurs when forced mechanical lifting of air impinging on the windward flanks leads to cooling of the air column, resulting in condensation and precipitation. Descent in the lee side leads to warming and drying and precipitation is suppressed. If the atmospheric conditions are stable the air mass flow may get diverted around the mountain or it may stagnate (fig. 5.1 b). The blocked air can cause ascent further windward of the range and can also enhance the lifting and hence the precipitation that does occur.

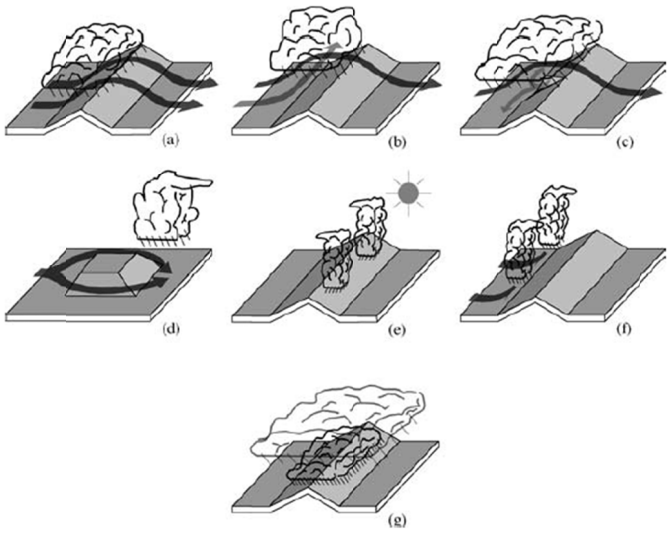

Figure 5.1: Mechanisms of orographic precipitation: (a) Seeder-feeder mechanism; (b) upslope condensation; (c) upslope triggering of convection; (d) upstream triggering of convection; (e) thermal triggering of convection; (f) leeside triggering of convection; (g) leeside enhancement of convection. Slanted lines below cloud base indicate precipitation. (from Roe 2005).

Melting and evaporating precipitation cools the air through which it falls and the result can be strong down-valley air flow (fig. 5.1 c); it is

possible, too that the diverted airflow itself can leads precipitation in the convergence region in the lee of the range, where ascent occurs (fig. 5.1d). Orographically induced clouds can take the form of cumulus or cumulonimbus when the air subjected to lifting is sufficiently moist and unstable (Figure 5.1 e): if the orography lifts air above its level of free convection (the level at which it becomes less dense than the surroundings) it will continue to rise. Thermal forcing occurs when daytime heating produces an elevated heat source and a corresponding thermally direct circulation, with convergence and convection at the top of the mountain (Figure 5.1f): this is responsible of the afternoon thunderstorms in summer (Roe 2005). Another effect is the "seeder-feeder" mechanism according to which precipitating hydrometeors that originate from a cloud layer aloft (the "seeder" cloud) grow at the expense of the water content of a cloud below (the "feeder" cloud) which, by itself, might not precipitate (Figure 5.1 g). Stratus and small cumulus clouds orographically formed over hills or mountains can be particularly effective feeder clouds. It is recognized however, that the complex interactions between cloud dynamics and microphysics, and orographic forcing are far from being completely understood.

The shape of the mountain can also have a significant influence on the intensity and distribution of precipitation. In the case of a concave ridge, the forward-reaching ridge arms inhibit diffluence upstream of the ridge and intensify the high pressure perturbation that develops on the windward slope (Jiang 2006). Watson and Lane (2011) pointed out on how the terrain geometry (straight, convex or concave ridge) influences the orographic precipitation dynamics.

Basics aspect of orographic precipitation have been recently reviewed by Roe (2005) and Smith (2006), highlighting influences of aspect and shape of the orographic barriers.

Several studies has been focus on the interaction between the topography and the patterns of precipitation, in order to predict flash floods, landslides, avalanches (Roe 2005). All these natural hazards, are mainly impacted by precipitation intensity in mountainous regions (e. g., Caracena et al. 1979, Caine 1980, Conway and Raymond 1993).

5.4 SALERNO UNIVERSITY MODEL OF THE OROGRAPHICALLY - INDUCED EXTREME-RAINFALL EVENTS

In Italy and, in particular, in Campania region, where flood induced by the local extreme rainfalls are of first order of frequency, the problem of the orographic precipitation is strongly felt.
The hydrology research group of the University of Salerno, directed by the profs. Fabio Rossi and Paolo Villani, since 1998 highlights the importance of the orographic barrier on the distribution, intensity and frequency of the extreme rainfalls.
Rossi et al. (2005) presented at the European Geosciences Union (EGU) the first study on the orographic barrier in the Campania region where was build up the law on the variation of the rainfall intensity and the morphometric features of the barrier.
Successively, the research group of Rossi (2006) presented, at the National Conference of Hydraulics and Hydraulics Engineering in Rome (HYDRA 2006), the geostatistical study on the regional analysis of the annual mean precipitation detected in a rain-gauges set influenced by the orographic barrier of the Cilento sub-region (Longobardi et al., 2006). At the same conference the Prof. Rossi, in his oral presentation, point out on the simplified meteo-morphological model on the extreme event orographically induced presented at the EGU in the 2005 (Rossi et al., 2005). The proposed model was based on simple regressions, linear on the windward side and power regression on the leeward side.
On the upwind hillslope the linear model is between the amplification factor **Y** of the precipitation, derived from the ratio between the intensity of the precipitation on a plain $\mathbf{p_1}$ (figure 5.2) and that at the beginning of the orographic barrier p_2 (figure 5.2), and the mean slope of the hillslope (**X**):

$$Y = 1 + a_1 \cdot X \qquad \textbf{Equation 5.1}$$

Where a_1 is constant value equal to 1.15.

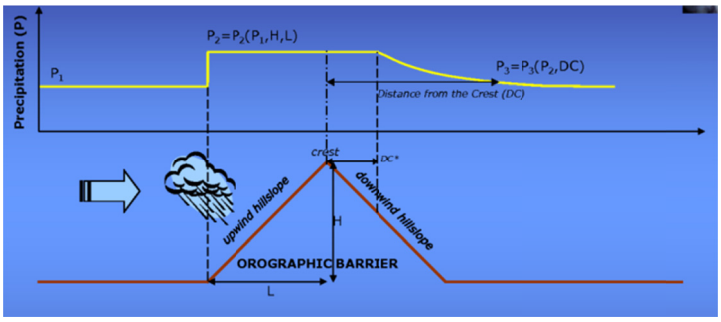

Figure 5.2: Schematic representation of the orographic barrier and the precipitation pattern related (from Rossi et al., 2005)

The model on the downwind hillslope is a power regression between the attenuation ratio (Z) and the distance of the rain-gauges station from the summit of the orographic barrier (u).

$$Z = a_3 \cdot u^{-a4}$$ **Equation 5.2**

The constants a_3 and a_4 have a value respectively equal to 21.08 and 0.37.
The recent italian literature about the topic relates the distribution of the precipitation only to the slope of the orographic barrier, otherwise other researchers took into account other factors, following Spreen (1947) that considered other factors as slope, orientation, exposition, relative relief and gradient of hillslope. Other studies have shown as the transversal amplitude of the orographic barrier influences the amplification and distribution of the precipitation (Rossi et al., 2005; Smith 2006; Bastard et al. 2007).
For years, the research studies on the orographic barriers were oriented on the analytical models performed on an idealized barrier, with an ellipse form. The above cited study of the University of Salerno was carried out on the mean value of the annual maximum precipitation pattern compared to the slope of the hillslope of the orographic barriers identified on the base of an expert judgment.
So, the central problem on the study of the orographic precipitations for the hydrological issue is to identify and delimitate objectively the boundaries and extention of the orographic barriers, in order to provide geomorphometric bases to more sophisticated physically based models.

5.5 GIS-BASED HIERARCHICAL, MULTISCALE OROGRAPHIC BARRIERS: CONCEPTS AND PROCEDURES

As above discussed, the interactions between the orographic barriers and wet air masses flow have different effects on the timing scale, at a mega-, meso - or micro- scale. So, in the present research, the choice was oriented to adopt a hierarchical-multiscale approach in order to allow the interdisciplinary researches among the geomorphology, the orography and hydrology.
Following specific references (Dramis et al. 2011, Orlavsky 1975), the table 5.3, proposes a comparative hierarchical scheme on the linkage between geomorphologic, climatic, and orographic entities here introduced.

Table 5.3: Space-temporal hierarchy of atmosphere phenomena (modified from Orlanvsky, 1975), geomorphologic entities (modified from Dramis et al., 2011) and the orographic taxonomy proposed in Cuomo et al. (2011) and adopted in the present study.

Level	Area (Km^2)	Scale	Geo- morph. Entity	Orography	Climate Entity	Meteo-phenomena
I	10^6	$1:15^6$	Continent	Orogen	Macro-scala α	Global circulation, long wave
II	10^5	$1:10^6$	Physiographic system	Belt	Macro-scala β	Baroclinic wave
III	10^5	$1:5^5$	Physiographic domain	Chain	Meso-scala α	Frontal systems, cyclones
IV	10^4	$1:2,5^5$	Physiographic region	System	Meso-scala β	Orographic effect
V	10^3	$1:1,0^5$	Physiographic provence	Range	Meso-scala γ	Storm systems
VI	10^2	$1: 5^4$	Morphologic system	Group	Micro-scala α	Storms
VII	10^1	$1:2,5^3$	Morphologic complex	Complex	Micro-Scala β	Tornadoes
VIII	10^0	$1:5^3$	Morphologic unit	Unit	Micro-scala γ	Storm cells

The comparative table was a guidelines to attempt a reasonable definition of the orographic entities.

So, the aim of this study is to build-up a GIS-based procedure to extracting and defining the orographic barrier at different scales within the Campania-Lucanian Apennine.
Considering that the expected results might be useful to improve the amplification and attenuation orographic factor in the coordinate GIS-based orographic precipitation models, in the following paragraphs the procedure will be described in detail and the resulting maps will be discussed.

5.5.1 GIS-based multiscale recognition

For the identification and delimitation of the orographic barriers an innovative procedure will be presented in this paragraph.
The materials utilized in the procedure were the regional technical map of the Campania region at a 1.5.000 scale (CTR-1998) from which was performed the DEM map with a cell size 20×20 m. The DEM was optimized with a specific GIS tools in order to eliminate the fill and the sinks (figure 5.3).

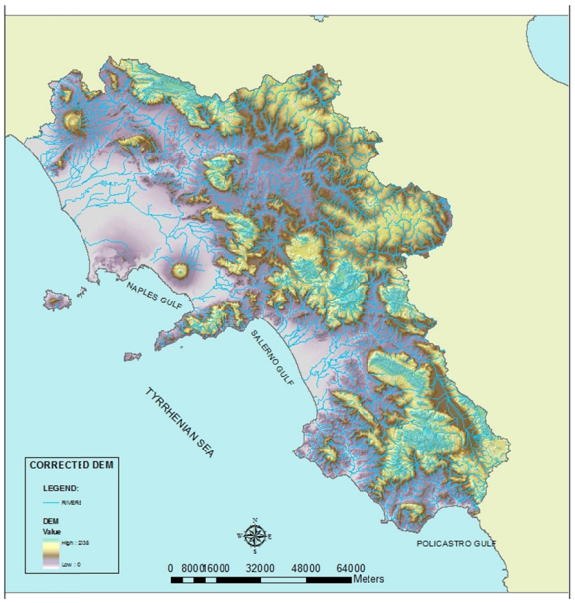

Figure 5.3: The DEM map of the Campania Region with a cell size 20×20 m

The methodology, as shown in figure 5.4, involves two distinctive and integrated procedures automatized in the Gis software, adopting the basic knowledge of the differential geometry and the classical geomorphometric functions.

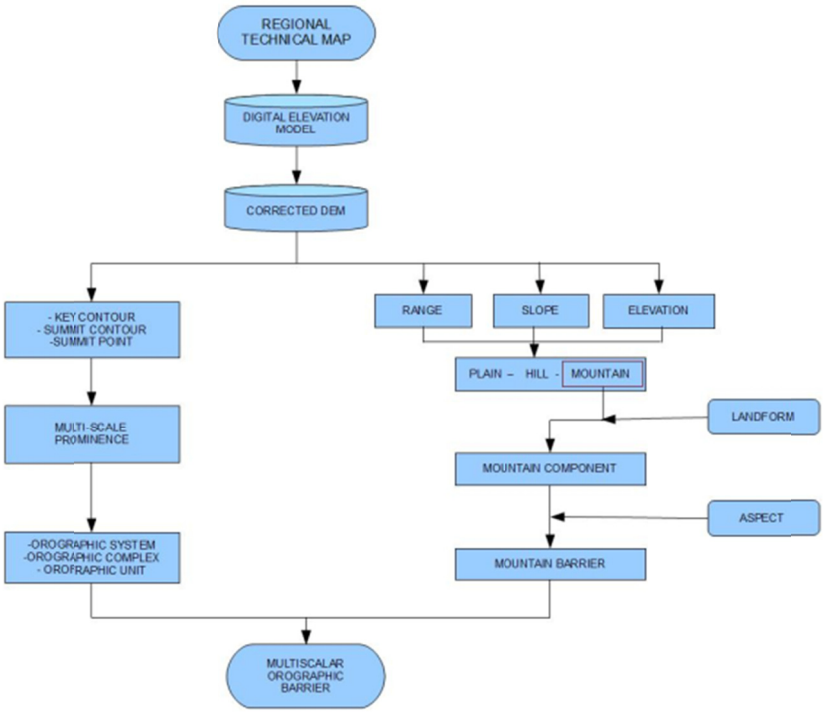

Figure 5.4: Flow chart on the procedure adopted for the identification of the orographic barriers (from Cuomo and Guida 2010 a, b).

The first procedure (on the left in figure 5.4) allows to obtain the hierarchical definition of the orography through the concept of "prominence" and "parent relationship" (Chaudhry and Mackaness, 2008). The second procedure allows to define the orographic barrier on the geomorphometric bases. Then, to explain clearly the procedure should be define some basic concepts.

The *Prominence* (P) describes the relative height of a mountain and can be defined as the differences in elevation between the peak of the mountain and the lower point of that. The peak point will named "*summit point*"

and the closed contour line that contains it but does not contains other closed lines within, will named "summit contour". The lower point dividing each mountain from another is commonly known as "saddle point". Each saddle point is situated between two or more closed contours that are the lowest contour lines of each mountain. This lines, to which corresponds the height of the lower point introduced for the prominence calculation, will named " *key contour*" and the related saddle, "key saddle".

The *mountain-parent relationship* (MPR) establishes a filiation relation between topographic points, lines and polygons, relevant in mountain orography. Several definitions of the concept exist. Bivouac.com (2004) defines it as "*the parent of each peak is the higher peak whose base contour surrounds the given peak and no other peak*" and, thus, such a peak is referred to as the topographic parent. Other systems in defining parent peaks exist: "*line parent*" and "*source parent*"; both are used more often than the topographic parent (Maizlish, 2003). According to the previous definitions, the *island parentage* or *encirclement parentage* method (Molenaar 1996, 1998; van Smaalen 2003; Chaudhry and Mackaness, 2006) was adopted to aggregate hierarchically nested mountain orders.

5.5.2 Hierarchical orography

This paragraph deals with the description of the first procedure adopted for the delimitation of the orographic barrier.

The first method used to build-up the orographic map is based on the use of orographic parameters, describing the mountain terrain "*as a whole*" (Ahnert, 1984): mountain prominence and order, and their relationships.

Mountain prominence, as above defined, is a first-order derivative of elevation, representing the height above all surrounding terrains or the relative elevation of a summit (Press and Siever, 1982; Summerfield, 1991). More precisely, it is the elevation difference between a peak and the saddle (*key saddle)* connected to the lowest contour (*key contour)* that encircles it and does not have higher peaks (Chaudhry and Mackaness, 2008).

Mountain order, as proposed by Yamada (1999), is defined by the contour lines on a topographic map in which each mountain is represented as sets of closed contour lines. These sets include only a single closed

contour line for each elevation *"unless a saddle (or pass) that divides the mountain has a height that exceeds the contour interval"* (Yamada, 1999). Referring to the basic concepts of the differential geometry, for the geomorphometric descriptions of the landscapes, it is possible to define the saddle mathematically (Takahashi 2004). The Earth's surface can be described as a differentiable function in R^2 and classes C^2 in the form z = f (x, y) that associates to each point x, y of the earth's surface its elevation z. The study of this function is focused on to finding the so-called "critical points", which correspond to the points of maximum, minimum and saddle, calculated by studying the Hessian matrix, whose components are the second derivatives of the function with respect to the variables x and y. All critical points have a common characteristic, i.e., have no local slope:

$$\frac{\sigma z}{\sigma x} = \frac{\sigma z}{\sigma y} = 0 \qquad \textbf{Equation 5.3}$$

In particular, the saddle point is defined as that point of coordinates (xo, yo) with the determinant of the Hessian matrix H <0 and:

$$\frac{\sigma^2 z}{\sigma x^2} > 0, \frac{\sigma^2 z}{\sigma y^2} < 0 \text{ or viceversa} \qquad \textbf{Equation 5.4}$$

Therefore, starting from the identification of morphological saddles, have been extracted the key contours and, by adopting the hierarchical-multiscale criterion, as defined in Table 5.3, each has been identified at different scales. Thus, the closed contour lines, contained in the Key contour, form a set of concentric shapes. Starting from the summits, each set of contour lines defines a 1st order mountain above a connected saddle or pass; two or more 1st order mountains produce a 2nd order mountain and so on. If the highest of the lower-order mountains are of level *m*, then the surrounding higher-order mountain, with a lower elevation than the m^{th} order mountain, is identified as an m^{+1th}-order mountain (figure 5.5).

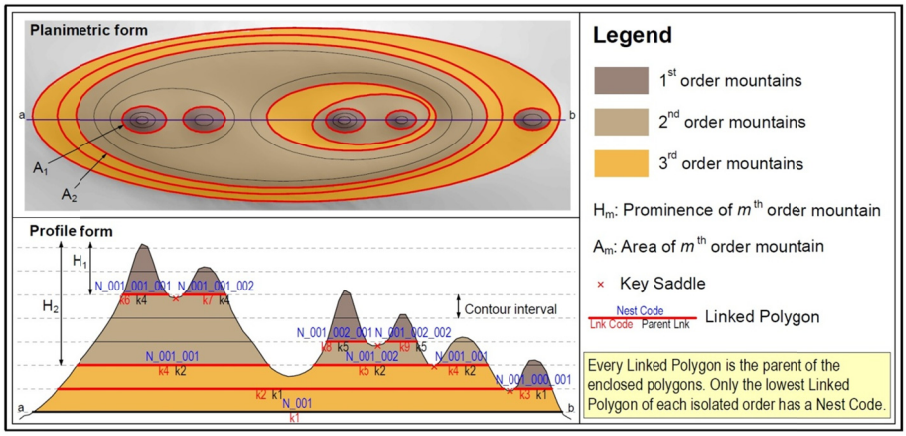

Figure 5.5: Scheme of order, prominence, area and parent relationship of the ordered mountains (modified from Cuomo et al., 2011).

The Yamada definition of mountain orders is similar and complementary to that defined for stream orders by Strahler (1952).
The procedure here proposed starts from the Yamada (1999) mountain ordering proposal but, before ordering the mountains, it automatically provides the identification of those contour lines or groups of contour lines encircling any positive (mountains) or negative (depressions) orographic volumes, using and processing polygons instead of polylines.
Based on the above background, concepts and materials, the applied methodology works with a GIS-based procedure, including five computer routines and several operational steps (figure 5.6). The first routine works on the polylines derived from the source DEM, starting with a polyline pre-processing, providing the *contour classification* and then extracting the related *contour lines* table, the *contour line type, surrounding ID* and the *contour line level* fields (Ackermann, 1978). The pre-processing routine is necessary first to identify the polyline surrounding all the "internal polylines". Thus, if for a generic contour value there are two contour lines one in the other (as in the case of a crater or volcanic rim), the procedure checks where the elevation value is greater than the contour value. If it happens inside the smallest contour lines, the geometry of the resulting polygon will coincide with the area encircled by the same polyline.

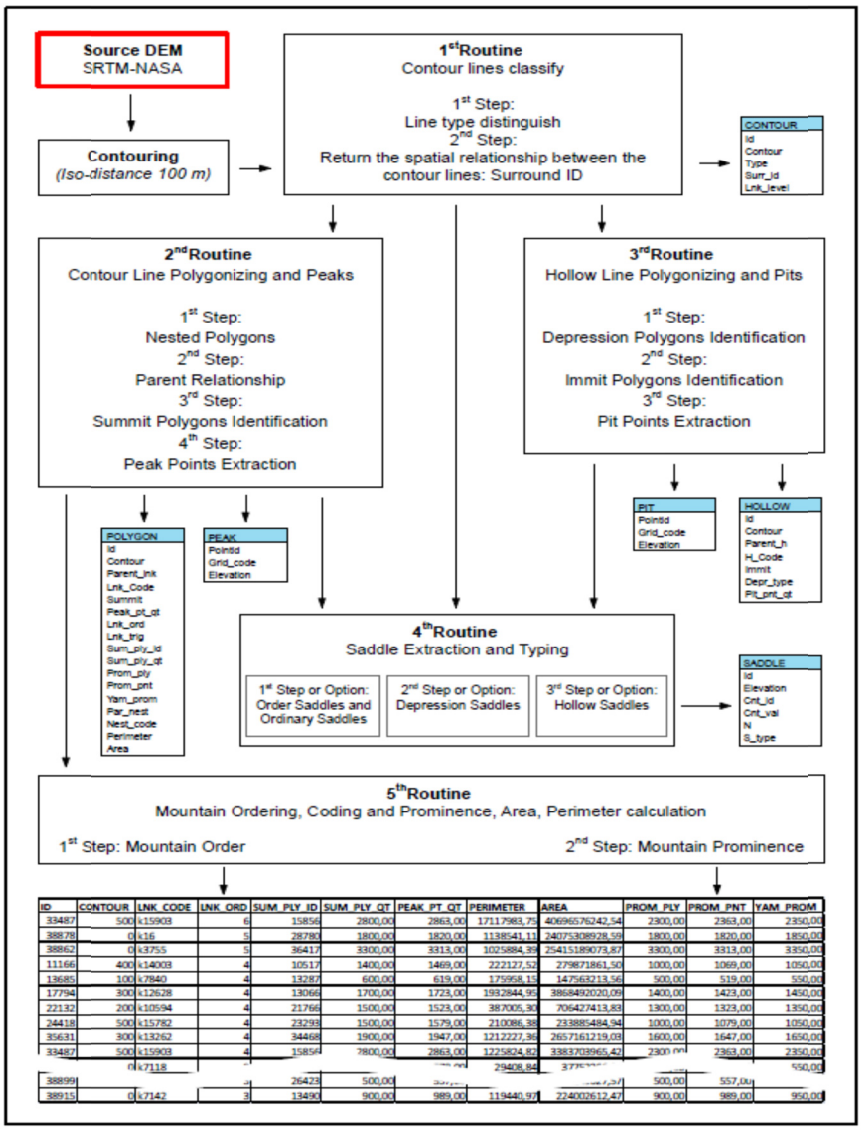

ID	CONTOUR	LNK_CODE	LNK_ORD	SUM_PLY_ID	SUM_PLY_QT	PEAK_PT_QT	PERIMETER	AREA	PROM_PLY	PROM_PNT	YAM_PROM
33487	500	k15903	6	15856	2800,00	2863,00	17117983,75	4069657624 2,54	2300,00	2363,00	2350,00
38878	0	k16	5	28780	1800,00	1820,00	1138541,11	24075308928,59	1800,00	1820,00	1850,00
38862	0	k3755	5	36417	3300,00	3313,00	1025884,39	25415189073,87	3300,00	3313,00	3350,00
11166	400	k14003	4	10517	1400,00	1469,00	222127,52	279871861,50	1000,00	1069,00	1050,00
13685	100	k7840	4	13287	600,00	619,00	175958,15	147563213,56	500,00	519,00	550,00
17794	300	k12628	4	13066	1700,00	1723,00	1932844,95	3868492020,09	1400,00	1423,00	1450,00
22132	200	k10594	4	21766	1500,00	1523,00	387005,30	706427413,83	1300,00	1323,00	1350,00
24418	500	k15782	4	23293	1500,00	1579,00	210086,38	233885484,94	1000,00	1079,00	1050,00
35631	300	k13262	4	34468	1900,00	1947,00	1212227,36	2657161219,03	1600,00	1647,00	1650,00
33487	500	k15903	4	15856	7800,00	2863,00	1225824,82	3383703965,42	2300,00	2363,00	2350,00
	0	k7118					29408,84	37			450,00
38899			3	26423	500,00				500,00	557,00	
38915	0	k7142	3	13490	900,00	989,00	119440,93	2240026 12,47	900,00	989,00	950,00

Figure 5.6: Flow chart of the adopted procedure, with routines, operative steps and related orographic data base table (from Cuomo et al 2011).

On the contrary, if it happens in the area between the contour lines, the resulting polygon will have a complex geometry with a hole corresponding to the smallest polyline.
The second routine provides the *polygon generation/classification* and working in four steps: the 1st step consists in a nested *polygonization* of those contour lines surrounding an orographic volume; the 2nd step works on the previous nested *polygons* to construct the *polygon parent relationships*.
In other words, once the procedure has derived the polygon set, it identifies all the polygons that are not encircled by any other polygon, calling them base polygons and, starting from these, it derives the parent relationship.
Adopting a bottom-up procedure, any specific base polygon is the parent of all the enclosed polygons; if out of all these there are two or more polygons at the same elevation, the procedure marks them as linked polygons. At this point, the procedure considers these polygons, as the parents of all the enclosed polygons, until there are again more than one polygon at the same elevation.
The 3rd step extracts the summit polygons from above nested polygons, identifying the polygon that doesn't have any other polygon included. The 4th step localizes and extracts the summit or peak points within the summit polygons and creates the table of the peak points, as the points with highest elevation within a summit polygon (within a first order mountain).
The 3rd routine manages the same steps for those contour lines that don't surround an orographic volume, identifying the hollow contour polygonization and depression polygons, to recognize immit polygons and, finally, to localize and extract the immit or pit points within the immit polygons and creating the pit points table.
Finally, the 5th routine derives the mountain orders from the polygon theme and calculates the prominences.
Meanwhile, this routine assigns the nest code only to those linked polygons owing rank of mountains that are the lowest linked polygons of each isolated order.

In order to validate the above procedure in a landscape containing most of the orographic entities above described, an orographic map of karst landscape of the Alburni Mts. (Aloia et al., 2010) was build-up at 1:5,000 scale (figure 5.7). This karst landscape was chosen because it is representative of the orographic conditions recurrent in the Apennine chain.

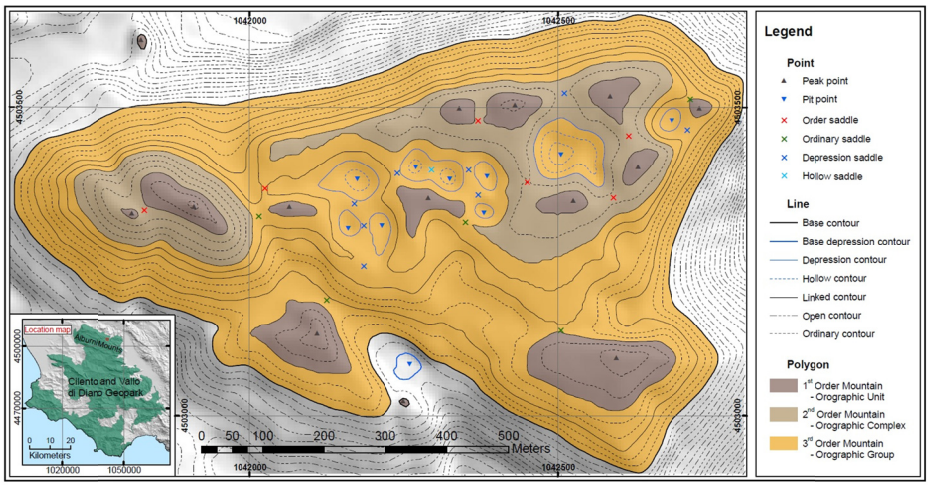

Figure 5.7: Orographic entity identification in a typical karst landscape (Alburni Mts – Cilento Geopark, Southern Italy) (from Cuomo et al 2011)

Therefore, the authors put forward a proposal of hierarchical taxonomy of the Apennine mountain orders organized in orographic entities (Table 5.4), following and modifying the previous Cuomo and Guida (2010a) proposal in orographic barrier studies.

Table 5.4: Proposal of the orographic entity hierarchy related to mountain order (modified from Cuomo and Guida 2010)

Mountain order	Orographic entity	Orographic and geological definition
8	**Orogen**	An extensive belt of rocks deformed by orogeny, associated in places with plutonic and metamorphic rocks
7	**Belt**	Typically thousands of kilometers long and hundreds of kilometers across and parallel continental coastlines or margins
6	**Chain**	A set of mountain systems, grouped together for geographical, i.e. continuity/ mean relative relief and geological reasons, i.e. continental orogenetic style, timing and uplift rates. At least two orographic system linked by a system key saddle
5	**System**	A group of mountain ranges tied together by common geological features. At least two orographic range linked by a range key saddle.
4	**Range**	A mountain range is a single, large land mass consisting of a succession of mountains or narrowly spaced mountain ridges, closely related in position, direction, formation, and age. A component part of a mountain system or a mountain chain. At least two orographic groups linked by a group key saddle
3	**Group**	At least two orographic complexes linked by a complex key saddle
2	**Complex**	At least two orographic units linked by a unit key saddle
1	**Unit**	Peak area inside summit polygons without saddles

In the figures 5.8 and 5.9 are reported the resulting orographic map where are shown the groups, the complexes and units hierarchical useful for the multiscale studies.

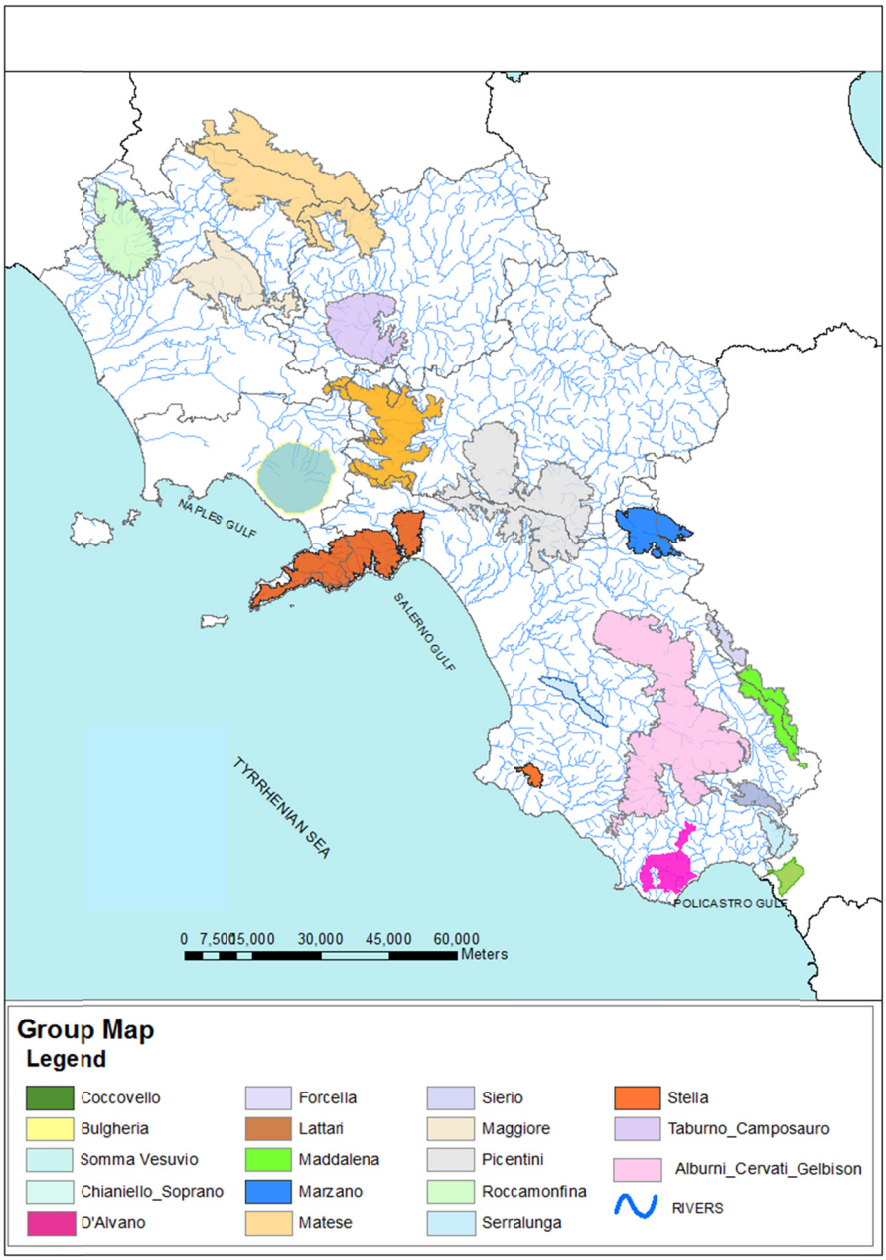

Figure 5.8: The map of the Orographic Groups of the Campania region.

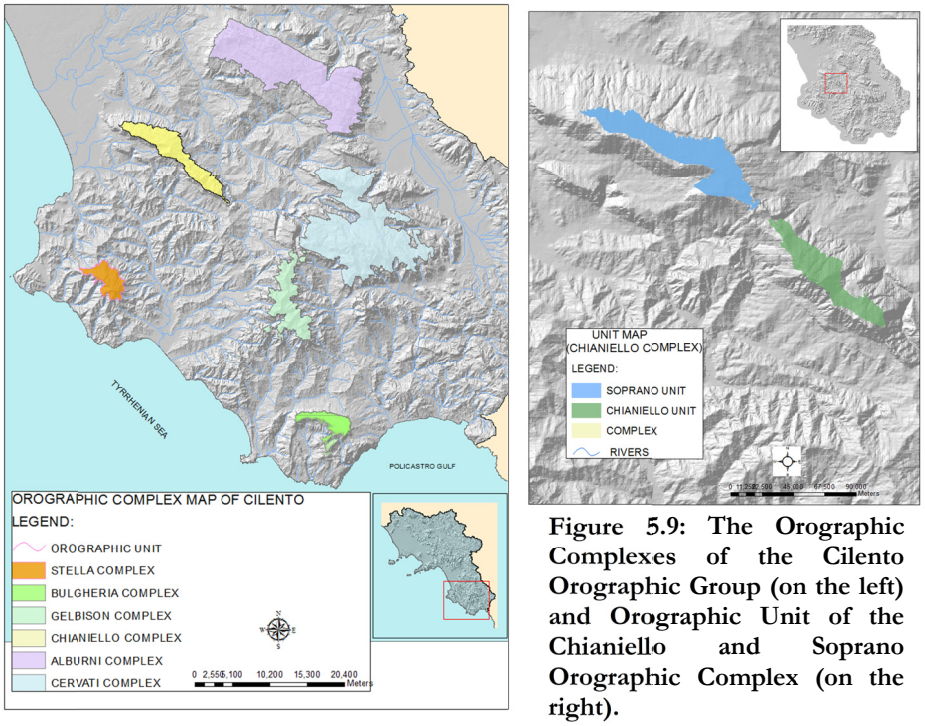

Figure 5.9: The Orographic Complexes of the Cilento Orographic Group (on the left) and Orographic Unit of the Chianiello and Soprano Orographic Complex (on the right).

5.5.3 Geomorphometric approach

The second procedure adopted, as above specified, allows the identification and delimitation of the mountains by geomorphometric analysis (Barsch and Caine ,1984; Ives et al., 1997;Beniston, 2000).
The first operation was to identify the three basic physiographic elements (plain, hill, mountain) to defining the extension of a mountain.

To this aim were studied the most relevant methods of the specific literature. Some researchers believe that the areal extend and the height is not a suitable classification (Penck, 1896; Supan, 1911), others that slope angles, rocky terrain and the presence of the snow and ice are crucial for define the mountains (Barsch and Caine, 1984; Ives et al., 1997; Beniston, 2000). Finally, Barsch and Caine (1984) point out that the definition of the mountain may be adapted to the area under investigations.
Following the criterion suggested in the literature, were adopted some morphometric parameters for the identification of the mountains, neglecting the landscape ecological criteria adopted by Troll (1975).
A combination of three relevant geomorphometric parameters were used: elevation, slope and range (or relative relief). Their values were classified each in three classes to distinguish plain , hillslope and mountain.
The first parameter elevation, derived by the DEM, was re-classify in the three classes (Penck, 1894; Hammond 1964):

i) 0-100 m for the coastal plains, flow flood plain and low coastal hillside;

ii) 100-600 m, identifying the low hilly areas;

iii) up to 600m for the high hilly and mountains areas (figure 5.10).

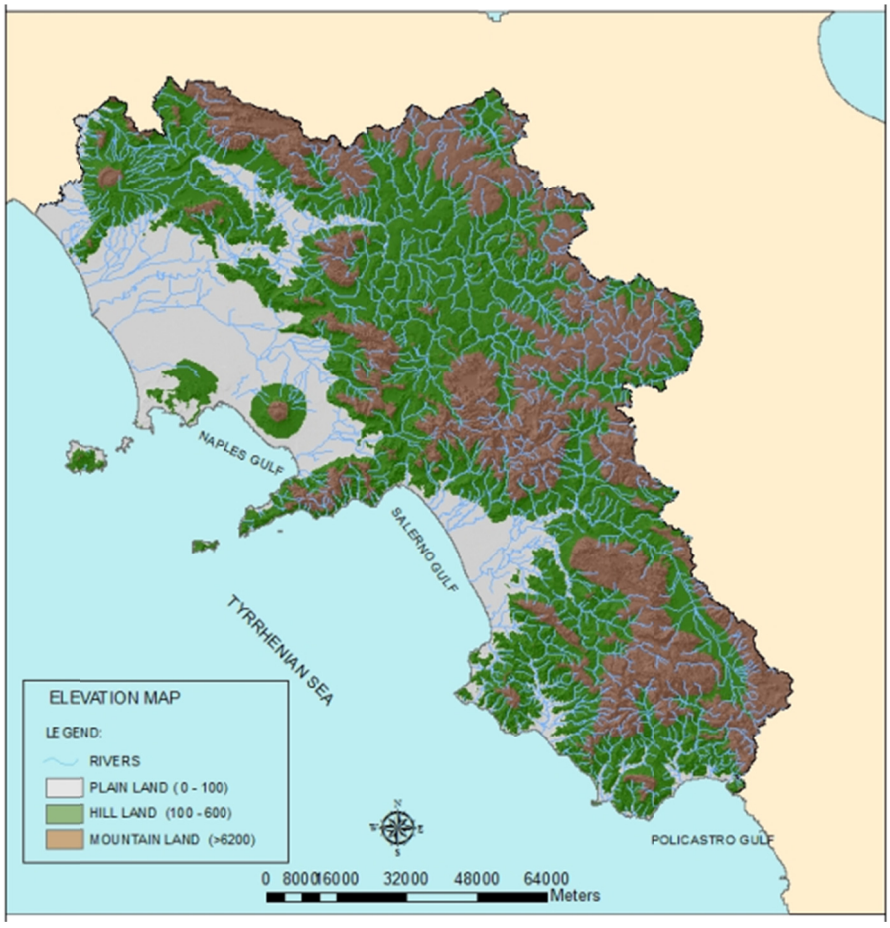

Figure 5.10: Three class elevation map to the identification of the plain-, hill- and mountain-lands (Cuomo and Guida, 2010).

The slope map was obtained by using the standard GIS tools and re-classified, following Barsch and Caine (1984), in:

i) 0-30%, for the plain ondulating lowlands;

ii) 30-50%, for the hilly landscapes;

iii) 50-80 % for the stepper mountain slopes (figure 5.11).

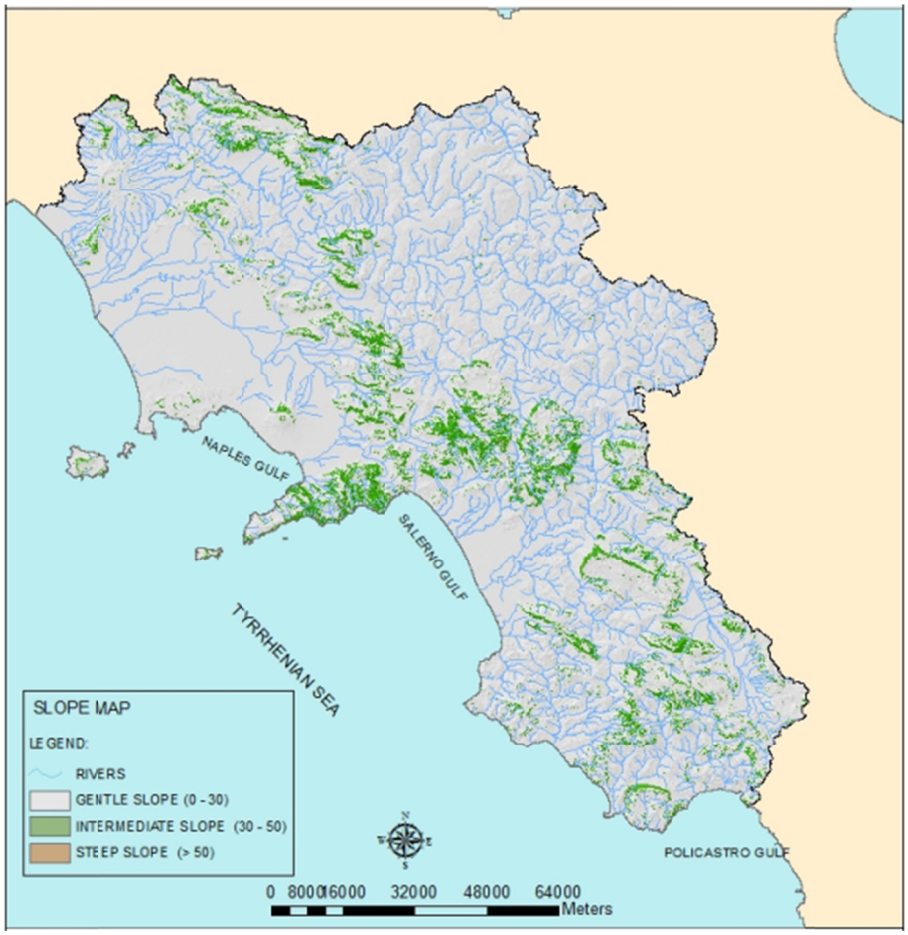

Figure 5.11: Slope class map identifying flat, hilly and stepper hilly areas.

The relative relief or range was obtained by using the apposite GIS function, as for the slope map, adopting a circular mobile windows with a 400 m diameter. This parameter was defined by Barsch and Caine (1984), as the differences between the elevation of the higher point and the lower point in a unit area or window.
The range of values utilized for relative relief to identify were:

i) 0 -20 m/km^2, for the low relief;

ii) 20 -200 m/km^2, for the middle relief and

iii) >200 m/km^2, for the hight relief (figure 5.12)

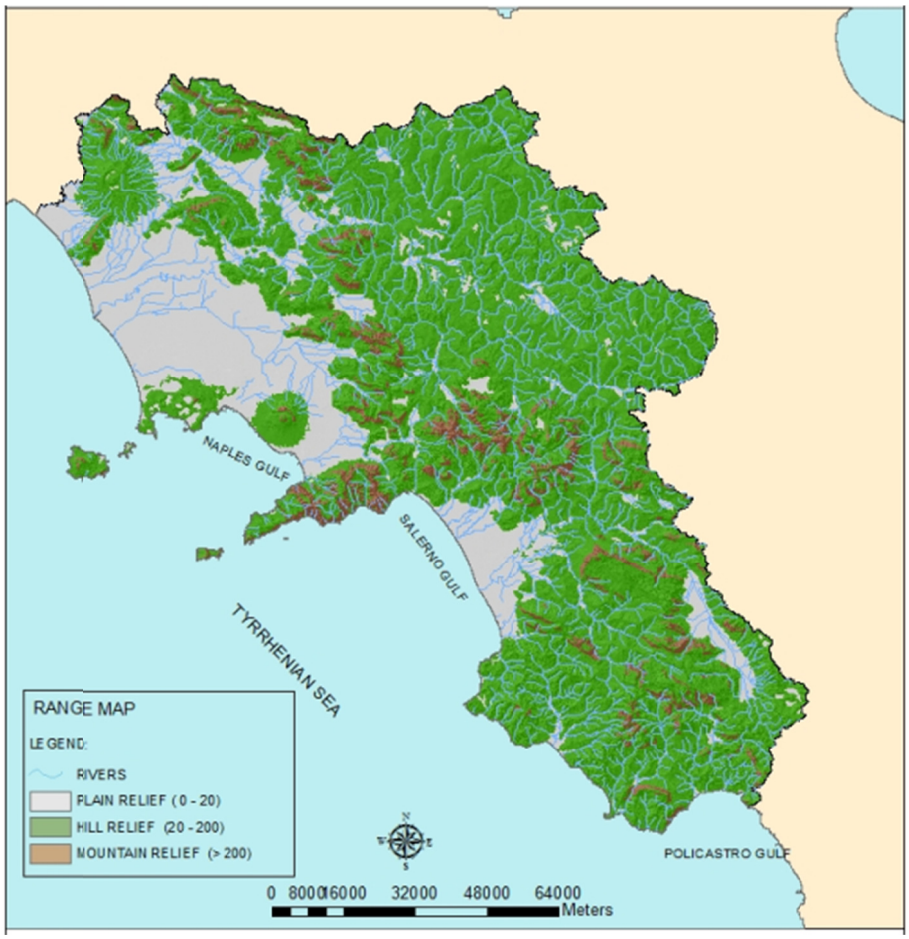

Figure 5.12: Range map of the Campania region

Necessary condition to defining mountain extension (Landscape map) was the contemporary of following conditions:

Slope > 50 %
Range > 200 m/m
Elevation > 600 m

Areas with plain relief above 600 m in elevation correspond to tableland or karst features.
In the figure 5.13 is reported the resulting landscape map.

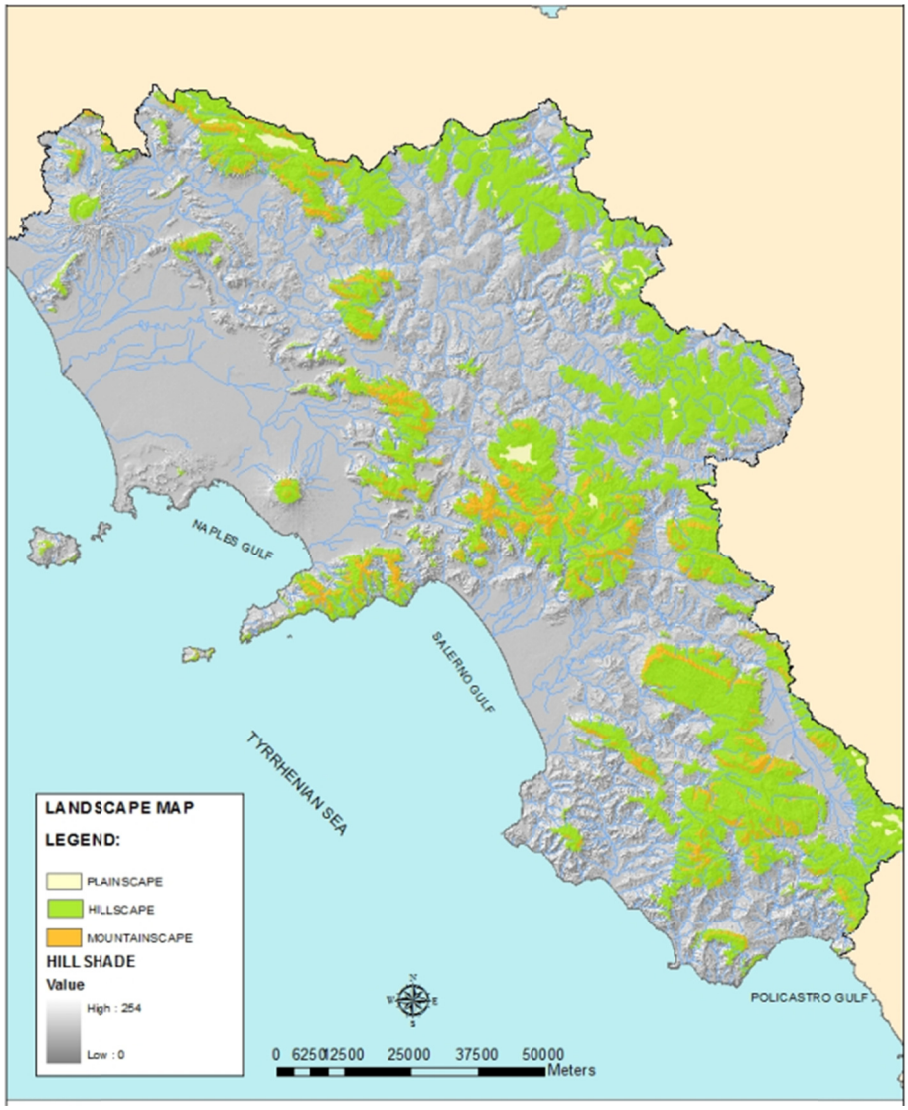

Figure 5.13: Landscapes map performed combining the elevation, slope and range maps

From the landscapes map, were selected the Mountain-scape only.
Then, each Mountainscape was characterized by three orographic components:
1.The summit or crest that is the highest area of the mountain;
2.The hillslope that is the sloped flank of the mountain;
3.The flood-plan or Plan dividing two or more mountain areas.

In the figure 5.14 are schematically summarized all the main components of the mountains.

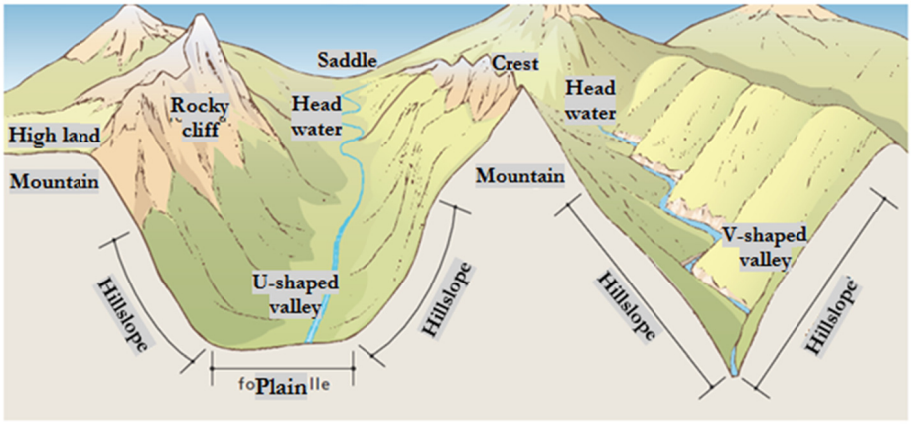

Figure 5.14: Simplified scheme of the landform component of a mountain region

To identify the basic components of the mountain, named lanforms, was used the original tool of Fels and Zobel (1995), Weiss (2001) and Tagil and Jenness (2008).

The tool, operating in the GIS software, calculate the Topographic Position Index (TPI) that is the relative position of every pixel based on digital elevation data, defined as the difference of the height value of a relative position from the surrounding mean height values.

The size of the neighborhood which is incorporated in the calculation is depending of the desired detail of the index. The calculation can be done with any focal window shape. The resulting index values are negative or positive with a range of value depending on the height differences in the focal window. Negative values indicate that the local position is deeper, positive values indicate that the location is higher than the neighborhood. Zero values occur at flat plains or at mid-slope positions. Based on that index values a very simple landform classification is possible, e.g. in valley, slope and ridge. The results of different sizes of focal windows can be used to derive more complex landform classes' e.g. small valley on a flat hill. The neighborhood size and shape of windows critical in this analysis and should be based on roughness of landscape feature being analyzed (fig. 5.15). To classify very small features like small streams or drainages, a small circular neighborhood was used. To

identify large canyons or mountains, a large circular neighborhood was used.

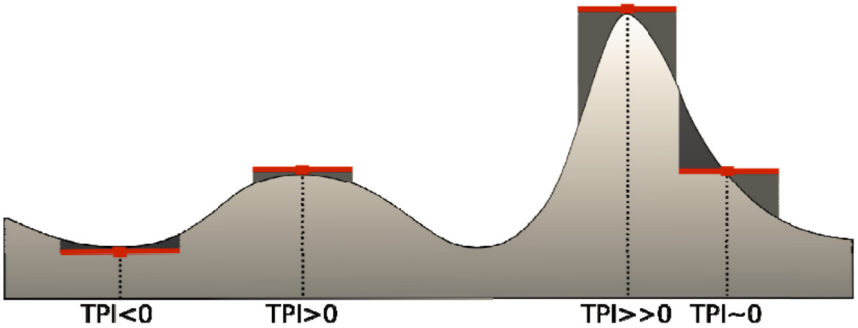

Figure 5.15: Semplified representation of the classification method adopting in the TagilandJenness (2008) studies to perform the landforms map

Choosing the correct neighborhood is generally an iterative process and depends from geostatistical structure and roughness on the landscape.
In order to define the correct couple of windows (large and small)to use for the identification of the landscape of mountains was introduced the Fragmentation Index (FI)(Monmonier 1974, Chou 1997). The FI of a map can be calculated as the ratio of the number of contiguous map regions (**m**), or the number of polygons that would result after classifying and dissolving the boundaries between same-valued neighboring polygons, to the number of original polygons (**n**):

$$FI = m/n \qquad \textbf{Equation 5.5}$$

This fragmentation index ranges from 1, complete fragmentation (where **m = n**), to 0, completely connected (where **m=0**).
For raster data, **m** equals the number of regions (the number of records in the attribute table after using RegionGroup function), while **n** equals the number of cells in the raster.
Therefore, were simulated some TPI maps with different coupled of windows size with circular features and were chosen only three of that maps with the coupled of windows size of 5-25 , 3-9 and 6-36 square metres (figure 5.16).

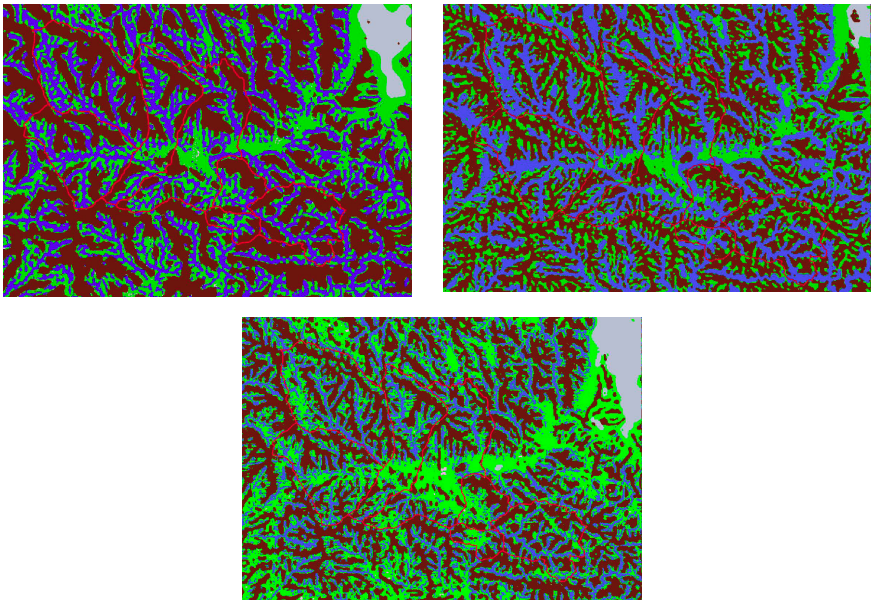

Figure 5.16: The three TPI maps, performed in the test-region, chosen for calculate the Fragmentation Index. On the upper left 5 - 25 coupled, on the upper right there is the coupled 6-36 and on the bottom center the coupled 3-9

Following the above procedure was calculated the FI (table 5.5):

Table 5.5: Fragmentation Index values for a few Campania region catchments

	REGION (windows_6_36)	REGION (windows_5_25)	REGION (windows_3_9)
BUSSENTO	1.92E-06	1.20E-06	2.05E-06
ALENTO	0.0169	0.0104	0.0176
MINGARDO	4.05E-06	2.67E-06	4.34E-06
TUSCIANO	0.0158	0.00873	0.01528

It is evident that, for all the windows adopted, was obtained a good results. Only for the Tusciano river was obtained a less value with the windows 5_25 than the others two couples.
Based on the above criteria, to draw-up the landform maps was definitely adopted a circular windows with a small size of 5 m^2 and the large one of 25 m^2.
In the figure 5.17 is shown the landforms map performed with the above illustrated procedure.

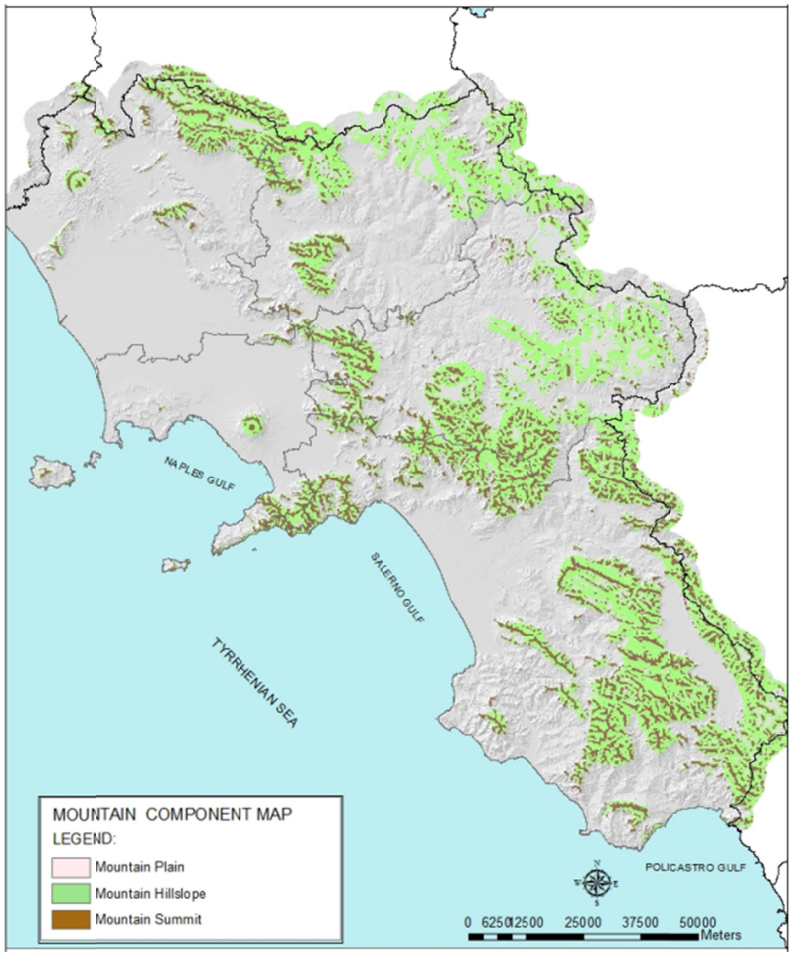

Figure 5.17: Landforms map of the Campania region

Finally, the mountain barriers identification was performed by intersecting the landform map with the aspect map (NE, SE, SW and NW), and extracting all the hillslope with the south-west orientation. This choice was derived taking into the analisis of Longobardi et al. (2006) and Blasi et al. (2001) were was specified that the air masses along the Tyrrhenian bordland involving storm event have a SW direction.
The mountain barrier map obtained is in the raster format including in each cell the morphometric features on the parameter utilized for performing the map (figure 5.18).

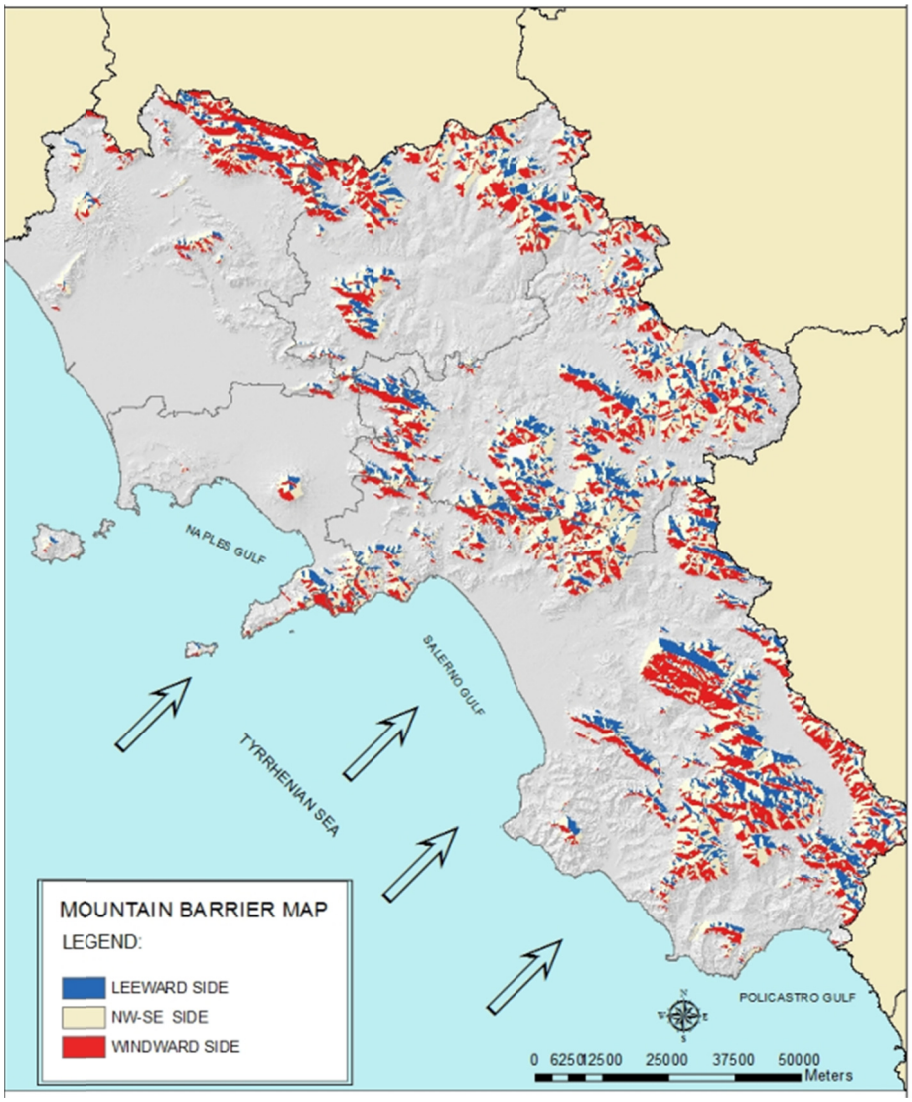

Figure 5.18: The mountain barrier map of the Campania region (Cuomo and Guida, 2010a)

5.6 MULTISCALE OROGRAPHIC BARRIER MAP

In the previous paragraphs were described the two approaches adopted for the identification of the orographic map, adopting the orographic procedure, and the mountain barrier, applying the morphologic procedure. Combining the resulting maps obtained by the two approaches, was drawn-up the Multiscale Orographic Barrier map (figure 5.19).

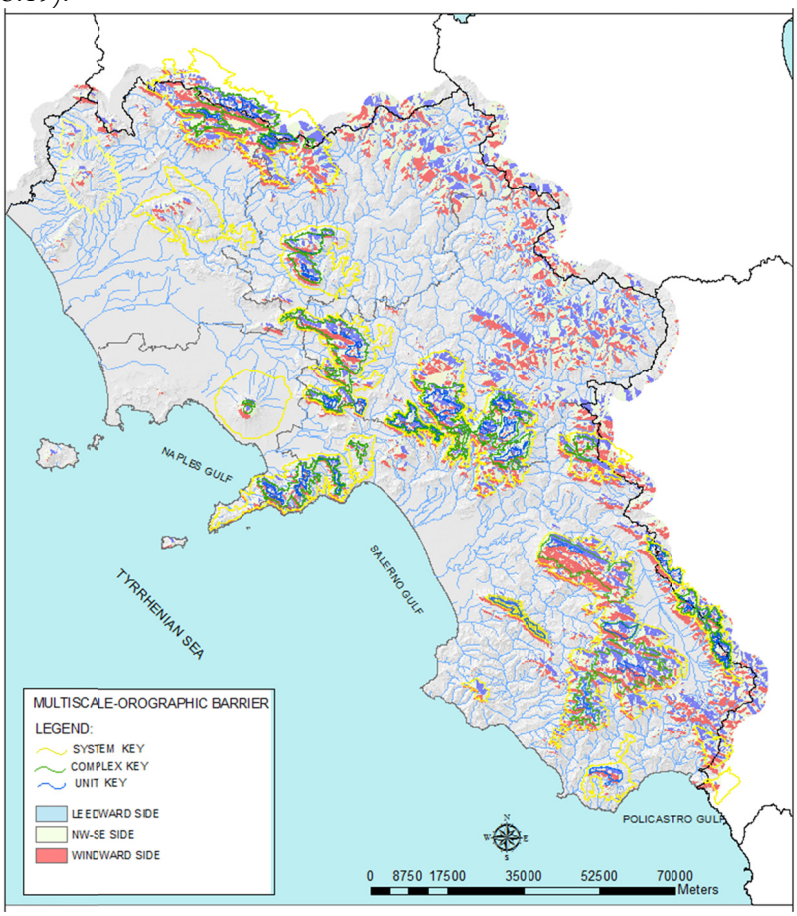

Figure 5.19: Multiscale orographic barrier map of the Campania region

The multi-scale orographic map includes a database of the orographic groups, complexes and units and for each one contains morphometric features to be employed in the spatial-temporal analysis for further analytical models on the orographic precipitations.

The figure 5.20 shows the advances performed by the above automatic procedure in respect to the expert judgment procedure used in Rossi et al. (2005).

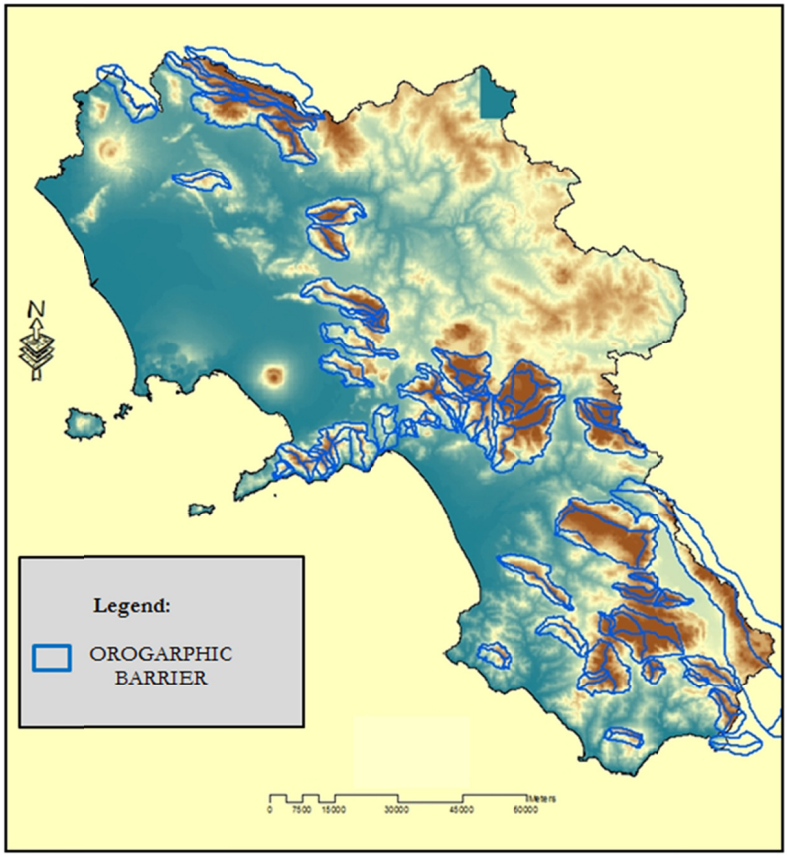

Figure 5.20: The orographic barrier map performed on the expert judgment based

Must to evidence that the delimitation of the group orographic barrier, drawn up adopting the above automatic procedure, is the same operated with the expert judgment. It is evident that the map of figure 5.20 was very static and did not take into account the hierarchical taxonomy derived by the adopted multiscale approach. Also, the same map (figure 5.19) is only a graphical spatial query from the orographic Informative System of Campania Region.

5.7 OROGRAPHIC BARRIER CHARACTERIZATION

The third objective of the orographic barrier topic was thei quantitative characterization (orographic signature). In the present paragraph will show the two method used for the classification of the orographic barrier, previously identified, delimitated and mapped.
As specified in the paragraph 5.3, the shape of the barrier, plus its elevation and slope influence the flowing of the air masses causing different consequences on the rainfall pattern and intensity (Jiang, 2006; Wang and Lane, 2011).
Considering the atmospheric dynamics, it seems to be important the classification of the mountains against their shape and to this aim were proposed the following two methods of characterizations:

i) The first is based on topographic indexing;

ii) The second is based on the Fractal dimension.

The first orographic barrier classification here proposed is based on a set of compound topographic index.
In order to classify the orographic groups, were considered relevant the following compound variables:

- *Prominence* (P), that, is defined as height difference between the summit point and the key contour- saddle (Chaudhry and Mackaness, 2008).

$$P = H_{SUMMIT\ POINT} - H_{KEY\ CONTOUR}$$

- The *Shape Complexity Index*, SCI (Hengl et al., 2003), commonly used to describe polygons on DEM slices indicating how compact or oval an orographic DEM slice is.

$$SCI = \frac{p}{2\pi R}$$

Where **p** is the perimeter of the barrier and **R** is the radius of the circle with the same perimeter of the orographic barrier.
There is a direct relation between the SCI and the classification of landforms (Olaya, 2009)

- The **Ruggedness**, RUGN (Melton, 1965), originally developped to characterize the drainage basin, it is also useful to defining the stature of a relief.

$$RUGN = \frac{RANGE}{\sqrt{A}}$$

Where **A** is the area of the orographic barrier, ***range*** is the difference between the highest and lowest values in the area being analyzed.

- The **Elevation-Relief Ratio**, ERR (Pike and Wilson, 1971), matematically equivalent to the hypsometric integral:

$$ERR = \frac{Z_{AVRG} - Z_{MIN}}{Z_{MAX} - Z_{MIN}}$$

Where Z_{avrg} is the mean elevation value of the mountain region, Z_{min} and Z_{max} are respectively the minimum and the maximum elevation in the same region.
For the above mentioned compound indexes, referred to each orographic groups, were performed a descriptive statistic in order to summarize all the value obtained calculating each parameter (table 5.6).

Table 5.6: Descriptive statistics parameters calculated for the orographic groups of the Campania region.

	P	SCI	RUGN	ERR
N	18.0	18.0	18.0	18.0
Min	364.0	1.5	464.9	5.4
Max	1288.0	5.2	1262.8	48.1
Sum	14392.0	58.7	16041.3	321.8
Mean	799.6	3.3	891.2	17.9
Std. error	71.4	0.2	60.1	3.0
Variance	91728.0	1.0	64945.3	161.7
Stand. dev	302.9	1.0	254.8	12.7
Median	729.0	3.1	915.5	12.9
Skewness	0.4	0.3	-0.3	1.1
Kurtosis	-1.3	-0.6	-1.0	0.4

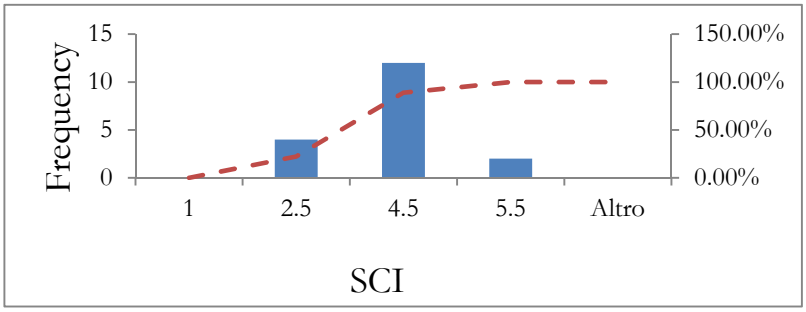

Figure 5.21: The SCI index frequency analysis

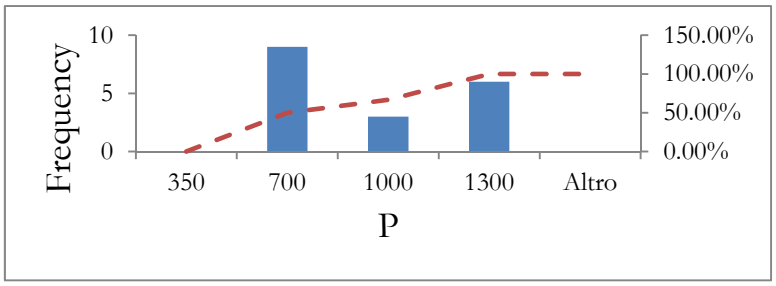

Figure 5.22: The P value frequency analysis

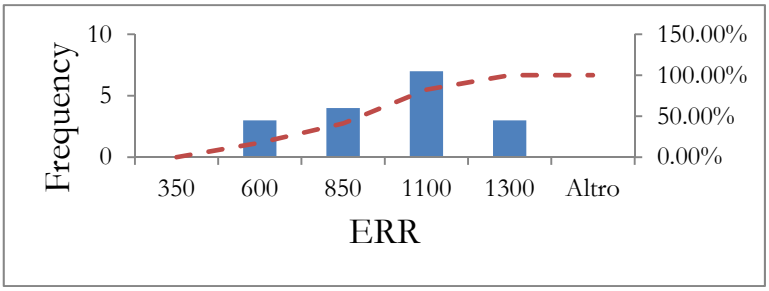

Figure 5.23: The ERR index frequency analysis

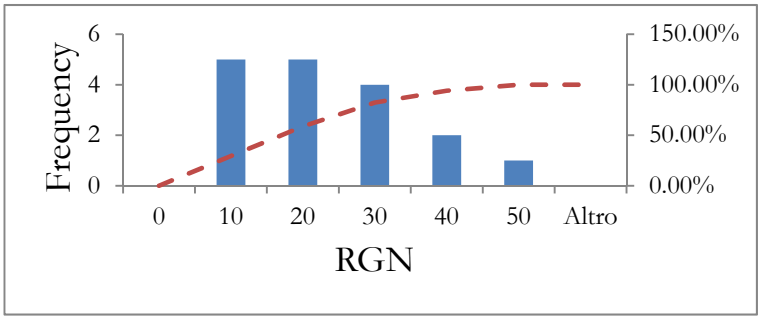

Figure 5.24: The RGN index frequency analysis

For regional classification of orographic barrier groups of Campania region, was used the simple multivariate procedure. The cluster analysis, is a multivariate procedure based on some measurement of distance

among object, calculated in a **c**-dimensional space, where **c** represents the number of attributes used in the cluster process (Mather, 1987).
Before to perform the cluster procedure, we have tested the correlation between the previously introduced indexes on the basis of a correlation matrix, reported in the table 5.7:

Table 5.7: Correlation matrix performed for the orographic parameters

	P	*SCI*	*ERR*	*RUGN*
P	1.0			
SCI	0.3	1.0		
ERR	-0.1	0.3	1.0	
RUGN	-0.5	-0.6	-0.1	1

It is evident that there is a good correspondence between the SCI and the RUGN indexes and the P and RUGN.
In the figure 5.26 is shown the Cluster analysis obtained combining the SCI and RUGN indexes, where the distances between classes are calculated by adopting the "Euclidean Distances" formula.

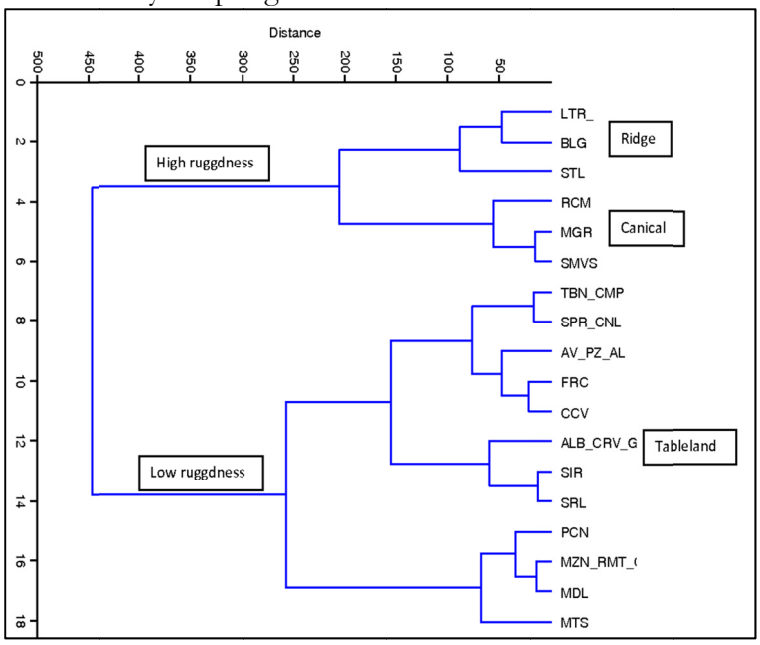

Figure 5.25: Cluster analysis of the orographic groups performed between the SCI and the RUGN indexes.

Analyzing the values of the distances was found that a first ranking of the groups is between high and low values of RUGN, while the distances calculated for the SCI ranged between a maximum of 2 and a minimum of about 1. In this case three intervals were chosen for the distinction in conical, tableland and ridges shapes respectively equal to 1-1.2, 1.3-1.6 and 1.7-2. This is a proposed method that could be extended to the other elements of the orography, such as the units or the groups, introducing some others parameters or adopting a more sophisticated method of analysis.

The second method for characterize the orographic groups is based on the fractal analysis. In the landscape issue, when are delineated some entities, such as rivers, islands, etc, may be interesting to characterize and quantify their spatial structure and their most fundamental properties.

Generally, object can lie either in Euclidean space, with an integer number of dimensions (0 for points, 1 for lines, 2 for surface, 3 for volumes) or in a fractal dimension, introducing a new way of characterizing the occupancy of the space by the objects (between 0 and 1 for clusters points, 1 and 2 for curves, 2 and 3 for surfaces and 3 and 4 for volumes) (Fortin and Dale, 2005)

The fractal dimension has attracted considerable attention from mathematicians because its fractional quality is in sharp contrast to the integer dimensions (zero, one, two and three) of Euclidean manmade shapes such as circles and squares (Hagerhall et al., 2004).

The development of fractal geometry was strongly linked to issues relating to the mathematical description of forms and shapes that are found in nature, such as rivers, mountain ranges and coastlines (Mandelbrot, 1983).

In order to give an idea on the characterization of the orographic barrier by using the Fractal Dimension (D) was used the prominence maps, performed with a cell size of 5x5 m, of the Stella and Chianiello Mounts, defined as orographic units in this study (fig. 5.9). Using continuous data the literature suggests to computed D as the slope of a log variogram assuming that the variogram is isotropic, linear and without a sill (Fortin and Dale, 2005).

$$2\gamma(h) = h^{4-2D}$$ **Equation 5.6**

Where the slope is (4-2D).

Therefore, firstly the geostatistic analysis was made on the prominence grid map of the two units considering two directions: the south-west and the north-west. Then, for each direction was build up the log variogram and the slope of that computed. In the figures 5.26-5.29 are show the analysis of the log-variogram.

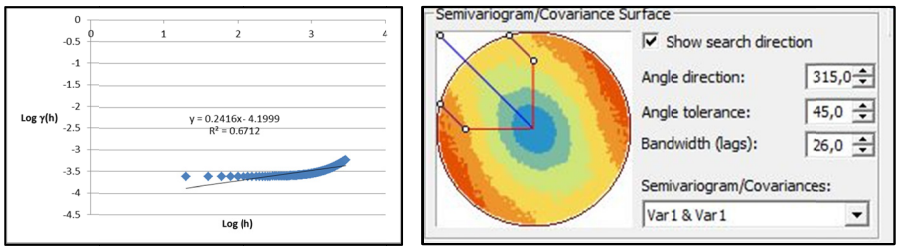

Figure 5.26: Example of the log variogram computed for the Stella Mount in the NW direction

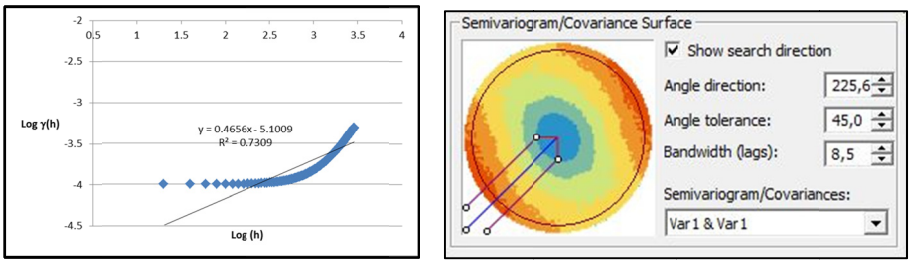

Figure 5.27: Example of the log variogram computed for the Stella Mount in the SW direction

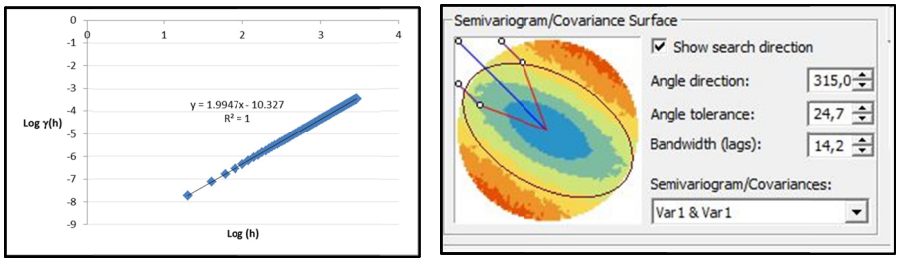

Figure 5.28: Example of the log variogram computed for the Chianiello Mount in the NW direction

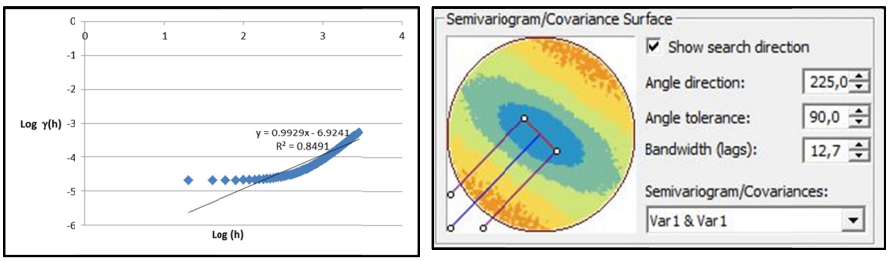

Figure 5.29: Example of the log variogram computed for the Chianiello Mount in the SW direction

In the table 5.8 are reported the fractal dimension calculated for the two units in the SW and NW directions.

Table 5.8: The fractal dimension D of Chianiello and Stella units

Units	D (SW)	D (NW)
Stella	2.8	2.9
Chianiello	2.5	2

The Stella mountain has the same D value in the two directions, so its features is similar to the circular one, whilst for the Chianiello mountain were obtained D=2 in the NW direction, similar to a linear shape, and D = 2.5 in the SW direction that is the central value between the elongate and circular shape.
The results are more closed on the realty. In fact the Chianiello Mount has an elongate shape and in the cluster analysis was classified as a Ridge, whilst the Stella mountain is more compacted (figure 5.30).

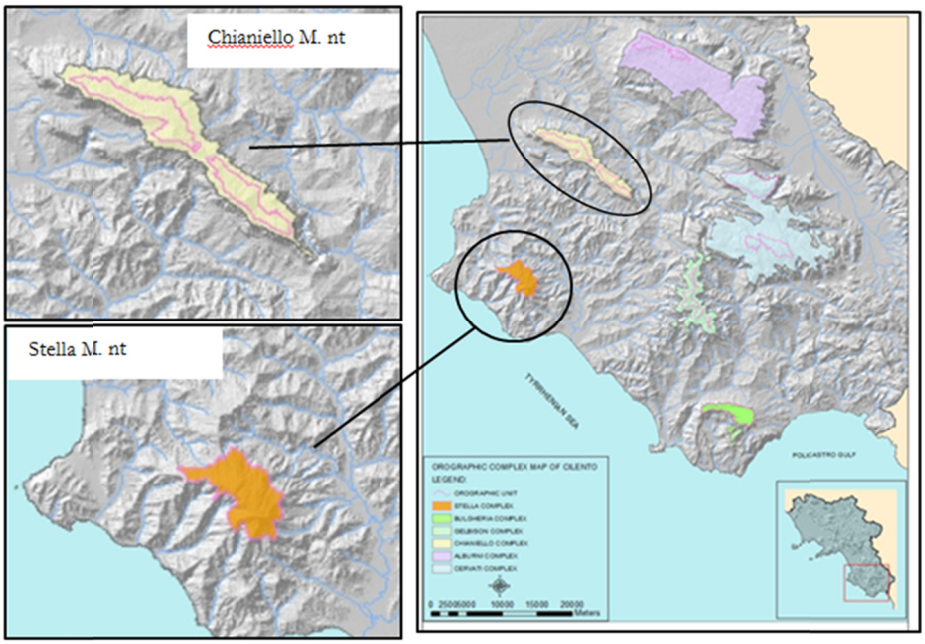

Figure 5.30: The Chianiello and Stella mountains

6 HYDRO-GEOMORPHOTYPES

6.1 INTRODUCTION

This chapter deals with the second main topic of the research: the "*hydro-geomorphotypes*".
Conceptually, the problem is related, in general, to the hydrological regionalization and, in particular, to the definition of the "basic land unit" in hydrological response of basin, at the space-time scales of analysis.
Strictly, the term "*hydro-geomorphotypes*" was firstly introduced by Rossi F. (1998) as "*territorial units which are homogenous for land use, geology and geomorphology*" as overall hydrological response in rainfall-runoff transformation, at regional sale and for planning purposes.
Untill the 2005, this term remains a neologism in the scientific literature and its conceptual meaning is not clearly stated, nor completely shared.
As just introduced in the first chapter, VAPI procedure is still utilized in the Campania region organization to evaluating the peak discharge for the flood hazard.
As shortly reported in cap.1, the rainfall-runoff model used in the Vapi was based on the hortonian infiltration excess mechanism, adapting a modified Rational Method at a regional scale with a classification of the regional territory in six hydrologic homogenous areas in respect to the rainfall distribution and in three permeability classes from regional geology bedrock.
In order to up-to-date the VAPI-Campania procedure (Rossi and Villani, 1995), a new research program with general aim to develop methods transferring hydrologic models and parameters in flood assessment, at sub-regional spatial scales was undertaken.
Following this progressive up-to-dating, at the National Conference of Hydraulics and Hydraulics Engineering in Rome, Rossi and Villani (2006) presented the research guidelines for the above mentioned updating of the VAPI-Campania procedure.
Among the other research proposals, one of that was oriented to the classification and zoning of the territory into "*hydro-geomorphotypes*" to

define the hydrological behavior of the catchment and small catchment with respect to their geology, pedology, geomorphometry and geomorphic functions.
Therefore, the concern of this topic is the definition and regionalization of hydro-geomorphometric characteristics in term of landform-soil relationship and attributes with hydrologic relevance on different spatial scales.
In the last decades, geomorphometric classification methods have supported the hydrologic modeling, at large to small scale. On a qualitative basis, it is well known that hydrologic processes are influenced by geomorphometric properties like local slope angle, total curvature or drainage density (Gregory and Walling, 1973).
There exist some approaches to quantifying these relations through drainage basin parameters (Moore et al., 1991) and model conceptions, like the Geomorphic Instantaneous Unit Hydrograph or GIUH (Blöschl and Sivapalan, 1995; Moore et al., 1991), as performing model of Instantabeous Unit Hydrograph (IUH).
Since the meaning of "hydro-geomorphotype", however, has never been precisely defined in terms of correct terminology, conceptual representation, structural constitution and functional behavior, the present chapter , as a part of this research project, give an original contribute to the topic.
In the following paragraphs, is presented firstly a brief scientific background about the disciplinary context on subject, illustrating successively previous effort in introducing the concept and finally offering the results of present research in spatial identification, objective delimitation and physical-based characterization of the "hydro-geomorphotypes" .
Applications in real world basin system modeling are, ultimately performed.

6.2 GENERAL BACKGROUND

The response of the rivers to the extreme precipitations on their basins is much more different: some produce flash floods of high magnitude

while others change only slowly their stream flow regimen (Schomocker-Fackel et al., 2007).
Among the many factors contributing to the hydrological behavior of a basin, a few of them, as the scale, topography, soils and bedrock are considered the major hydrological control, factors influencing heavily the main processes of runoff/sediment production after the rainfall: infiltration, filtration, catchment/aquifer storage capacity, sapping and channel initiation.
The role of this factors is studied by rainfall-runoff transformation model synthetically exposed in the Chapter 1.
In gauged basins, the rainfall-runoff transformation models derive from the analysis of some of the above hydrologic factors using i. e. measured rainfall, temperature and discharge data. A lot of basin or catchment are un-gauged and characteristic factors calibration is not easily pursued. Infact, it is difficult to identify the parameters correctly and to prove that the model is a valid representation of the processes in a catchment (Beven, 2001; Grayson et al., 1992; Naef 1981).
The aim of the more recent researches is the implementation of many different aspects of runoff formation in a rainfall-runoff modeling, such as the direct runoff, fast and delayed sub-surface return flow and the groundwater contribution to the streamflow to the deep percolation.
To integrate these academic researches into rainfall-runoff modeling, useful in planning and designer, a methodology is needed to define the spatial distribution of the runoff production processes in a catchment (Schomocker-Fackel et al., 2007) and the land surface units to which these processed are related.
The classical example of a spatially differentiated method is the above mentioned SCS CN method, developed by the U.S. Soil Conservation Service for small un-gauged streams (Soil Conservation Service, 1972). It used the Runoff-Curve Number to taken into account of the soil type and land use properties.
Another widely used indicator of topographically-induced hydrological behavior is the Topographical Wetness Index (Beven and Kirkby, 1979) characterizes the hydrological behavior based on upslope contributing area and local slope.
For instance, Schmidt et al. (2000) studied the runoff processes with respect to geomorphometry and geology and introduced the concept of "*geomorphometric-hydrological landforms*" (figure 6.1)

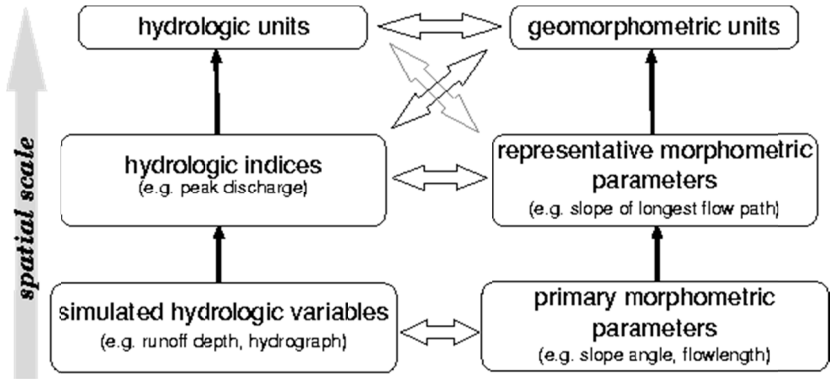

Figure 6.1:Relationship between hydrological, geomorphometric units and their indices, parameters and variables, modified from Schmidt et al. (2000).

This approaches consider the complex hydro-geomorphic linkages at basin and catchment scale and highlights that insights into hydro-geomorphic linkages are needed to elucidate spatial and temporal attributes of flow paths that affect both headwater and downstream channel systems, including cumulative impacts of land use (Sidle and Hornbeck, 1991; Burgess et al., 1998; Sidle et al., 2000).
Winter (2001) introduced the concept of "*hydrological landscape",* based on the idea that the complete hydrologic system interacts with a single, simple physiographic feature, and that this features becomes the basic building block of all hydrologic landscapes, classified the catchment into hydrological landscape units (upland, valley side and lowland), exploiting the combination of topographic, geological and climatic conditions. He also suggested a quantitatively use of the hydrological-landscapes for define and map hydrological-setting regions of the United States, as provided by Wolock et al. (2004), based on dominant runoff mechanisms. Three landscape classes are distinguished: wetland, hillslope and plateau, corresponding to three dominant hydrological regimes: saturation excess overland flow, storage excess sub-surface flow, and deep percolation. In their opinion, topography, geology and land use hold the key to identifying these landscapes.
The topographical wetness index was further modified by Hjerdt et al. (2004), who took into account downstream conditions considering how

far a water particle needs to move to lose a certain amount of potential energy.
The topography was also used to investigate the relationship of catchment transit times with numerous catchment characteristics such as flow path length, gradient and connectivity (McGuire et al., 2005; Jencso et al., 2009, 2010) or drainage density (Hrachowitz et al., 2009, 2010) using tracer techniques.
Other tracer studies have directly linked topography and hydrological behavior (Uhlenbrook et al., 2004; Tetzlaff et al., 2007).
A wide range of additional topographical indices have been suggested, describing, among other aspects, the shape, dimension and stability of a catchment, such as the hypsometric integral (Ritter et al., 2002) and its correlation with catchment processes (Singh et al., 2008).
Other studies correlated topographical indices with soil type and hydrological behavior (Park and van de Giesen, 2004; Lin and Zhou, 2008; Pelletier and Rasmussen, 2009; Behrens et al., 2010; Detty and McGuire, 2010).
In spite of the rich information content of topography, its general usefulness for hydrology is controversial. It has been argued that climate and geology exert stronger influence on the rainfall runoff behavior of a catchment than topography (Devito et al., 2005).
Furthermore, it was shown that flow patterns may be dominated by bedrock, rather than surface topography (McDonnell et al., 1996; Tromp-van Meerveld and McDonnell, 2003). According to McDonnell (2003) the "*catchment hydrologist will need to develop hypotheses from non-linear theory that are testable on the basis of observations in nature. This will not come about via model intercomparison studies or DEM analysis*".
These comments highlight the perception that DEM analysis alone may be of limited value for gaining deeper understanding about catchment processes and that this needs to be brought into a wider context, accounting for the subtle interplay of topography, geology, climate, ecology and hydrology.
In spite of the catchment processes complexity and due to the frequent lack of data for bottom-up modeling approaches, relatively simple, lumped conceptual models can, due to the self-organizing catchment behavior, be efficient in identifying dominant flow generation processes and modeling runoff (cf. Sivapalan et al., 2003; Savenije, 2010).

However, even for these top-down models additional data, other than precipitation and stream flow, are desirable for enhancing physical significance of model parameters and evaluation(Nalbantis et al., 2011).
Recently, Rennò et al. (2008) formalized the Height Above the Nearest Drainage (HAND) metric and employed it for landscape classification. This metric may be more adequate to identify hydrologically different landscape units than the traditionally used elevation above mean sea level. HAND calculates the elevation of each point in the catchment above the nearest stream it drains to, following the flow direction.
In addition elevation data (Nobre et al., 2011), showing that HAND is a stronger topographical descriptor than height above sea level by analyzing long term piezometer data.
Landscape classification based on HAND is potentially sensitive to different aspects, such as the definition of the threshold for channel initiation when deriving streams from a DEM, the seasonal fluctuations of the channel initiation, and the resolution of the DEM. Furthermore, it is unknown to what extent local landscape features can introduce a bias and how robust HAND is to the resolution of observed points (sample size) and the locations of the observed calibration
points. Hence, the application of HAND is still subject to considerable uncertainties. In addition, it is not well understood how HAND relates to other landscape descriptors, such as the topographical wetness index.
Based on hydrologically meaningful landscape analysis (Nobre et al., 2011); Savenije (2010) suggested that as topographical features are frequently linked to distinct hydrological functioning, they can be used to construct a conceptual catchment model perceived of hydrological units within a catchment.
The classification model suggested by Gharari et al. (2011), based on HAND was compared with the topographical wetness index and a clear relation between classified landscape and groundwater table based on binned values of the topographical wetness index values was found.
Such landscape classification results could in future work be refined by using additional information i.e. distributed soil moisture or groundwater data, for establishing a yet stronger link between landscape classes and runoff processes.
The resulting maps show a relatively realistic, high accuracy landscape classification presumably associated closely to the dominant runoff generation processes in the individual parts of the study catchment. Such results can in the future serve as basis for the development of conceptual

hydrological models by assigning different model structures to the individual landscape classes, thereby potentially improving model realism without the need for further parameters.
Other different modern approaches exist based on the classifying the hydrology of soils such as the HOST (Hydrology Of Soil Types) where the soils were grouped according to whether a similar hydrological reaction. Other authors as McGlynn and McDonnel (2003), Sidle et al. (2000), Merz and Mosely (1998) and Uhlenbrook et al. (2004) which considered the definition of landscape as puzzle of geomorphological units with similar hydrological behavior to identify the hydrological classification. Successively, Peschke (1999) et al. and in Scherrer and Naef (2003)determined the runoff processes on a plot scale using soil data, geology, topography and vegetation. More recently, Schomocker-Facker et al. (2007) follow the approach used by Scherrer and Naef (2003) at catchment scale and tested it with hydrologic observations during flood events.
Another approach for the identification and regionalization of runoff processes is based on a Gis-based and statistical approach and require three basic datasets in terms of permeability: simplified geological maps, digital elevation model and land use maps (Muller, et al. 2009)
Topography, land use and geology have also been used to directly infer dominant runoff processes within a catchment (Flugel, 1995; Naef et al., 2002; Schmocker-Fackel et al., 2007; Hellebrand and van den Bos, 2008; Muller et al., 2009; Gharari et al., 2011)).
As results of the above up-to-date review, emerge the need to find an unified approach in the definition of hydrologic units that having physical consistency, in term of topography, structure and function.
With respect to the significance of geomorphometric properties in hydrology, scaling effects have to be considered, meaning that (1) runoff-morphometry relations, which tend to be invariant over certain spatial ranges and (2) spatial thresholds affecting changes in these relations have to be determined (Blöschl and Sivapalan, 1995; Wood, 1995).
In general, local scale, hillslope scale and catchment scale are often used to distinguish different spatial scales in hydrology (figure 6.2).

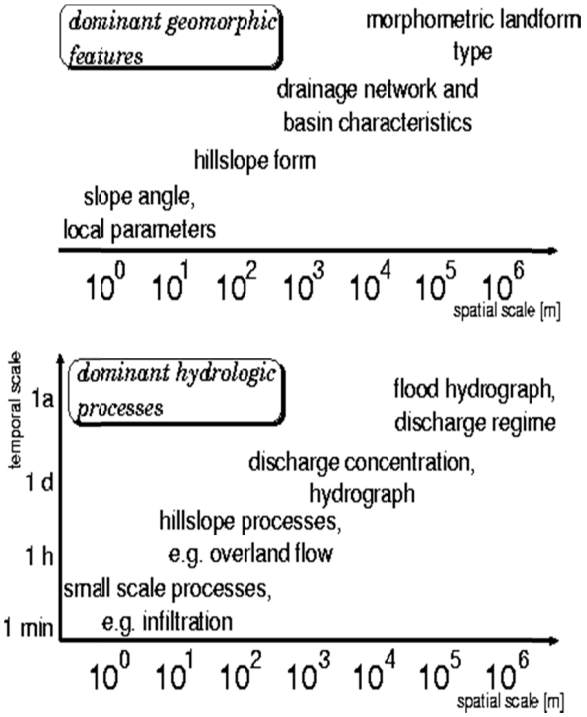

Figure 6.2: Scales in hydrology and geomorphology. The figure shows in a crude way some dominant features of each discipline in a spatial and spatio-temporal context. Translating scale properties from one discipline to the other is an open research question (Anderson and Burt, 1990).

On the local scale water flow path geometries, flow velocities and discharge are influenced directly by parameters like slope angle and upslope drainage area. Additionally, geomorphometry affects hydrologic processes indirectly through their dependency on several other factors (like soil parameters and vegetation).

The hillslope scale is dominated by runoff production mechanisms influenced by soil properties (partitioning of overland flow and subsurface flow) and hillslope form. Extracting of typical 'hillslope stripes' has been one strategy to represent hillslope hydrology within larger scale catchments.

6.3 SPECIFIC BACKGROUND: FROM THE "HYDROTYPE" TO "HYDRO-GEOMORPHOTYPE" CONCEPT

In hydrological scientific literature, the problem of the basic unit in catchment regionalization is a big issue not yet shared by hydrologist.
Since the SCS-CN method, the most popular method for computing of surface runoff for rainfall event, involving the use of simple empirical formula and readily available tables and curves, emerge the need of basics units. It is only one method, which can incorporate the land-use for computation of runoff from rainfall. SCS-CN method provides a rapid means for estimating runoff change due to land-use change. The SCS-CN method continues to be most satisfactory when used for different types of hydrologic problems that were designed to solve evaluating the effects of land-use changes (ACI-ASCE, 1985). The GIS and SCS-CN method were combined to the model rainfall-runoff relations and the watershed parameters were estimated while computation of other parameters required significant user interaction (White, 1988; Bhaskar et al, 1992). Purwanto and Donker (1991) proposed semi-distributed hydrologic modeling using SCS-CN method and assessed the effect of land-use change for hypothetical cases of reforestation and deforestation conditions. When hypothetical case of 5% reforestation or deforestation conditions considered, the peak flow was reduced by 14 % for reforestation and increased by 12 % for deforestation case for hydrologic soil group C when compared to normal land-use (Beker and Braun, 1999).
The advent of improved spatial data sources and tools to handle this type of information has enabled a number of authors to suggest various combinations of land-surface characteristics that can be used to defined areas of similar hydrological response.
Kite and Kouwen (1992) describe a catchment disaggregation approach that involves subdivision at regional-scale catchment into a number of hydrotypes with similar land-use characteristics. Comparison was made between using a lumped hydrological model and using a version of the same model applied successively to different land uses within sub-basins. A watershed in the Rocky Mountains of British Columbia was divided into three contributing sub-basins, and each of these was further subdivided by land cover classification using Landsat images. A hydrological model was applied separately to each land cover class in each sub-basin, and the resulting hydrographs were routed to the

subbasin outlet and then through lower subbasins. The final hydrographs were compared to those obtained using the model on the basin as a whole. It was found that using a semidistributed model gives goodness of fit statistics that are better than the lumped basin approach. The land class dependent parameter values found through optimization confirm the physical variations in storages and infiltration rates that would be expected in a mountain basin. The advantage of the semi-distributed model is that relating the parameter values to land cover characteristics provides a method of investigating land use changes and allows the model to be more easily transferred to other basins.

Liang et al. (1994) also describe a catchment disaggregation approach based on distinct vegetative characteristics and Flügel (1995) incorporated additional complexity into the hydro-type delineation process by classifying areas containing unique combinations of slope, aspect, soil and land-use. High sensitivity was found for parameters describing the water-holding capacity of unsaturated storages, which were defined in terms of the rooting depth of vegetation. It was concluded that the incorporation of land-use in the hydro-type delineation process was essential in regionalizing heterogeneity in regional-scale catchments.

Mitchell and DeWalle (1998) utilized elevation and land use information for predicting streamflow in a regional-scale catchment, where snowmelt was known to dominate. To account for climatic variation with elevation the catchment was first divided into four elevation zones. The elevation zones were then further divided into forested and nonforested areas. The results indicated that the accuracy of streamflow predictions was improved with the use of combined elevation and land-use zones compared to the standard elevation zones.

Jain et al. (1998) also divided a catchment into a number of hydro-types according to elevation and land cover information. Rather than having unique combinations of land cover and elevation zones, each hydrotype contained a number of different land covers. The basic requirement of the hydrotype was that the distribution of land covers and elevations were known and that the hydrotype contributed runoff to a definable stream channel.

Krysanova et al. (1998) applied a three-level disaggregation scheme to model streamflow and sediment transport within a mesoscale catchment. The disaggregation process involved subdividing the mesoscale catchment into regional-scale sub-catchments. Hydrotypes or elementary

units were then delineated within each sub-catchment based on land-use and soil types.

Becker and Braun (1999) considered up to nine different areal disaggregation schemes based on land-use, land cover (vegetation), soil-type and slope class for a small-scale river basin.

A sensitivity study of predicted streamflow showed that four hydrotypes needed to be modelled separately: (i) sealed areas; (ii) shallow ground water areas; (iii) forested areas with deep ground water tables; and (iv) arable land with deep ground water tables.

From the studies cited above it is evident that the hydrotype-disaggregation method can overcome the critical effects of averaging associated with lumped land-surface representations, as well as being more realistic in terms of data requirements and computational time as compared to the distributed modeling approach.

Numerous key questions, however, still remain unanswered.

Firstly, it is not clear on which land-surface characteristics can best beused as adequate (dominant) parameters in the disaggregation process at particular scales.

Secondly, concerns have been raised that by obtaining an integrated response from the aggregation of hydro-types, the question of scale has been sidestepped by ignoring the natural heterogeneity of parameters and processes within the individual hydrotypes (e.g. Band and Moore, 1995; Bonta,1998).

Recent developments in hydrological modelling of river basins are focused on prediction in un-gauged basins, which implies the need to improve relationships between model parameters and easily-obtainable information, such as satellite images, and to test the transferability of model parameters.

A large-scale distributed hydrological model has been used in several large river basins in Brazil. The model parameters are related to classes of physical characteristics, such as soil type, land use, geology and vegetation. The model uses two basin space units: square grids for flow direction along the basin and GRU—*group response units*—which are hydrological classes of the basin physical characteristics for water balance. Expected ranges of parameter values are associated with each of these classes during the model calibration. Results are presented of the model fitting in the Taquari-Antas River basin in Brazil (26000 km^2 and 11 flow gauges). The model was then applied to the Upper Uruguay River basin (52000 km^2), having similar physical conditions, without any

further calibration, in order to test the transferability of the model (Collischonn et al., 2007).
As the modelling scale increases to contain a sufficient sample of the small-scale variabilities in soil, vegetation and topographic characteristics for a region, it is no longer necessary to take account of the pattern of those characteristics, but only their statistical characterisation (Moore and Clarke, 1981; Entekhabi and Eagleson, 1989; Avissar, 1992).
Such statistical characterisation can be approximated by continuous analytical functions, or probability density functions (PDFs). The PDF approach considers the frequency of occurrence of variables of certain ranges without regard to the location of a particular occurrence within the area. Such an approach thus allows for the fact that the underlying variability may still be important in controlling hydrological fluxes, but that the pattern is less important.
The **representative elementary area** (REA) was an initial attempt by Wood et al. (1988) to determine the scale, at which small-scale organization in catchment characteristics is no longer important.
Using a hypothetical study of the effects of variable topography, soils and rainfall and, at least for short rainfall correlation lengths, Wood et al. (1988) showed that the REA for runoff generation predicted by their particular model and catchment characteristics was of the order of 1 km^2.
Subsequent research has shown that it may be, for some conditions, that there is no scale at which the variance in runoff response reaches a minimum, whereas in general it should be expected that if an REA scale exists, it might vary between environments and processes (Blöschl et al., 1995). Even if it is difficult to define an REA scale unequivocally, Beven (1995) and others have suggested that it may still be possible to use an approach based on the distribution functions of variables (or parameters) to provide realistic predictions of discharge and evapo-transpiration fluxes within heterogeneous terrain.
The quasi-distributed Variable Infiltration Capacity (VIC) hydrological model (Wood et al., 1992) was developed in an attempt to reproduce larger-scale hydrological response. The VIC model incorporates the saturation–overland flow mechanism with a continuous PDF to describe the relationship between soil moisture content and saturation, with relevant hydrological quantities determined by integration over this distribution. In essence, the distribution allows different parts of the catchment to have different significance in terms of runoff generation

potential. It also takes into account that the relationship between different catchment areas may change with wetting and drying.
The advantage of the PDF modelling approach lies in its ability to reproduce catchment response with a smaller number of physically meaningful parameters than the more traditional distributed models. This reduction in parameters is in line with the principle of parsimony that requires the modeller to seek the simplest model parameterization consistent with available evidence (Jakeman and Hornberger, 1993).
Another example was the quasi-distributed Variable Infiltration Capacity (VIC) hydrological model initially proposed by Wood et al. (1992) and subsequently modified by Kalma et al. (1995) and Sivapalan and Woods (1995).
The VIC model adopts a statistical distribution of storage elements across the catchment to allow for the fact that small-scale variabilities of soil, vegetation and topography will cause different parts of the catchment to have different soil moisture storage.
On the basin scale, the hydrograph is influenced by basin morphometry which can be expressed by representative attributes for catchment height distribution (relief indices), length and form of the basin (form indices) and parameters describing the drainage network (Cooke and Doornkamp, 1990; Gregory and Walling, 1973, Schmidt et al., 2000).
Recent advances in the analysis of landform geomorphometry through the availability of high resolution Digital Elevation Models (DEMs) and diffusion of GIS software enhance further quantitative research efforts within this topic.
The above illustrated literature rewiev deserve as start point to "*Up-to-dating VAPI Project*". Preliminary results of this researches are presented in Guida et al., (2007) in order to define multi-scale geo-morphometric landform types, reflecting similarities in their soil-landforms relationship and hydrologic behaviour, using a simple hydrologic-geomorphometric landform classification and a pre-defined model of terrain classification. In the EGU poster session (2007), the Authors show a proposal of defining and mapping *Hydro-geomorphological Units* at regional, basin and watershed scale from automated land-system recognition, referring to the GIS-based experiences carried out in Campania region.
Geomorphometric classification scheme follows previous approaches (Weiss, 2001), using original algoritms proposed in Guida et al. (2007) and producing *hydro-geomorphological units* according to the basic runoff

generation models: i) hortonian overland flow, ii) saturated overland flow, iii) subsurface flow and iv) deep percolation.
The Authors highlight that the hydrological behaviour in large basins is controlled by complex interactions between geomorphic, hydrological, hydro-geological, biological processes and land uses practices on hillslope, small catchments, watersheds and riparian zones and the studies related to this topics must be carried out within on shared interdisciplinary approaches. In fact, linkages between hydrologic behavior and geomorphic-soil attributes affect nonlinear or threshold responses of the hydrologic functions as runoff generation from open hillslope and colluvial hollows, expansion of preferential flow networks, redistribution of subsurface water storage in soils (Sidle et al.,2000) and groundwater contribution from bedrock.
So, in this chapter we proposed a new approach for the identification and delimitation of *hydro-geomorphotypes*, starting from the above cited proposals (Rossi and Villani, 2006); Guida et al., 2007, following a modified procedure proposed by Schmocker (2007), at plot and catchment scale, and integrating it by the hierarchical, multiscale implementation of the nested landform units.
The proposed procedure was applied and tested at catchment scale in representative gauged basins of the Campania Region and successively extended at regional scale to un-gauged basins. One part of this research concerns the definition and regionalisation of geomorphometric characteristics and attributes with hydrologic relevance on different spatial scales.
The resulting maps can be used to inferring hydro-geomorphotype in the up-to-dating VPI prodedure at catchment scale.
The introduction of this unit could be usefully adopted to evaluate both surface and the sub-surface response of basins, i.e., to highlight the fast and delayed response of a basins to the rainfall inputs.

6.4 METHODOLOGICAL APPROACH

The approach used for performed the hydro-geomorphologic types map was based on the hierarchical multiscale approach.
As mentioned in the introductory paragraphs, the methodological approach developed in the present research, starts from the scientific

guideline of Rossi (2006) and is build-up from the prototypal work of Guida et al. (2007), Blasi et al. 2007, Guida et al. 2007, 2009).
In the cited guidelines, a preliminary conceptual model of hydro-geomorphotype was developed for the mountain carbonate landscape with the pyroclastic soil cover, surrounding the volcanic complexes of the Campania region (Southern Italy).
The figure 6.3 shows the relationship between morphological units (and their morphological components, i.e the zero order basin component in the headwater valley unit), soil-bedrock lithology and dominant infiltration-filtration hydrological model.

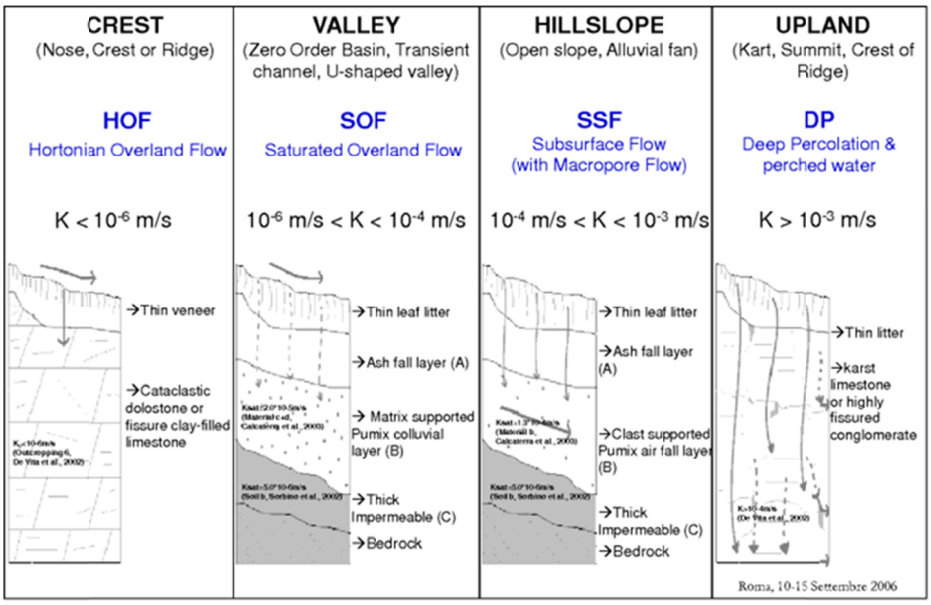

Figure 6.3: Relationship between morphological units and dominant infiltration-filtration model referred to the pyroclastic soil-mantled, carbonate landscape, surrounding the volcanic complexes of the Campania region (Southern Italy).

The figure 6.4 shows the Hydrogeomorphological Map resulting from a preliminary automatic, GIS-based, grid-oriented procedure applied to the Campania region, performed from a DEM with a cell size 20x20 m.

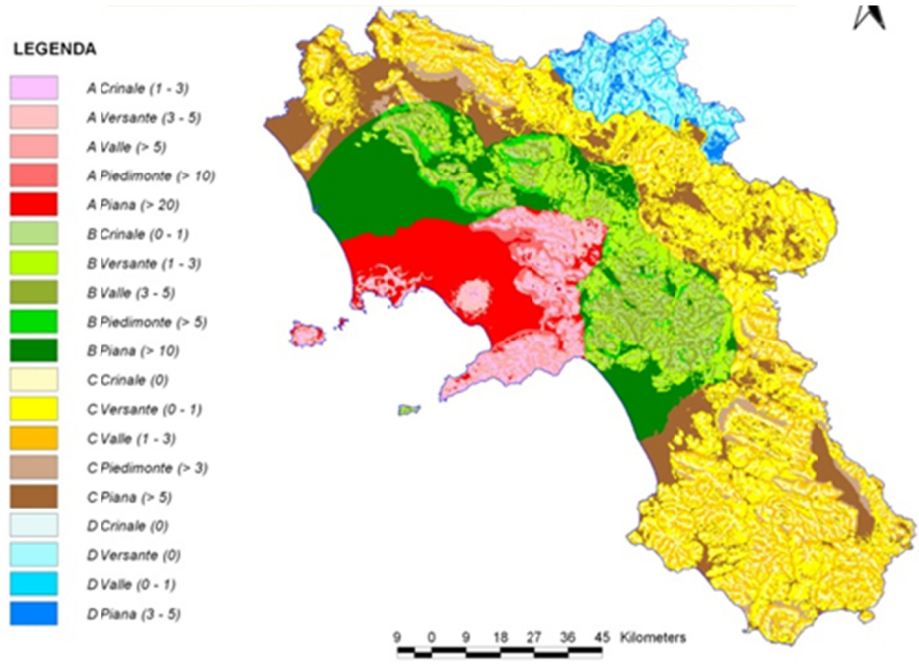

Figure 6.4: Preliminary Hydro-geomorphological Map of the Campania region (Guida D., in Rossi and Villani, 2006)

The method presented in Rossi (2006) gives the opportunity to objectively define the above cited Hydro-geomorphotypes and regionalize them in a map unit with a hydrological relevance on different spatial and temporal scales.
The central issue of the approach was: what is the basic unit geomorphologically consistent and hydrologically functioning?
Based on the scientific literature concerning the specific topic, the researches carried out by Troch et al. (2002) was considered appropriate. The study of Troch and collegues is based on the solution of the Boussinesq equation to describe the sub-surface flow from a one dimensional hillslope (figure 6.5) and on his application to a "*nine basic hillslope types*".

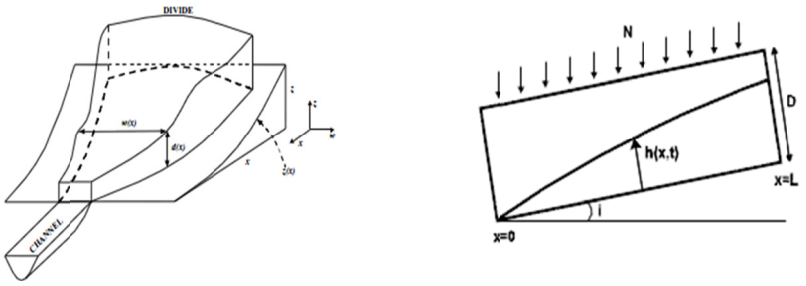

Figure 6.5: Definition of the cross -section of a hillslope aquifer (modified by Troch et al. 2002)

The nine hillslope types considered by Troch et al. (2002) are shown in the figure 6.6 and they will named *Basic Geomorphometric Type* (BGT) in the present research.

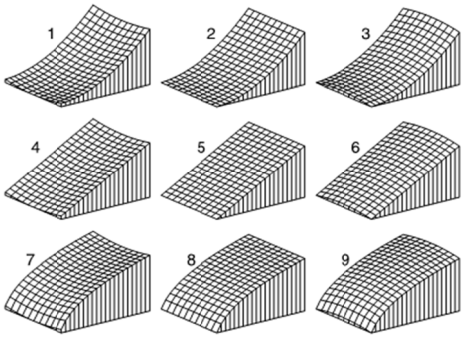

Figure 6.6: The nine form element, corresponding to Basic Geomorphometric Types (BGT): 1. Concave in plan and in profile; 2. Straight in plan and convex in profile; 3. Concave in plan and convex in profile; 4. Convex in plan and straight in profile; 5. Straight in plan and profile; 6. Concave in plan and straight in profile; 7. Convex in plan and concave in profile; 8staight in plan and concave in profile;9. Convex in plan and in profile.

Referring to the multiscale analysis, the basic landforms types cannot be disaggregates further (this are named in geomorphology "*elementary form*" (Dramis et al. 2011, Minar & Ivans, 2008), but they can be aggregate for the upscaling mapping (Consistently with the discussion in section 6.2). The figure 6.5 contained the representation of the typical illustration of the hierarchical ordering used in the literature for the multiscale

mapping. This figure was adapted to the specific issue of the hydro-geomorphotypes where were specified the range of scale adopted for each level.

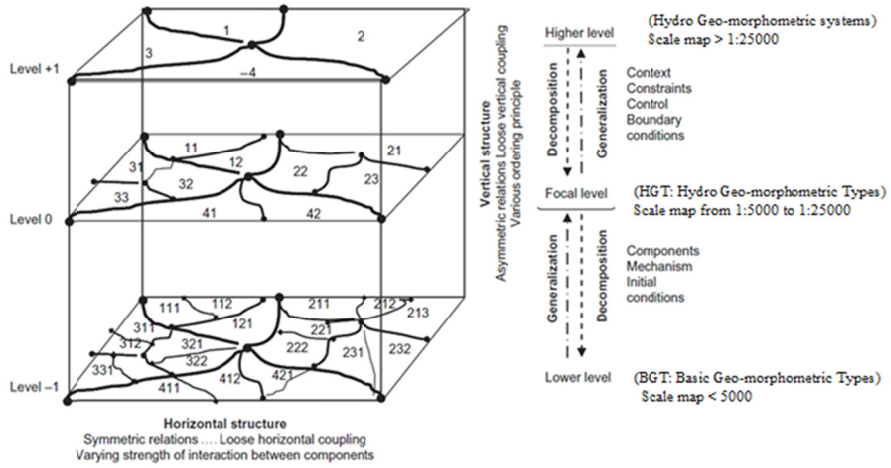

Figure 6.7: Hierarchical relationships between focal and higher/lower levels (modified from Dramis et al., 2011).

For the identification of the hydro-geomorphometric types, were firstly individuate the nine basic hillslope of Troch (BGT), so, referring to the figure 6.7, the procedure will start from the lower level and then, using the generalization method, that will explained in the following, the BGTs will be combined to build up the focal level.
Troch et al. (2002) to performing the nine basic types compared the profile and planar curvature. He used the polynomial function of Stefano et al. (2000) to describe the profile curvature function z(x) as:

$$z(x) = E + H\left(1 - \frac{x}{L}\right)^n \qquad \textbf{Equation 6.1}$$

Where: E is the elevation difference of the bedrock along the hillslope, L is the corresponding slope length and n defines profile curvature, for $n>1$ the profile is concave, $n<1$ define convex profile and for $n=1$ the profile is linear.

Adding a quadratic term to the equation 6.1, for describing the slope shape in the width direction, the formula becomes:

$$z(x) = E + H\left(1 - \frac{x}{L}\right)^n + \omega y^2 \qquad \textbf{Equation 6.2}$$

Where: ω is a plan curvature parameter and y is the distance from the slope center.

Combining the three plan curvatures ω and the three profile curvature n it is possible defining the nine basic hillslope types or Basic Geomorphometric Types (BGT), as defined in the present topic.

Also Troch et al. (2002) have computed the drainage response function for each BGT solving the continuity equation and the kinematic form of Darcy's law, adopting a proposed simplified method of Fan and Bras (1998) to map the three-dimensional soil mantle into a one-dimensional storage capacity function. This approach takes into account how plan shape and profile curvature are dominant topographic controls on flow processes along hillslopes. In the figure 6.8 is reported the plan view of the drainage of the nine hillslope.

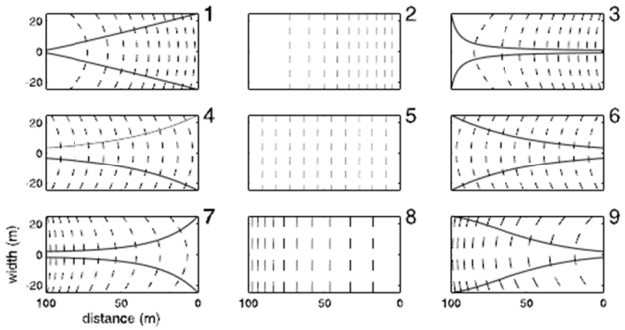

Figure 6.8: Plan view of drainage devides (solid lines) and contour lines (dashed lines of nine BGTs. The upslope devide is at x=0 (Troch et al., 2002)

It is evident the flow behavior of the BGT 1, 4 and 7 that is convergent, whilst, the divergent flow occurs for the types 3, 6 and 9 which have a concave - straight curvature.

The figure 6.9 shows, on the left, the sub-surface flow rate at different location along the hillslope (solid line: x=100 m is the outlet, dashed line:

X= 75 m, dash-dotted line: X= 50 m, dotted line: X= 25 m) and, on the right, soil moisture storage for characteristics time steps during the free drainage (dotted line: initial time t=0, dash-dotted line: t = 5 days, dashed lines: t =10 days, solid lines t = 15 days)

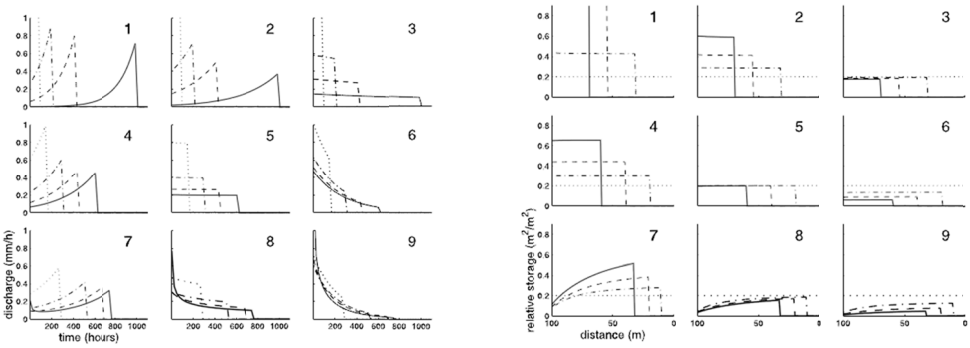

Figure 6.9: The hydrological behavior of the nine Basic geomorphometric Types (BGT):on the left, the sub-surface flow rate at different location along the hillslope; on the right, soil moisture storage for characteristics time steps during the free drainage (Troch et al., 2002)

Troch et al. (2002) have demonstrated that these nine hillslopes show quite different dynamic behavior during free drainage and rainfall recharge events.

Associating to each BGT a distinctive hydrologic behavior of figure 6.9 each one can be named, in the present study, "*Basic Hydro-Geomorphometric Types*" (BHGT), as minimal units reflecting the soil and topographic control on the surface and subsurface flow processes.

It evident in the figure 6.9 that, as explained by Troch "… *where there is a low bedrock slope near the exit, as for the BHGT 1, 2, 3, the flow drain slowly. The outflow for the 1, 2 and 4 increase with the time due to the increasing of the soil moisture storage near the exit. The outflow of hillslope 3 stays nearly costant for a long time as the soil moisture storage at the outlet stays close to the its initial value before to dropping. All convergent solpe (1. 4 and 7) have increcession outflow with the time, again because the soil moisture storage at the outlet increases in time . The soil moisture storage near the outlet of the diverging hillslope (3, 6 and 9) decrease with the time . The outflow of the hillslope 5 stays costant.*"

So, the Troch analytical approach was used for integrate the prototypal work of Guida et al. (2007) in the objectively individuation the nine BHGT and characterize them in respect to the sub-surface flow and the soil moisture capacity.
The Troch's method of is analytically very rigorous, but it is very difficult in applications at the basin scale to simulate the hydrological behavior of complex landscape, as the karst basins or the glacial basins. Also, this method gives information on the sub-surface flow and the soil moisture storage, but does not allows on the identification of the dominating runoff.
For these reasons, it was been crucial find a more effective method to integrate to the Troch's analytical approach of and obtaining a simplified procedure to individuate the land units with dominant rainfall-runoff transformation processes.
After detailed analysis of the specific literature on a simplified procedure to define the runoff production mechanisms, was used as the method proposed by Scherrer et al. (2003) (figure 6.10) at a catchment scale, successively applied by Schomocker-Fackel et al. (2007), on plot and catchment scale.

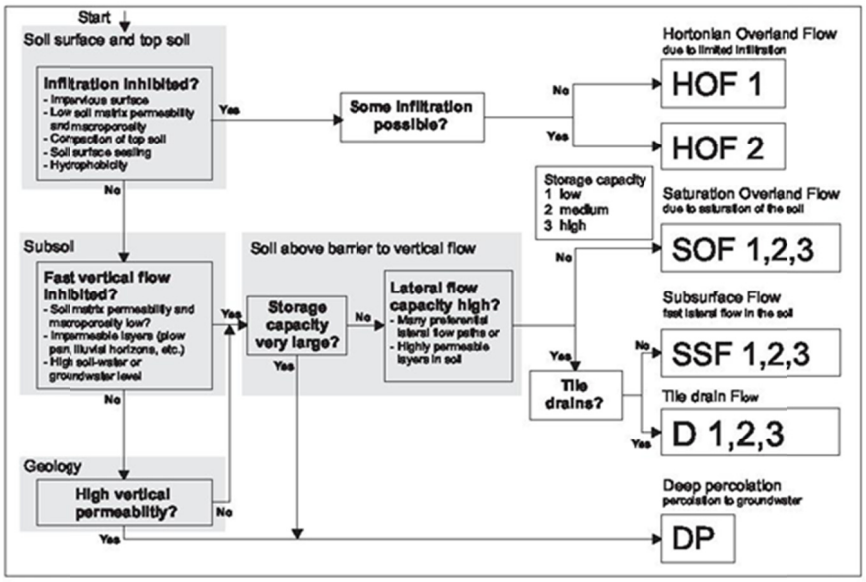

Figure 6.10: Decisional scheme to identify the dominant runoff processes

This procedure was based on large number of sprinkling experiments conducted by Faeh (1997), Scherrer (1996), Weiler and Naef (2003). Scherrer and Naef (2003) and was used this as a basis for developing process decision schemes to determine the dominant runoff on a soil profile. The procedure do not took into account the morphometric characteristics of the basin, as shown in the figure 6.10, and was adopted exclusively in the urban areas.
So, the method proposed for the identification of the hydro-geomorphotypes of the Campania region combines the prototypal procedure of Guida et al. (2007), objectively identify on the basis of the automatic recognition of the nine BGT of Troch (2002), and the results studies carried out by Scherrer et al. (2003).
The propotypal procedure of Guida et al. (2007) was an usefull guidelines for the interpretation of geomorphometric unit into a corrispondent hydrologic behaviour of the sub-soil, while the method of Scherrer et al. (2003) was a good example of decision scheme for the identification of mechanisms of the runoff wich are reduced to three classes in the approach used for the campania region, as shown in figure 6.11.

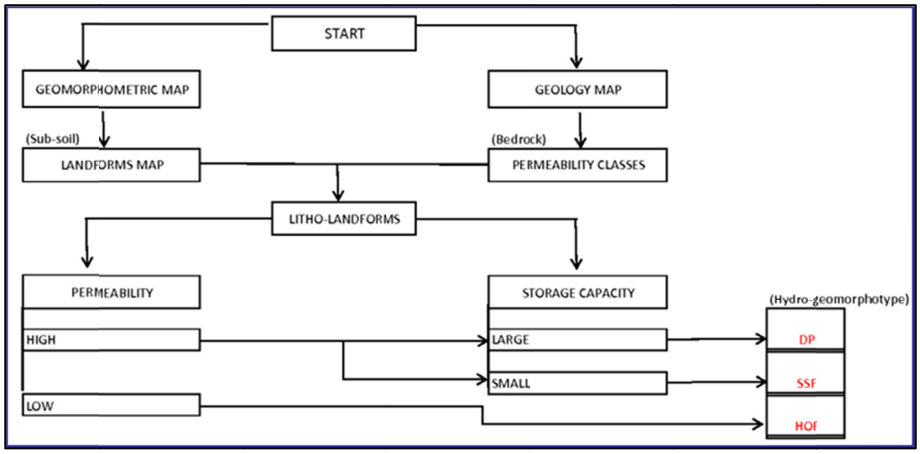

Figure 6.11:Decision scheme for the identification and delimitation of hydro-geomorphotypes in the Campania Region

The procedure adopted is based on two approaches. The first approach is geomorphological based and consists on the performing the

Geomorphometric map following the method of Troch to obtain the nine BGT and the BHGT.
Combining the BHGT at catchment scale, were produced a wide range of Hydro-geomorphological Units (HGU), traditionally considered in hydrology and geomorphology, performing the Landforms map.
In the procedure above described , the identification, delimitation and classification of the HGU results by grid-based and object-based GIS techniques, using the following recent studies of Summerel et al., (2005). In this paper, the authors demonstrate with models and examples the shared assumption that location and distribution of landform shape and size describe and categorize many features of a catchment, indicating, among others, soil types, geological features, hydrological influences, and even shallow groundwater systems. The paper describes an objective method for delineating major landforms of a catchment on the basis of hydrological terrain analysis. It allows comparisons to be made within and between catchments. The method uses the UPNESS index from the Fuzzy Landscape Analysis Geographic Information System (FLAG) model (Roberts et al., 1997) that is derived from digital elevation data. UPNESS was developed as an index of surface and shallow subsurface water accumulation, fitting a five-parameter sigmoidal function to the cumulative distribution function (cdf) of the natural log (ln) of UPNESS. The point of inflection of the *cdf* of the UPNESS index is defined from the first derivative of the five-parameter sigmoidal function as the point of maximum concavity. The second and third points are defined by determining the maximum upward concavity and minimum downward concavity from the second derivative of a five-parameter sigmoidal function (referred to as break points). The inflection and break points from the UPNESS index are used to segment the cdf into three regions that represent four different landform elements. Landform categories based on these points represent **ridge tops** and **upper slopes**, **midslopes**, **lower slope**, and **in-filled valley/alluvial deposits**. The shape of the *cdf* curve indicates the dominance of major landforms within a catchment, providing an objective means for classifying this catchment characteristic. Examples are given showing how landform discrimination compares to geological maps. The landforms index presented in the above paper offers an useful technique to differentiate complex landforms in a landscape using terrain analysis, attempting to represent dominant hydrological soil formation processes.

This statement have been followed in this research, adopting simplification and adaptation to perform a multiscale application in supporting flood hazard assessment in Campania region.
The second approach used, as basic map, the regional geologic map reclassified in three relative permeability classes, obtaining the Permeability Map.
Combining the two approaches and relative database on the permeability and storage dataset, the *Effective Hydro-geomorphological Units* (EHGU) were obtained, according to the basic runoff generation models: hortonian overland flow, saturated overland flow, subsurface flow and deep percolation.
The procedure proposed was firstly tested on two experimental watershed of the Campania Region and successively extended to the Campania region. In the following paragraphs will describe in detail the proposed procedure and will show the obtained map.

6.5 GIS-BASED, AUTOMATIC RECOGNITION

The procedure described above was firstly applied at a catchment scale in the Upper Bussento, because it was one of the experimental basins of the VAPI project, for its geological and geomorphological characteristics and for the particular hydrological behavior already described in the chapter 4.
The Upper Bussento river drains with its water the mountain basins, that, as recently stated by several researches, are responsible of the discharge water in the lowland area (Viviroli & Weingartner 2004, Viviroli et al, 2011). For this raison, in this research, it was chosen as experimental basin for the reliability of the methodology.
For the identification of the EHGU of the Upper Bussento river, were utilized the hydro-geological map at 1:25000 scale, provided by the Left Sele Basin Authority (AdB), and a DEM of the catchment obtained by the Technical Regional Map at 1:5000 scale with a cell size of 5x5m. The choice of cell size was dictated by the correspondence to the scale of analysis chosen.
Following the procedure shown in the figure 6.11, the Hydro-geological Map (figure 6.12) was adopted to define bedrock permeability classes.

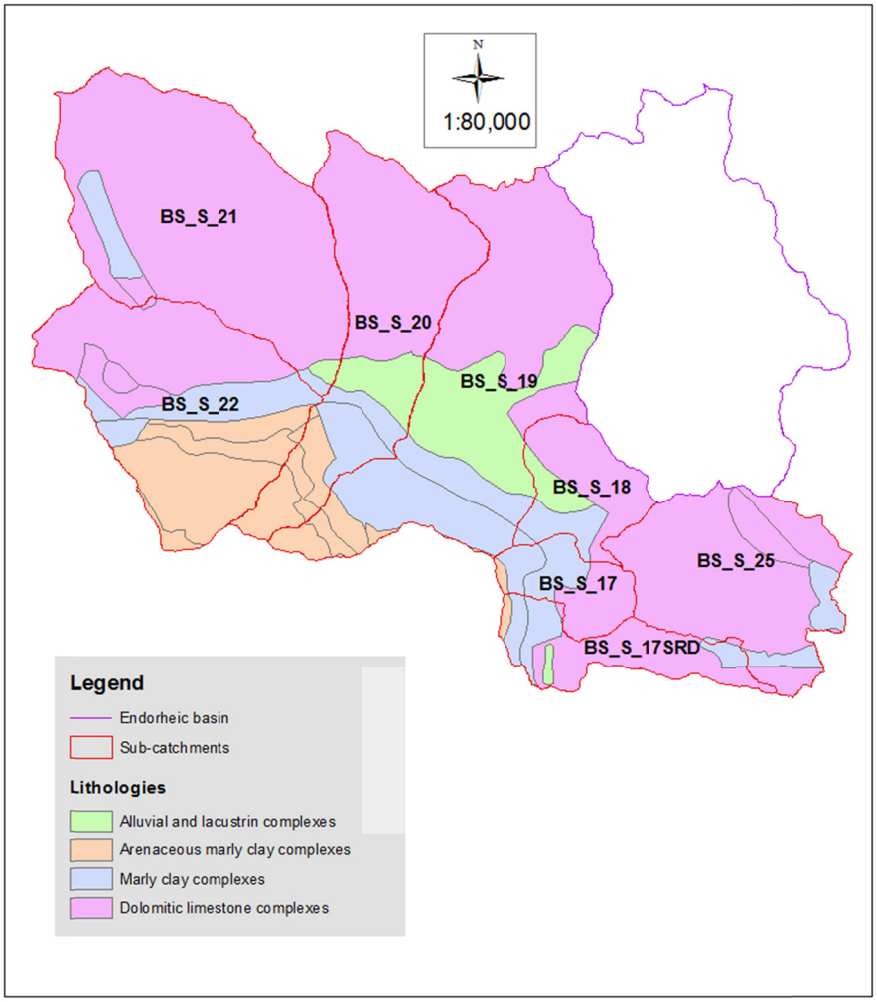

Figure 6.12: Hydro-geological map of the Upper Bussento river

Starting from a first classification of the relative bedrock permeability in: high, medium and low permeability, it was been reclassified in two classes: permeable or not permeable, according to the VAPI procedure (figure 6.13).

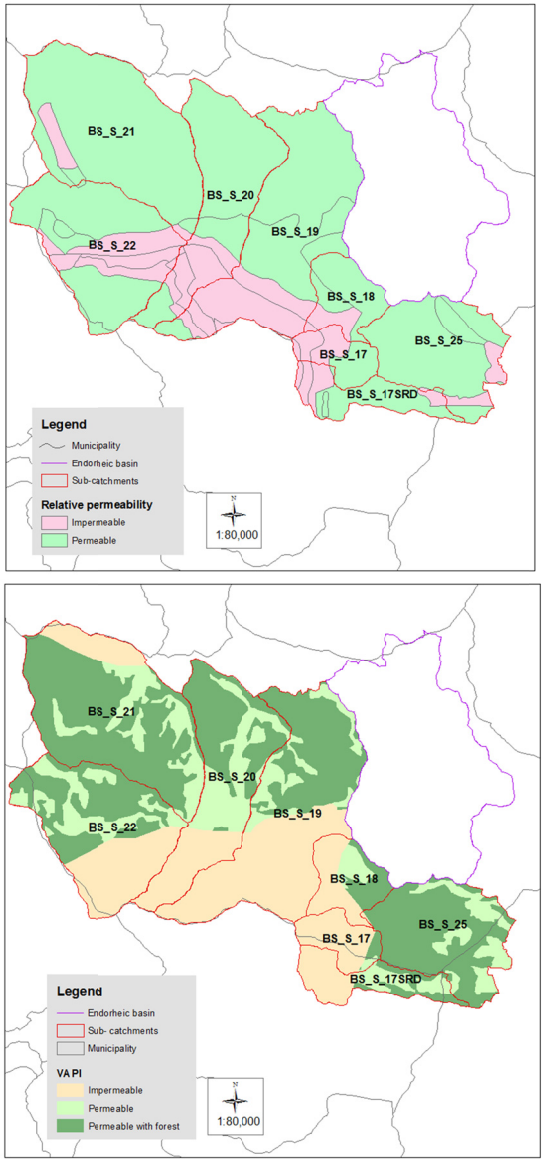

a)

b)

Figure 6.13: a) Permeability Map compared with the hydro-geological map used in the VAPI procedure.

Then, to define the hydrologic behavior of the sub-soil, the Landform Map was dawn-up, by using two softwares, e-Cognition (licensed by D. Guida) in object oriented analysis and the ArcMap (licensed by CUGRI) in the elaboration of the grid maps.

The e-Cognition software, currently used in the Image Analysis, in earth sciences it is used to develop rule sets for the automatic spatial analysis from remote sensing data and DEM's, using the segmentation techniques and classification rule-set. The e-Cognition software was used to identificate the nine basic geomorphometric types (BGT) and perform their aggregation, deriving from the DEM, slope, planar and profile curvature, and flow accumulation by fuzzy-set rules based on adequate parameter thresholds (figure 6.14 and 6.15).

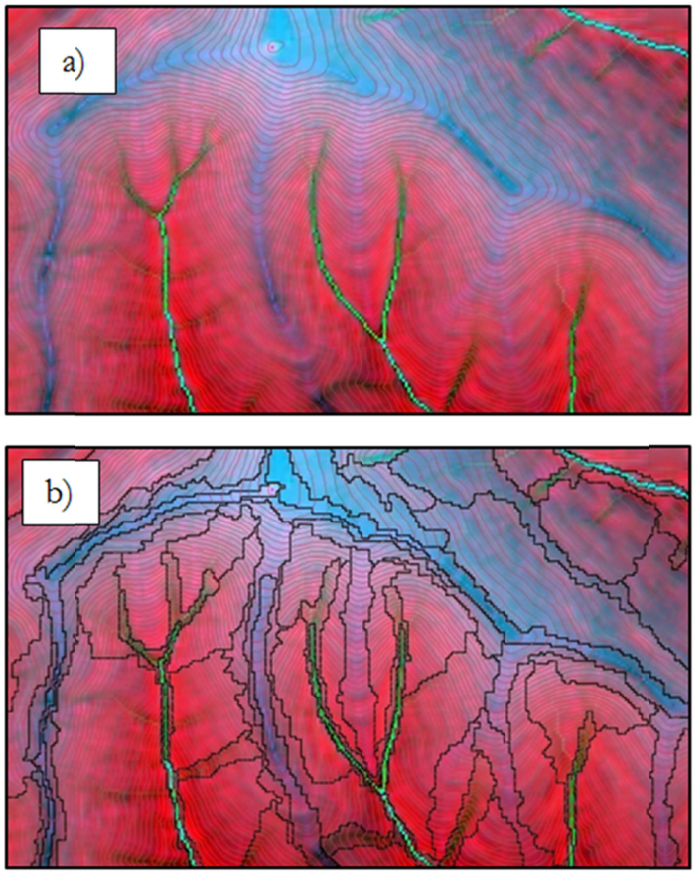

Figure 6.14: a) the map is a composed of the DEM, slope, planar and profile curvature, and flow accumulation (grid image); b) the results map of the segmentation algorithm is shown (object image)

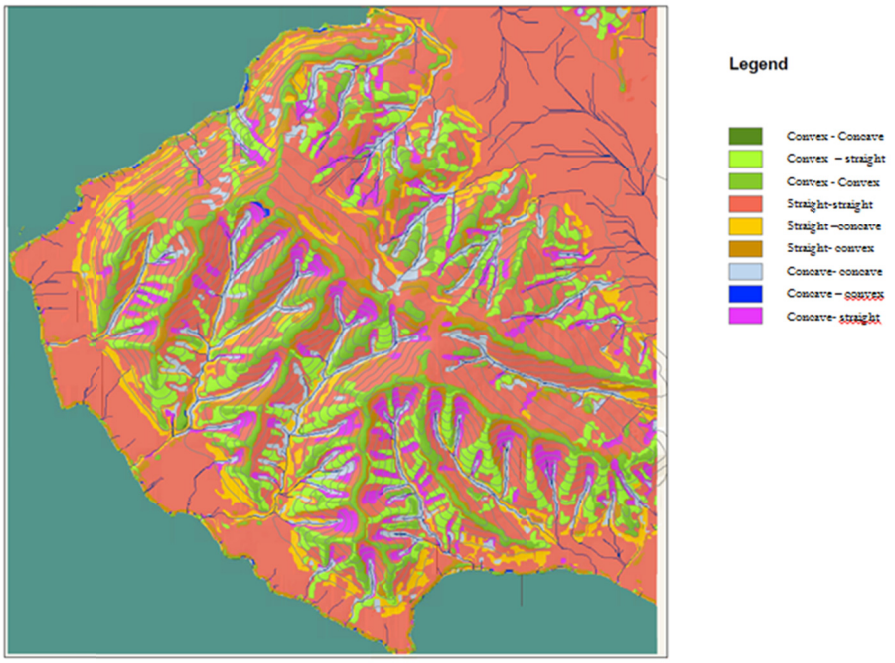

Figure 6.15: Elementary unit of landforms defining the nine Basic Geomorphometric Types (BGT)

Identified the BGT map, to each one was associated a relative soil moisture storage capacity considering the approach of Troch et al. (2002). The BGTs were selected in two groups.
The first one includes the types 1, 2, 4 and 7, having a convergent flow and showing an increase of the sub-surface flow with the time due to the increasing of the storage. For these was assigned in the database a large storage capacity. The second one includes the types 3, 5, 6, 8 and 9 for witch the soil moisture storage decrease with the time. To these were assigned the small storage in the database.
By assigning these characteristics to the BGT, they become Basic Hydro-geomorphometric Types) BHGT.
In the natural landscape, each basic landform could be seen as an association of two or more BGT or BHGT.
For example, a "Ridge" is formed by two BGT straight in plan and convex in profile, connected in the summit (figure 6.16). The Zero

Order Basin (ZOB) is formed by two BGT straight in plan and concave in profile, connected to the base (Figure 6.17).

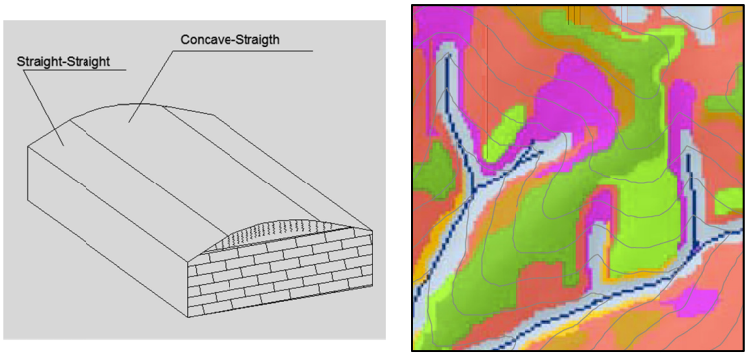

Figure 6.16: On the left is shown the schematic ridge and on the right its identification on the landforms map (object in green).

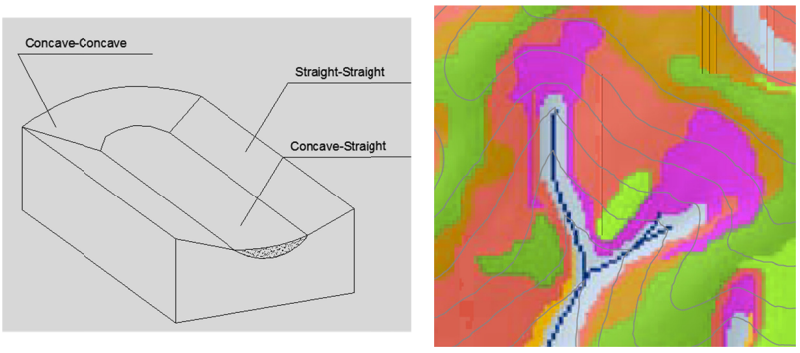

Figure 6.17: on the left is shown the schematic Zero Order Basin and on the right its identification on the landforms map (object in pink and violet)

So, considering the hydrological behavior of this landforms as storage capacity, the ZOB may have a large capacity of storage as demonstrate by Troch for the straight-concave units and for the ridges must be expected a lower storage capacity than the previous.
Following the criteria above described and following Summerell et al. (2005), in E-Cognition software has proceeded to a suitable combination of the BHGT to obtaining the following landforms: summit, open slopes, deep incised valley, U-shaped valley and plains.

The figure 6.18, shows the Landform Map of the Upper Bussento river.

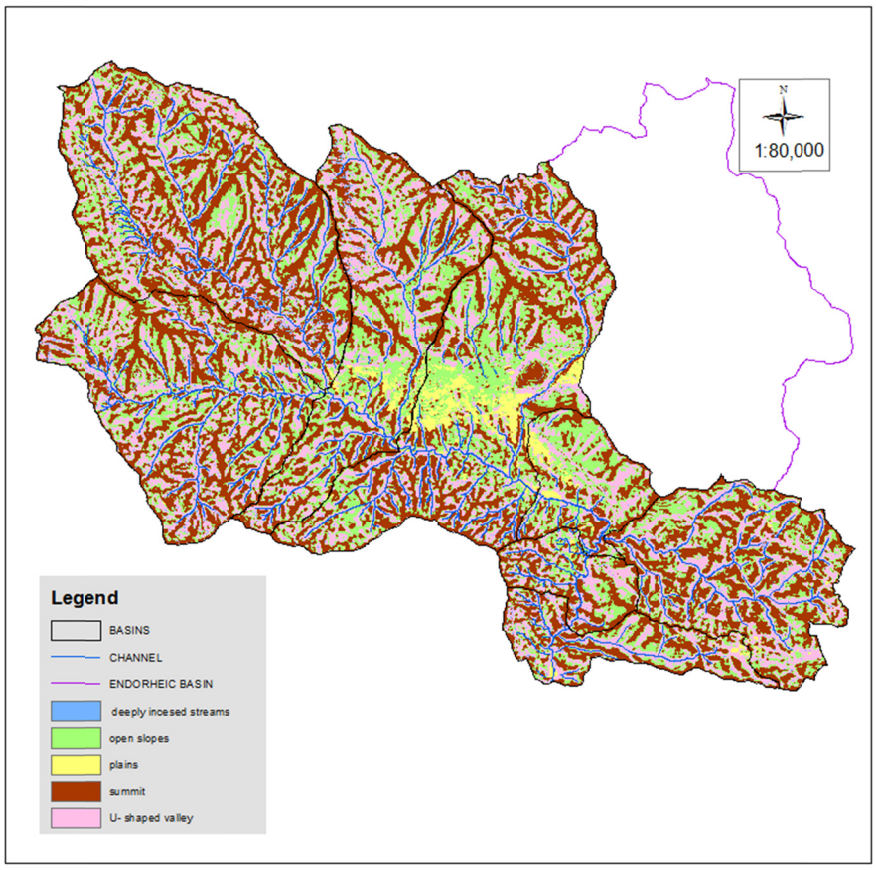

Figure 6.18: Landform Map of the Upper Bussento

The Landform Map, consisted of HGU has a graphical and not graphical database. This last contains information on the storage runoff capacity. Combining the BHGT (to obtain the HGU), each hydrologically described with a specific analytical equation on the storage capacity of Troch (2002), an integration to the present research will be programmed to solve the system of transfer equations on the storage capacity at the linkage between two BHGT. Appropriate boundary condition must be placed at the transition from one BHGT to another. This problem was not object of the present research study and this for the specific aim of

the topic oriented to the individuation and delimitation of the hydro-geomorphotypes, only.
To complete the hydrological behavior of each landform, the storage capacity must be linked to the bedrock permeability. In fact, the proposed procedure includes the merging of the Landforms map with the permeability map. The results map, named the Litho- landforms map is shown in figure 6.19.

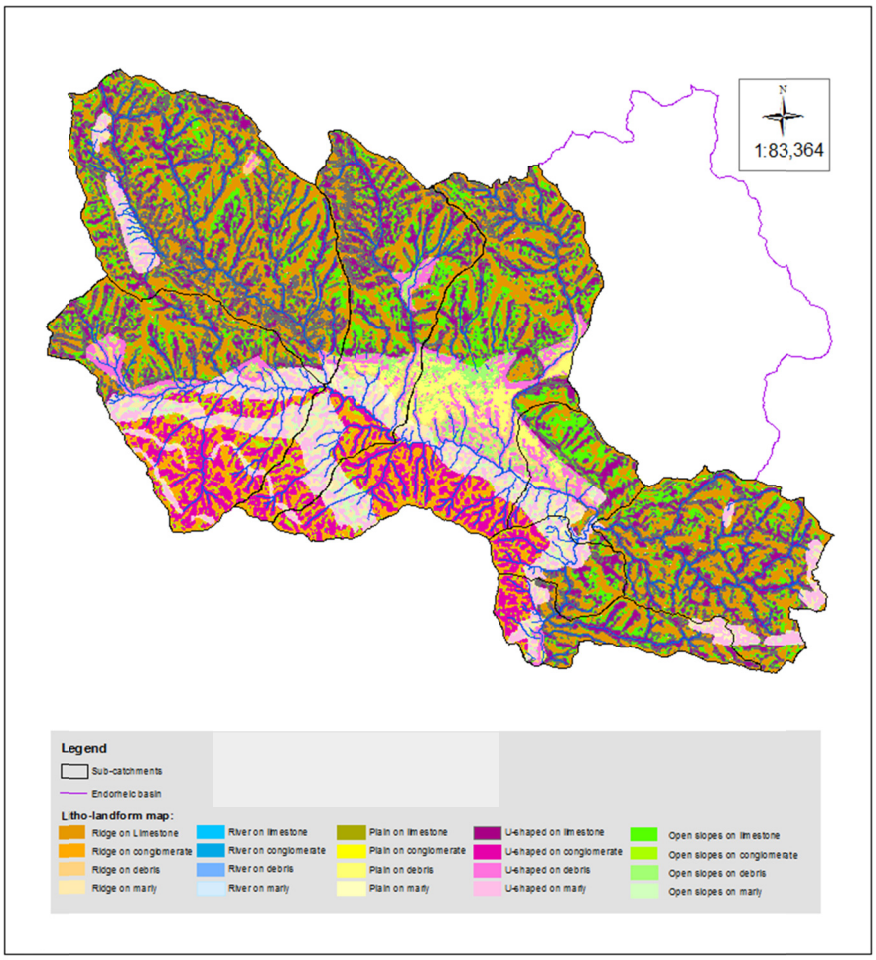

Figure 6.19: The Litho-landforms Map of the Bussento river basin

The above Litho-landform Map consists of a graphical and not graphical database with a dataset on the permeability of the bedrock and on the storage capacity of the soil and subsoil. This step allowed to identify the so named *Effective Hydro-Geomorphological Units* (EHGUs) to which one is associated a specific runoff production following the scheme of Naef (2003). In particular, it was considered the results obtained by Scherrer et al. (2007) on some investigated plot (figure 6.20, 6.21).

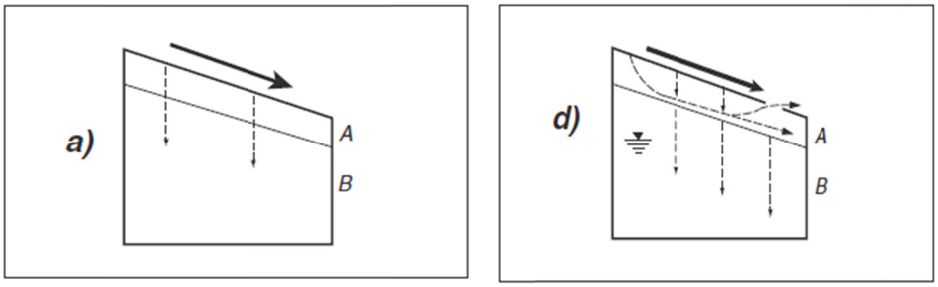

Figure 6.20: The Hortonian Overland Flow (HOF) is considered for conditions: on the left infiltratin restricted by a low permeability layer in the A or upper B horizon caused by compaction; on the right on nearly saturated shallow soils, infiltration quickly causes saturations (modified from Scherrer et al., 2007)

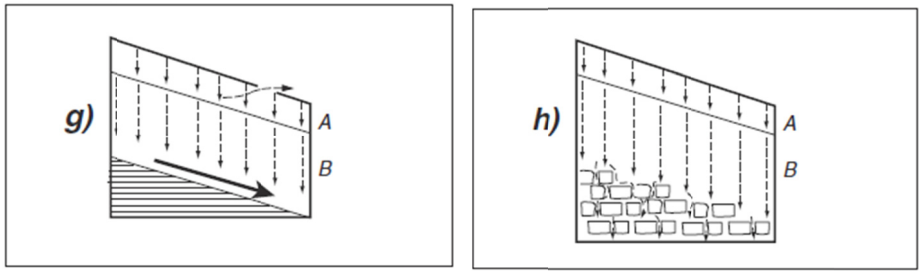

Figure 6.21: The subsurfce flow is shown on the left. Shallow soils on an impervious layer. Good vertical and lateral permeability are required; the deep percolation is on the right. Permeable soils with good vertical permeability in combination with a pervious geology (modified from Scherrer et al., 2007)

Referring to the Scherrer study, his results were adapted to the local geology and geomorphology and following the instruction collected in the table 6.1 were individuated the EHGUs and performed the hydro-geomorphological map (figure 6.22).

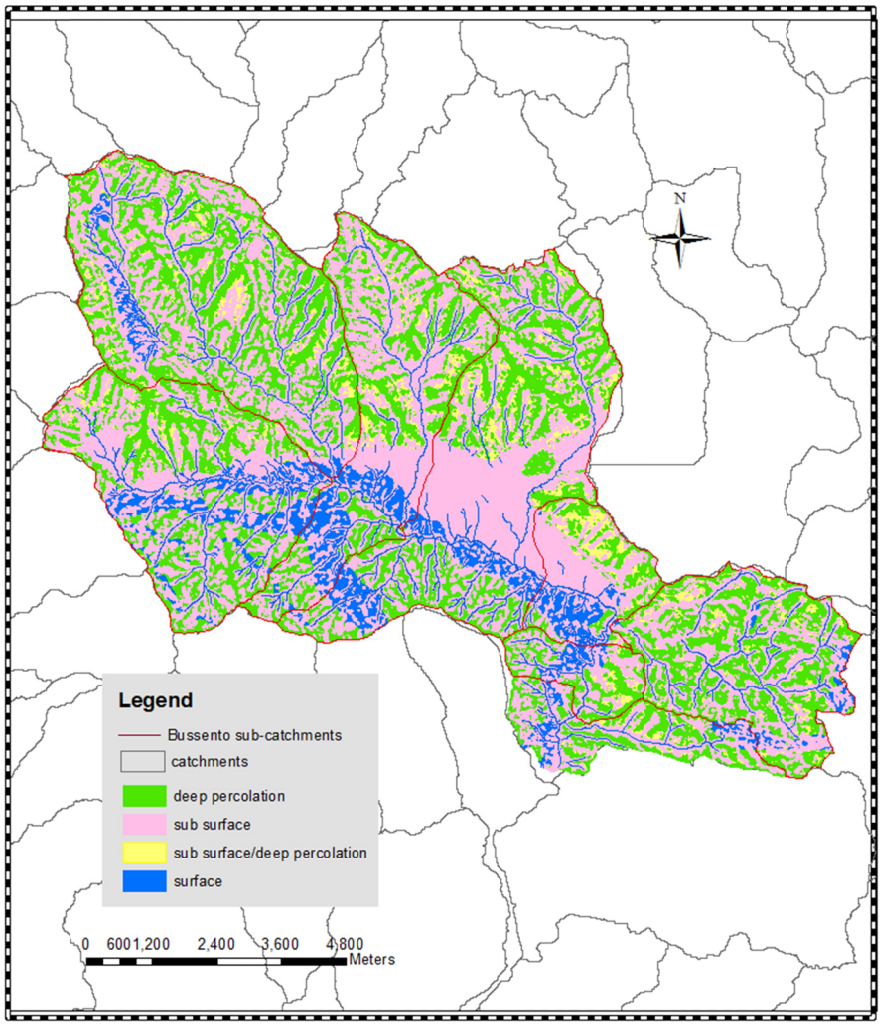

Figure 6.22: EHGU map of the Upper Bussento river basin

Table 6.1: Dominat mechanisms of production of the runoff compared to the lithology anf geomorphology

BEDROCK	LANDFORM	SOIL	DOMINANT INFILTRATION	EFFECTIVE HYDRO-GEOMORPHOLOGICAL UNIT
Limestone Dominant high or very high permeability due to fracture and Hypo-karst	Summit (Ridge, Peak, Crest or Nose and related Shoulders)	Thin and discontinuous veneer of organic and residual soils in blanket and pockets	Dominant infiltration and deep percolation (DP). Very low runoff production. Ephemeral, diffuse springs along the transition from highly fissured hypo-karst zone and fractured limestone below after prolonged rainfalls.	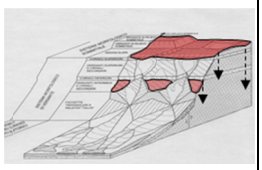
Limestone Dominant high or very high permeability due to fractures and joints	Open Slope (Hillslope, Sideslope, Scarp)	Soils on colluvial and debris cover with lower boundary on fractured limestone bedrock	Dominant excess saturation and sub-surface rainfall-runoff transformation model, partly deep percolation via sub-cutanean infiltration (P. W. Williams, 1983) Paul W. Williams (1983) The role of the subcutaneous zone in karst hydrology - Journal of Hydrology Volume 61, Issues 1–3, February 1983, Pages 45–67 - V.T. Stringfield Symposium - Processes in Karst Hydrology	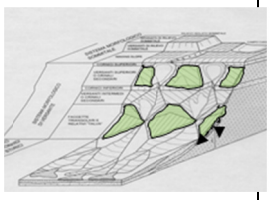

Limestone Dominant high or very high permeability due to fracture and Hypo-karst	U- Shaped Valley	Soils on colluvial infilling by diffusion processes in hollows and swales on argillic B-horizons	Dominant excess saturation and sub-surface rainfall-runoff transformation model, very low deep percolation via sub-cutanean infiltration (P. W. Williams, 1983)	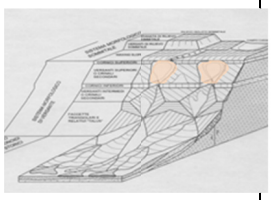
Limestone high permeability due to fracture	Deep Incised Valley	Bedrock or boulder stream	Surficial permanent or intermittent streamflow	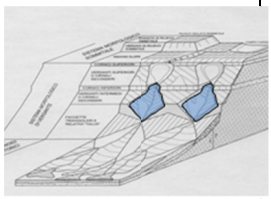
Limestone Dominant high or very high permeability due to fracture and Hypo-karst	Plain (dolines, poljes and limestone pavements)			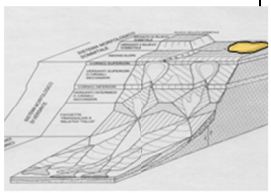

Conglomerate-sandstone Dominant high or very high permeability due to fractures and porosity	Summit (Ridge, nose and crest) Plain (Shelves, Esplanade)	Thin to tick soil and weathered regolite and saprolite	Dominant infiltration and deep percolation. Very low runoff production. Ephemeral, diffuse springs along the transition from highly weathered zone and fractured sandstones.	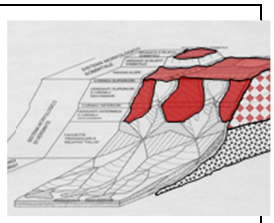
Conglomerate- sandstone Dominant high or very high permeability due to fractures and porosity	Open slopes U- shaped Valley		Dominant excess saturation and sub-surface rainfall-runoff transformation model, partly deep percolation	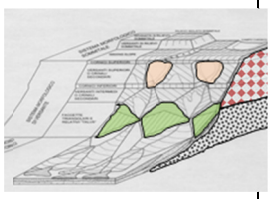
Conglomerate- sandstone Dominant medium permeability due to fractures and porosity	Deep incised valley	Bedrock or boulder stream	Surficial permanent or intermittent streamflow	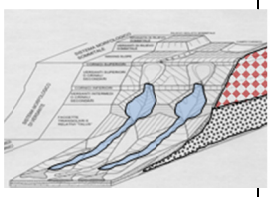
Marly clayey arenaceous	Open slopes Summit U- shaped Valley Deep incised valley Plain	Incept- soils and regosoils	All landforms have a dominant superficial or infiltration excess runoff production prevalent quick return flow, except concave valleys and swales	
Colluvium-debris	Open slopes Summit U-shaped Valley Deep incised valley Plain	Thick to very thick soils	All landforms have a dominant sub-surficial or saturation excess runoff production inducing prevalent delayed return flow	

6.5.1 Testing of the procedure

The proposed procedure was firstly applied to the Bussento river and then was extended to the Campania region. Before doing so the testing of the procedure was made to verify the reliability of that.
The procedure above described was applied to the Upper Bussento river basin located in the Southern of Campania Region and National Park of the Cilento and Vallo di Diano, where some catchments namely BS22 and BS21 were monitored by hourly and monthly discharge surveys, radon concentration measures and physical-chemical analysis. These catchments were utilized to testing the reliability of the proposed procedure and were chosen for their particular and distinctive hydrogeologic characteristics and hydro-geomorphological features.
In particular, the catchment BS21 (Inferno creek catchment) is characterized by dominant carbonate formations with a prevalently karst behavior. The catchment BS22 (Persico creek catchment) is composed in the right half-basin by terrigenous bedrock and in the right area by karst carbonate bedrock.
The geological and hydrogeological features of the catchments, descripted in the paragraph 3.4.2 and illustrated in the figure 3.17, suggest the possible hydro-geomorphological response of both.
The catchment BS21 must have a very large groundwater reservoir and the delay time response might be slower than the catchment BS22.
For the catchment BS22, must be expected lower response time and a lower storage capacity than the previous one.
To compare the results, a preliminary analysis was made on the distribution of the areas with a dominant mechanisms of production of the runoff. For this analysis another catchment was considered, it was the BS30 or Giumenta creek catchment, characterized exclusively by terrigenous bedrock only, so it might expected a lower storage capacity than the BS22. In the figure 6.23 is reported the EHGU maps for the experimental sub-catchments.

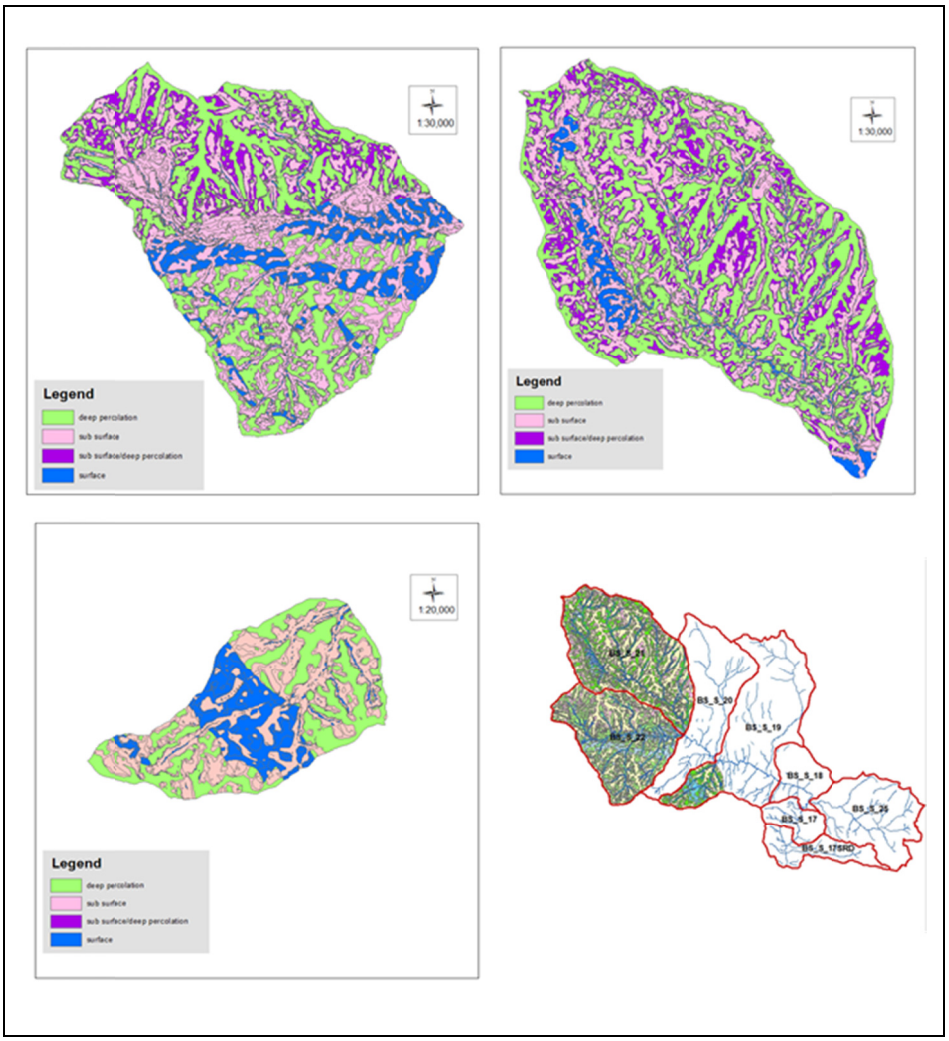

Figure 6.23: Catchment case-studies in the Upper Bussento river basin: on the bottom right, the BS21, BS22 and BS30 catchments, on the bottom left, the EHGU map of the BS30, and on the upper right and left, respectively, the EHGU map of the BS21 and BS22 catchments.

The figure 6.24 shows the distribution of the areas with dominant mechanisms of runoff production in the three catchments.

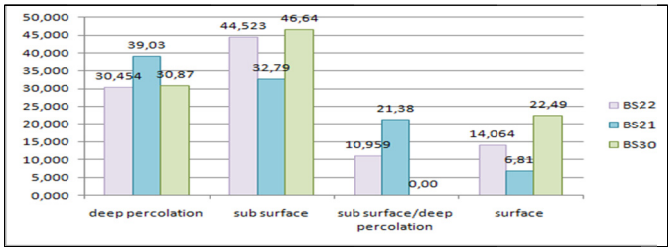

Figure 6.24: Distribution of the areas relative to the mechanisms of runoff production in the catchments BS21, BS22 and BS30.

As expected, the catchment BS21 has the higher percentage of areas with the deep percolation mechanism than the other two catchments. The two terrigenous catchments have a major percentage of areas contributing to the runoff production with sub-surface mechanisms firstly and the surface mechanisms then, congruent with their bedrock and the hydrogeologic behavior.

The second analysis was carried out on the discharge data of the catchments BS21 and BS22. Firstly, were considered the discharge dataset monthly collected from October 2009 to December 2010 at the outlet of the two catchments and, successively, was carried out the analysis on the hourly discharge datasets collected at the outlet rivers of BS21 and BS22, described in the chapter 4. More specifically, the monthly discharge data were collected at least a week after the last intense precipitations to detect, essentially, the sub-surface and deep percolation component in the hydrograph.

On the annual hydrograph was performed the separation between the sub-surface and the baseflow components, analyzing the hydrograph recession limb of in order to obtaining the storage capacity of the catchments. The base flow separation have been widely studied (Hall, 1968; Tallaksen, 1995) for his importance in the stream flow of many catchments (Gonzales et al., 2009), also to enhance karst baseflow contribution to the flood flow.

Several method are known in the hydrologic literature for the hydrograph separation and are divided in the *graphical method* (Linsley et al., 1975; Szilagyi &Parlange, 1998), which define the points where baseflow intersects the recession and falling limbs of the quickflow response, the *filtering method*, by which the data processing of the entire

stream hydrograph derives a baseflow hydrograph and the *tracer based method* using hydrochemical or environmental isotopes.
In the present research was used principally the simple graphical method integrated with the electrical conductivity informations measured with integrate DL/N70 instruments at the BS22 and BS21 river stations, for individuate the point of separations between the components of the total flow. Using the graphical method, the hydrograph was plotted on a semi-logarithmic scale identifying a straight line as groundwater flow. So, the groundwater was approximated with linear reservoir concept (Gonzales et al., 2009). The most used method for describing the baseflow of rivers is the Maillet formula (Maillet , 1905) that models the response of the groundwater aquifer as a linear reservoir of parameter K. This assumption leads to the following equation for the groundwater recession hydrograph:

$$Q(t) = Q(t_o)\ \exp(-t/k) \qquad \textbf{Equation 6.3}$$

where $Q(t)$ is the baseflow at time t; $Q(t_o)$ is a reference baseflow discharge at time t_o, and k is the recession constant for baseflow, representing a characteristic storage delay in the watershed.
So, the Maillet formula was applied to the annual base flow of the BS21 and BS22 and, following the procedure above described, were calculated the k parameter and the groundwater storage volume (figure 6.25).

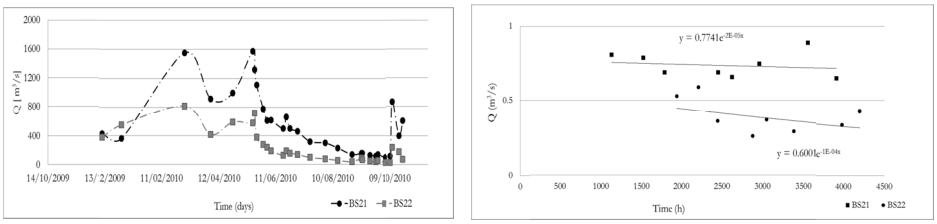

Figure 6.25: On the left: The annual hydrograph of the catchments BS21 and BS22; On the right: straight regression of the baseflow datasets

Appling the Maillet formula to the recession curve was estimated the groundwater storage for the two catchments and the results are reported in the table 6.2.

Table 6.2: Storage coefficient and grandwater volume of in the BS21 and BS22 aquifers

Catchment Code	Storage coefficient k	Storage W (Mm^3)
BS21	0,00002	58,30
BS22	0,0001	12,36

The results of the test on the annual hydrograph encourage the present research. In fact, the volume of water storage in the reservoir of the BS21 is about five times higher than the BS21 (table 6.2).
The second test was made on some hourly data events to verifying the reliability of the method on the role of the EHGU at the storm events scale and, in particular, in respect to the sub-surface component.
In the figure 6.26 are shown the hydrographs detected from the BS21 and BS22 catchments with hourly datasets from November 2010 to April 2011.

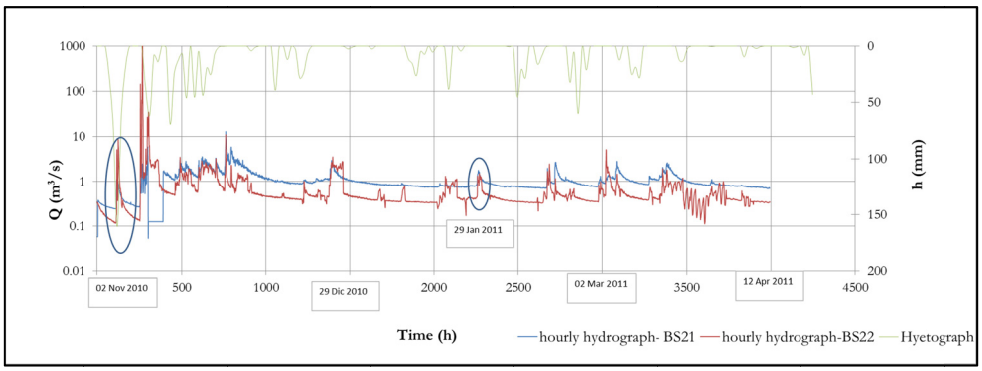

Figure 6.26. Hydrograph of the catchments BS21 and BS22 detected from October 2010 to April 2011. The blue line evidence the two event storms analyzed

The procedure adopted was similar to annual hydrograph analysis. Elaboration of the hourly dataset was possible to separate the sub-surface component into the fast and delay response of the catchments.

In fact, after selecting the storm event, plotting the hydrograph on a semi-logarithmic scale the discharge point were aligned along three lines with a different slope that is decreasing with the response time of the catchments depending upon the components of the runoff analyzed as the surface, fast and delayed sub-surface runoff and deep percolation.
All the components were analyzed with the Maillet formula in order to describe each one as linear reservoir characterized by a K value.
The value of the K coefficients were calculated for two events occur in 2 November 2010 and 29 January 2011 (indicated in the figure 6.26 with a blu circular line) measured at the station BS21 and BS22 . The event of the 2 November is typicall of no antecedent raining period and with a dry soil, otherwise the event of the 29 January occurred during the raining period with wet soils. The soil moisture antecedent conditions influenced the timing response of the catchments and the amount of rains that runs off (Scherrer et al., 2007), for this reason were selected this two events.
In the figure 6.27 are illustrated the hydrographs measured at the river station BS21 and BS22 for the events of the 2 November 2010 and 29 january 2011.

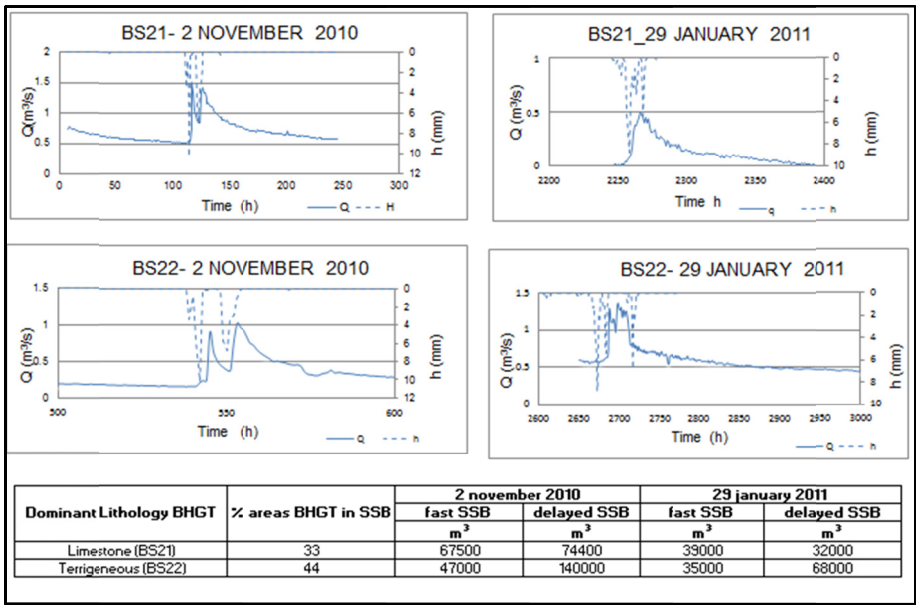

Dominant Lithology BHGT	% areas BHGT in SSB	2 november 2010		29 january 2011	
		fast SSB	delayed SSB	fast SSB	delayed SSB
		m^3	m^3	m^3	m^3
Limestone (BS21)	33	67500	74400	39000	32000
Terrigeneous (BS22)	44	47000	140000	35000	68000

Figure 6.27: the hydrograph measured at the river station BS21 and BS22 for the events of the 2 November 2010 and 29 january 2011.

For the two events was estimated the storage volume in the aquifer as fast and delayed sub-surface flow using the Maillet formula. The table of the figure 6.27 summarize the estimated volumes for the two catchments. It is evident, that the volume of the delayed sub-surface flow storaged in the BS22 aquifer is two times higher than the volume estimated for the BS21. This last, as explained previously, has a dominant limestone bedrock with a 33% of areas that contribute to the runoff with the sub-surface flow (obtained from the BHGT map) respect to the BS22 for which the 44% of the catchment's areas contribute to the runoff with the sub-surface process and the 14 % with the surface flow.

The testing has provided good results on the reliability of the method here presented, so the procedure will be extended to the Campania region and, in particular, to their mountain catchments.

The finality of the proposed method is to support the up-dating of the VAPI project hydro-geomorphological insights regarding differentiate infiltration models to be considered.

It is well know that the VAPI was made considering only the hortonian mechanisms for excess of infiltration, but the literature is giving consideration to the base flow and the sub-surface flow as an important components of the total flood flow (Gonzales et al., 2009), especially if it was performing hydrologic analysis at the temporal and spatial scale.

In the VAPI procedure, the runoff coefficient was utilized to define the volume of water that runs off with the hortonian excess infiltration mechanism during the flood events, so the coefficient was regionalized through the linear correlation with the percentage of the permeable areas of the basins. This last, representing the physiographic basin characteristic, was used as the independent variable of the models.

As previously cited, at the conference IDRA 2006 the Proff. Rossi and Villani conferring on the up-dating of the VAPI. They introduced the new concept of the Hydro-geomorphotypes in order to consider, in the storm event analysis and at the catchment scale, the sub-surface components besides the surface flow.

So, in the present research it was performed the above method for the individuation and delimitation of the EHGT, which is an up-dating corresponding of the permeability class of the VAPI and gives information on the components of the total discharge.

The elaborated map will be used to estimate a new parameter that will be stronger than the percentage of permeability because it gives additional hydrological information.
To this aim were proposed some indexes derived from the mapping spatial analysis of the EHGU modifying , in part, the method of Hellebrand et al. (2007) that regionalized the winter storm flow coefficients through a correlation with the permeability of the lithologies and the dominating runoff processes.
The use of the new index, as an independent parameter in a regression model, may open possibilities for flood event predictions in un-gauged basins concerning their runoff coefficient.
Firsly, the runoff coefficient was calculated for all the sub-catchments of the Upper Bussento, using the VAPI formula:

$$C_f = C_{f1}\left(\frac{A_1}{A}\right) + C_{f2}\left(\frac{A_2}{A}\right) \qquad \textbf{Equation 6.4}$$

Where: Cf_1 = 0,42; Cf_2 = 0,56; A_1 is the permeable area and A_2 is the impermeable area.
Then, were calculated some indexes as the ratio between the areas of a particular EHGU in a catchments and its total area.
The results are collected in the table 6.3.

Table 6.3: The coefficient of the sub-catchments of the upper Bussento and the runoff coefficients values: Adp=area in Km² contributing to the deep percolation, Asb=area in Km² contributing to the sub-surface flow, As=area in Km² contributing to the hortonian overland flow, Ab=catchments area in Km² , As+Asb= sum areas of the hortonian overland flow and sub-surface flow (km²), Asb_dp= area in km² contributing, both with the sub-surface flow and the deep percolation .

Sub catchment	Ab (Km²)	Adp/Ab	Asb/Ab	Asb_dp/Ab	As/Ab	As+Asb/Ab	Cf
BS17	96.052	0.301	0.382	0.157	0.093	0.475	0.22
BS21	19.187	0.390	0.328	0.214	0.068	0.396	0.12
BS22	14.730	0.305	0.445	0.110	0.141	0.586	0.21
BS23	7.789	0.319	0.418	0.224	0.039	0.457	0.14
BS25	10.902	0.394	0.336	0.218	0.052	0.389	0.12
BS30	2.838	0.309	0.466	0.000	0.225	0.691	0.3

The correlation matrix was firstly performed to check the degree of dependence between each index and the coefficient of runoff, using the common Pearson correlation coefficient, which is sensitive only to a linear relationship between two variables (table 6.4):

$$r = \frac{\sum_{i=1}^{n}(X_i-\bar{X})(Y_i-\bar{Y})}{\sqrt{\sum_{i=1}^{n}(X_i-\bar{X})^2}\sqrt{\sum_{i=1}^{n}(Y_i-\bar{Y})^2}} \qquad \textbf{Equation 6.5}$$

Table 6.4: Correlation matrix between the runoff coefficient and the geomorphometric parameter

	Adp/Ab	Asb/Ab	Asb_dp/Ab	As/Ab	As+Asb/Ab	Cf
Adp/Ab	1.00					
Asb/Ab	-0.84	1.00				
Asb_dp/Ab	0.59	-0.78	1.00			
As/Ab	-0.52	0.73	-0.99	1.00		
As+Asb/Ab	-0.71	0.92	-0.96	0.94	1.00	
Cf	-0.75	0.79	-0.96	0.93	0.93	1.00

As expected, the parameter calculated with the areas contributing to the runoff with the deep percolation (Adp) or as combination of deep percolation and sub-surface flow (Assb_dp) have a negative correlation with the coefficient of runoff. In addition, the best positive correlation was found between the parameter calculated with the areas contributing to the runoff with surface processes (As). Similar correlation was found for the runoff coefficient and the index calculated considering the sum of the areas contributing runoff with the hortonian and sub-surface mechanisms (As+Assb) and the runoff coefficient.
So, in the figure 6.28 are reported all the linear correlations between the runoff coefficient and the two parameters SI=As/Ab (Surface Index), SSI=Asb/Ab (Sub-Surface Index) and the new RI=(As+Asb)/Ab (Runoff Index).

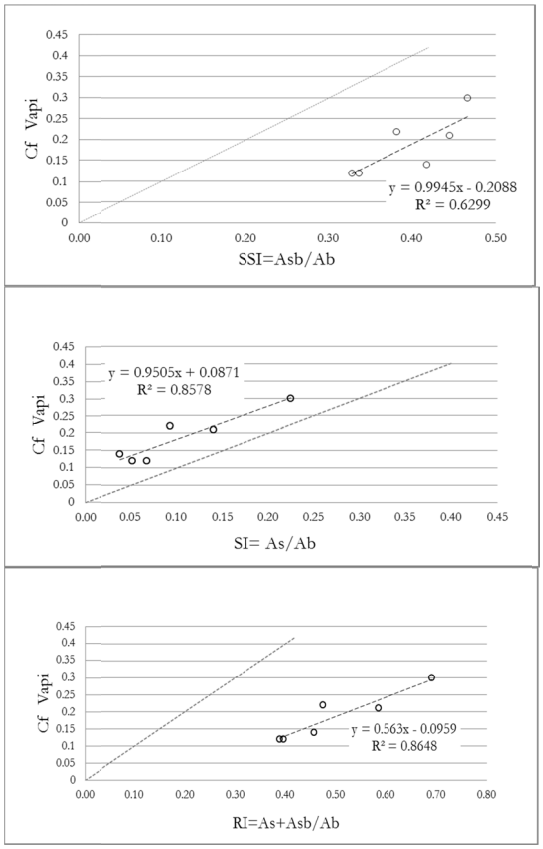

Figure 6.28: Straight line equation between the SSI and Cf, SI and Cf, RI and Cf

The new coefficient proposed in this research was named Runoff Index (RI) (figure 6.28) and was calculated as the ratio between the sum of the areas characterized by the hortonian overland flow and sub-surface flow and the total area of the catchment:

$$RI = \frac{A_{HOF}+A_{SSF}}{A_{basin}} \qquad \textbf{Equation 6.6}$$

Where: A_{HOF} is the area related to the hortonian overland flow; A_{SSF} is the area related to the Sub-surface flow; A_{basin} is the area of the catchment.

This geomorphometric parameter shows a good linear correlation with the runoff coefficient, allowing to improve the correlation the runoff coefficient should be calculate on an experimental basis.
So, in the following paragraphs the procedure will extend to the Campania region and then the correlation will repeat on datasets collected on other mountain catchments to estimating the runoff coefficient with pre-existing experimental data.

6.6 EXTENSION OF THE PROCEDURE TO THE CAMPANIA REGION

In the previous sections were descripted the method for the identification of the hydro-geomorphometric types and the test for the reliability of the procedure on the Upper Bussento river basin.
The testing procedure gives a good results and it is encouraged to use the maps produced in updating the VAPI.
To this aim, in the present paragraph the method will extend to the Campania region.
The materials used to applying the method are similarly the DEM of the Campania region with a 20 × 20 and the regional hydro-geologic map provided by the CUGRI (figure 6.29).

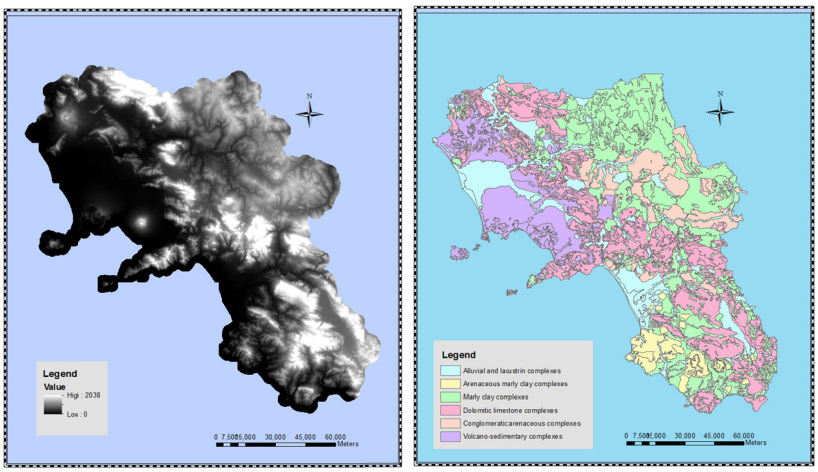

Figure 6.29: The DEM with a cell size 20× 20 m (on the left) and the hydro-geologic map of the Campania region (on the right)

In figure 6.30 is reported the EHGU regional map, of the Campania region.

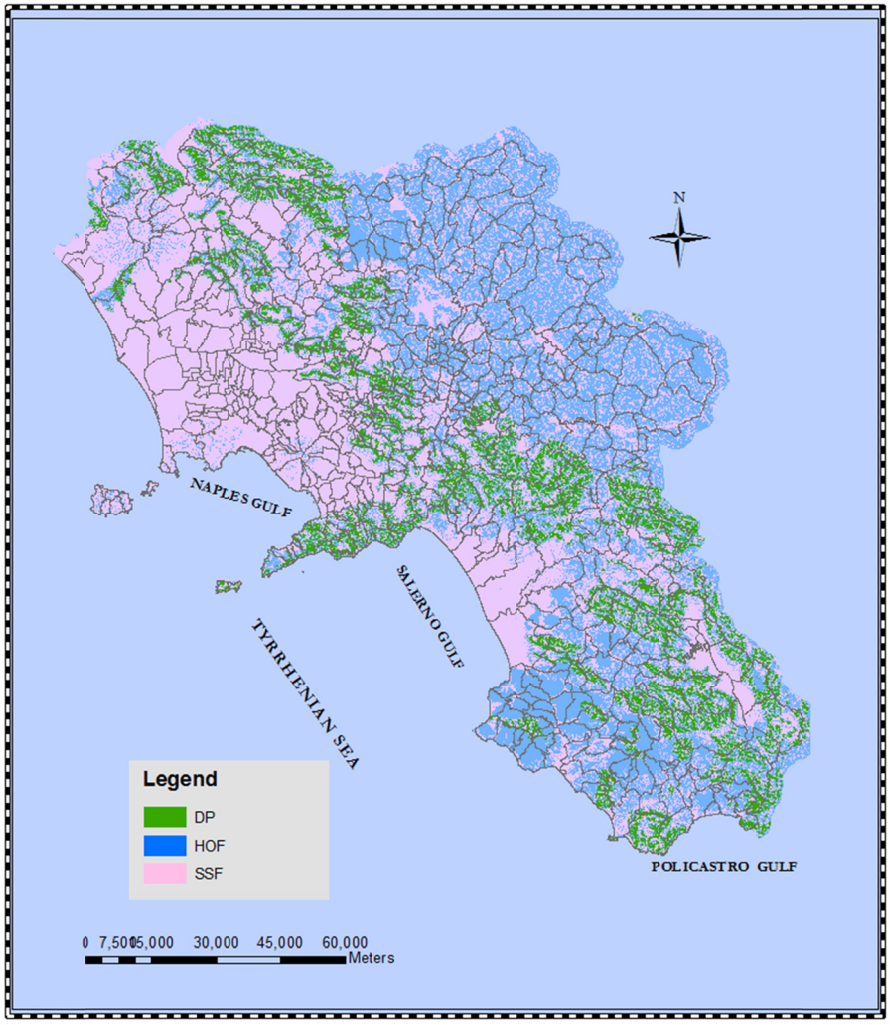

Figure 6.30: EHGU map of the Campania region

In the paragraph 6.5 has been proposed the linear correlation of the Runoff Index with the runoff coefficient to be used for the un-gauged basins. To this aim, the hydrological dataset of mountain catchments of Upper Alento, Carmine, Mennonia, Nocellito and Torna were analyzed adopting the same procedure as the BS21 and BS22.

The upper Alento and Carmine catchments have mainly of a clayey-marly bedrock, whilst the Nocellito, Mennonia and Torna are dominated by conglomerate-sandstone complexes.
In the figure 6.31 is reported the Hydro-geomorphometric Map of the cited catchments.

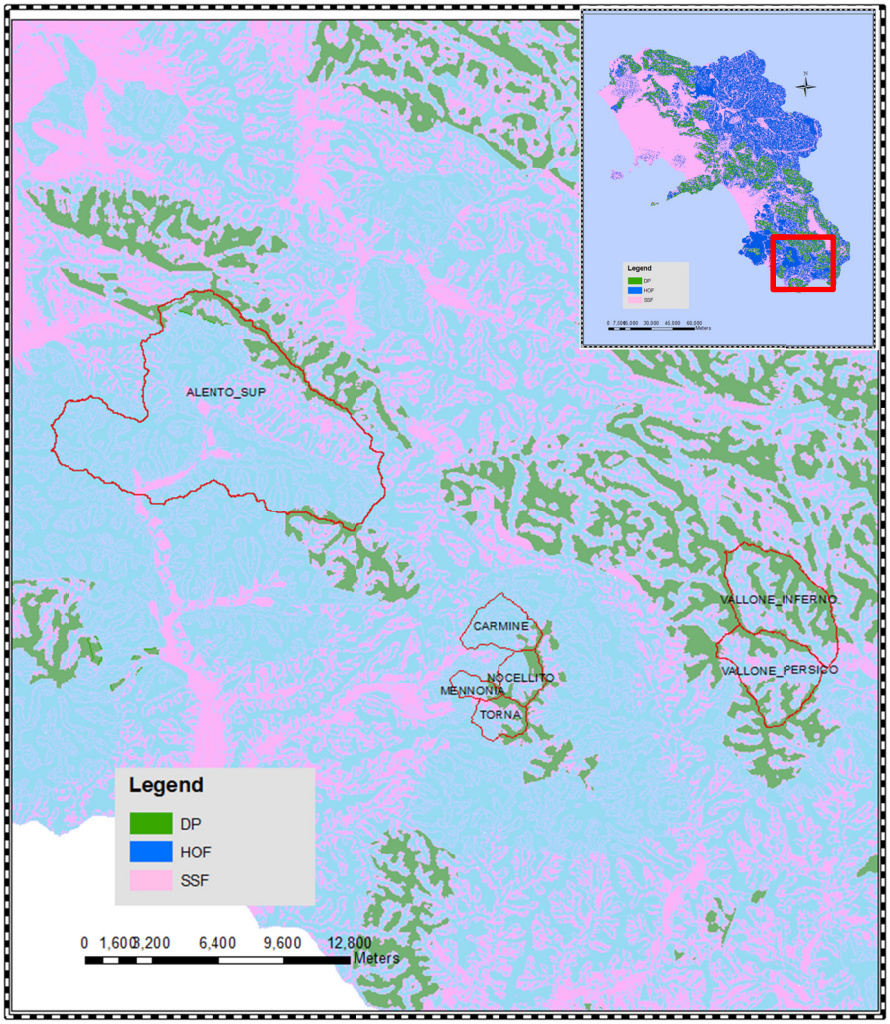

Figure 6.31: The hydro-geomorphometric map of the Upper Alento, Crmine, Mennonia, Nocellito and Torna sub-catchments.

For each catchments was calculate the Runoff Index (RI) to be used for the correlation with the runoff coefficient (figure 6.32).

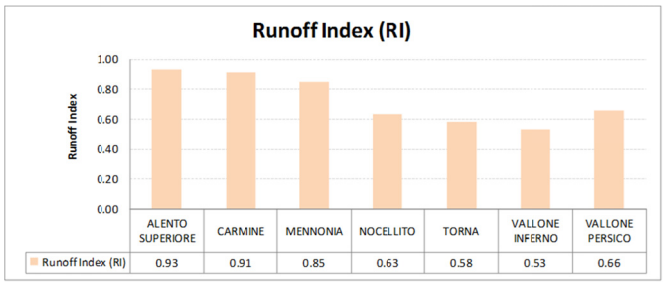

Figure 6.32: Distribution of the areas with a dominant runoff production processes calculated for the Upper Alento, Mennonia, Carmine, Torna, Nocellito, Persico and Inferno catchments.

As expected, the lower value of RI is for the catchments with a conglomerate complexes as Torna, Nocellito and the catchments of the upper Bussento, whilst the higher one is obtained for the catchments dominated by impermeable lithologies (clay and marl).
In order to make a correlation between the runoff coefficient and the RI, as for the upper Bussento catchments, and between the delay time and the RI, were analyzed the hydrographs of the catchments (figures 6.33-6.37)

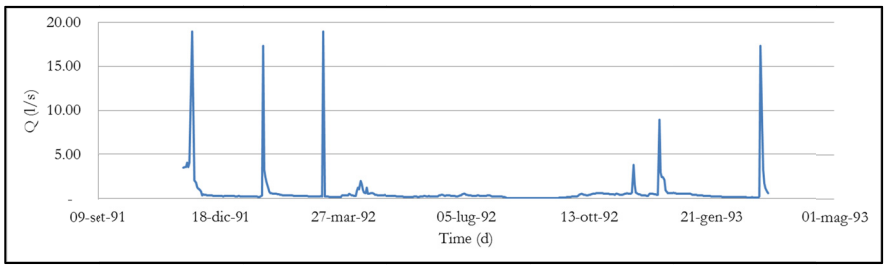

Figure 6.33: The hydrograph of the upper Alento catchments detected from 18 november 1991 to 8 march 1993

It is evident that the upper Alento aquifer remains constant throughout the year at events of remarkable intensity, showing an hydrological response typical of impermeable basin with a dominant hortonian infiltration mechanism.

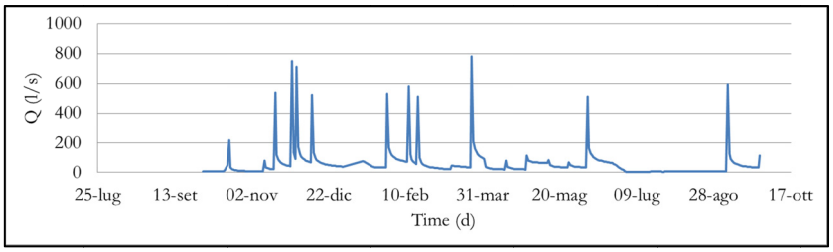

Figure 6.34: The hydrograph of the Carmine catchments detected from 1 october 1975 to 26 september 1976

The hydrological behaviour of the Carmine catchments is similar to the upper Alento one. The analysis of the RI, too, show a similar behavior.

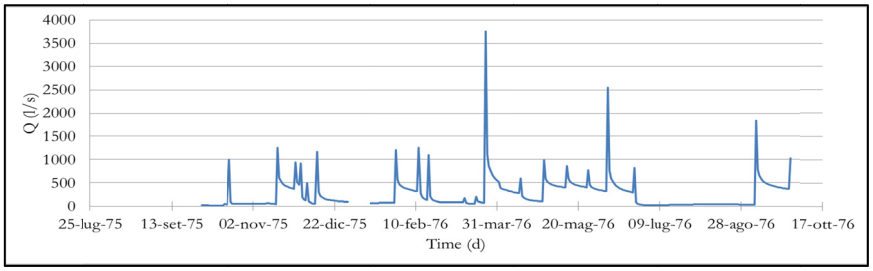

Figure 6.35: The hydrograph of the Nocellito catchments detected from 1 october 1975 to 27 september 1976

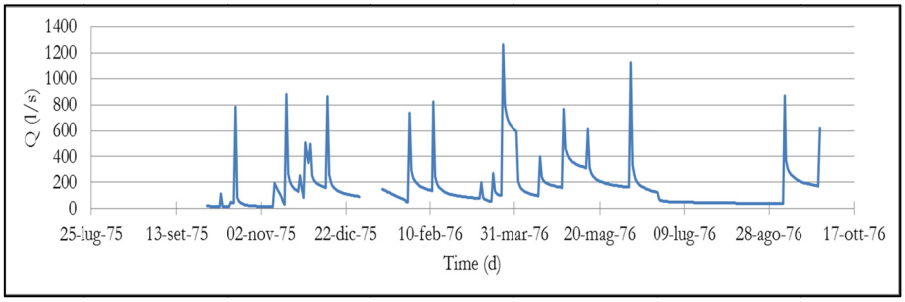

Figure 6.36: The hydrograph of the Mennonia catchments detected from 1 october 1975 to 27 september 1976

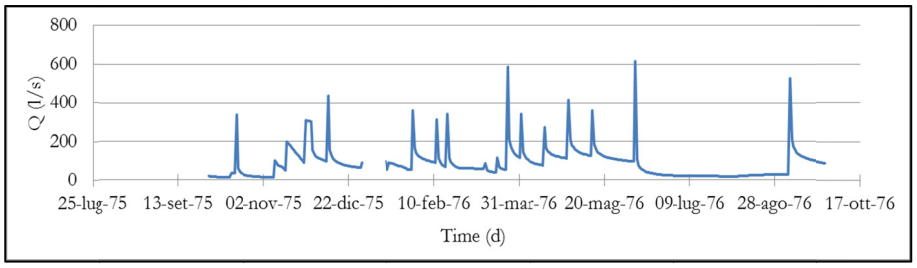

Figure 6.37: The hydrograph of the Torna catchments detected from 1 october 1975 to 27 september 1976

The Torna, Mennonia and Nocellito catchmens, with a conglomerate bedrock, are affected by an evident seasonal increasing of the baseflow component.
For each catchments were individuate and analyzed isolated and independent storm events and for each one were estimated:

- The event runoff coefficient
- The response time for the delayed and the fast sub-surface flow

In the table 6.5 are reported the mean coefficient of runoff and the delay time estimated for the catchments and the mean slope of the catchments.

Table 6.5: Runoff coefficient and the delay time estimated for the experimental catchments

Catchments	RI	Cf	tr (delayed) (h)	tr (fast) (h)	p
Upper Alento	0.93	0.3	16.39	3.13	0.39
Carmine	0.91	0.28	18.81	6.07	0.41
Mennonia	0.85	0.26	30	7	0.31
Nocellito	0.63	0.26	25	3	0.38
Torna	0.67	0.2	21	5	0.65
Inferno Valley	0.53	0.15	66	25.5	0.18
Persico Valley	0.66	0.24	66.80	21.11	0.18

The cross correlation between attributes is given in Table 6.6. It can observe a good correlation between RI and Cf and a partial correlation between the tr (fast or delayed) and RI.

Table 6.6: The cross correlation matrix

	RI	*Cf*	*tr (delayed)*	*tr (fast)*
RI	1			
Cf	**0.83**	1		
tr (delayed)	-0.67	-0.62	1	
tr (fast)	-0.62	-0.68	0.97	1

In order to improve the correlation between the delay times and the RI, this last was multiply for the mean slope of the catchments, **p** (table 6.7).

Table 6.7: The cross correlation matrix

	RI	*Cf*	*tr (delayed)*	*tr (fast)*	*RI*p*
RI	1				
Cf	0.83	1			
tr (delayed)	-0.67	-0.62	1		
tr (fast)	-0.62	-0.68	0.97	1	
RI*p	0.62	0.45	**-0.91**	**-0.84**	1

It is now evident the good correlation between RI*p and the fast and delayed response times of the sub-surface mechanism. In the figures 6.38, 6.39 and 6.40 are reported the regression analysis between the parameter with a good correlation.

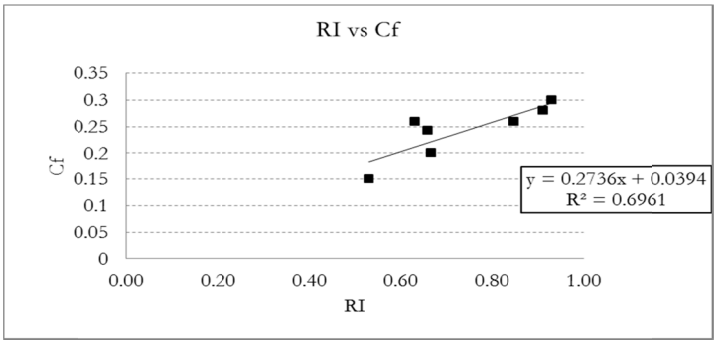

Figure 6.38: RI-Cf linear regression for the studied catchments.

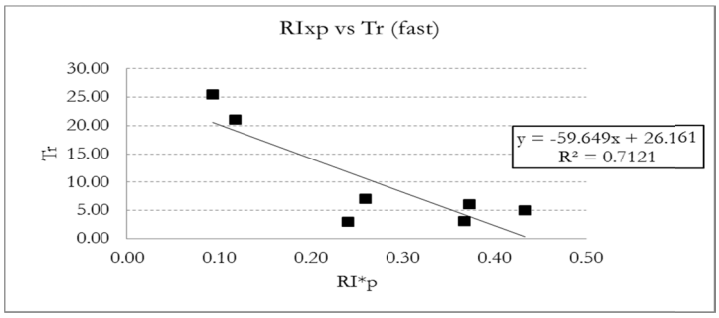

Figure 6.39: RI*P-fast Tr linear regression for the studied catchments.

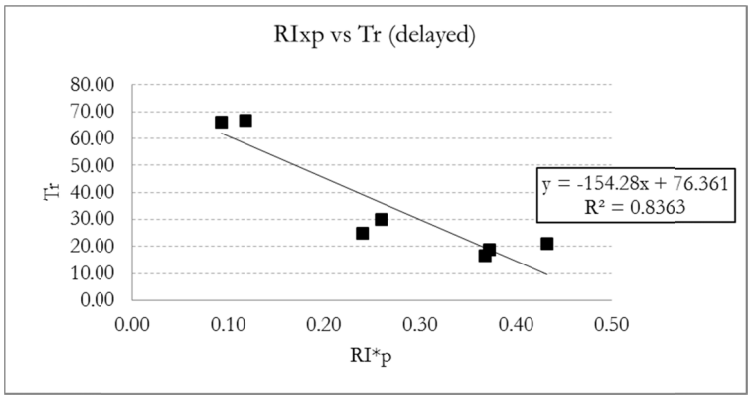

Figure 6.40: RI*P-delayed Tr linear regression for the studied catchments.

In order to evaluate the statistically significance in the regression analysis, the statistical technique of one-way analysis of variance (ANOVA) was used.

Figure 6.41: The test ANOVA results

Regression	F	Fcrit	p-value
Cf-RI	64.51	4.75	3.6105E-06
Tr (del) - RI*P	17.32	4.75	0.00132
Tr (fast) - RI*P	7.99	4.75	0.01525

The regression between the Cf and RI provided a significant result with a $p << 0.01$. The p-value was of 0.00132 for the linear regression between

Tr delayed and RI, and turned out to be higher than 0.01 for the correlation between Tr fast and RI.
In conclusion, the regression analysis with a higher statistical significance was between the Cf and RI, with the following linear equation:

$$\boldsymbol{C_f = 0.27\,RI + 0.04 + \varepsilon} \qquad \textbf{Equation 6.7}$$

The proposed linear model appeared to perform well in describing the runoff coefficient when RI served as independent parameters. Therefore, its applicability on the un-gauged basins will be suitable. In addition, the good correlation between the two parameter will attempt in the implementation in widely used hydrologic software for the Rainfall-runoff transformation in order to considering a stronger and adequate hydro-geomorphologic features of the catchments.

7 DISCUSSIONS ON APPLICATIONS TO THE MOUNTAIN CATCHMENTS

7.1 INTRODUCTION

In the previous chapter was described, tested and extended to the Campania region the method for the identification and delimitation of the Effective Hydro-Geomorphological Units (EHGUs) map, useful to improve the VAPI procedure to catchment scale. A spatial analysis was used to estimate the basic parameter named Runoff Index (RI) to predict the runoff coefficient in the un-gauged catchments, considering both infiltration and saturation excess overland flow models.
Then, in order to use the EHGU map as support for the estimation of the hydrologic parameters, another procedure was build up in the calculation of the delay time of both the sub-surface fast and delayed runoff component, using as independent variable the product of the above cited RI and the mean slope of the catchments.
The goal of this chapter is to calibrate and validate the applicability of the parameters evaluated in the previous chapter, on the catchments with available stream flow data and on un-gauged catchments on a selected orographically induced rainfalls, by using a widespread hydrological distributed model.
To this aim was utilized the software HEC-HMS of the U.S. Army Corps of Engineers' that is designed to simulate the precipitation-runoff processes of dendritic watershed systems.
In the following, after a brief description of the HEC-HMS software will explain the approaches adopted for the simulations. Finally will describe their applications on two mountain catchments of the Campania region and the simulated results will show.

7.2 HEC-HMS SOFTWARE

HEC-HMS has been developed for the U.S. Army Corps of Engineers to simulate the hydrologic response on the watershed driven by the precipitation that falls on it. The software was tested in several geographic zones with critical hydrologic events and verified in small and large basins or in the urban areas.
To run the HEC-HMS hydrologic simulation is need to specify three datasets:
1. The Basin Model: containing the physiographic representation of the watershed;
2. The Meteorologic Model: including meteorological data of input on the rainfall and on the evapotranspiration
3. The Control Specifications: temporal information on the simulation

The Basin Model is a component of the software that works in the Arc Map software to which it is linked. In the environmental GIS, with the tool named Arc Hydro, it is possible to calculate and specify the components of the basin and to input hydro-geomorphological parameters.
In this phase, in fact, the river network is divided in segment and the basin is divided in catchments with the outlet at the end of each segment river. For each catchment it is possible to introduce springs and wells linked to the segments river and to the centroid of the catchments to form a network. For each catchment of the watershed is possible to simulate the hydrologic response to the rainfall input data in accord to the land use and the morphologic and geologic characteristics of the watershed.
The Meteorologic Model is the component used to input the rainfall pattern that may be based on the observed rainfall from a hystorical events, may be a frequency based hypothetical rainfall event, or may be an event that represents the upper limit of the precipitation possible to a given location. The rainfall pattern may be specific for each catchment of the watershed and it is possible to specify the rainfall for the river, as the radar datasets.
The Control Specification component storage all the input datasets, the temporal range to utilized for the calculation and the output simulation, too. All the results obtained from the hydrologic simulation may be represents in the graphic form or on tables.

The HEC-HMS computes the runoff volume calculating all the possible losses as interception, infiltration, evaporation and so on. The software consider that all land and water in a watershed can be categorized either:

- Directly - connected impervious surface, or
- Pervious surface

Precipitation on the pervious surfaces is subject to losses which are calculates in the simulation with the following alternative models:

- The initial and constant - rate loss model;
- The deficit and constant - rate loss model;
- The SCS curve number (CN) loss model
- The Green and Ampt loss model

Estimated the losses and subtracted these from the precipitation, must be calculate the base flow and separate this from the runoff. The next is to calculate the Syntetic Unit Hydrograph (US). The software proposed to use the following three method for the calculation of the UH, as suggested by Chow, Maidment and Mays in the 1988:

- methods that relate the UH characteristics (such as the UH peak and the peak time) to watershed characteristics. Snyder's UH is similar to synthetic UH;
- Those that based upon a dimensionless UH. The SCS UH is such a synthetic UH;
- Those that are based upon a quasi-conceptual accounting for watershed storage. Clark' s UH and the ModClark model do so.

All these synthetic UH models are included in HEC-HMS.

7.2.1 Simulation method

The simulations described in this chapter are made using the HEC-HMS software sintetically described above. As seen the software includes several methods for the estimation of the losses and the UH.
For the specific study it was chosen to use the following methods for the simulations:

- The Snyder's method was used for the transformation of the rainfall into runoff;
- The SCS Curve Number was used for estimate the losses;
- The Lag method for the simulation of the channel flow.

All this methods include synthetic parameters evaluable through physical formulas available in the literature. Moreover the losses for evapotranspiration can be neglected and the base flow was interpreted as a spring inflowing with a constant discharge.
The Snyder's UH is found on the calculation of two parameter: the standard lag tp, like the delay time of the flood wave and the peaking coefficient Cp that avoid in the evaluation of the features of the hydrograph. The standard lag is the difference in the time of the UH peak and the time associated to the centroid of the excess rainfall hyetograph. This may be evaluate with the following equantion:

$$t_p = 0.7133(S_{pc})^{-0.39}(LL_C)^{0.3}$$

Equation 7.1

Where: S_{pc} is the mean slope of the main stream, L is the length along the main stream from the outlet to the divide, L_C is the length along the main stream from the outlet to a point nearest to the centroid.
The peaking coefficient Cp is depending by the Ct, that is a calibration parameter which depends from the percentage of the permeable area I:

$$C_P = 0.89C_t^{0.46}$$

Equation 7.2

Where:

$$C_t = 7.81(I)^{-0.78}$$

Equation 7.3

For evaluating the infiltration losses was adopted the Soil Conservation Service (SCS) Curve Number (CN) method.
This model estimates the precipitation excess as a function of the cumulative precipitation, soil cover, land use and antecedent moisture, using the following equation:

$$P_e = \frac{(P - I_a)^2}{P - I_a + S}$$

Equation 7.4

Where: Pe = accumulated precipitation excess at time t; P= accumulated rainfall depth at time t; Ia = the initial abstraction (initial loss); and S = potential maximum retention, a measure of the ability of a watershed to abstract and retain storm precipitation. Until the accumulated rainfall exceeds the initial abstraction, the precipitation excess, and hence the runoff, will be zero. Analysing the results of many experimental watersheds, the SCS developed an empirical relationship of Ia and S:

$$I_a = 0.2S$$

Equation 7.5

Therefore, the cumulative excess at time t is:

$$P_e = \frac{(P - 0.2S)^2}{P + 0.8S}$$

Equation 7.6

Incremental excess for a time interval is computed as the difference between the accumulated excess at the end of and beginning of the period. The maximum retention , S, and watershed characteristics are related through an intermediate parameter, the curve number (CN) as:

$$S = \frac{1000 - 10CN}{CN}$$

Equation 7.7

CN value range from 100 (for water bodies) to approximately 30 for permeable soil with high infiltration rates. The CN for a watershed can be estimated as a function of the land use, soil type and antecedent watershed moisture using tables published by the SCS.
The Lag Model is the simplest routing models of the HEC-HMS. With it, the outflow hydrograph is simply the inflow hydrograph, but with all ordinates translated by a specific duration. The flows are not attenuated, so the shape is not changed. If observed flow hydrograph are available, at two cross section along a river, the lag time can be estimated from these as the elapsed time between the time of the centroid of areas of the two hydrographs.
The simulated hydrograph carried out in the HEC-HMS software is useful for check the usefulness of the EHGU map, of the Runoff Index (RI) and the relationships between the RI and the runoff coefficient or the delay time. To do this were choice two catchments:

- The BS22, is a catchment of the Upper Bussento, just described in the chapters 3 and 4. It was choice for the availability of stream flow data and for its particular geology and hydro-geological behavior described in the chapter 3. The river basin extension falls entirely in the Centaurino M.nt delimited as complex entities by the orographic procedure.

- The Dragone river, that is the experimental basin in doctoral thesis of Spatuzzi (2012). It was choice for the presence of the pyroclastic soils covered the limestone bedrock and to simulating the storm event, defined by the hydrologists as flash floods, that occurred on September 2010 causing damage and loss of human life. The particular events was selected because orographically induced by the units entities individuate on the Lattari Mount.

Three typologies of simulations have been performed, as resumed in the following:

1. In the first simulation were adopted the critical parameter describing the synthetic UH of Snyder, above introduced (formula 7.1, 7.4, 7.7)

2. In the second simulation is provided the experimental estimation of the standard lag utilizing the flowstream data available on the monitored catchment, introduced in the chapter 6, the BS22.

   The experimental data allowed to estimating, after individuating the three components of the total runoff, the standard lag or delay time for the direct runoff, sub-surface flow and the deep percolation at the outlet of the catchment BS22.
   The software, with the "Basin model" component, splits the the BS22 in sub-catchments and for each one must be define the hydrologic parameters. To this aim, the delay time has estimated at the outlet of each sub-catchments adopting the following proportion equation:

   $$t_{P\_C} : A_{BHGU\_C} = t_{p\_SC} : A_{BHGU\_SC} \qquad \textbf{Equation 7.8}$$

   where: t_{P_C} = delay time estimated for the catchment for a specific component (direct, sub-surface flow or deep percolation); A_{BHGT_C} = area of BHGU in the watershed (C) corresponding to the component considered; t_{p_SC} = delay time calculated for the sub_ catchment (sc) for a specific component; $A_{BHGT\_SC=}$ area of BHGU calculated in the sub_ watershed and corresponding to the component considered.
   The software requires a only delay time for the outlet of the catchment or sub-catchment. In order to obtain the total delay time a weighted mean depending on the distributions of the EHGU, was used:

   $$t_{p-sottobacino} = t_{p-direct} \times \frac{A_{surface}}{A_{sottobacino}} + t_{p-subsurface} \times \frac{A_{subsurface}}{A_{sottobacino}} + t_{p-deep} \times \frac{A_{deep}}{A_{sottobacino}}$$

   Equation 7.9

3. In the last simulation is introduced the runoff coefficient Cf for take into account the infiltration losses, in place of the SCS method. It was estimated for the gauged catchments of the upper

Bussento. To translating the value to the sub-catchments was use the same formulation used for the delay time, where the RI was introduced because of the significance linear model between the RI and C_f:

$$C_{fsc} = C_{f\_C} \frac{RI_{SC}}{RI_C} \qquad \text{Equation 7.10}$$

Where: C_{f_SC} = runoff coefficient calculated for the sub-catchment (SC); C_{f_C} = runoff coefficient estimated for the catchment (C); RI_{SC} = runoff index calculate in the sub-watershed; RI_C = runoff index calculate in the watershed.

For the Dragone river, that is an un-gauged watershed, was, instead, adopted the linear model found in the previous chapter between Cf and RI (equation 6.7).
In the following paragraphs, will describe the obtained results applying the three procedure proposed.

7.3 RAINFALL-RUNOFF SIMULATION

7.3.1 Catchments BS22

The present paragraph deals with the simulation runs on the catchment BS22 and the discussions on the obtained results. The description of the catchments is in the chapter 3. At the outlet of the catchment BS22 were collected hourly flow stream data in the period from the November 2010 to April 2011, just shown in the chapter 4. The dataset on the temporal precipitation pattern was available at the stations of Sanza e Rofrano (figure 7.1), provided by the curtesy of the Civil Protection of the Campania Region.

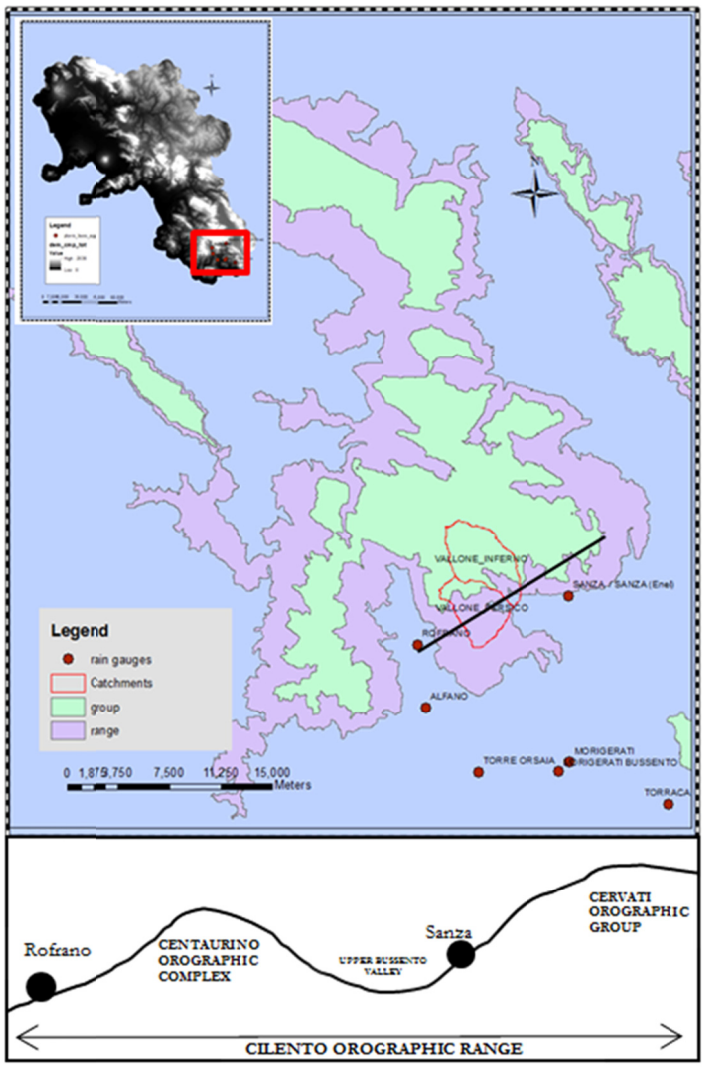

Figure 7.1: Orographyc Map-Transect, and location of the rain gauges used for the experimental rainfall pattern (Rofrano and Sanza).

The map of figure 7.1 shows in background the Cilento orographic range, Aburni, Cervati and Chianiello groups and Centaurino complex.
In the figures 7.2 and 7.3 are reported the rainfall hyetograph of the storm events for which the hydrograph was simulated: the 2 and 9-11 november 2010.

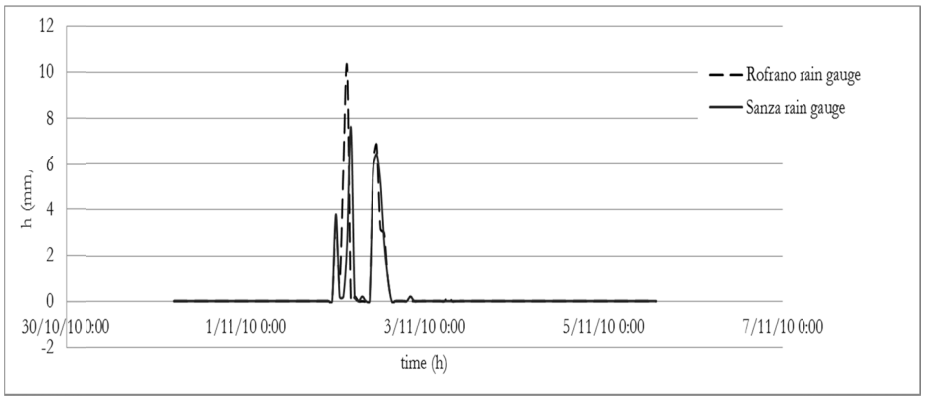

Figure 7.2: The Hyetographs of the 2 November 2010 at the Rofrano and Sanza rain gauges

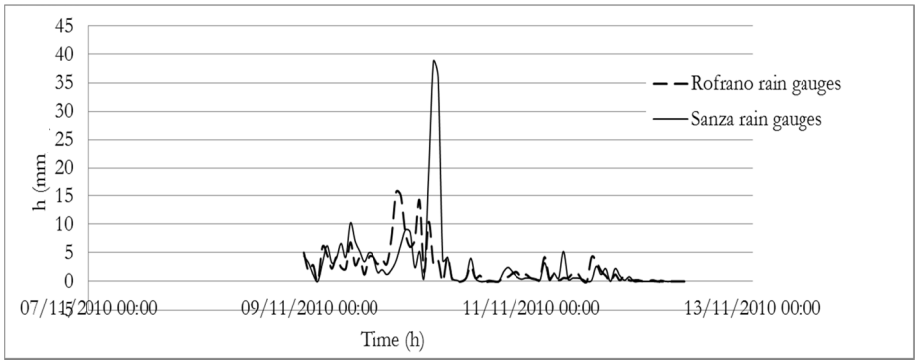

Figure 7.3: The rainfall hyetographs of the 9-11 November 2010 at the Rofrano and Sanza rain gauges.

The two events occur in the same rainy period and were selected because the soil moisture condition and tree cover are the same for the two events. The first was a typical Mediterranean local event, the last a frontal system, affecting heavy both Sele Plain and Diano Valley, with an extention up to hundreds kilometers.
In the figure 7.2, it is evident that the events having a duration of 5 hours can be defined as single storm events, according to Orlansky (1975). In addition, the higher peak intensity, recorded at the Rofrano station, is decreasing in intensity, moving the event toward the Sanza rain gauge. This can be explained with the most straightforward mechanism of orographic precipitation: the "stable upslope ascent" (Roe 2005) for

which the air masses, impacting over the windward flank, is mechanical forced resulting in condensation and precipitations. This mechanism occur at the scale of large midlatitude mountain range with a wide of 4 Km and height on 1.5 Km (Smith et al. 2003). Considering the typical dimensions of the mountain for which occurs the "stable upslope ascent" mechanism and the typology of rainfall, the event of the 2 november was caused by the presence of the group with a prominence of 1Km and height of 1.5 km.

The event of 9-11 November 2010, had a duration of up to 1-2 days and, as defined by Orlansky, it can be between "storm system" and "frontal system". In the figure 7.3, it is evident that the peak rainfall event occur at the Sanza rain gauge, with a lower intensity at Rofrano. This mechanism may be explained with the lee side convergence where ascent occur and lead to precipitation, at range orographic level. This was generated for the presence of the orographic range with a lower height than the orographic group and for the stable atmosphere with a flow not strong enough to ascend over the orographic range.

For these two events were simulated the hydrographs following the three procedures previously described.

At begin of the simulation, the morphometric and hydrologic parameters of the catchments must be calculate. So, the DTM of basin BS22 , with a cell size of 5 x 5 m (figure 7.4) was used in order to split the catchments in sub-catchments and obtain all the geomorphometric parameters on the watershed and the river network (table 7.1).

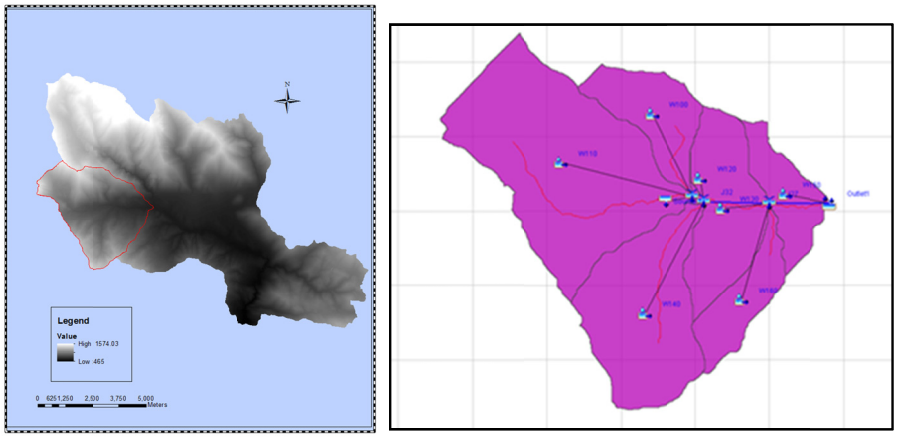

Figure 7.4: DEM of the catchment BS22 of the upper Bussento (left) and the BS22 splits in sub-catchments (right)

Table 7.1: Geomorphometric parameters calculated in the ArcMap fo the BS22 sub-catchments.

Sub-basin	Area	Lenght main trunk	Lenght c	Slope
-	[kmq]	[km]	[km]	[%]
w100	1.40	1.2	1.61	25
w110	5.66	3.35	2.7	11
w120	0.04	0.19	0.17	8
w130	2.11	1.06	0.7	6
w140	3.28	2.32	1.93	15
w150	0.97	0.94	0.75	7
w160	1.05	0.75	1.53	13
BS22 Total Area	14.51			

These parameters, calculated in the ArcMap, composed the not-graphical database of the sub-catchments.
Next, importing the map of sub-catchments in the HEC-HMS all the morphometric parameter were introduced within and were selected the models to be used for the first simulation, as described in the paragraph 7.2.1: the Snyder's UH, the SCS Curve Number estimating the infiltration losses and the lag method for models the stream flow.
So, in the table 7.2 are collected all the parameters calculate with the Snyder's equations, where the percentage of permeable area was calculate from the simplified Permeability Map of the catchments (figure 7.5).

Table 7.2: BS22 Hydrologic parameters calculated for the Snyder formulation

Sub_Catch	L	Lc	Slope	**tp**	I tot	Ct	**Cp**
-	[km]	[km]	[%]	**[ore]**	[%]	-	**-**
w100	1.2	1.61	25	0.25	99	0.22	0.44
w110	3.35	2.7	11	0.54	84	0.25	0.47
w120	0.19	0.17	8	0.11	21	0.72	0.76
w130	1.06	0.7	6	0.32	53	0.35	0.55
w140	2.32	1.93	15	0.39	78	0.26	0.48
w150	0.94	0.75	7	0.30	33	0.51	0.65
w160	0.75	1.53	13	0.27	70	0.28	0.50

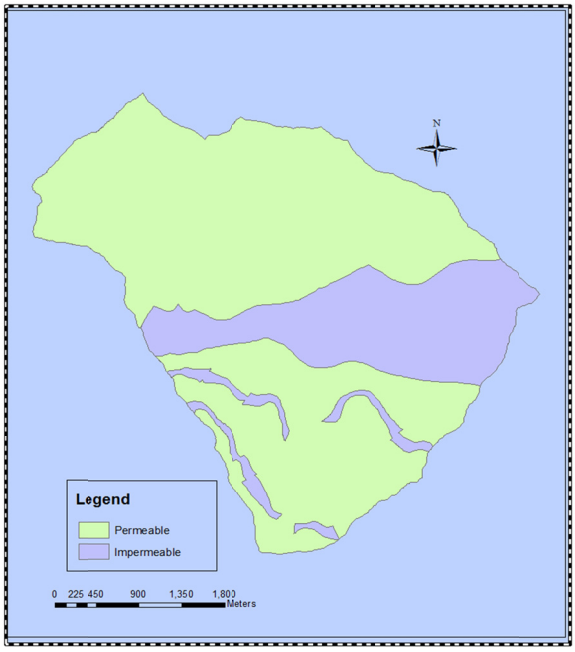

Figure 7.5: Simplified Permeability Map of the BS22

The Curve Number was selected from a table defined by the SCS method and it is related to the land use and the antecedent moisture conditions of the soil. The CN of the catchment BS22 was of 60 because the catchment soil is of group B (Group B soils have a moderately low runoff potential due to moderate infiltration rates) and for the presence of wood.
The first event implemented in the software was the 2 November 2010 storm. It is a typical event of the end of the dry period, when the low flow conditions occur and the river discharge is mainly sustained by the baseflow. The raining period considered has a monthly mean temperature of 15 °C. The initial and the evapotranspiration losses were detracted to the rainfall in a percentage of 80 %.
The figure 7.6 shows the cumulative pattern of the precipitation measured at the Rofrano rain gauge, successively used for the simulation, and the experimental hydrograph measured at the outlet of the catchment and used to verify the simulated results.

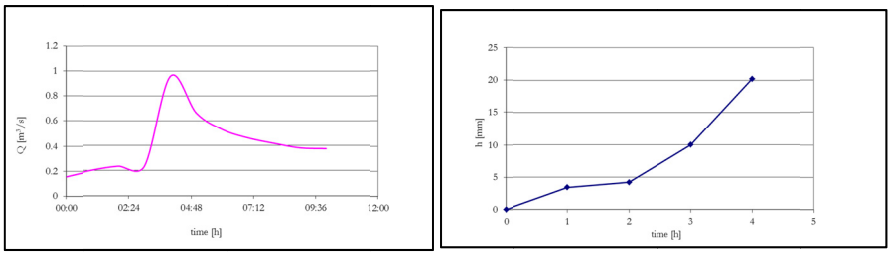

Figure 7.6: The experimental hydrograph registered at the outlet of the BS22 (on the left) and the cumulative rainfall for the event of the 2 November registered at the Rofrano rain gauge.

After the introduction of all the inputs data required, the simulation was started and the simulated hydrograph was compared to the experimental one (figure 7.7).

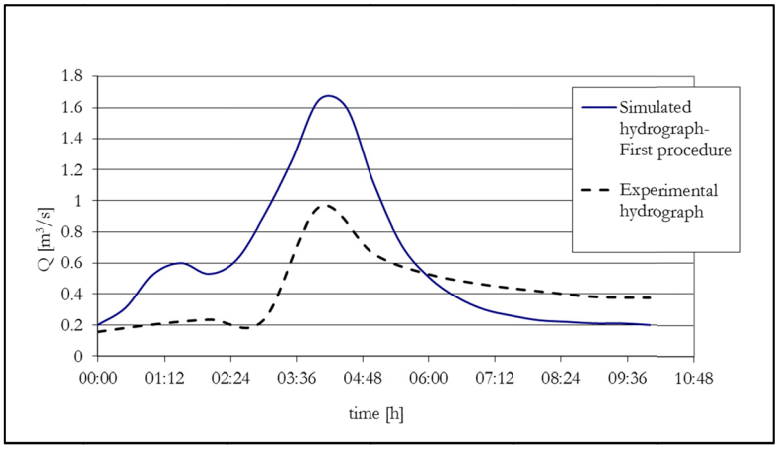

Figure 7.7: Comparison between the experimental and the simulated hydrographs for the event occurred the 2 november 2010

It is evident that the two hydrographs have a temporal correspondence of the peak flow, but the volume of discharge simulated is of 30% bigger than the effective. The response time of the components on the total runoff seems to be highly discordant.
As described above, on the same event storm, was run the second simulation where the delay times of the catchments were calculated from the experimental data. The delay time was determined for the direct runoff and sub-surface flow, applying the graphic separation of the

hydrograph method with the help of the electrical conductivity, too (par. 4.5, fig. 4.53).
The table 7.3 reports the delay times calculated for the direct runoff and for the slow and quick sub-surface flow, for the specific storm event of the 2 November 2010.

Table 7.3: The delayed time estimated at the outlet catchment BS22

Component	tr
	[min]
Slow SUB-SUPERF	66
Quick SUB-SUPERF	21
Direct RUNOFF	2

The delay times were estimated at the outlet of the catchment BS22. These was transfer to the outlet of the sub-catchments considering the distributions of the hydro-geomorphotypes in each sub-catchments and applying the equation 7.8.
The total delay time of the sub-catchment was done as a weighted mean time on the basis of the hydro-geomorphotypes correspondent to each delay time estimated for the component to the total discharge. The formula adopted was the equation 7.9. The table 7.4 contains the delay times and the total delay time of each sub-catchment.

Table 7.4: The sub-catchments response time of the, weighted on the areas of hydro-geomorphometric type.

	sub-catchemnts	Tr delayed	Tr fast	Tr direct	TR
W100	W100	2.88	0.60	0.01	1.47
W110	W110	7.30	3.55	0.08	3.61
W120	W120	0.04	0.02	0.00	0.02
W130	W130	2.08	1.52	0.06	1.22
W140	W140	5.36	2.42	0.06	3.17
W150	W150	0.70	0.54	0.05	0.34
W160	W160	1.41	0.79	0.03	0.83

The so estimated delay times were then introduced in the software and the simulation was re-started. The resulting modeled hydrograph is compared to the experimental one in the figure 7.8.

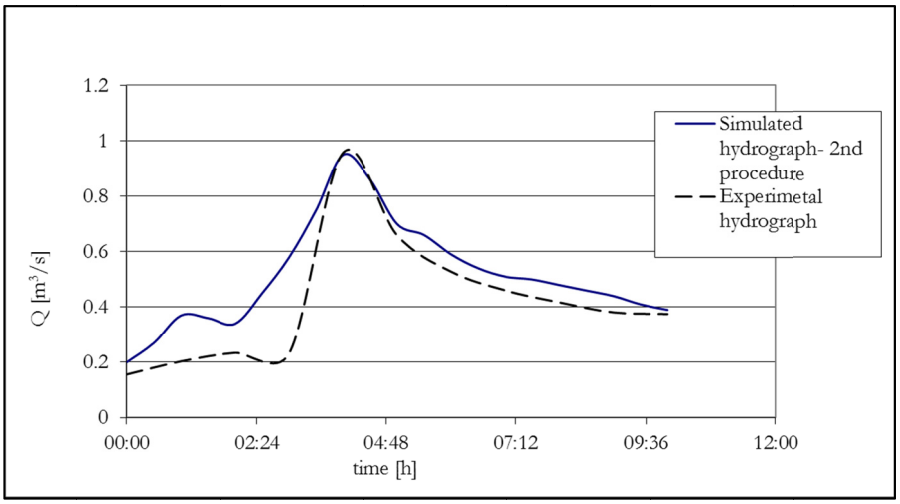

Figure 7.8: The hydrograph simulated with the second procedure is compared to the experimental one.

Comparing the two discharge pattern is evident the correspondence in the timing and in the value of peak discharge, and the volume of the simulated hydrograph is of 15% bigger than the experimental one. The recession limb of the two hydrographs seems to be the same pattern.
In order to improve the method of simulation and make the results more realistic was introduced the third method of simulation concerning the replacement of the SCS method with the runoff coefficient. The runoff coefficient was estimated for the catchment BS22 and then calculate at each sub-catchment adopting the formula 7.10 (table 7.5)
In the table 7.5, the last column contains the coefficient of runoff calculated adopting the linear equation found in the section 6.6. It is evident that these values do not differ much from those calculated with the weighted mean and from experimental data.

Table 7.5: Coefficient of runoff calculated for the sub-catchments

Sub-catchments	RI	Cf_BS22	$Cf_{\_subcatchments}$	C_f (equation 6.7)
W100	0.34	0.24	0.12	0.13
W110	0.53		0.19	0.18
W120	0.79		0.29	0.25
W130	0.70		0.25	0.23
W140	0.64		0.23	0.21
W150	0.75		0.27	0.24
W160	0.70		0.26	0.23

The simulation was run adopting the delay time calculated in the second procedure and the runoff coefficient of table 7.5. In the figure 7.9 the simulated hydrograph is compared to the experimental one.

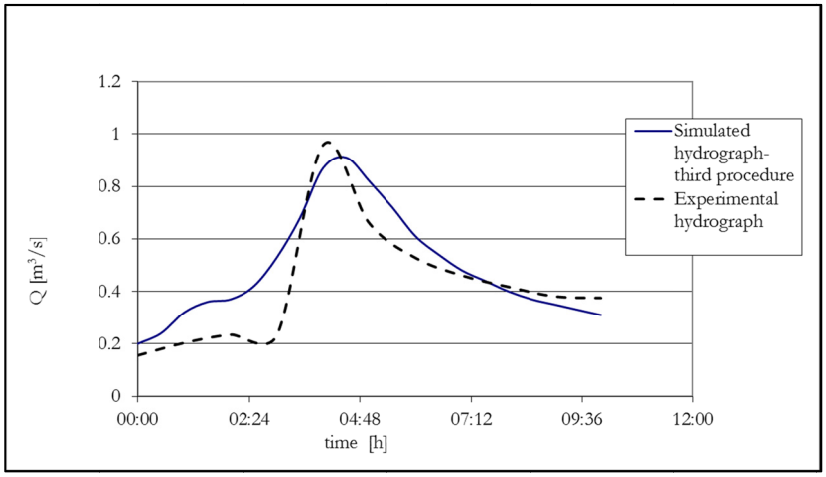

Figure 7.9: Comparison between the simulated and experimental hydrograph

Comparing the two hydrograph pattern is evident that the simulated peak discharge is slightly more delayed and lower in a value than the real one. The recession limb of the simulated hydrograph is less adherent than the real. It may be for the high percentage of losses introduced.
The second event considered occurs on the 9-11 november 2010. The precipitation has a duration of 24 hours with a volume of rainfall of 586000 m^3.
The experimental hydrograph measured at the outlet of the BS22 is in figure 7.10.

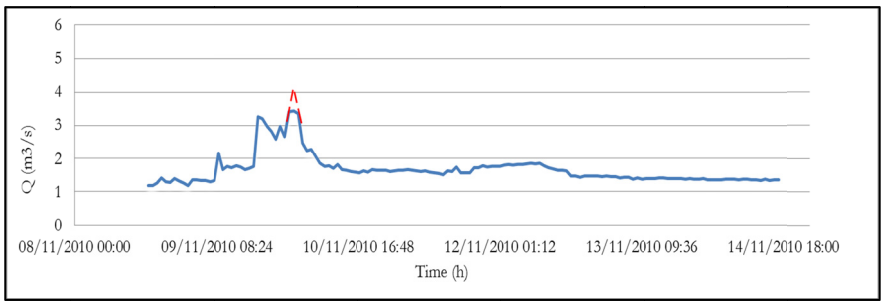

Figure 7.10 The observed hydrograph for the event of the 9-11 november 2010. The line in red indicate the effective water level.

This event shown two peaks. It is evident that the second peak has a flat shape that may be explained by the high water levels in rivers causing river bank overtopping. For this storm event were performed the three simulations. The first simulation was run introducing the Snyder's parameter, which are the same calculated for the event of 2 November 2010, and in figure 7.11 are compared the two hydrographs.

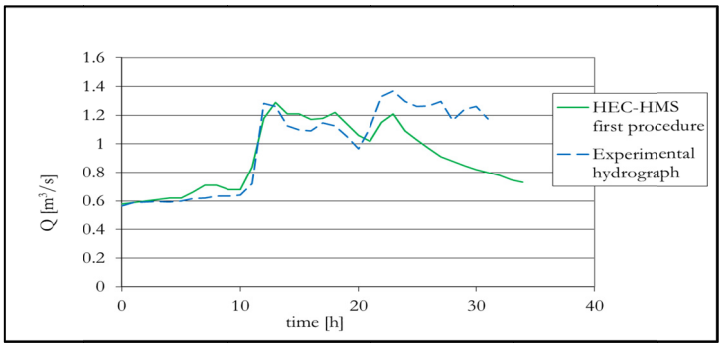

Figure 7.11: Comparison between the simulated and experimental hydrographs.

The two hydrographs are not perfectly adherent in the recession limb.
For the second procedure were estimated the delay times for the components of total flow at the outlet of the BS22 using the temporal flowstream pattern detected experimentally (table 7.6).

Table 7.6: The delay times estimated at the outlet of the BS22

Component	tr
	[min]
Slow SUB-SUPERF	55
Quick SUB-SUPERF	9
Direct RUNOFF	3

In the table 7.7 are collected the total delay time calculated for each sub-catchments with the formula 7.15.

Table 7.7: The response time (h) calculated for the sub-catchments considering the distribution of the hydrogemorph types

Sub-catchments	Tr delayed	Tr fast	Tr direct	TR
W100	4.84	1.08	0.03	2.50
W110	12.27	6.43	0.26	6.29
W120	0.07	0.04	0.01	0.03
W130	3.51	2.74	0.19	2.16
W140	9.01	4.38	0.20	5.50
W150	1.18	0.98	0.16	0.62
W160	2.37	1.43	0.09	1.46

For the third simulation were estimated the runoff coefficient, reported in the table 7.8 for each sub-catchments, applying the formula 7.16.

Table 7.8: Coefficient of runoff calculated for the sub-catchments

Sub-catchments	RI_{SC}	Cf_BS22	$Cf_{\_SC}$	Cf_{SC} (linear equation)
W100	0.34	0.24	0.12	0.13
W110	0.53		0.19	0.18
W120	0.79		0.29	0.25
W130	0.70		0.25	0.23
W140	0.64		0.23	0.21
W150	0.75		0.27	0.24
W160	0.70		0.26	0.23

All the simulation were operated considering three temporal rainfall patterns (figure 7.12):

- In the first was used the rainfall pattern measured at Sanza station, that may be influenced the second peak discharge;
- In the second simulation was used the data detected at the Rofrano rain gauge, that may be influenced the first peak discharge;
- In the third simulation mean of the previous datasets were used to verify to improving the procedure.

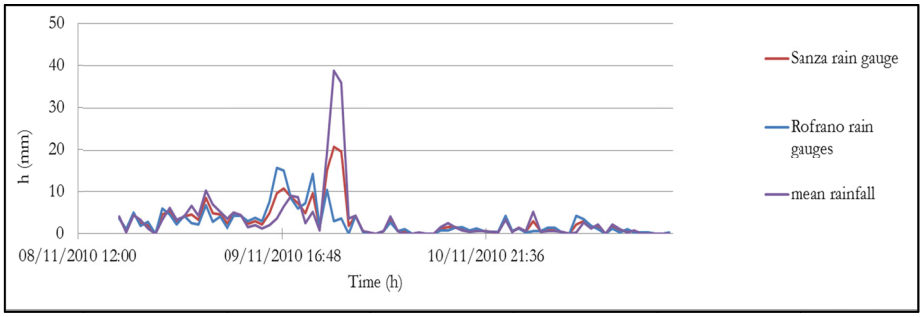

Figure 7.12: The hyetograph of the rainfall measured at the Rofrano and Sanza rain gauges

In the figure 7.13, 7.14 and 7.15 are compared the hydrographs obtained from the second and third simulating procedure.

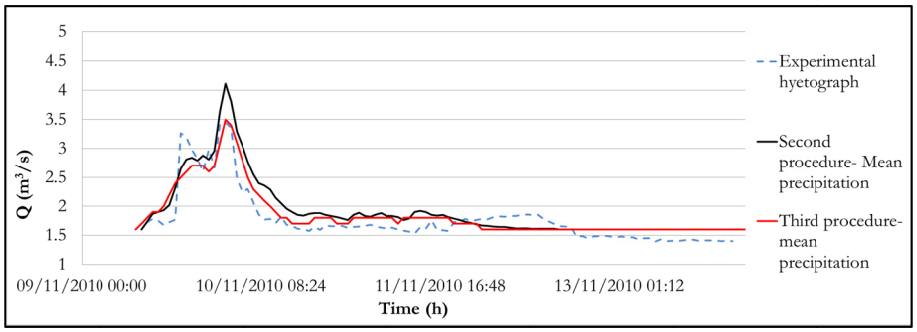

Figure 7.13: Comparison between the hydrographs simulated with the second and third procedure and the experimental one. The rainfall intensity used is the mean value of the Rofrano and Sanza precipitation.

In the figure 7.13 the storm event was simulated with the mean rainfall intensity of Rofrano and Sanza. Following the second simulation the hydrograph have the second peak flow bigger than the measured one. Otherwise with the third simulation a good correspondence in the value was found. The two simulated recession limb are quite correspondent to the experimental one.
As explained, the measured hydrograph is affected by the banks river overtopping in correspondence of the second peak and the effective water level occurred is indicated in red in the figure 7.10.
Therefore, the resulted hydrograph, obtained with the second simulation, seems to be more correspondent to the realty than the other one obtained with the third procedure.
The figure 7.14 and 7.15 contained the simulated hydrograph correspondent to, respectively, the Rofrano and Sanza rainfall inputs.

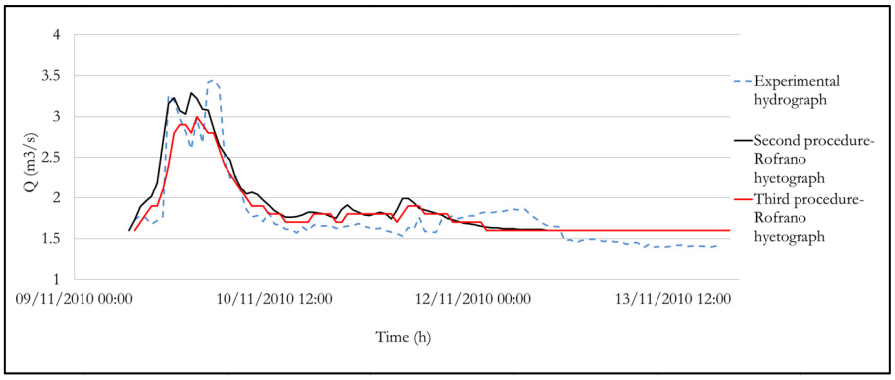

Figure 7.14: The comparison between the hydrographs simulated with the second and third procedure and the experimental one. In the simulations was used rainfall of the Rofrano station.

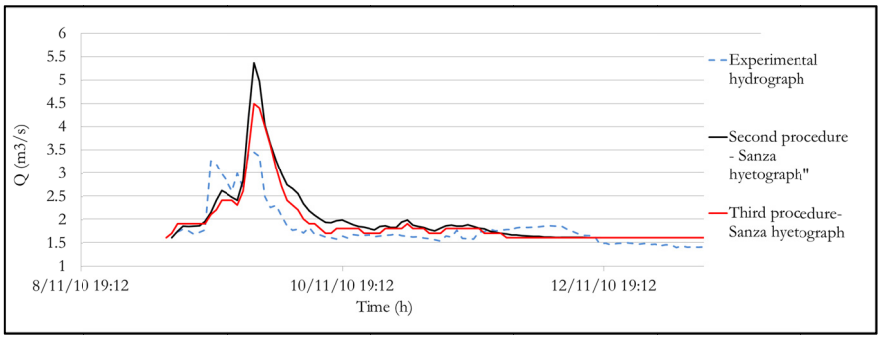

Figure 7.15: The comparison between the hydrographs simulated with the second and third procedure and the experimental one. In the simulations was used rainfall of the Sanza station

A good simulation of the first peak was obtained introducing, in the second simulation procedure, the precipitation pattern of Rofrano station (figure 7.14), while the second peak was better simulated with the precipitation intensity registered at the Sanza Station, because the simulated peak includes the volume of water overtopping the banks river (figure 7.15), as for the figure 7.13.

Finally, considering the construction of the real peak discharge of the figure 7.10 seems taht the simulation made with the mean precipitation is closer to reality.

7.3.2 Rainfall-Runoff simulation for the Dragone river

The Dragone catchments is the second watershed where was performed the simulation above applied. It is located on the Amalfitana coast, in Campania region (figure 7.16), and it characterized prevalently of limestone covered of pyroclastic soil. So, the geology make it hydrologically different from the Bussento river basin.

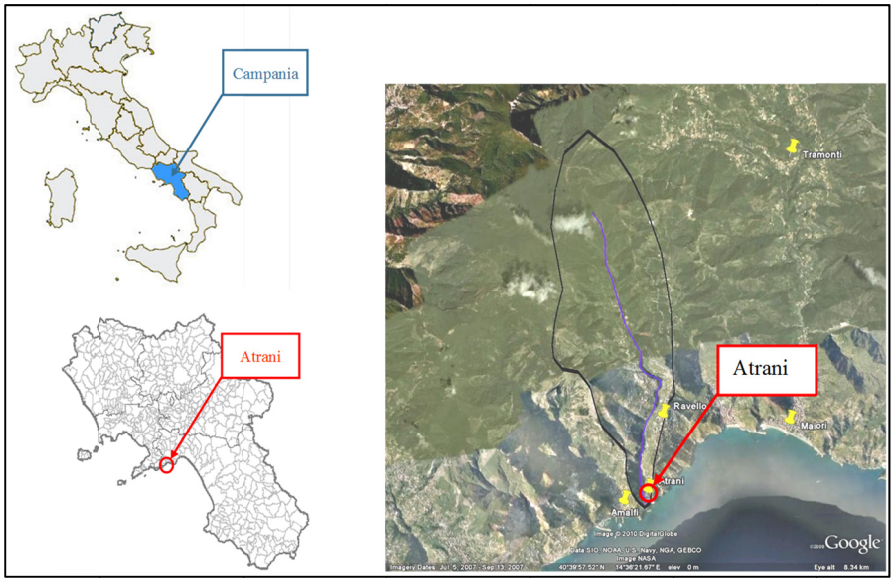

Figure 7.16: Location of the Dragone river basin

The event storm to simulate is occurred in the 9 september 2010 (figure 7.17). The temporal precipitation pattern was collected at the Ravello station, but the hydrograph was not available.
The figure 7.17 shows spatial pattern of the cumulative rainfall at 10, 30 and 60 minutes from the rainfall starting time, demonstrating the SW-NE displacement of the perturbation and an evident amplification due to the orographic barrier, at the orographic unit level. This results confirm the assumption stated in the chapter about the orographic barriers, on the interrelations, at hierarchical level behavior, between meteorological events and orographic unit.

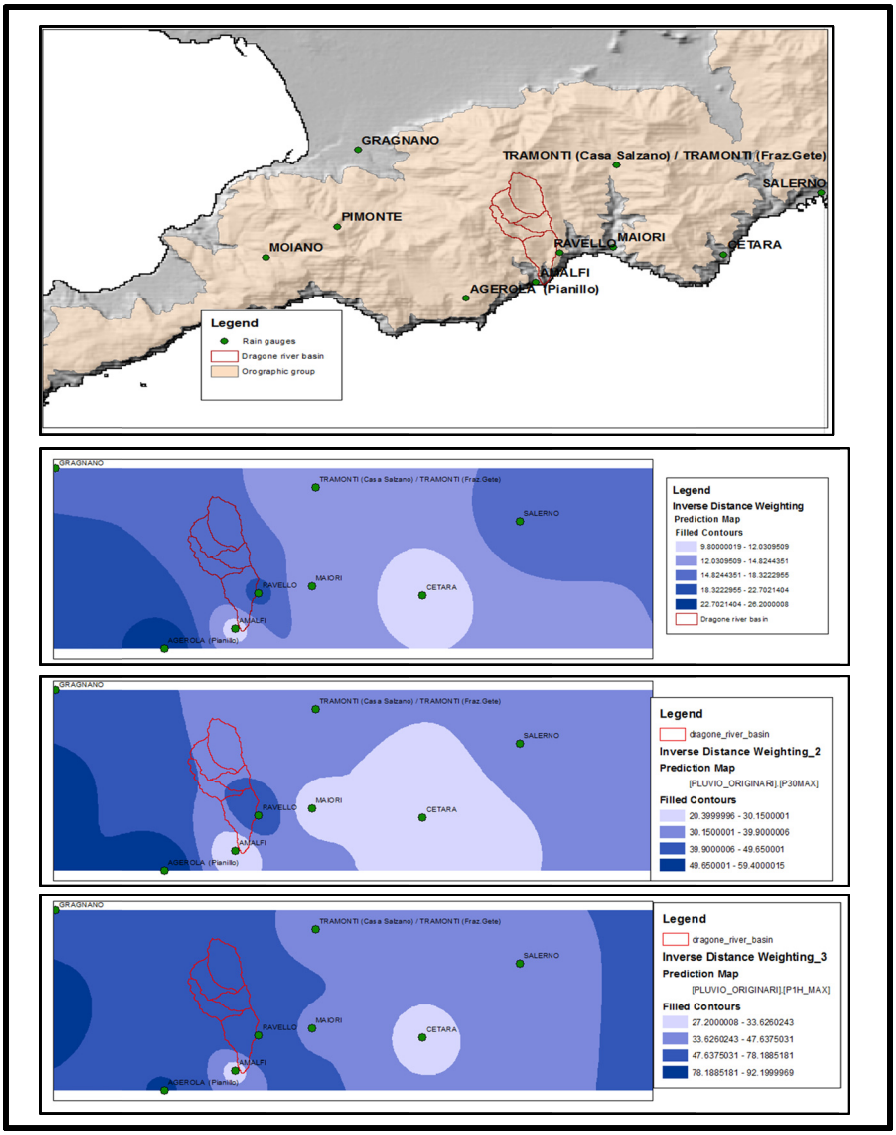

Figure 7.17: The spatial-temporal pattern cumulative rainfall at 10 and 30 minutes and 1 hour from the beginning of the precipitation.

In the figure 7.18, is reported the cumulative rainfall intensity used in the simulation, affected by unit hydrograph barriers.

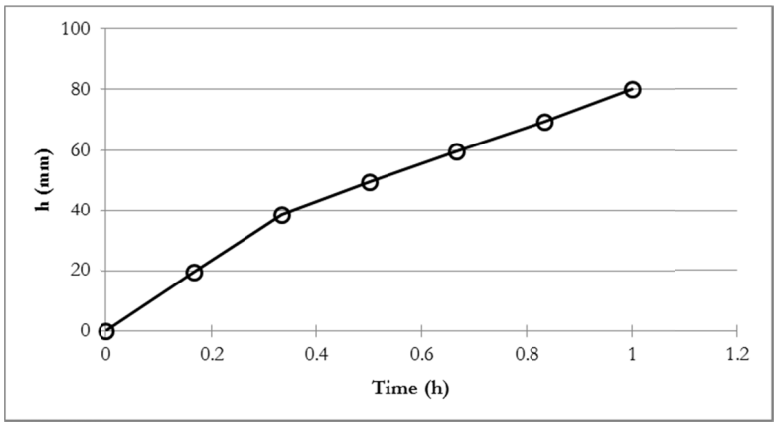

Figure 7.18: Cumulative rainfall pattern detected at the Ravello rain gauges (at t=0 it starts to rain)

Photos, surveys and inspections were used to reconstruct the hydrograph (Spatuzzi 2012) (figure 7.19).

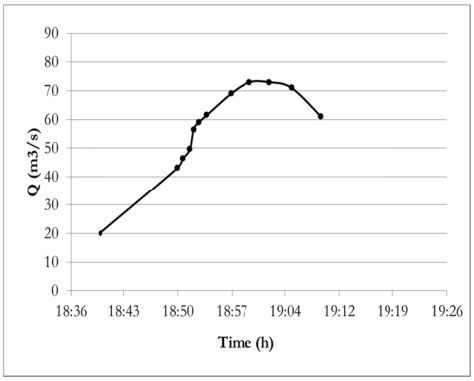

Figure 7.19: The hydrograph reconstruct using photos, surveys and inspections

To perform the simulation, the catchment was firstly divide in sub-catchments (figure 7.20) in the ArcMap software and the morphometric parameters for each one were derived (table 7.10)

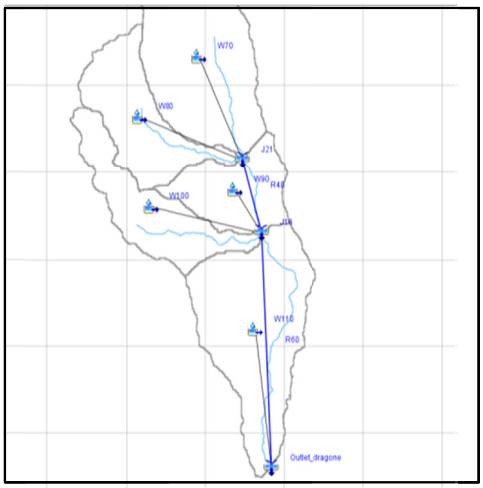

Figure 7.20: The Dragone basin splitted in sub-catchments

Table 7.9: The morphometric parameters calculate for each sub-catchments

Sub-catchments/ river reach	Area [km²]	Lenght of river [km]	Mean slope of channel [%]	Snyder's tp [h]
W70	2.65			0.52
W80	1.46			0.44
W90	1.11			0.51
W100	1.36			0.4
W110	2.66			0.68
R40	-	0.99	9	
R60	-	3.4	11	

For the simulation were used the three procedure above introduced in the paragraph 7.2.1..
In the table 7.11 are listed the Snyder's parameter, need for the first method.

Table 7.10: The Snyder's parameter

Sub-catchment	Permeable area [%]	C_t	Snyder's C_p
W70	52	0.36	0.56
W80	47	0.35	0.55
W90	46	0.39	0.58
W100	67	0.29	0.51
W110	72	0.28	0.49

The parameter to be used in the second method are the delay times.
The event type (isolate cell) was short and intense , with a quick basin response. For this reason the delay times were calculated from the recession limb only for the fast components (surface and fast sub-surface flows). Then, with the formulas 6.14 and 6.15 were calculated the total delayed times for the sub-catchments.
The same was done for the runoff coefficient and was used the linear equation, to be used in the third simulation.
To apply the citied formulas was firstly calculate the RI from the EHGTs map (figure 7.21).

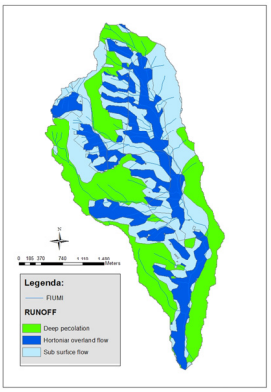

NAME	RI
W70	0,812
W80	0,775
W90	0,637
W100	0,474
W110	0,531

Figure 7.21: The EHGTs map of the Dragone river basin and the Runoff Index calculated for the sub-catchments.

In the table 7.11 are reported the delay times and the runoff coefficient calculated for the sub-catchments.

Table 7.11: The hydrologic parameters calculated for the sub-catchments of the Dragone river

NAME	**cf**	**tr** surface (h)	**tr** sub (h)	Total Tr
W70	0.372	0.0361	0.0265	0.0244
W80	0.355	0.0344	0.0253	0.0222
W90	0.292	0.0283	0.0208	0.0153
W100	0.217	0.0211	0.0155	0.0084
W110	0.243	0.0236	0.0173	0.0108

In the figures 7.22, 7.23 and 7.24 are shown the hydrographs results from the performed simulation and the hydrograph reconstructed.
In particular, the figure 7.22 contains the reconstructed hydrograph compared to the hydrograph simulated with the physically based equations operated by Spatuzzi (2012) in her doctoral thesis with the Flo2d software.

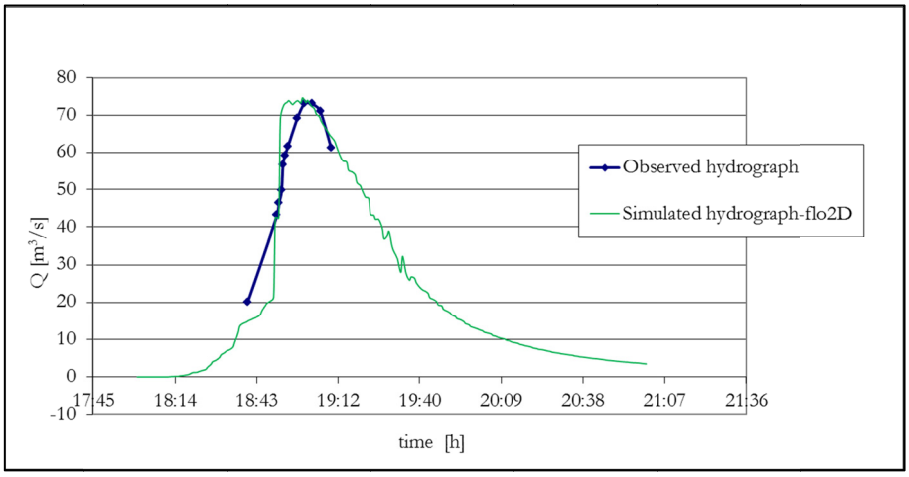

Figure 7.22: The flo2D hydrograph compared to the experimental one.

The flo2d peak discharge is comparable to the observed one, but shows a longer persistence and an anticipated response time.
The figures 7.23 and 7.24 contains respectively the hydrographs simulated with the first and the third procedures.

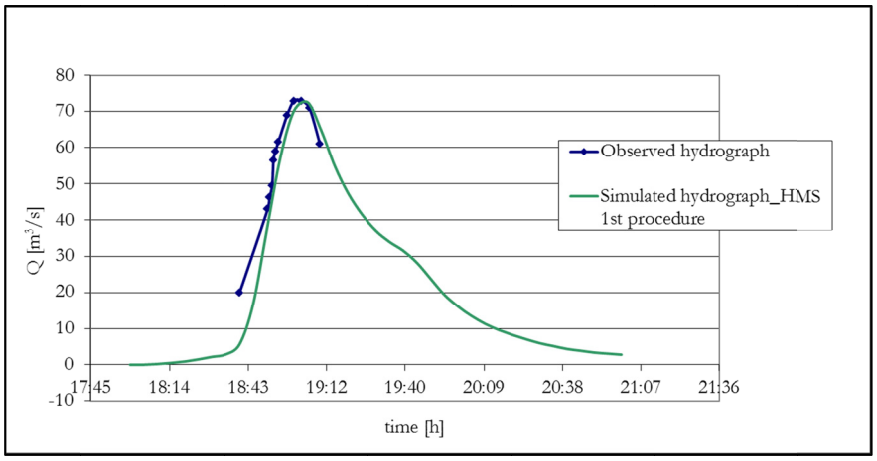

Figure 7.23: The hydrograph obtained with the first procedure is linked to the experimental one.

In this case, the simulate hydrograph shows a good correspondence of the peak discharge with the reconstructed hydrograph, also for the rising limb.

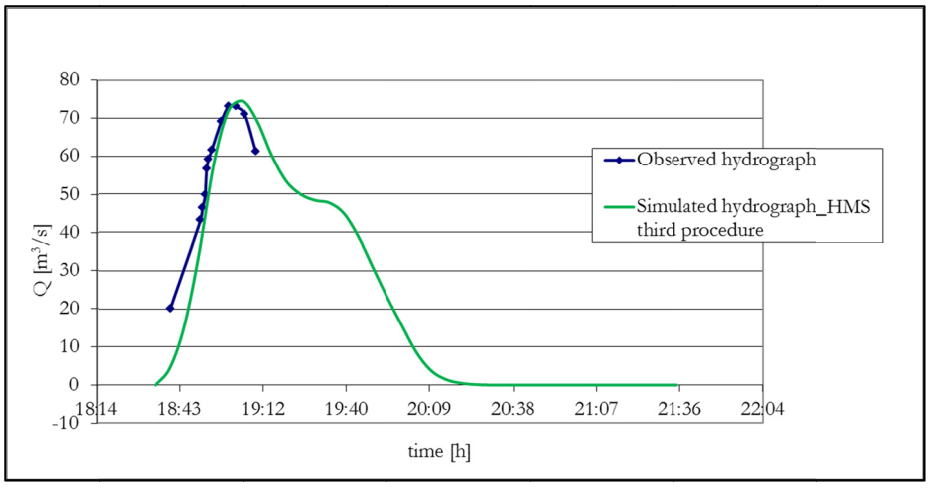

Figure 7.24: The hydrograph obtained with the third procedure is linked to the experimental one.

For the last simulation are observed a better correspondence in the rising limb with the observed one but the peak discharge is slightly delayed. The peak discharge value is comparable.

In conclusion, the above simulations demonstrated the feasibility of the EHGU approach also for un-gauged basin, in the landscape of the Campania region not considered to testing the reliability of the procedure.

8 CONCLUSIONS

This thesis presents the results of the research carried out on 'hydro-geomorphological contribution to up-date the VAPI-Campania procedure' (Rossi and Villani, 1995) and synthesizes the contents of scientific papers published by the writer on national and international journals and proceedings. In particular, this research demonstrates advances in the methodological insights, procedural innovations and spatial modeling of two main topics: orographic barriers and hydro-geomorphotypes. The proposed hierarchical-multiscale approach and performed algorithms and GIS routines (grid- and object-based) has demonstrated to be of strong support to the interdisciplinary hydro-climatological analysis and modeling, at any spatial and temporal scales.

The results obtained in the first topic consist of an innovative GIS-based procedure allowing the automatic individuation, objective delimitation and distinctive characterization of the orographic barriers in order to overcome both the heuristic delimitation (expert judgment based) used in the simplified model on the orographically induced rainfalls of Rossi et al. (2005) and the extreme geometrical shape reduction adopted in the physically-based orographical barrier modeling. Also, the results will support ongoing geo-statistical analysis on the distribution, intensity, frequency and persistence anomalies in the distribution of the orographically-induced rainfalls.

The results obtained on the second topic offer new insights in the automatic individuation of the hydro-geomorphotypes, that become a more suitable basic land unit in the VAPI-Campania rainfall-runoff transformation procedure. The adopted procedure integrates the prototypal work of Guida et al. (2007), performed exclusively on the pyroclastic-cover landscape of the Campania region and modifies the decisional scheme of Scherrer and Naef (2003), and identifies three dominant mechanisms in rainfall-runoff transformation. The procedure was designed for mountain regions, without considering the hydrologic

behavior and geomorphologic features of the floodplains and urban areas.

In particular, the new insights into orographic mountains definition allowed to draw-up the hierarchical-multiscale orographic barrier map of the Campania region (Cuomo and Guida, 2010), suitable in interdisciplinary studies relating type and magnitude of meteorological events to the hierarchically correspondent orographical entity. Recently, in Cuomo et al., 2011, the procedure was just applied and extended to the Apennines chain, Sicily and Sardinia islands, producing a digital orographical map, useful in performing ongoing researches in oro-hydrographic regionalization of Europe. Some characterization methods were proposed in order to classify the orography, at a given spatial scale, based on shape and ruggedness improving the analysis of the event storms types and their linkage to the orography shape. This last issue was recently addressed in the literature by Jiang (2006) and Watson and Lane (2011).

The second topic of research has allowed to conceptualize the hydro-geomorphotypes as basic hydrological units with effective behavior at the catchment and sub-catchment scale. Based on these findings, a GIS based procedure allows to drawn-up the hydro-geomorphotypes map of the Campania region. Spatial hydrological analysis on the experimental catchments have allowed to propose the Runoff Index (RI), as synthetic hydro-geomorphological parameter containing quantitative morphological and geological control in hydrologic response of a river basins. This index, tested on some mountain catchments with respect to their effective geology and hydrological behavior (using hourly discharge and rainfall data), provides several advantages in planning assessment, containing more detailed data on the different components of the total streamflow, at the catchments and sub-catchments scale. Also, the linear relation performed rather well to describe the runoff-producing processes, where the runoff coefficient is in a linear dependence with the RI, used as independent variable. Model performance, using the ANOVA test, indicates the statistical significance of the simplified model. Anyway, this model must be improved with additional hydrological analysis on others mountain catchments.

We modeled the integrated hydro-geomorphological approach and procedure on rainfall-runoff transformation using the well-know HEC-HMS software, on two catchments for two storm events with different orographically-induced rainfall temporal pattern. The simulations showed the suitability and the implementation in digital hydrologic analysis of the RI and EHGU's. Also, the rainfall-runoff transformation modeling demonstrated the accuracy of integrated hierarchical-multiscale taxonomy linking the orographic entities and precipitations.

REFERENCES

Abbott, M. B., Bathurst, J. C., Cunge, J. A., O'Connell, P. E., & Rasmussen, J. (1986a). An introduction to the European Hydrologic System-Systeme Hydrologique Europeen, SHE, 1: History and philosophy of a physically-based, distributed modeling system. *Journal of Hydrology, 87*, 45-59.

Abbott, M. B., Bathurst, J. C., Cunge, J. A., O'Connell, P. E., & Rasmussen, J. (1986b). An introduction to the European Hydrologic System-Systeme Hydrologique Europeen, SHE, 2: History and philosophy of a physically-based, distributed modeling system. *87*, 61-77.

ACI-ASCE Committee, 3. (1985). Recommendations for design of beam column joints in monolithic reinforced concrete structures. *J.Am. Concr. Inst.,*, 82(3), 266–283.

Ackermann, F. (1978). Experimental investigation into the accuracy of contouring from DTM. *Photogrammetric Engineering and Remote Sensing, 44*, 1537-1548.

Ahnert, F. (1984). Local relief and height limits of mountain ranges. *American Journal of Science, 268*, 1035-1055.

Aloia, A., De Vita, A., Guida, D., Toni, A., & Valente, A. (1-3 October 2011 (in press)). National Park of Cilento and Vallo di Diano:geodiversity, geotourism, geoarchaelogy and historical tradition. *Proceedings of the European Geopark Conference.* Lesvos, Greece.

Alonso, M., Chaminè, H., Gomes, A., Fonseca, P. E., Marques, J. M., Guimaraes, L., et al. (2006). Urban hydrogeomorphology and geology on the POrto metropolitan area (NW Portugal): a multidisciplinary approach. *Pre-Congress Proceedings of the X IAEG*

International Congress.Engineering geology for tomrrow's cities, Nottingham (p. 1-9). London: The geological society of London.

Amore, F. O., Bonardi, G., Ciampo, G., De Capoa, P., Perrone, V., & Sgrosso, I. (1988). Relazioni tra "Flish interni" e domini appenninici:reinterpretazione delle formazioni di Pollica, San Mauro e Albidona nel quadro della evoluzione inframiocenica delle zone esterne appenniniche. *Memorie Società Geologica Italiana, 41*, 285-297.

Anderson, M. G., & Burt, T. (1978). The role of topography in controlling throughflow generation. *Earth Surface Processes and Landforms, 3*, 331-344.

Augusti, G., Borri, C., & Niemann, H. J. (2001). Is aeolian risk a s a significant as another environmental risk? *Reliability Engineering and System Safety, 74*, 227-237.

Austin, P. M., & Houze, R. A. (1972). Analysis of the structure of precipitation patterns in New England. *Journal of Applied Meteorology, 11*, 926-935.

Avissar, R. (1992). Conceptual aspects of a statistical-dynamical approach to represent landscape subgrid-scale heterogeneities in atmospheric models. *Journal of Geophysical Research, 97*, 2729-2742.

Babar, M. (2005). *Hydrogeomorphology: foundamentals, applications and techniques.* New India Publishing Agency, New Delhi.

Bakalowicz, M. (1995). The infiltration zone of karst aquifers. *Hydrogeologie, 4*, 3-21.

Band, L., & Moore, I. (1995). Scale: Landscape Attributes and Geographical Information Systems. In J. D. Kalma, *Scale Issues in Hydrological Modelling* (p. 159-180). Wiley,Chichester, UK.

Band, L., Tague, C., Brun, S., Tenenbaum, D., & Fernandes, R. (2000). Modeling watersheds as spatial object hierarchies: structure and dynamics. *Transactions in GIS, 4*(3), 181–196.

Barros, A. P., & Lettenmaier, D. P. (1994). Dynamic modeling of orographically induced precipitation. *Reviews of Geophysics, 32*, 265–284.

Barsch, D., & Caine, N. (1984). The nature of the mountain geomorphology. *Mountain Research and Development, 4*(4), 287-298.

Barstad, I., Grabowski, W. W., & Smolarkiewicz, P. K. (2007). Characteristics of large-scale orographic precipitation: Evaluation of linear model in idealized prolems. *Journal of Hydrology, 340*, 78-90.

Basists, A. N. (1989). A comparison of orographic effects on precipitations at 10 region worldwide. *Master Thesis, University of Georgia*.

Beasley, D. B., Huggins, L. F., & Monke, E. J. (1980). ANSWERS: a model for watershed planning. *Transactions of the American Society of Agricultural Engineers*(23), 938-944.

Becker, A., & Braun, P. (1999). Disaggregation, aggregation and spatial scaling in hydrological modelling. *Juornal od hydrology, 217*, 239-252.

Behrens, T., Zhu, A.-X., Schmidt, K., & Scholten, T. (2010). Multi-scale digital terrain analysis and feature selection for digital soil mapping. *Geoderma, 155*, 175-185.

Beker, A., & Braun, P. (1999). Disaggregation , aggregation and spatial scale modeling in hydrological modelling. *Journal of Hydrology, 17*(2-3), 239-252.

Beniston, M. (2000). *Envirnmental changes in mountains and uplands*. Edward Arnold, London.

Berz, G. (1997). Catastrophes and climate change: Risks and (re-)actions from the viewpoint of an international reinsurer. *Ecologae Geologicae Helvetiae*, 375-379.

Beven, K. (2000). *Rainfall-Runoff modelling: The Primer*. Chichester, New York, Weineim, Brisbane, Singapore, Toronto: John Wiley and Sons.

Beven, K. (2001). How far can we go in distributed hydrological modelling? *Hydrology and Earth System Sciences*, 5(1), 1-12.

Beven, K. J. (1991). 'Scale considerations. In D. S. Bowles, & P. E. O'Connell, *Recent Advances in the Modeling of Hydrologic Systems* (p. 357-371). Kluwer, Dordrecht.

Beven, K. J. (1995). Linking parameters across scales: Subgrid parameterisations and scale dependent hydrological models. In J. D. Kalma, & M. Sivapalan, *Scale Issues in Hydrological Modelling*. Wiley, Chichester, UK.

Beven, K. J., & Kirkby, M. J. (1979). Toward a simple physically-based variable contributing area of catchment hydrology. *Working paper No. 154*.

Bhaskar, N., James, W., & Devulapalli, R. (1992). Hydrologic parameters estimation using Geographic Information System (GIS) Journal of Water . Resources Planning and Management, ASCE 118(5) , 492-512.

Bisson, R., & Lehr, J. (2004). *Modern groundwater exploration: discovering new water resources*. John Wiley and Sons Inc, Hoboken, NJ.

Blasi, C., Carranza, M. L., Frondoni, R., & Rosati, L. (2000). Ecosystem classification and mapping: a proposal for italian landscape. *Applied vegetation sciences, 3*, 233-242.

Blasi, C., Guida, D., Siervo, V., Paolanti, M., Michetti, L., Capotorti, G., et al. (2007). An integrated, hierchical, multiscale, GIS based approach to defining and mapping the landscape of Italy. *Geophysical Research Abstracts. 9*. Vienna: European Geosciences Union.

Blösch, G., & Silvapan, M. (1995). Scale Issues in hydrological modelling: a review. *Hydrological processes, 9*, 251-290.

Blöschl, G., Grayson, R., & Sivapalan, M. (1995). On the Representative Elementary Area (REA) concept and its utility for distributed rainfall-runoff modelling',. In J. D. Kalma, & M. Sivapalan, *Scale Issues in Hydrological Modelling* (p. 71-88). Wiley, Chichester, UK.

Bonardi, G., Amore, F. O., Ciampo, G., De Capoa, P., Miconnet, P., & Perrone, V. (1988). Il complesso Liguride Auct.: stato delle conoscenze e problemi aperti sull'evoluzione pre-appenninica ed i suoi rapporti con l'arco calabro. *Memorie Società Geologica Italiana, 41*, 17-35.

Bonnet, S., & Crave, A. (2003). Landscape response to climate change:Insights from experimental modeling and implications for tectonic versus climatic uplift of topography. *Geology, 31*, 123-126.

Bonta, J. (1998). Spatial variability of runoff and soil properties on small watersheds in similar soil-map units. *Transactions ASAE, 41*, 575-858.

Bookhagen, B., & Strecker, M. R. (2008). Orographic barriers, high-resolution TRMM rainfall, and relief variations along the eastern Andes. *Geophysical Research Letters, 35*, 1-6.

Brooks, N., & Adger, N. W. (2003). Country level risk measures of climate-related natural disadters and implications for adapatation to climate change. *Tyndall Centre Working Paper*(8), 8.

Bull, W. B. (1975). Allometric change of landforms. *GSA Bull., 86*(11), 1489-1498.

Burgess, S. S., Adams, M. A., Turner, N. C., & Ong, C. K. (1998). The redistribution of soil water by tree root systems. *Oecologia, 115*, 306-311.

Bush, B., Prentice, M. L., Bishop, M. P., & Shroder, J. F. (2004). Modelling global and regional climate system: Climate forcing and topography. In M. P. Bishop, & J. F. Shroder, *Geographic Information System and Mountain Geomorphology* (p. 403-419). Springer, Chilchester, UK.

Caine, N. (1980). The rainfall intensity: duration controls on shallowlandslides and debris flow. *Geografiska Annaler Series A, 62*, 23-27.

Cammarosano, A., Danna, M., De Rienzo, F., Miele, F., & Nardi, G. (2000). Il substarto del gruppo del Cilento tra il M. Vesalo e il M. Sacro (Cilento, Appennino Meridionale). *Bollettino Società Geologica Italiana, 119*, 395-405.

Cannarozzo, M., D'Asaro, F., & Ferro, V. (1993). *Valutazione delle piene in Sicilia.* CNR-GNDCI, Palermo.

Cannon, T. (1994). Vulnerability analysis and the explanation of "Natural" Disaster. In A. Varley, *Disaster, Development and Environmet.* London: John Wiley & Sons Ltd.

Cao, C., Piga, E., Salis, M., & Sechi, G. M. (1991). *Valutazione delle piene in Sardegna.* Rapporto regionale Sardegna, CNR-GNDCI, LINEA 1,, Istituto di Idraulica, Università di Cagliari.

Caracena, F., Maddox, R., Hoxit, L., & Chappell, C. F. (1979). Mesoscale analysis of the Big Thompson storm. *Monthly Weather Review, 107*, 1-17.

Carrara, A. (1983). Multivariate models for landslide hazard evaluation. *Mathematical gaology, 15*(3).

Carrara, A., Cardinali, M., & Guzzetti, F. (1992). Uncertainity in assessing landslide hazard and risk. *ITC journal*(2), 172-183.

Carrara, A., Cardinali, M., Detti, R., Guzzetti, F., Pasqui, V., & Reischenbach, P. (1991). GIS techniques and statistical models in evaluating landslide hazard. *Earth surface processes and landforms, 16*, 427-455.

Carrara, A., Cardinali, M., Guzzetti, F., & Reischenbach, P. (1995). GIS tecnology in mapping landslide hazard. In A. Carrara, & F. Guzzetti, *Geographical Information Sistems in natural hazards* (p. 135-175). Kluver Academin Publishers, Dordrecht, Notherlands.

Chaudhry, O. Z., & Mackaness, W. A. (2006). *Modelling Geographic Phenomena at Multiple Levels of Detail.* Proceeding of AutoCarto Research Symposium in Vancouver, WA, Jun 2006.

Chaudhry, O. Z., & Mackaness, W. A. (2008). Creating Mountain of Mole Hills: Automatic identification of hill and range using morphometric analysis. *Transaction in GIS,, 12*(5), 567-589.

Chou, Y. (1997). *Exploring spatial analysis in GIS*. Onword Press.

Chow, V., Maidment, D., & Mays, L. W. (1988). *Applied hydrology*. McGrawHill.

Cinque, A., & Ascione, S. (2001). Evoluzione geomorfologica e caratetri oro-idrografici della Campania. In A. Vallario, *Ambiente geologico della Campania*. Liguori, Napoli.

Clarke, R. T. (1973). A review of some mathematical models used in hydrology, with observations on their calibration and use. *Journal of Hydrology*(19), 1-20.

Collischonn, W., Allasia, D., Da Silva, B. C., & Tucci, C. E. (2007). The MGB-IPH model for large-scale rainfall—runoff modeling. *Hydrological Sciences Journal, 52*(5).

Conway, H., & Raymond, C. F. (1993). Snow stability during rain. *Journal of Glaciology, 39*, 635-642.

Cooke, R. U., & Doornkamp, J. C. (1990). Geomorphology in environmental management. 2nd ed Oxford University Press, Oxford.

Copertino, V., & Fiorentino, M. (1992). *Valutazione delle piene in Puglia*. CNR-GNDCI, Potenza.

Coppus, R., & Imeson, A. C. (2002). Extreme events controlling erosion and sediment transport in a semi-arid sub-Andean valley. *Earth Surf.Earth Surf., 27*, 1367-1375.

Cuomo, A., & Guida, D. (2010a). Definizione Gis_Based delle Barriere Orografiche dell'appennino Campano-Lucano (Italia Meridionale). *Atti del XXXII Convegno Nazionale di Idraulica e Costruzioni Idrauliche, Palermo, ISBN 978-88-903895-2-8*, 288.

Cuomo, A., & Guida, D. (2010b). Orographic barriers GIS-based definition of the Campania-Lucanian Apennine. *Session Poster "Complex System in Geomorphology", Geophysical Research Abstracts, 12,*.

Cuomo, A., Guida, D., & Palmieri, V. (2011). Digital orographic map of peninsular and insular Italy. *Journal of Maps, 7*(1), 447-463.

D'Argenio, B., Ferreri, V., Stanzione, D., Brancaccio, L., & Ferreri, M. (1983). I travertini di Pontecagnano (Campania). Geomorfologia,Sedimentologia, Geochimica. *Bollettino Società Geologica Italiana, 102*, 123-136.

D'Argenio, B., Pescatore, T., & Scandone, P. (1973). Schema geologico dell'Appennino meridionale (Campania e Lucania). *In:Moderne vedute sulla geologia.Accademia Nazionale dei Lincei*, *183*, p. 49-72.

D'Argenio, B., De Castro, P., Emiliani, P., & Simone, L. (1975). Geologic notes: Bahamian and Limestones identical lithofacies and age. *American Association of Petroleum Geologists, 59*(3), 524-533.

De Vivo, B., G., R., & B., G. P. (2001). New constraints on the pyroclastic eruptive. In B. De Vivo, & G. Rolandi, *Mt. Somma Vesuvius and Volcanism of* (Vol. 73, p. 47-65). Spec. Issue Mineral. Petrol.

D'Elia, G., Guida, M., & Terranova, C. (1987). Osservazioni sui fenomeni di deformazione gravitativa profonda nel bacino del Fiume Bussento. *Boll. Soc. Geol. Ital., Vol. CVI*.

Detty, J. M., & McGuire, K. J. (2010). Topographic controls on shallow groundwater dynamics: implications of hydrologic connectivity between hillslopes and riparian zones in a till mantled catchment. *Hydrological Processes, 24*, 2222-2236.

Devito, K., Creed, I., Gan, T., Mendoza, C., Petrone, R., Silins, U., et al. (2005). A framework for broad-scale classification of hydrologic response units on the Boreal Plain: is topography the last thing to consider? *Hydrological processes, 19*, 1705-1714.

Dikau, R. (1990). Geomorphic landforms modelling based on Hierarchy Theorie. *In: Proc. 4th International Synopsium on Spatial Data Handling, 23-27 July, Zurich, 230-239*.

Dilley, M., Chen, R. S., Deichmann, U., Lerner-Lam, A. L., Arnold, M., Agwe, J., et al. (2005). *Natural disaster hotspots: a global risk analysis.* Synthesis report, The world bank and Columbia University, Washington.

Dooge, J. C. (1959). A general theory of the Unit Hydrograph. *Journal of Geophysical Research, 64*(2), 241-256.

Dooge, J. C. (1982). Parameterization of hydrologic processes. In P. S. Eagleson, *Land Surjace Processes in Atmospheric General Circulation Models.* (p. 243-288). Cambridge University Press, London.

Dooge, J. C. (1986). Looking for hydrologic laws. *Water Resources Research, 22*, 46S-58S.

Dramis, F., Guida, D., & Cestari, A. (2011). Nature and Aims of geomorphological mapping. In M. Smith, P. Paron, & J. S. Griffiths, *Geomorphological mapping: Methods and applications* (Vol. 15). Elsevier, Developments in Earth Surface Processes.

Dunne, T., & Black, R. (1970). Partial area contributions to storm runoff in a small New England watershed. *Water Resources Research*, 6:1296-1311.

El-Kady, A. I. (1991). Watershade models and their applicabilityto conjuntive use management. *Journal of the American Water Resources Association, 25*(1), 25-137.

Elshorbagy, A., & Ormsbee, L. (2006). Object-oriented modeling approach to surface water quality management. *Environmental Modelling & Software* (26), 689-698.

Encyclopedia. (2004). *Mountain Hierarchies. Canadian Mountain Encyclopedia.*

Entekhabi, D., & Eagleson, P. (1989). Land surface hydrology parameterization for the atmospheric general circulation models including subgrid-scale variability. *J. Climate, 2*, 816–831.

Espinha Marques, J., Duarte, J. M., Constantino, A. T., Martins, A. A., Aguiar, C., Rocha, F. T., et al. (2007). Vadose zone characterisation in a mountain hydrogeologic system: Serra de Estrela (Cantral Portugal) case study. In L. Chery, & M. G. (Eds), *Aquifer System Management: Darcy's Legacy in a Word of Impeding Water storage,Selected paper in Hydrogeology* (p. 207-221). IAH Special Publications. Taylor & Francis CRC Press.

Espinha Marques, J., Marques, J., Chaminè, J. M., Carreira, H. I., Fonseca, P., Sampera, J., et al. (2006). Hydrogeochemical model of low temperature geothermal system in a mountainous terrain, Serra de Estrela, Central Portugal. *Geothermal Resources Council Transactions, 30*, 913-918.

Faeh, A. (1997). *Understanding the processes of discharge formation under extreme precipitation – A study based on numerical simulation of hillslope experiments,*. PhD thesis, Swiss Federal Institute of Technology, Zurich.

Fan, Y., & Bras, R. (1998). Analytical solution to hillslope subsurface storm flow and saturation overland flow. *Water Resource Research, 34*(4), 921-927.

Fels, J. E., & Zobel, R. (1995). *Landscape position and classified landtype mapping for statewide DRASTIC mapping project.* . North Carolina State University Technical Report.

Ferrari, E., Versace, P., & Villani, P. (1990). Terzo livello di analisi delle piene in Calabria. In *In F. Rossi: Previsione prevenzione degli eventi idrologici estremi e loro controllo, Rapporto 1998*. GNDCI-CNR.

Florio, G., Fedi, M., Cella, F., & Rapolla A. (1999). The Campanian Plain and. *Journal of Volcanology, 91*, 361-379.

Flügel, W. (1995). Delineating Hydrological Response Units (HRU's) by GIS analysis for regional hydrological modelling using PRMS/MMS in the drainage basin of the River Bröl, Germany. . *Hydrological Processes, 9*, 423-436.

Ford, D., & Williams, P. (1989). *Karst geomorphology and hydrology*. London, England: Unwin Hyman.

Fortin, M. J., & Dale, M. (2005). *Spatial Analysis: a Guida for ecologists*. Cambridege: Cambridege University Press.

Frich, P., Alexander, L., Della Marta, P., Gleason, B., Haylock, M., Klein Tank, A., et al. (2002). Observed coherent changes in climatic extremes during the second half of the twentieth century. *Climate Resources, 19*, 193-212.

Gagerall, C. M., Purcell, T., & Taylor, R. (2004). Fractal dimension of landscape silhouette outlines as a predictor of landscape preference. *Journal of Environmental Psychology, 24*, 247–255.

Galewsky, J., Roe, G., Anderson, R., Meyer, G., & Flowers, G. (2008). Climate Over Landscapes: Workshop on Atmospheric Sciences and Surface Processes. *Boulder, Colorado, 1–3 October 2007, Eos Trans. AGU, 89(16), 151, doi:10.1029/2008EO160004*.

Gharari, S., Hrachowitz, M., Fenicia, F., & G., S. H. (2011). Hydrological landscape classification: investigating the performance of HAND based landscape classifications in a central European meso-scale catchment. *Hydrological and Earth System Sciences*, 15, 3275-32791, doi:10.5194/hess-15-3275-2011.

Gonzales, A. L., Nonner, J., Heijkers, J., & Uhlenbrook, S. (2009). Comparison of different base flow separation method in a lowland catchment. *Hydrology and earth system sciences discussions, 6*, 3483-3515.

Gonzales, A. L., Nonner, J., Heijkers, J., & Uhlenbrook, S. (2009). Comparison of different base flow separation methods in a lowland catchment. *Hydrology and Earth System Sciences Discussions, 6*, 3483-3515.

Goodrich, D. C., & Woolhiser, D. A. (1991). Catchment Hydrology. *Reviews of Geophysics*(29), 202-209.

Grayson, R., Moore, I. D., & McMahon, T. (1992). Physically based hydrologic modelling. Is the concept realistic? *Water Resource Resurces*, 26(10), 2659-2666.

Gregory, K., & Walling, D. E. (1973). *Drainage Basin Form and Processes.* . Edward Arnold Scrap Processors Inc., London., 456 pag.

Guida, D., Cestari, A., Lanzara, R., & Siervo, V. (2007). Hydrogeomorphological units at a regional, basin and watershed scale from automated land-system recognition: GIS-based experiences in Campania region (Southern Italy). *Geophysical Research Abstracts*, *9*. Vienna.

Guida, D., De Pippo, T., Cestari, A., Siervo, V., & Valente, A. (2009). Applications of the hierarchic GIS- based geomorphological mapping system. In M. Marchetti, & M. Soldati (A cura di), *Third AIGEO National Conference*, *13-18 September*, p. 109-110. Modena, Italy.

Guida, D., Guida, M., Cuomo, A., Siervo, V., & Guadagnuol, o. D. (2008). Radon-prone Areas Assessment in Campania Region. Applications of a Hierarchical and Multi-scale Approach to the Environmental Planning. *Journal of Technical & Environmental Geology, XVI, 2 (April/June), 38-62.* .

Guida, D., Guida, M., Luise, D., Salzano, G., & Vallario, A. (1980). Ricostruzione di sequenze morfoevolutive nell'area ad W di M. Sacro (Cilento. *Geologia applicata e idrogeologia, 15*, 1-22.

Guida, D., Longobardi, A., & Villani, P. (2005). Hydrological modelling for river basin management in an highly hydro-geological conditioned environment. In J. F. Martin-Duque, C. A. Brebbia, D. Emmanouloudis, & U. Mander, *Geo-Environment & Landscape Evolution II.* (p. 283-292). SOUTHAMPTON, WIT Press. ISBN:1-84564-168-X .

Gupta, V. K., Rodriguez-Iturbe, I., & Wood, E. F. (1986). *Scale Problems in Hydrology.* D. Reidel, Dordrecht.

Hack, J. T., & Goodlett, J. (1960). Geomorphology and forest ecology of a mountain region in the central Appalachians. *United States Geological Survey Professional Papers*, 347.

Hagerhall, C. M., Purcell, T., & Taylor, R. (2004). Fractal dimension of landscape silhouette outlines as a predictor of landscape preference. *Journal of Environmental Psychology, 24*, 247–255.

Hahn, D. G., & Manabe, S. (1975). The role of mountains in the south Asian monsoon circulation. *Journal of Atmospheric Sciences, 32*, 1515-1541.

Haigh, M. (1987). The holon hierarchy theory and landscape research. *Catena*, 181-192.

Hall, F. R. (1968). Base flow recessions:a review. *Water Resources Research, 4*(5), 973-983.

Hall, F. R. (1968). Base-flow recessions- A review. *Water Resources Research, 4*(4), 973-983.

Hammond, E. H. (1964). Analysis of the properties in land forms geography: An application to broad- scale in land form mapping. *Annals of the Association of American Geographers, 54*, 11-19.

Hancock, P., Hunt, R., & Boulton, A. (2009). Hydroecology, the interdisciplinary study of groundwaetr dependent ecosystems. *Hydrogeology journal, 17*(1), 1-3.

Hellebrand, H., & van den Bos, R. (2008). Investigating the use of spatial discretization of hydrological processes in conceptual rainfall runoff modelling: a case study for the meso-scale. *Hydrological Processes*, 22, 2943–2952, doi:10.1002/hyp.6909, .

Hellebrand, H., Hoffmann, L., & Pfister, L. (2007). Assessing winter storm flow generation by means of the permeability of the lithology and the dominating runoff production processes. *Hydrology and Earth System Sciences, 11*, 1673-1682.

Hengl, T., Gruber, S., & Shrestha, D. P. (2003). Digital terrain analysis in ILWIS. *Lecture notes. International Institute for Geo-Information Sciences & Earth Observation (ITC), Enschede*, 56.

Hewlett, J., & Hibbert, A. (1967). Factors affecting the response of small watersheds to precipitation in humid areas. *In Proceedings of the International Symposium on Forest Hydrology, Sopper WE, Lull HW (eds). Pergamon: New York*, 275-290.

Hjerdt, K. N., McDonnell, J. J., Seibert, J., & Rodhe, A. (2004). A new topographic index to quantify downslope controls on local drainage,. *Water Resources Research, 40, W05602, doi:10.1029/2004WR003130.*

Holley, B. P. (1969). The problem of scale in time-space researce. In T. Carlstein, D. Parkes, & N. Thrift, *Time and Regional Dynamics* (p. 5-18). John Wyley and Sons, New York).

Hornberger, G. M., & Boyer, E. W. (1995). Recent advances in watershed modelling. U. S. report to IUGG, 1991-1994. *Reviews of Geophysics, American Geophysical Union, Suppl.*, 949-957.

Horton, R. E. (1945). The erosional development of streams and their drainage basins: Hydrophysical approach to quantitative morphology. *Bulletin of the Geological Society of America, 56*, 275-370.

Hrachowitz, M., Soulsby, C. D., Dawson, J. J., & Malcolm, I. A. (2009). Regionalization of Transit Time Estimates in montane catchments by integrating landscape controls. *Water Resource Research, 45, W05421, doi:10.1029/2008WR007496*.

Hrachowitz, M., Soulsby, C., Tetzlaff, D., Malcolm, I. A., & Schoups, G. (2010). Gamma distribution models for transit time estimation in catchments: Physical interpretation of parameters and implications for time-variant transit time assessment. *Water Resources Research, 46, W10536, doi:10.1029/2010WR009148*.

Huw, D. (s.d.). Mesoscale Atmospheric System- Observation and Modelling. http: ams.confex.com/ams/pdfpapers/96718.pdf. Tratto da www.ams.confex.com.

Ives, J. D., Messerli, B., & Spiess, E. (s.d.). Mountains of the world- A global priority. In B. Messerli, & J. D. Ives, *Mountains of the world- A global priority* (p. 1-15). Parthenon, London.

Jain, S., Kumar, N., Ahmad, T., & Kite, G. (1998). SLURP model and GIS for estimation of runoff in a part of Satluj catchment, India,. *Hydrological Sciences Journal, 43*, 875-884.

Jakeman, A., & Hornberger, G. (1993). How much complexity is warranted in a rainfall-runoff model?,. *Water Resources Research, 29*, 2637-2649.

Jencso, K. G. (2010). Hillslope hydrologic connectivity controls riparian groundwater turnover: Implications of catchment structure for riparian buffering and stream water sources. *Water Resources Research, 46, W10524, oi:10.1029/2009WR008818*.

Jencso, K. G., McGlynn, B. L., Gooseff, M. N., Wondzell, S. M., Bencala, K. E., & Marshall, L. A. (2009). Hydrologic connectivity between landscapes and streams: transferring reach- and plotscale understanding to the catchment scale,. *Water Resources Research, 45, W04428, doi:10.1029/2008WR007225*.

Jiang, Q. (2003). Moist dynamics and orographic precipitation. *Tellus, 55A*, 301-316.

Jiang, Q. (2006). Precipitation over Concave Terrain. *Journal of Atmospherc Sciences, 63*, 2269-2288.

Kalma, J., Bates, B., & Woods, R. (1995). Predicting catchment-scale soil moisture status with limited field measurements,. In J. D. Kalma, & M. Sivapalan, *Scale Issues in Hydrological Modelling* (p. 203-225). Wiley, Chichester, UK.

Kirkby, M., & Chorley, R. (1967). Throughflow, overland flow and erosion. *Bulletin of the International Association of Scientific Hydrology, 12*, 5-21.

Kite, G. W., & Kouwen, N. (1992). Watershed modeling using land classifications. . *WATER RESOURCES RESEARCH, 28*(12), 3193-3200, doi:10.1029/92WR01819].

Klein, J. T., & Newell, W. H. (1998). Advancing Interdisciplinary Studies. In W. H. Newell, *Interdisciplinarity: Essays from the Literature* (p. 3-22). New York.

Klemes, V. (1983). 'Conceptualisation and scale in hydrology. *Journal of Hydrology*, 1-23.

Klijn, F. (1988). Milieubeheergebieden. CML-report 37/RIVM.

Koestler, A. (1967). *The Ghost in the Machine.* Macmillan, New York.

Kronert, R., Steinhardt, U., & Volk, M. (2001). *Landscape Balance and Landscape Assessment.* Springer-Verlag, Berlin.

Krysanova, V., Muller-Wohlfeil, D., & Becker, A. (1998). Development and test of a spatially distributed hydrological/water quality model for mesoscale watersheds. *Ecological Modelling, 106*, 261-289.

Lambiase, S., & Ruggiero, A. (1980). La forra del Torano (Matese centrale): un caso di convergenza tra morgogenesi carsica e fluviale. *Societa' Toscana di Scienza Naturali, Vol. LXXXVII.*

Lastoria, B., Simonetti, M. R., Casaioli, M., Mariani, S., & Monacelli, G. (2006). Socio-economic impacts of major floods in Italy from 1951 to 2003. *Advances in Geosciences, 7*, 223-229.

Leavesley, G. H., & Stannard, L. G. (1990). Application of remotely sensed data in a distributed parameter watershed model. *Workshop on Applications of Remote Sensing in Hydrology.* Saskatoon: National Hydrologic Research Center, Environment Canada.

Liang, X., Lettenmaier, D. P., Wood, E. F., & Burges, S. J. (1994). A simple hydrologically based model of land surface water and energy fluxes for general circulation models. *Geophysical Research, 99*(D3), 14415-14428.

Lin, H., & Zhou, X. (2008). Evidence of subsurface preferential flow using soil hydrologic monitoring in the Shale Hills catchment,. *European Journal od Soil Sciences, 59*, 34-49.

Lin, Y. L. (2007). *Mesoscale Dynamics.* New York: Cambridge University Press.

Linseley, R. K., Kohler, M. A., & Paulhus, J. L. (1975). *Hydrology for engineers.* McGraw Hill.

Linsley, R. K., Kohler, M. A., & Paulhus, J. L. (1975). *Hydrology for engineers.* McGraw-Hill.

Linton, D. (1951). The delimitation of morphological regions. In L. D. Stamp, & S. W. Wooldridge, *London Essays in Geography, Annals of the Association of American Geographers* (Vol. 41(3), p. 199-218).

Loague, K., Heppner, C. S., Mirus, B. B., Ebel, B., Ran, Q., Carr, A., et al. (2006). Physics- based hydrologic-response simulation-foundantion of hydroecology and hydrogeomorphology. *Hydrological processes, 20*(5), 1231-1237.

Longobardi, A., Cuomo, A., Guida, D., & Villani, P. (s.d.). Water Resources Assessment for Karst Aquifer Conditioned River Basins: Conceptual Balance Model Results and Comparison with Experimental Environmental Tracers Evidences. In I. A. Dar, & M. A. Dar, *Earth and Environmental Sciences* (p. 276-298). InTech, December, 2011, 978-953-307-468-9.

Longobardi, A., Rossi, F., & Villani, P. (2006). Criteri per un'analisi regionale della pioggia media annua. *Proceeding of the XXX° Convegno di Idraulica e Costruzioni Idrauliche - IDRA.*

Mackay, R., & Riley, M. S. (1991). The problem of scale in the modelling of groundwater flow and transport processes. *In Chemodynamics of Groundwaters. Proc. Workshop November 1991, Mont Sainie-Odile. France. EAWAG, EERO, PIR "Environment" of CNRS, IMF Universite Louis Pasreur Strasbourg*, (p. 17-51).

Maillet, O. E. (1905). *Essais d'hydraulique soutteraine et fluviale.* Paris: Hermann.

Maizlish, A. (2003). *Prominence and Orometrics: A Study of the Measurement of Mountains. http://www.peaklist.org/theory/theory.html.*

Mandelbrot, B. B. (1983). *The fractal geometry of nature.* New York: W.H. Freeman and Company.

Mather, P. (1987). *Computer Processing of Remotely-sensed Images.* Wiley, New York, 353pp.

McDonnell, J. J. (2003). Where does water go when it rains? Moving beyond the variable source area concept of rainfall-runoff response. *Hydrological processes*, 17, 1869–1875, doi:10.1002/hyp.5132,.

McDonnell, J. J., Freer, J., Hooper, R., Kendall, C., Burns, D., Beven, K. J., et al. (1996). New method developed for studying flow on hillslopes. EOS, Trans. AGU, 77, 465–472.

McGlynn, B. L., & McDonnell, J. J. (2003). Role of discrete landscape units in controlling catchment dissolved organic dynamics. *Water Resource Resurces, 39*(4), 1090-1117.

McGuire, K. J., McDonnell, J. J., Weiler, M., Kendall, C., McGlynn, B. L., Welker, J. M., et al. (2005). The role of topography on catchment-scale water residence time. *Water Resources Research, 41, W05002, doi:10.1029/2004WR003657*.

Meentemeyer, V. (1989). Geographical perspectives of spaces, time, and scale. *Landscape Ecology, 3*, 163-173.

Melton, M. A. (1965). The geomorphic and paleoclimatic significance of the alluvial deposits in southern Arizona. *Journal of Geology, 73*, 1-38.

Merz, J., & Mosley, M. P. (1998). Hydrological behaviour of pastoral hill country modified by extensive landsling, Northern Hawkes's Bay, Neww Zealand. *Journal of Hydrology, 37*(2), 113-139.

Miglietta, M. M., & Rotunno, R. (2005). Simulation of moist nearly neutral flow over a ridge. *Journal of Atmospheric Sciences, 62*, 1410-142.

Minar, J., & Evans, I. (2008). Elementary forms for land surface segmentation: The theoretical basis of terrain analysis and geomorphological mapping. *Geomorphology,, 95*, 236-259.

Mitchell, K., & DeWalle, D. (1998). Application of the Snowmelt Runoff Model Using Multiple-Parameter Landscape Zones on the Towanda Creek Basin, Pennsylvania. *Journal od Ammerican water resources assessment, 34*, 335-354.

Molenaar, M. (1996). A syntactic approach for handling the semantics of fuzzy spatial objects. In P. Burrough, & A. Frank, *Geographic objects with indeterminate boundaries* (p. 207-222). Taylor & Francis, London.

Molenaar, M. (1998). *An Introduction to the Theory of Spatial Object modelling for GIS*. Taylor & Francis, London.

Monmonier, M. (1974). Measures of pattern complexity for choroplethic maps. *The American Cartographer, 1*(2), 159-169.

Montgomery, D. R., & Buffington, J. (1998). Channel processes, classification, and response. . In R. J. Naiman, & R. E. Bilby, *River Ecology and Management* . Springer Verlag.

Montgomery, D., & Dietrich, W. E. (1989). Channel initiation, drainage density and slope. *Water Resources Research,*(8), 1907-1918.

Moore, I. D., O'Loughlin, E. M., & Burch, G. J. (1988a). A contour-based topographic model for hydrological and ecological applications. *Earth Surface Processes Landforms, 13*, 305-320.

Moore, I. D., Pamuska, J. C., Grayson, R. B., & Srivastava, K. P. (1988b). Application og digital topographic modeling in hydrology, Publication No. 07-88. In S. J. American Society of Agricultural Engineers (A cura di), *Int. Symposium on Modeling Agricultural, Forest and*, (p. 447-461).

Moore, I., R.B. Grayson, R. B., & Ladson, A. R. (1991). Digital Terrain Modeling: A Review of Hydrological, Geomorphological, and Biological Applications. *Hydrological processes, 5*, 3-30.

Moore, R., & Clarke, R. (1981). A distribution function approach to rainfall runoff modelling. *Water Resources Research, 17*, 1367-1382.

Mostardini, F., & Merlini, S. (1986). Appennino Centro - Meridionale. Sezioni geologiche e proposta di modello strutturale. *Memorie Società Geologica Italiana, 35*, 177-202.

Muller, C., Hellebrand, H., Seeger, M., & Schobel, S. (2009). Identification and regionalization of dominant runoff processes – a GISbased and a statistical approach. *Hydrology and Earth System Sciences*, 13, 779–792, doi:10.5194/hess-13-779-2009.

Mulvani, T. J. (1850). On the use of the self registering rain and flood gauges. *Proceedings - Institution of Civil Engineers, 4*, 1-8.

Murakami, M. (1987). Orography and Monsoons. In C. P. Chang, & T. N. Krishnamurti, *Monsoon Meteorology* (p. 331-364). Oxford University Press.

Naef, F. (1981). Can we model the rainfall-runoff process today? *Hydrological Sciences Bulletin, 26*(3), 281-289.

Nalbantis, I., Efstratiadis, A., Rozos, E., Kopsiafti, M., & Koutsoyiannis, D. (2011). Holistic versus monomeric strategies for hydrological modelling of human-modified hydrosystems. *Hydrolologic and Earth System Sciences* , 15, 743–758, doi:10.5194/hess-15-743-2011.

Nash, J. E. (1957). The form of the instantaneous unit hydrograph. *The International Association of Hydrological Sciences, 45*(3), 114-121.

Nir, D. (1987). Regional geography considered from the system approach. *Geofurum, 18*(2), 187-202.

Nobre, A. D., Cuartas, L. A., Hodnett, M., Renn´o, C. D., Rodrigues, G., Silveira, A., et al. (2011). Height above the Nearest Drainage, a hydrologically relevant new terrain model. *Journal of Hydrology*, 404, 13–29.

O'Neill, R., DeAngelis, D., Waide, J., & Allen, T. (1986). A Hierarchical Concept of Ecosystems. *Princeton University Press, Princeton.*

Okunishi, K. (1974). Slopes and their processes. *Transactions, Japanese Geomorphological Union, 10A*, 13-22.

Okunishi, K. (1991). Hydrogeomorphological interactions—a review of approach and strategy. *Transactions, Japanese Geomorphological Union, 12*, 99-116.

Okunishi, K. (1994). Concept and methodology of hydrogeomorphology. *Transactions, Japanese Geomorphological Union, 15A*, 5-17.

Olaya, V. (2009). Basic land-surface parameters. In T. Hemgl, & H. I. Reuter, *Geomorphometry: concepts, softwares, applications* (Vol. 33, p. 141-170). Hartemink A. E. and McBratney A. B., Amsterdam, The Netherlands.

O'Neill, R. V. (1988). Hierarchy Theory and Global Change. In T. Rosswall, R. G. Woodmansee, & P. G. Risser, *Scales and Global Change.* John Wiley & Sons Ltd,Chichester/London.

Orlanski, I. (1975). A rational subdivision of scales for atmospheric processes. *Bulletin of the American Meteorological Society, 56*, 527-530.

Park, S., & van de Giesen, N. (2004). Soil-landscape delineation to define spatial sampling domains for hillslope hydrology. *Journal of Hydrology, 295*, 28-46.

Patacca, E., Scandone, P., Bellatalla, M., Perilli, N., & Santini, U. (1992). *La zone di giunzione tra l'arco appenninico settentrionale e l'arco meridionale nell'Abruzzo e nel Molise.* Studi Geologici Camerti, vol. spec. 1991/2, CROP 11:417-441, Camerino.

Pelletier, J. D., & Rasmussen, C. (2009). Geomorphically based predictive mapping of soil thickness in upland watersheds,. *Water resources research*, 45, W09417.

Penck, A. (1896). Die Geomorphologies als genetische Wissenschaft. *Comptes Rundus, 6. Inbternationales Geographisches Kongress,*, *C*, p. 735-752. German.

Pereira, G. (2002). A typology of spatial and temporal relations. *Geographical Analysis, 34*(1), 21-33.

Peschke, G., Etzenberg, C., Topfer, J., Zimmermann, S., & Muller, G. (1999). Runoff generation regionalization: analysis and a possible approach to a solution. *IASH pubblication 254 (Regionalization in Hydrology)*, 147-156.

Phillippee, J. T., & Wiggert, J. M. (1969). *Instantaneous Unit Hydrograph response by harmonic analysis.* Bulletin 15, Water Resources Research Center, Virginia Polytechnic Institute, Virginia.

Pielke, R. (2001). Influence of spatial distribution of vegetation and soils on the prediction of the cumulus convective rainfall. *Rev. Geophysics, 39*(2), 931-944.

Pike, R. J., & Wilson, S. E. (1971). Elevation relief ratio, hypsometric integral, and geomorphic area-altitude analysis. *Geological Society of Amrica Bulletin, 82*, 1079-1084.

Pnck, A. (1894). *Morphologie der Erdoberflache.* Engelhorn -Verlag, Stuttgart, Germany.

Press, F., & Siever, R. (1982). *Earth* (3 edn ed.). W.H. Freeman & Co., San Franciso, CA.

Purwanto, E., & Donker, N. (1991). Semi-distributed hydrologic modeling of the humid topical upper Cimandiri catchment (west Java) using HEC-1 model. International Journal of Applied Earth Observation and Geoinformation (ITC) 1991-4, 241-253.

Ramírez, J. A. (2000). Prediction and Modeling of Flood Hydrology and Hydraulics. In *Inland Flood Hazards: Human,Riparian and Aquatic Communities* (p. 293-329). Cambridge: Ellen Wohl.

Renn´o, C. D., Nobre, A. D., Cuartas, L. A., Soares, J. V., Hodnett, M. G., Tomasella, J., et al. (2008). HAND, a new terrain descriptor using SRTM-DEM: Mapping terra-firme rainforest environments in Amazonia. *Remote Sensing of Environment*, 112, 3469–3481.

Rigon, R., D'Odorico, P., & Bertoldi, G. (2011). The geomorphic structure of the runoff peak. *Hydrol. Earth Syst. Sci. Discuss.*, 8, 1031-1058, doi:10.5194/hessd-8-1031-2011.

Ritter, D. F., Kochel, R. C., & Miller, J. R. (2002). Process geomorphology. Mc-Graw Hill, Boston.

Robe, F., & Emanuel, K. (2001). The effect of vertical wind shear on radiative-convective equilibrium states. *Journal of Atmospheric Sciences, 58*, 1427-1445.

Roberts, D., Dowling, T., & Walker, J. (July 1997.). FLAG: A Fuzzy Landscape Analysis GIS Method for Dryland Salinity Assessment. *CSIRO Land and Water Tech Report 8/97, Canberra.*

Rodriguez-Iturbe, I., & Gupta, V. K. (1983). Scale problems in hydrology. *Journal of Hydrology, 65*, (Special issue).

Rodríguez-Iturbe, I., & Valdés, J. B. (1979). The geomorphologic structure of hydrologic response. *Water Resources Research, 15*(6), 1409-1420.

Roe, G. H. (2005). Orographic precipitation. *Annual Review Earth and Planetary Sciences , 33*, 645-671.

Ross, C. N. (1921). The calculation of flood discharge by the use of time contour plan isochrones. *Transaction of the Institute of Engineers*(2), 85-92.

Rossi, F. (1998). Idrologia e Controllo degli eventi estremi". *XXVI Convegno di Idraulica e Costruzioni Idrauliche*, (p. 81-99). Catania.

Rossi, F. (2006). L'analisi statistica degli eventi idrologici estremi. *XXX Convegno di Idraulica e Costruzioni Idrauliche*. Roma.

Rossi, F., & Villani, P. (1994). *Valutazione delle piene in Campania.* Dipartimento di Ingegneria Civile, Università di Salerno. CNR-GNDCI.

Rossi, F., Fiorentino, M., & Versace, P. (1984). Two- Component Extreme Value distribution for flood frequency analysis. *Water Reosurce Researches, 20*(7), 847-856.

Rossi, F., Furcolo, P., Guida, D., & Tropeano, R. (2005). The effect of orography on extreme rainfall: a simplified meteo-morphological model. *Session Poster, European Geosciences Union, Vienna.*

Rotunno, R., & Ferretti, R. (2001). Mechanisms of intense Alpine rainfall. . *Journal of Atmospheric Sciences, 58*, 1732-1749.

Salvati, S., Stark, C. P., Rossi, M., & Guzzetti, F. (2010). Societal landslides anf flood risk in Italy. *Natural Hazards and Earth System Sciences, 10*, 465-483.

Savenije, H. H. (2010). HESS Opinions "Topography driven conceptual modelling (FLEX-Topo)". *Hydrologic and Earth System Sciences*, 14, 2681–2692, doi:10.5194/hess-14-2681-2010.

Scheidegger, A. E. (1972). Hydrogeomorphology. *Journal of Hydrology, 20*, 193-215.

Scherrer, S. (1996). *Abflussbildung bei Starkniederschl¨agen – Identifikation von Abflussprozessen mittels kunstlicher Niederschlage (Translation: Runoff formation under extreme precipitation – Identification of runoff processes by means of sprinkling experiments).* PhD thesis, Swiss Federal Institute of Technology, Zurich.

Scherrer, S., & Naef, F. (2003). Adecision scheme to identify dominant flow processes at the plot scale for the evaluation of contributing area at the catchments scale. *Hydrological Processes, 17*(2), 391-401.

Schmidt, J., Hennrich, K., & Dikau, R. (2000). Scales and similarity in runoff processes with respect to geomorphometry. *Hydrological Processes, 14*, 1963-1979.

Schomocker-Fackel, P., Naef, F., & Scherrer, S. (2007). Identifying runoff processes on the plot and catchment scale. *Hydrology and Earth System Sciences*, 11, 891-906.

Seelbach, P., Wiley, M., Kotanchik, J., & Baker, M. (1997). *A landscape-based ecological classification system for river valley segments in lower Michigan (MI-VSEC Version 1).* Fisheries Division Research Report 2036, Department of Natural Resources, State of Michigan, Lansing, USA.

Shermann, L. K. (1932). Stream flow from rainfall by unit-graph method. *Engineering News Records*(108), 501-505.

Sidle, R. C. (2006). Field observation and process understanding in hydrology: essential components in scaling. *Hydrological Processes, 20*, 1439-1445.

Sidle, R. C., & Hornbeck, J. W. (1991). Cumulative effects: a broader approach to water quality research. *Journal of Soil and Water Conservation, 46*, 268-271.

Sidle, R. C., & Onda, Y. (2004). Hydrogeomorphology: overviw of an emerging science. *Hydrological processes, 18*, 597-602.

Sidle, R. C., Tsuboyama, Y., Noguchi, S., Hosoda, I., Motohisa, F., & Shimuizu, T. (2000). Stormflow generation in steep forested headwater: a linked hydrogeomorphic paradigm. *Hydrological Processes, 14*, 369-385.

Simonovic, S., Fahmy, H., & Elshorbagy, A. (1997). The use of object oriented modeling for water resources planning in Egypt. *Water Resources Management, 11* (4), 243-261.

Singh, O., Sarangi, A., & Sharma, C. M. (2008). Hypsometric integral estimation methods and its relevance on erosion status of northwestern lesser Himalayan watersheds. *Water Resources Management, 22*, 1545-1560.

Singh, V. P., & Fiorentino, M. (1996). *Geographical Information Systems in hydrology.* Boston: Kluver Academic.

Singh, V. P., & Woolhiser, D. A. (2002). Mathematical modeling of watershade hydrology. *Hydrologic Engineering, 7*(4), 270-292.

Sivapalan, M., & Woods, R. A. (1995). Evaluation of the effects of general circulation model's subgrid variability and patchiness of rainfall and soil moisture on land surface water balance fluxes. In J. D. Kalma, *Scale Issues in Hydrological Modelling* (p. 453-473). Chichester, UK.

Sivapalan, M., Bloschl, G., Zhang, L., & Vertessy, R. (2003). Downward approach to hydrologic prediction. *Hydrological processes*, 17, 2101–2111, doi:10.1002/hyp.1425,.

Smith R. B. and I. Barstad. 2004: : Vol. 61, N. (2004). A Linear Theory of Orographic Precipitation. *Journal of Atmospheric Sciences, 61*(12), 1377-1391.

Smith, R. B. (2003). A linear uplsope-time delay model for orographic precipitation. *Journal of hydrology, 282*, 2-9.

Smith, R. B. (2006). Progress on the theory of orographic precipitation. *Geological Society of America, Special paper 398*, 1-16.

Soil Conservation Service, H. (1972). *Sec.4 of National Engineering Handbook*. Washington, D. C.: Soil Conservation Service, U. S. Department of Agriculture.

Spatuzzi, S. (2012). Modelli di previsione dei fenomeni di Flash-Floods nei piccoli bacini. *Tesi di dottorato*.

Speight, J. (1988). Land classification. In R. C. McDonald, R. F. Isbell, J. Speight, J. Walker, & M. Hopkins, *Australian soil and land survey field handbook*. 2nd Edn. (Inkata Press: Melbourne).

Spreen, W. C. (1947). A determination on the effect of topography upon precipitation. *Transanctions American Geophysical Union, 28*, 285-290.

Stefano, C., Ferro, V., Porto, P., & Tusa, G. (2000). Slope curvature influence on soil erosion and deposition processes. *Water Resources Research, 36*(2), 607-617.

Strahler, A. N. (1952). Hypsometric (area-altitude) analysis of erosional topography. *Geologic Society of America, 63*, 1117-1142.

Summerell, G. K., Vaze, J. T., Grayson, R. B., Beale, G., & andDowling, T. I. (2005). Delineating the major landforms of catchments using an objective hydrological terrain analysis method. *Water Resources Research, 41, W12416, doi:10.1029/2005WR004013*.

Summerfield, A. M. (1991). *Global Geomorphology*. Longman, London.

Sun, Y., Solomon, S., Dai, A., & Portmann, R. (2007). How often will it rain? *Journal of Climate and Applied Meteorology, 20*, 4801-4818, doi: 10.1175/JCLI42631.

Supan, A. (1911). *Grundzuge der physischen Erdkunde.* Veit & Co., Leipzig, German.

Szilagyi, J., & Parlange, M. B. (1998). Base flow separation based on analytical solutions of the Boussinesq equation. *Journal of Hydrology, 204*(1-4), 251-260.

Szilagyi, J., & Parlange, M. B. (1998). Base flow separation based on analytical solutions of the Boussinesq equation. *Journal of hydrology, 204*(1-4), 251-260.

Tagil, S., & Jenness, J. (2008). Gis-Based automated landform classification and topographic, landcover and geologic attributes of landforms around the Yazoren Poje Turkey. *Journal of Applied Sciences, 8*(6), 910-921.

Takahashi, S. (2004). Algorithms for extracting surface topology fron digital elevation models. In S. Rana, *Topological data structures for surfaces* (p. 31-51). John Wiley and Sons, Ltd, England.

Tallaksen, L. (1995). A review of baseflow recession analysis. *Journal of Hydrology, 165*, 349-370.

Tallaksen, L. M. (1995). A review of base flow recession analysis. *Journal of Hydrology, 165*, 149-370.

Teixeira, J., Chaminé, H. I., Espinha Marques, J., Gomes, A., Carvalho, J. M., A., P. A., et al. (2008). Integrated approach of hydrogeomophology and gis mapping to the evaluation of groundwater resources: an example from the hydro-mineral system of Caldas da Cavaca, NW Portugal. In *Global Groundwater Resources and Management, Selected paper from the 33rd International Geological Congress, Genaral Synopsium: Hydrogeology, Oslo (Norway), August 6-14* (p. 227-249). Paliwal B. S.

Tetzlaff, D., Soulsby, C., Waldron, S., Malcolm, I. A., Bacon, P. J., Dunn, S. M., et al. (2007). Conceptualization of runoff processes using a geographical information system and tracers in a nested mesoscale catchment. *Hydrological Processes, 21*, 1289-1307.

Thorncroft, C., Hoskins, B., & McIntyre, M. (1993). Two paradigms of baroclinic wave life-cycle behavour. *Quarterly Journal of the Royal Meteorological Society, 119*, 17-55.

Todini, E. (1988). Rainfall-Runoff modeling - Past, present and future. *Journal of Hydrology, 100*(13), 341-352.

Todini, E. (2007). Hydrological catchment modelling: past, present and future. *Hydrology & Earth System Sciences, 11*(1), 468-482.

Troch, P., van Loon, E., & Hilberts, A. (2002). Analytical solutions to a hillslopes-storage kinamatic wave equation for subsurface flow. *Advances in Water Resources , 25*, 637-649.

Troll, C. (1975). VegleichendeGeographie der Hochgebirge der Erde in landchaftsokologischer Sicht. *Geographische Rundschau, 27*, 185-198.

Tromp-van Meerveld, H. J., & McDonnell, J. J. (2006). Threshold relations in subsurface stormflow: 2. The fill and spill hypothesis. *Water Resources Research*, 42, W02411, doi:10.1029/2004WR00380.

TsuKamoto, Y. (1961). An experiment on subsurface flow. *Journal of the Japanese Forestry Society, 43*, 62-67.

Tucker, G. E., & Bras, R. L. (1998). Hillslope processes, drainage density and landscape morphology. *Water Resources Research, 34*, 2751-2764.

Uhlenbrook, S., Roser, S., & Tilch, N. (2004). Hydrological processes representation at the meso-scale: the potential of a distributed, conceptual catchment model. *Journal of Hydrology, 291*, 278-296.

Van Smaalen, J. W. (2003). Automated Aggregation of Geographic Objects: A New Approach to the Conceptual Generalisation of Geographic Databases. *Doctoral Dissertation. Wageningen University and Research Centre, The Netherlands.*

Versace, P., Ferrari, E., Fiorentino, M., Gabriele, S., & Rossi, F. (1989). *La valutazione delle piene in Calabria.* CNR-GNDC, LINEA1, CNR-IRPI. Cosenza: Geodata.

Villi, V., & Bacchi, B. (2001). *Valutazione delle piene in Tiveto.* CNR-GNDCI, Padova-Brescia.

Viviroli, D., & Weingartner, R. (2004). The hydrological significance of mountains – from regional to global scale. *Hydrology and Earth System Sciences, doi:10.5194/hess-8-1017-2004, 8*, 1016-1029.

viviroli, D., & Weingartner, R. (2004). The hydrological significance of mountains: from regional to global scale. *Hydrology & Earth System Sciences, 8*(6), 1016-1029.

Viviroli, D., Archer, D. R., Buytaert, W., Fowler, H., Greenwood, G. B., Hamlet, A., et al. (2011). Climate change and mountain water resources: overview and recommendations for research, management and policy. *Hydrology and Earth System Sciences, 15*, 471-504.

Viviroli, D., Archer, D. R., Buytaert, W., J., F., Greenwood, G. B., Hamlet, A. F., et al. (2011). Climate change and mountain water

resources: overview and recommendations for research, management and policy. *Hydrology and Earth System Sciences, 15*, 417-504.

Viviroli, D., Durr, H. H., Messerli, B., & Meybeck, M. (2007). Mountains of the world, water towers for the Humanity: Typology, mapping, and global significance. *Water Resources Research, 43, W07447*, 1-13.

Vos, F., Rodriguez, J., Below, L. R., & Guha- Sapir, D. (2010). *Annual disaster statistical Review 2009: The numbers and trends.* Centre of Research on the epidemiology of disasters. Brussels: CRED.

Wang, J., Endreny, T. A., & Hassett, J. M. (2005b). A flexible modeling package for topographically based watershed hydrology. *Journal of Hydrology*(314), 78–91.

Wang, J., Hassett, J., & Endreny, T. (2005a). An object-oriented approach to the description and simulation of watershed scale hydrological processes. *Computers and Geosciences*(31), 425-435.

Watson, C. D., & Lane, T. P. (2011). Sensitivities of orographic precipitation to terrain geometry and upstream conditions in idealized simulations. *Journal of Atmospheric Sciences*, doi:10.1175/JAS-D-11-0198.1, in press.

Webster, P. J. (1987). The variable and interactiveMonsoon. In C. Chang, & T. N. Krishnamurti, *Monsoon Meteorology* (p. 269-329). Oxford University Press.

Webster, R. (1977). *Quantitative and Numerical Methods in Soil Classification and Survey.* Clarendton, Oxford.

Weiler, M., & Naef, F. (2003a). Simulating surface and subsurface initiation of macropore flow. *Journal of Hydrology, 273*, 139-154.

Weiler, M., & Naef, F. (2003b). An experimental tracer study of the role of macropores in the infiltration in grassland soils. *Hydrological Processes, 17*, 477-493.

Weiss, A. (2001). Topographic position and landforms analysis. *Poster presentation, ESRI User Conferences, San Diego, CA.*

White, D. (1988). Grid-based Application of Runoff Curve number. Journal of Water Resources Planning and Management, ASCE 114(6), 601-612.

White, W. (1969). Conceptual models for carbonate aquifers. *Ground-Water, 7*, 15-21.

Winter, T. C. (2001). The concept of hydrologic landscapes. *Journal of the American Water Resources Association, 37*(2), 335-349.

Wolock, D. M., Winter, T. C., & McMahon, G. (2004). Delineation and evaluation of hydrologic landscape regions in the United States using geographic information system tools and multivariate statistical analyses. *Environmental Management, 34*, 71-88.

Wood, E. (1994). Scaling, soil moisture and evapotranspiration in runoff models. *Adv. Water Resour, 17*, 25-34.

Wood, E. F., Sivapalan, M., & Beven, K. (1990). Similarity and scale in catchment storm response. *Reviews of Geophysics , 28*, 1-18.

Wood, E., Lettenmaier, D., & Zartarian, V. (1992). A landsurface hydrology parameterization with subgrid variability for general circulation models. *Journal of geophysical research, 97*, 2717-2728.

Wright, R. L. (1972). Principles in a geomorphological approach to land classification. *Z. Geomorph, 16*(4), 351-373.

Wu, J. (1999). Hierarchy and scaling: extrapolating information along a scaling ladder. *Canadian Journal of Remote Sensing, 5*(4), 367-380.

Yamada, S. (1999). Mountain ordering: A method for classifying mountains based on their morphometry. *Earth Surface Processes and Landforms,, 24*(7), 653-660.

Young, R. A., Onstad, C. A., Bosch, D. D., & Anderson, W. P. (1989). AGNPS: A nonpoint source pollution model for evaluating agricultural watershed. *Journal of Soil and Water Conservation*(44), 168-173.